In vitro and *in vivo* analysis of the assembly of the non-collagenous tectorial membrane matrix

A thesis submitted towards fulfilment of the requirement for the degree of Philosophy Doctor

by

Julia Jurievna Korchagina

to

The University of Sussex

School of Life Sciences

July 2013

This thesis is dedicated to Richard Goodyear and Guy Richardson who trusted me and gave me the opportunity to carry on my work in the lab.

ACKNOWLEDGEMENTS

First of all, I want to break the traditions of how acknowledgements are usually written and thank the following people: Tony Robertson, Kishani Ranatunga, Naomi Clifton, Claire Thomas, Helen Prance, Richard Goodyear and Guy Richardson. Without them I would not be where I am now.

I am deeply grateful to my main supervisor, Professor Guy Richardson, who contributed in so many ways to help me complete this degree. He has given me endless guidance, support, inspiration and encouragement and it is difficult to express in words how much has he done for me over these four years. I also thank Dr. Kevin Legan, my second supervisor, who supported me with my work in every possible way. Dr. Richard Goodyear deserves special thanks for being a constant source of help and advice (or a constant victim of me demanding help and advice).

I want to thank Professor James Bartles, Dr. Marcelo Rivolta and Dr. Jing Zheng for the reagents they kindly provided. Many thanks to Dr. Richard Goodyear for his contribution to electron microscopy imaging, and to Mr. Souvik Naskar for his excellent assistance with western blotting. Furthermore I also want to express my gratitude to Prof. Guy Richardon and Dr. Kevin Legan for their help with transgenic animals and to Mrs. Lindsey Welstead for genotyping. I thank Dr. Martyn Stenning for his help in organising my trips to Madrid and Baltimore. I am grateful to the University of Sussex and Action on Hearing Loss for the financial support of this project. I would also like to thank Dr. Nikolai Nikitin who once played a huge role in my career giving me the chance to apply for the place at Sussex four years ago.

I would never be able to survive through this journey without the love and support of my dearest parents, Valentina Korchagina and Juriy Korchagin. I thank my friends

David Theobald, Alejandro Vicente-Grabovetsky, Marina Salorio-Corbetto, Nicola Allen, Ash Robinson, Terri Roberts, Kirsty Bennett, Vera Medvedeva, Ekaterina Vlasova and Anna Dzarasova for being the best friends ever and always being around me when I needed them. Also, my life in the lab would not have been so much fun if it was not for my best friend, Richard Goodyear.

Finally, I want to say a big thank to Kevin Costello who was brave enough to be around me during the tough period of thesis writing and for giving me his love and support in situations where most people would kill me. I am also so grateful to him for making sacrifices in his own life in order to go with me to France, just to allow me to follow my dream.

UNIVERSITY OF SUSSEX

JULIA JURIEVNA KORCHAGINA

SUBMITTED FOR THE DEGREE OF PHILOSOPHY DOCTOR

***IN VITRO* AND *IN VIVO* ANALYSIS OF THE ASSEMBLY OF THE NON-COLLAGENOUS TECTORIAL MEMBRANE MATRIX**

SUMMARY

Alpha- and beta-tectorin (Tecta and Tectb) are major non-collagenous components of the tectorial membrane (TM). The presence of a zona pellucida (ZP) domain in both tectorins suggests that Tecta and Tectb can form hetero- or homopolymers. It is unclear, however, how these proteins assemble to form the TM matrix. The mechanisms of apical targeting, secretion and processing of the tectorins are also unexplored. I used fluorescently-tagged tectorin constructs for stable transfection into polarised epithelial MDCK cells or transient expression in mouse cochlear cultures to develop an *in vitro* model of TM matrix assembly. Significant amounts of matrix were not observed with stable tectorin expression in monolayer cultures of MDCK cells. In contrast, I observed substantial amounts of dense extracellular matrix on the apical surfaces of outgrowth zone cells when cochlear cultures were transiently transfected with either Tecta or Tectb. When ectopically expressed in hair cells, Tecta and Tectb locate to the distal tips of the hair bundle.

To study the role of the inner-ear protein Ceacam16 in hearing, we generated a *Ceacam16* functional null mouse model. The *Ceacam16* gene was inactivated by targeted replacement of exons 2-5 with the bacterial *lacZ* gene. β-gal staining I performed reveals that Ceacam16 is expressed in the epithelial cells of the spiral limbus and inner sulcus, and in both the pillar cells and Deiter's cells. I first detected the

presence of Ceacam16 in the TM at P12, four days before the defined striated-sheet matrix is observed. Transmission electron microscopy reveals a complete loss of striated-sheet matrix in *Ceacam16* null mice in comparison to the wild-type.

The results of this thesis suggest neonatal mouse cochlear cultures as a model for studying tectorin-based extracellular matrix production and also reveal that Ceacam16 is required for normal formation and/or maintenance of striated-sheet matrix.

TABLE OF CONTENTS

LIST OF FIGURES

LIST OF TABLES

LIST OF ABBREVIATIONS

ABR - auditory brainstem response

ADNSHL - autosomal dominant non-syndromic hearing loss

AG - chicken βactin/rabbit β-globin hybrid promoter

AP - alkaline phosphatase

APS - ammonium persulfate

ARNSHL - autosomal recessive non-syndromic hearing loss

BCIP - 5-bromo-4-chloro-3-indolyl phosphate

BM - basilar membrane

BSA - bovine serum albumin

BSD - backscatter detector

CaCo2 cells - human colorectal adenocarcinoma 2 cells

CAG - promoter composed of the CMV IE enhancer sequence connected to the AG promoter

CAP - compound action potential

CCD - charge-coupled device

Ceacam - carcinoembrionic antigen-related cell adhesion molecule

CF - characteristic frequency

CG - ammonia-polymerised collagen

CL4 - LLC-PK1-CL4 cells

CMM - collagen - BD Matrigel^{TM} master mix

CMV/CMV IE - human cytomegalovirus immediate early promoter

Co-IP - co-immunoprecipitation

DFNA4 - deafness autosomal dominant 4

DIV - days *in vitro*

DMEM - Dulbecco's modified Eagle's medium

DMSO - dimethyl sulfoxide

dNTPs - deoxynucleotide triphosphates

DPOAE - distortion product otoacoustic emissions

E - embryonic day

EDTA - ethylenediaminetetraacetic acid

EGFP - enhanced green fluorescent protein

EMC - extracellular matrix

Ent - entactin domain

ES cells - embryonic stem cells

FBS - fetal bovine serum

FITC - fluorescein isothiocyanate

G418 - geneticin

GER - greater epithelial ridge

GFP - green fluorescent protein

GPI - glycosylphosphatidylinositol

HBSS - Hank's balanced salt solution

HEPES - hydroxyethyl-piperazine ethanesulafonic acid

HEK 293 cells - human embryonic kidney 293 cells

HMM - high molecular mass

Ig - immunoglobulin

IgCAM - immunoglobulin superfamily of cell adhesion molecules

IHC/IHCs - inner hair cell/cells

IRES - internal ribosome entry site

LB - lysogeny broth

LM - laminin

LMM - low molecular mass

MCS - multiple cloning site

MDCK cells - Madin-Darby canine kidney cells

MEM - minimum essential medium

MG - Matrigel™

MMM - medium molecular mass

NBT - nitro-blue tetrazolium chloride

OCT - optimal cutting temperature

OD - optical density

OHC/OHCs - outer hair cell/cells

ORF - open reading frame

OTOG - otogelin

OTOGL - otogelin-like

P - postnatal day

pBK - plasmid backbone

PBS - phosphate buffered saline

PCR - polymerase chain reaction

PDL - poly-D-lysine

PVDF - polyvinylidene difluoride

PVP – polyvinylpyrrolidone

RCM - rat cochlear culture medium

RFP - red fluorescent protein

SBA - soybean agglutinin

SDS-PAGE - sodium dodecyl sulphate polyacrylamide gel electrophoresis

SEI - secondary electron image

SEM - scanning electron microscopy

SOC - super-optimal broth with catabolite repression

TBE - Tris-borate EDTA

TCA - trichloracetic acid

Tecta - alpha-tectorin

Tectb - beta-tectorin

TEM - transmission electron microscopy

TEMED - tetramethylethylenediamine

TIL - trypsin inhibitor like cysteine rich domain

TM - tectorial membrane

UV – ultraviolet

vWFC/vWFD - von Willebrand factor type C/type repeat

ZA - zonadhesin-like domain

ZAN - zonadhesin

ZP - zona pellucida

βgal - β-galactosidase

CHAPTER 1

General Introduction

1.1. Anatomy and physiology of the mammalian auditory periphery

The mammalian ear comprises three parts, each of which plays a particular role in the perception of sound; these are the outer, middle and inner ears (Fig.1.1). The outer ear is composed of an external cartilaginous section referred to as the pinna or the auricle. The pinna, in turn, consists of the concha, which forms a reverberating hollow space connected by the ear canal (external auditory meatus) to the eardrum or tympanic membrane (Fig.1.1) (Geisler, 1998). The outer ear collects sound waves, transmitting them to the more interior portions. It selectively strengthens and weakens sound stimuli of particular frequencies and directions (Rosowski, 1996). The eardrum is an elastic, fine membrane that separates the outer and middle ears.

The middle ear transmits sound from the ear canal to the inner ear. Its primary function is to compensate for the impedance mismatch between the two different media of the ear: the air-filled outer ear and the liquid-filled inner ear (Pickles, 1988). The ossicles (Fig.1.1), a chain of minute bones named the malleus (hammer), the incus (anvil) and the stapes (stirrup), render sound transmission through the mammalian middle ear (Pickles, 1988; Geisler, 1998). The malleus is most lateral and adjoins the medial aspect of the eardrum. The footplate of the stapes is affixed to the oval window in the bony wall of the inner ear (Pickles, 1988).

The inner ear includes the vestibular system (the organ of balance), and the cochlea (the organ of hearing) (Klinke, 1986). The cochlea translates sound waves into action potentials encoding auditory information for processing in the central nervous system.

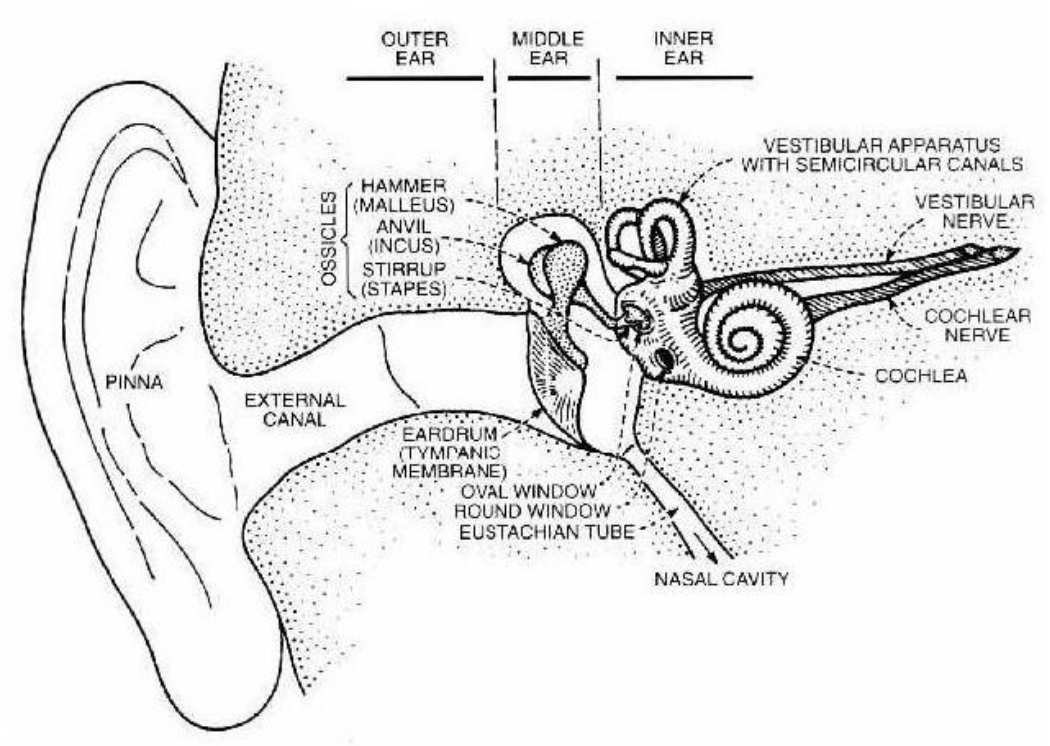

Figure1.1. The outer, middle and inner ears in man. The size of the inner and middle ear structures has been magnified (from Geisler, 1998).

1.2. General structure of the cochlea

The cochlea ("snail" in Latin) is a small, coiled, bony structure split into three ducts filled with liquid: scala vestibuli, scala media and scala tympani (Fig.1.2) (Geisler, 1998). Scala vestibuli and scala tympani are filled with perilymph, which is akin to extracellular fluid (Pickles, 1988) and scala media is filled with endolymph, resembling intracellular fluid (Bosher and Warren, 1978). Scala vestibuli begins at the oval window, a membrane between the middle ear and the inner ear which is in direct contact with stapes (Fig.1.1). Scala tympani terminates at the round window, another membrane

within the osseous wall of the cochlea, which is situated below the oval window (Fig.1.1) and allows the pressure caused by the quivering of the stapes to be released back in the middle ear. A small hole, the helicotrema, provides a connection between scala vestibuli and scala tympani at the cochlear apex.

Scala media is enclosed between scala vestibuli and scala tympani (Fig.1.2) and its boundaries are formed by two elastic membranes. Reissner's membrane separates scala media from scala vestibuli and is insensitive to sound waves (von Bekesy, 1960). The basilar membrane (BM) forms the boundary between scala media and scala tympani and is sensitive to sound waves. The BM consists of collagen fibres embedded in an amorphous matrix. It stretches radially from the osseous spiral lamina to the spiral ligament, located at the outer wall of the cochlea (Geisler, 1998; von Bekesy, 1948). The fluid content of scala media is referred to as the endolymph.

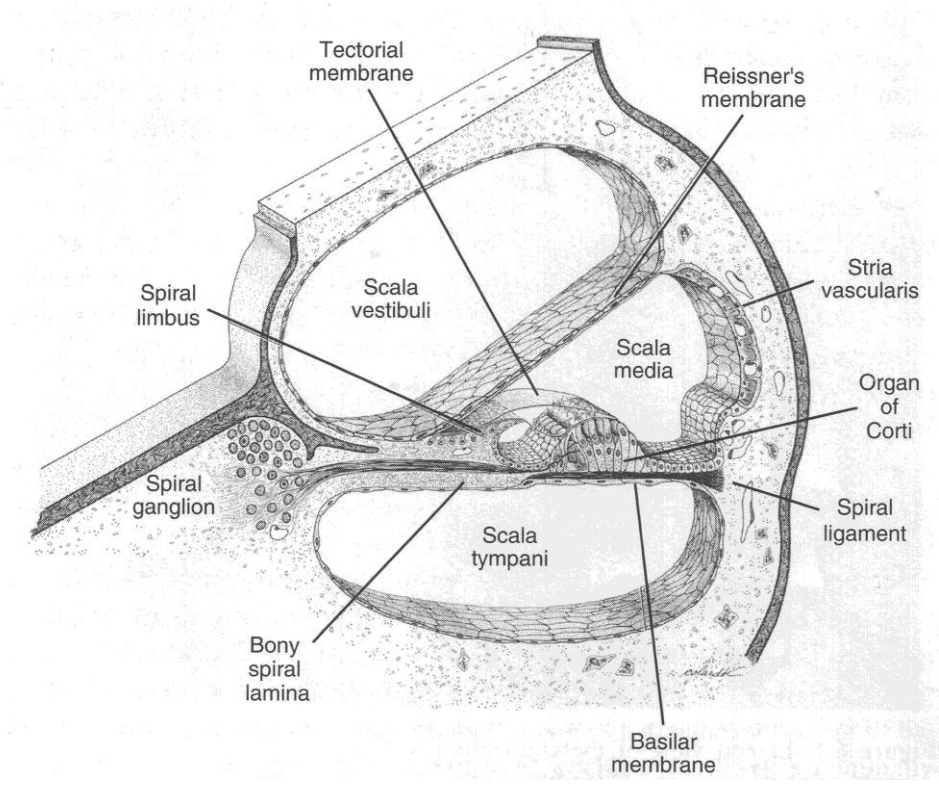

Figure 1.2. A cross-section through the cochlea displaying the scalae and related structures of the mammalian cochlea (from Geisler, 1998).

The cochlea acts as a frequency analyser (von Bekesy, 1960). It separates a complex sound wave into its component frequencies and maps them along the BM (Dallas, 1992; von Bekesy, 1960). The motion of the BM occurs in a form of a travelling wave which starts at the base of the cochlea and terminates at the apex (von Bekesy, 1960). The place where the BM displacement reaches its maximum depends on the frequency of the stimulus, and is the characteristic frequency (CF) of this point along the BM. High frequencies cause maximum vibrations at the base of the cochlea, and low frequencies peak at the apex (von Bekesy, 1960). This is reflected in the shape and physical properties of the BM which is thick, narrow and stiff in the basal turn of the cochlea, but is broad, thin and floppy at cochlear apex (von Bekesy, 1960).

1.3. The structure of the organ of Corti

On upper surface of the BM sits the complex, cellular structure referred as the organ of Corti. The organ of Corti is comprised of the hair cells, which are the receptor cells that transform sound oscillations into neural activity, and the supporting cells that provide structural support and play the diverse roles in the development and maturation of the sensory epithelia.

Two distinct types of hair cells are distinguished in the organ of Corti: the inner hair cells (IHCs) and outer hair cells (OHCs). The IHCs are arranged linearly along the modiolar face of the tunnel of Corti and their lateral boundaries are defined by the inner pillar cells (Fig.1.3). The OHCs are arranged into three rows on the other side of the tunnel of Corti. Both types of hair cells are crowned at their apical surfaces with a stiff cuticular plate comprised of actin and other cytoskeletal proteins, from which the hair bundles protrude (Fettiplace and Hackney, 2006). Supporting cells surround the hair cells and prevent them from directly contacting each other. The apical extremities of

supporting and hair cells are joined together by tight junctions, adherens junctions and desmosomes to produce the reticular lamina (Raphael and Altschuler, 2003). Deiters' cells support the OHCs at their base and apex (Geisler, 1998) and form protrusions which extend to the reticular lamina and fill spaces between OHCs (Raphael and Altschuler, 2003). An inner phalangeal cell and a border cell support and isolate an IHC. The pillar cells form the tunnel of Corti and provide mechanical coupling between the BM and the reticular lamina (Tolomeo and Holley, 1997). Tall columnar Hensen's cells adjacent to the third row of Deiter's cells (Fig.1.3) might regulate the ion balance of the endolymph (Lagostena et al., 2001; Sugasawa et al., 2013). The organ of Corti is covered by the tectorial membrane (TM), an acellular structure which is attached to the spiral limbus and extends parallel to the BM (Fig.1.3). Transverse oscillations of the BM in response to sound stimulation induce a radial shearing movement of the hair cells against the TM, deflecting their hair bundles thus causing their depolarisation and transmitter release (Geisler, 1998).

The IHCs have dense afferent innervation and are thought to be the main sensory cells of the cochlea. Their hair bundles are free-standing and are stimulated by the fluid motion in the subtectorial space. The OHC hair bundles are imbedded in the TM (Kimura, 1966). Efferent fibres synapse directly on the OHCs and on the afferent dendrites under IHCs (Spoendlin, 1985). The OHCs are able to change their length and shape in response to electrical stimulation (Brownell et al., 1985). This property known as somatic electromotility serves to amplify the vibrations of the BM at low sound pressure levels and compress the BM response at high sound pressure levels (Robles and Ruggero, 2001).

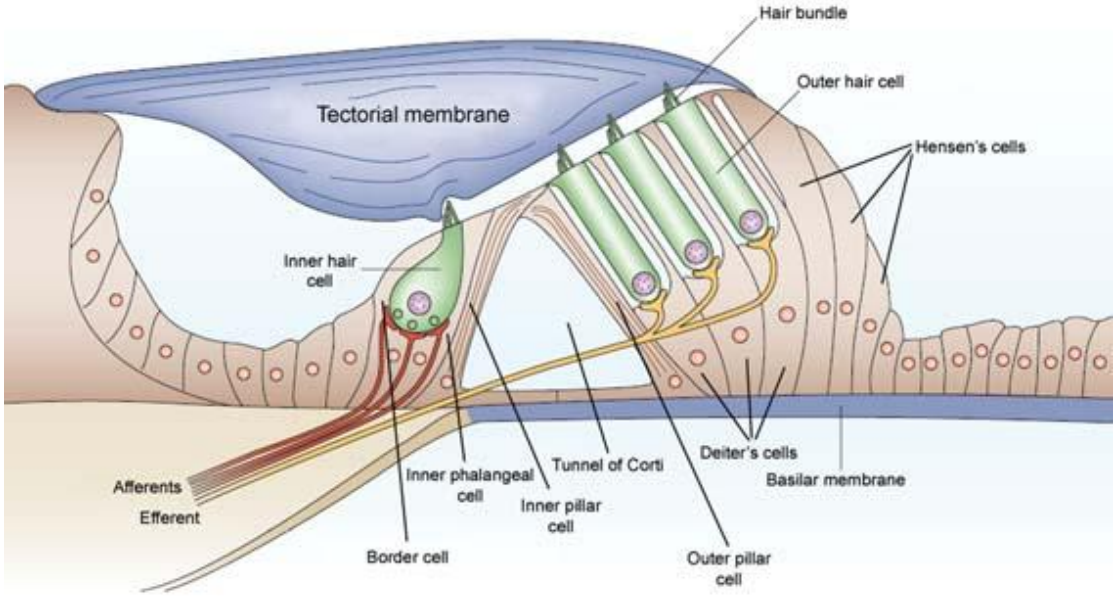

Figure 1.3. Cross-section through the organ of Corti (modified from Fettiplace and Hackney, 2006).

1.4. The tectorial membrane

1.4.1. The structure of the tectorial membrane

The tectorial membrane (TM) comprises three distinct zones (Fig.1.4): the marginal zone consisting of the marginal band; the middle zone which forms the main body of the TM; and the limbal zone where the TM attaches to osseous spiral limbus.

The main body of the TM is packed with striated-sheet matrix and bundles of collagen fibres (Fig.1.4). Its upper surface is covered by the covernet, which merges into the marginal band. Hensen's stripe and Kimura's membrane are situated on the lower surface of the TM (Fig.1.4). The tallest row of stereocilia on each OHC is imbedded into Kimura's membrane, which lies over all three rows of OHCs and continues into the marginal band (Kimura, 1966; Lim, 1980). The position of Hensen's stripe corresponds to the row of IHCs (Lim, 1980; Rueda et al., 1996).

The TM contains three types of collagen, types II, IX and XI, and the non-collagenous glycoproteins: alpha-tectorin (Tecta) and beta-tectorin (Tectb) (Legan et al., 1997; Richardson et al., 1987), otogelin (Cohen-Salmon et al., 1997), and the recently described protein Ceacam16 (Zheng et al., 2011). Recent studies suggest that otogelin-like (OTOGL) (Yariz et al., 2012) and otolin (Deans et al., 2010) are non-collagenous glycoproteins that contribute to the TM.

Collagen bundles are interwoven with the striated-sheet matrix. The *Tectb*$^{-/-}$ mice (Russell et al., 2007) and mice with a functional null mutation in Tecta (*Tecta*$^{\Delta ENT/\Delta ENT}$) (Legan et al., 2000) lack a striated-sheet matrix suggesting that it is formed of Tecta and Tectb proteins. Another possible component involved in striated-sheet matrix formation is Ceacam16 protein which was shown to interact with Tecta (Zheng et al., 2011). Although Kammerer et al., 2012, generated a *Ceacam16*$^{-/-}$ mouse model they did not performed full ultrastructural analysis. However, it was shown that Ceacam16 protein appears in the TM from a postnatal day 12 (P12), coincidentally with the onset of hearing in mice (Kammerer et al., 2012). The data of Simmler et al., 2000, indicate that otogelin is involved in the TM fibrillar network and might be associated with collagen fibrils. In the otogelin null mice, large areas of the TM have a disrupted fibrillar organization with collagen bundles forming either scattered, wavy strands or dense, rod-like fibrils (Simmler et al., 2000). The striated-sheet matrix in the otogelin null mouse is unaffected (Simmler et al., 2000). The roles of OTOGL and otolin are yet to be identified.

Striated-sheet matrix is formed of two types of filaments, light-staining and dark-staining, of about 7-9 nm in diameter (Hasko and Richardson, 1988). The composition of light and dark filaments is unclear. They may be homomeric, formed from either

alpha-tectorin or beta-tectorin, or heteromeric (Legan et al., 1997). Tectorins are also present in the covernet fibrils, the marginal band and Hensen's stripe, denser structures within which there is no striated-sheet matrix.

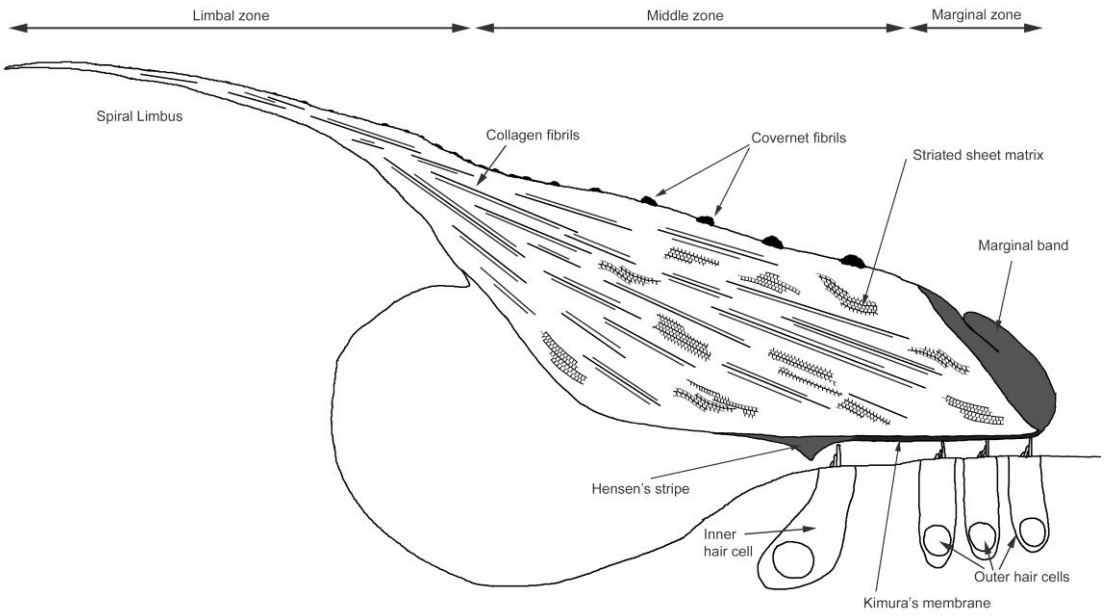

Figure 1.4. Organ of Corti and tectorial membrane structure (provided by R. Goodyear).

1.4.2. Development of the tectorial membrane

The first appearance of the TM in the mouse is observed by electron microscopy at embryonic day 16 (E16) as an amorphous substance, known as the primordial TM, over the greater epithelial ridge (GER) (Fig.1.5, a) (Lim and Rueda, 1992). As the primordial TM develops, it extends and thickens to form the major TM by E18 (Lim, 1987). The major TM covers the surface of the GER including the developing IHCs. A structure known as the minor TM is first observed by E19 (Lim and Rueda, 1992) and covers the lesser epithelial ridge and developing OHCs (Fig.1.5, b). At birth the minor TM is recognised as a covering sheet that attaches to the Hensen's cells, the supporting cells behind the outermost row of the OHCs, and extends to the major TM (Lim and Rueda,

1992; Rueda et al., 1996). A loose subtectorial meshwork connects the supporting cells with the undersurface of the minor TM (Fig.1.5, c).

Between the fifth and sixth postnatal days (P5 and P6) the GER recedes, forming the inner spiral sulcus (Rueda et al., 1996). During the next week of development, the major TM and minor TM fuse to form the tectorial membrane properly (Fig.1.5, c). This process is guided by marginal pillars, interim structures that exist between P6 and P14 on the apical surface of the third row of Deiter's cells, on the lateral edge of the organ of Corti (Rueda et al., 1996). As a result of the maturation of the organ of Corti the IHCs move inwards and their hair bundles become detached from the TM whilst the OHCs hair bundles remain imbedded in the TM (Rueda et al., 1996).

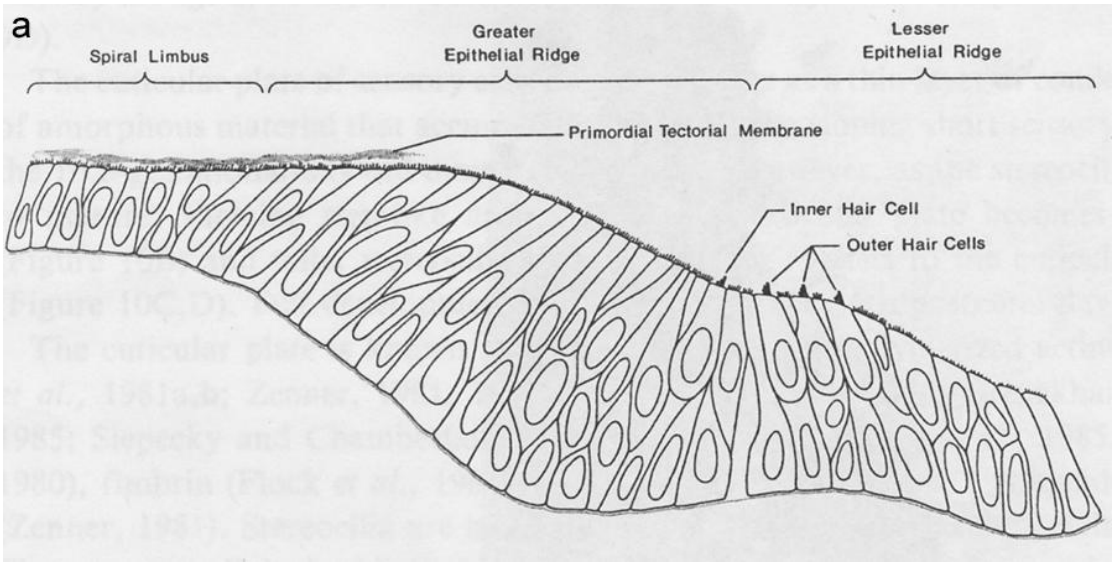

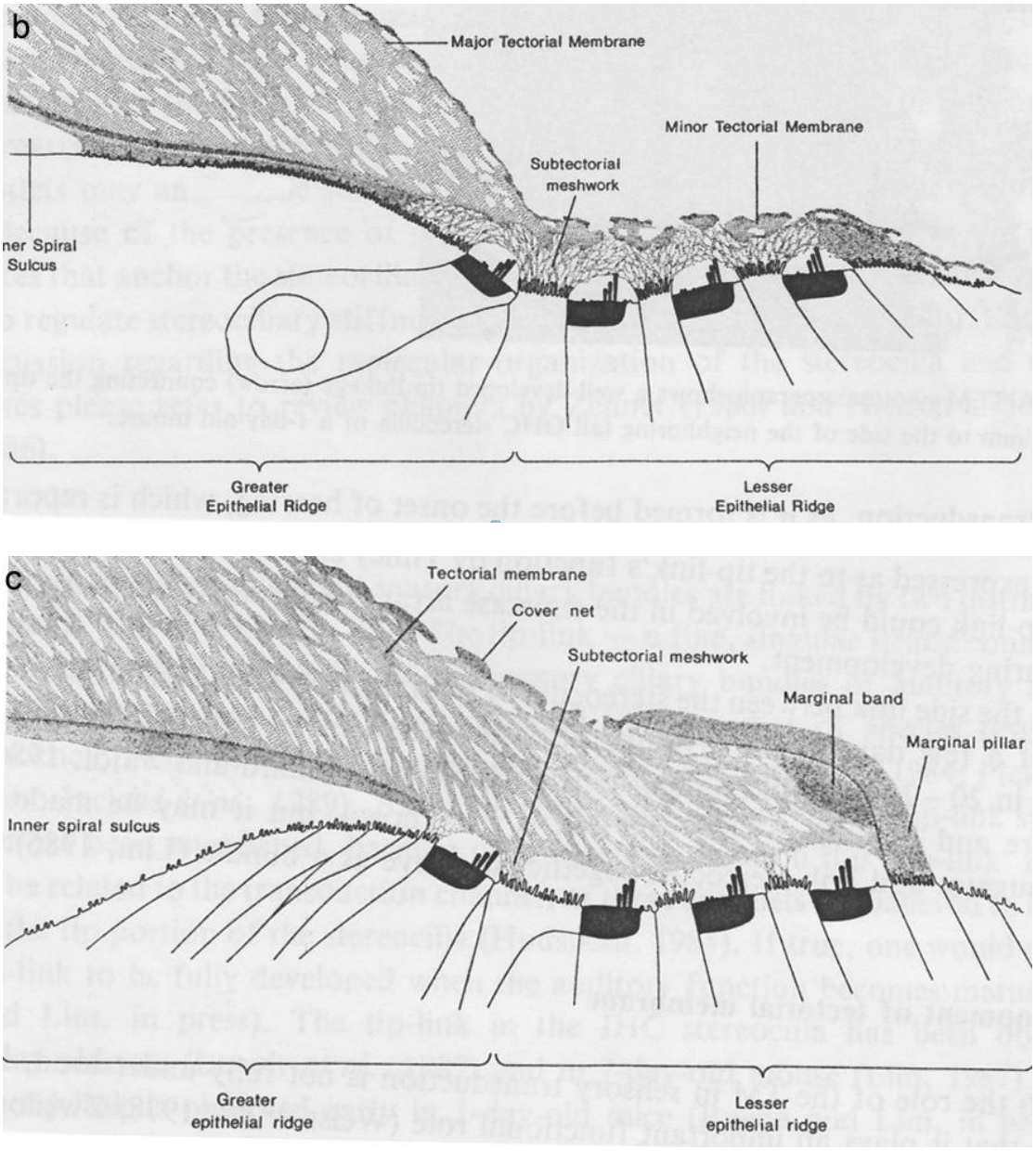

Figure 1.5. Schematic representations of the development of the tectorial membrane. A - the primordial TM formation, b - the major TM and minor TM formation, c - fusion of the major TM and minor TM. Modified from Lim and Rueda, 1992.

1.4.3. Function of the tectorial membrane

The function of the TM is yet to be fully elucidated. However, the fact that mutations in its proteins lead to deafness underlines the importance of the TM in hearing. Mutations in the gene encoding collagen XI cause non-progressive autosomal dominant non-syndromic hearing loss (ADNSHL) across the middle frequencies in American and

Dutch families (McGuirt et al., 1999). A moderate autosomal recessive non-syndromic hearing loss (ARNSHL) is described for subjects with mutations in the otogelin gene *OTOG* (Schraders et al., 2012) and the otogelin-like gene *OTOGL* (Yariz et al., 2012). Missense mutation in *Ceacam16* gene leads to progressive ADNSHL with a late onset in an American family (Zheng et al., 2011). Mutations in *Tecta* gene are the most common reason of ADNSHL. They can, however, also lead to ARNSHL (Hildebrand et al., 2011).

Data on $Tecta^{\Delta ENT/\Delta ENT}$ mutant mice with a targeted deletion in *Tecta* gene indicate that the TM is a resonant structure that provides an inertial mass against which the OHCs react at the CF of the BM (Legan et al., 2000). The TM allows the OHCs to provide feedback to the BM with optimal gain and at the appropriate time in the BM motion cycle (Legan et al., 2000). It also plays an important role in activating IHCs by complex fluid movements in the subtectorial space that excite the hair bundles at the CF (Legan et al., 2005). As the BM, the TM is more narrow and stiff at its base is more wide and floppy at its apex (Freberg, 2009). It was shown that the TM is not a mechanically stiff structure, but possesses visco-elasticity and thus can support travelling waves (Abnet and Freeman, 2000). This travelling wave can stimulate hair cells and couple with the BM travelling wave to affect cochlear sensitivity and tuning (Ghaffari et al., 2007).

1.5. The components of the striated-sheet matrix of the tectorial membrane

1.5.1. Tectorins

1.5.1.1. Tecta and Tectb

Tecta is a large modular glycoprotein of about 240 kDa with 33 potential N-glycosylation sites (Legan et al, 1997). It has an entactin domain at its N-terminus, which is akin to the G1 domain of the basement membrane glycoprotein entactin, a central zonadhesin-like (ZA) domain which includes three full and two partial von Willebrand factor type C (vWFC V0) or D repeats (vWFD V1, V2, V3 and V4), a sole zona pellucida (ZP) domain located at the C-terminal region and three trypsin inhibitor like cysteine rich domains (TIL1, 2, 3) (Fig.1.6) (Hildebrand et al., 2011). Tectb is a much smaller glycoprotein, ~36 kDa, with 4 potential N-glycosylation sites (Legan et al., 1997). It contains a single ZP-domain (Fig.1.6). Both tectorins have a signal sequence for transit into the endoplasmic reticulum located at the N-terminus of the protein.

Sequence data indicates that tectorins contain the glycosylphosphatidylinositol-anchor (GPI-anchor) located downstream of a tetrabasic furin-like cleavage site (Fig.1.6). The GPI-anchor is thought to target tectorins to the apical surface of the cochlear epithelium, where they can be released into the extracellular space by specific endoproteases (Legan et al., 1997).

When run on a SDS-PAGE (sodium dodecyl sulphate polyacrylamide gel electrophoresis) gel under reducing conditions, native tectorins of the TM resolve as three broad bands: high, medium and low molecular mass (HMM, MMM and LMM)

tectorins of corresponding masses ~173, ~60 and ~45 kDa (Richardson et al., 1987). HMM, MMM and LMM tectorin products are mainly derived from proteolytic processing of the Tecta molecule (Killick and Richardson, 1997; Legan et al., 1997). However, the LMM tectorin fraction is also partly represented by Tectb (Legan et al., 1997). Fig.1.7 indicates the possible cleavage pattern of Tecta protein. The predicted polypeptides generated after processing would have masses of ~34 (LMM), ~147 (HMM) and ~47 kDa (MMM) (Legan et al., 1997). The difference between predicted masses and masses observed on SDS-PAGE gels under reducing conditions is likely to be due to glycosylation, and the broad nature of the bands due to glycosylation heterogeneity.

Transient expression of tectorin-encoding plasmids in CL4 cells showed that tectorins are effectively targeted to the cell apical surface (Witteveen, 2008). However, when CL4 cells are transiently transfected with plasmids encoding tectorins with deleted GPI-anchors, both tectorins are retained within the cell (Witteveen, 2008). Cells, transfected with full-length tectorin DNA, but treated with tunicamycin, an inhibitor of protein N-glycosylation, also accumulate tectorins in the cytoplasm (Witteveen, 2008). These data indicate that both the GPI-anchor and the correct N-glycosylation are required for the apical targeting of the tectorins (Witteveen, 2008).

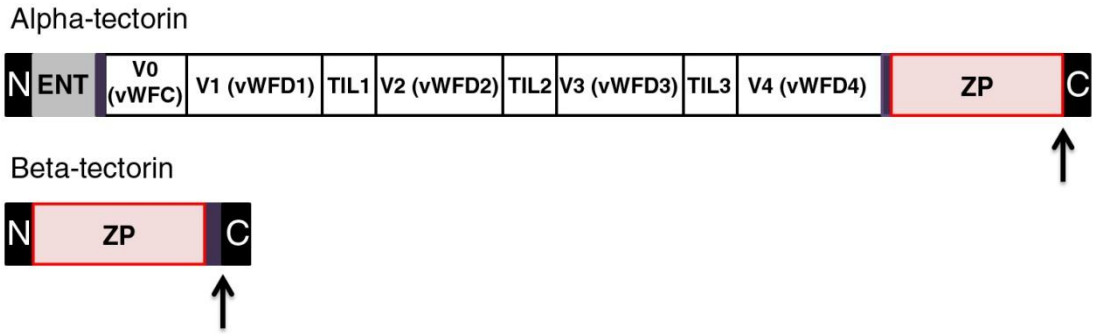

Figure 1.6. Schematic structure of Tecta and Tectb proteins. The N-terminal signal sequence and the C-terminal characteristic of GPI-anchored proteins are shown as black bars. The endoproteinase cleavage sites in Tecta and Tectb are labelled by arrows. ENT is the entactin domain. V0 (vWFC) is a partial von Willebrand factor C domain; V1, V2, V3 and V4 are von Willebrand factor D domains where V4 is a partial domain (Xia et al., 2010). TIL 1, 2 and 3 stand for Trypsin Inhibitor Like cysteine rich domain. ZP - zona pellucida domain, shown as a red rectangle. Regions with no significant homology to other proteins are depicted as dark violet bars. Modified from Hildebrand et al., 2011 and Goodyear and Richardson, 2002.

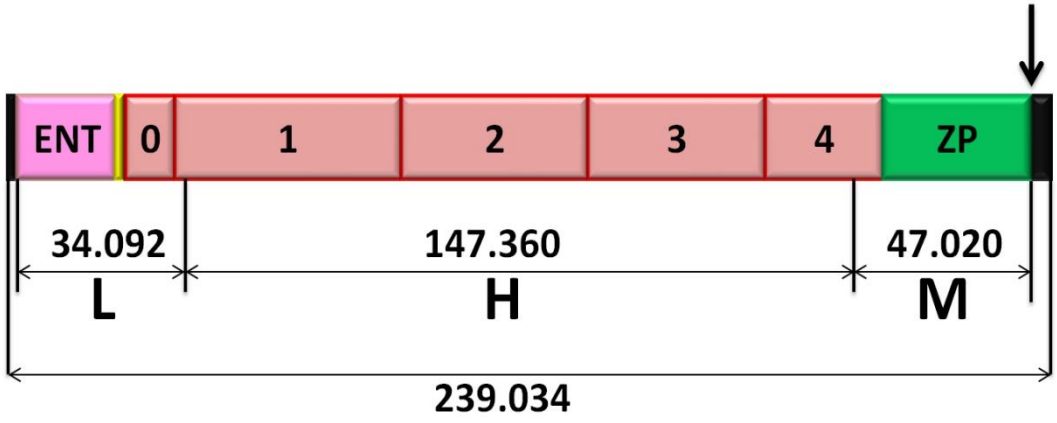

Figure 1.7. Tecta cleavage sites that might result in HMM, MMM and LMM Tecta suggested by N-terminal sequence obtained by Edman degradation. The predicted masses of polypeptides are shown above the arrows (Legan et al., 1997).

The ZP domain found in both tectorins is a motif of ~260 amino acids with 8 conservative cysteine residues involved in forming intrachain disulfide bonds (Bork and Sander, 1992). The ZP domain is a common sequence of various extracellular proteins

that are able to form filaments or matrices (Jovine et al., 2002). It is considered to be an element that enables proteins to polymerise (Jovine et al., 2002). The presence of a ZP domain in both Tecta and Tectb suggests that tectorins may either self-assemble as homomeric filaments or form heteromeric filaments via interactions between their respective ZP domains (Jovine et al., 2005; Legan et al., 1997).

Alternative interactions between Tecta and Tectb might occur via the Tecta ZA domain (Legan et al., 1997). This domain contains vWFC and vWFD subunits and is highly homologous to the sperm transmembrane protein zonadhesin (ZAN) which is responsible for sperm - zona pellucida binding (Lea et al., 2001). Even the order of vWF repeats in Tecta protein is the same as in the ZAN molecule. Sperm-egg binding is mediated by zona pellucida glycoproteins of an oocyte. The similarity with the sperm-egg adhesion system suggests that tectorins might interact in a similar way, with the ZA domain of Tecta interacting with ZP domains of Tectb and/or other Tecta molecules (Legan et al., 1997).

The presence of vicinal cysteines in vWFD subunits of Tecta might provide an alternative model of tectorin interactions. The vicinal cysteines are thought to have protein disulphide isomerase activity which enables them to form a disulphide bond between their side chains (Carugo et al., 2003). It is then possible that von Willebrand factors which contain D repeats form multimers due to disulfide bond formation between the vicinal cysteine residues. Thus Tecta might form homomeric filaments via its ZA domain and interact with Tectb via its ZP domain. There is, however, no evidence of Tecta multimers in the TM (Legan et al., 1997).

The data on the Tectb knock-out mouse model (Russell et al., 2007) suggests a possible role of Tectb protein in striated-sheet matrix organisation. Striated-sheet matrix is

absent in these mice. Tecta protein is, however, able to form disorganised filaments within the TM body, suggesting that Tectb might act as a crosslinker between Tecta filaments.

1.5.1.2. Tectorin expression pattern and timeline

In situ hybridisation experiments reveal Tecta and Tectb mRNAs are expressed in the basal end of the developing mouse cochlea at E12.5 (Rau et al., 1999). The patch of developing epithelial cells expressing Tectb mRNA is smaller than the area expressing Tecta mRNA (Rau et al., 1999). At E14.5 tectorin mRNA expression spreads into all turns of the cochlear duct (Rau et al., 1999). The expression of tectorin mRNA in the basal end of the developing mouse cochlea, thus, foreshadows the differentiation of sensory hair cells which starts at E14.5 with inner hair cells (Munnamalai et al., 2012). The patterns of Tecta and Tectb expression visible from E14.5 develop from the base of the cochlea to the apex and include two bands of expression for Tecta and three narrower bands of expression for Tectb (Fig. 1.8) (Rau et al., 1999). Tecta mRNA expression is detected throughout the GER and in the inner phalangeal cells around IHCs. A narrow zone of Tecta expression is also found in the first two rows of Hensen's cells adjacent to the third row of Deiter's cells (Fig.1.8). Tectb expression is seen in a narrow region of the GER alongside the IHCs, in the inner and outer pillar cells and in the third row of the Deiter's cells. Tectb is also detected in the first and second rows of Deiter's cells in the apex of the cochlea at early postnatal stages of development (Rau et al., 1999).

By P8, Tecta expression at the base of the cochlea stops and the levels of Tectb expression are reduced. Expression of both tectorin mRNAs almost entirely stops by

P15 (Rau et al., 1999). Tectorin proteins, however, are stable and survive throughout the life of the organism.

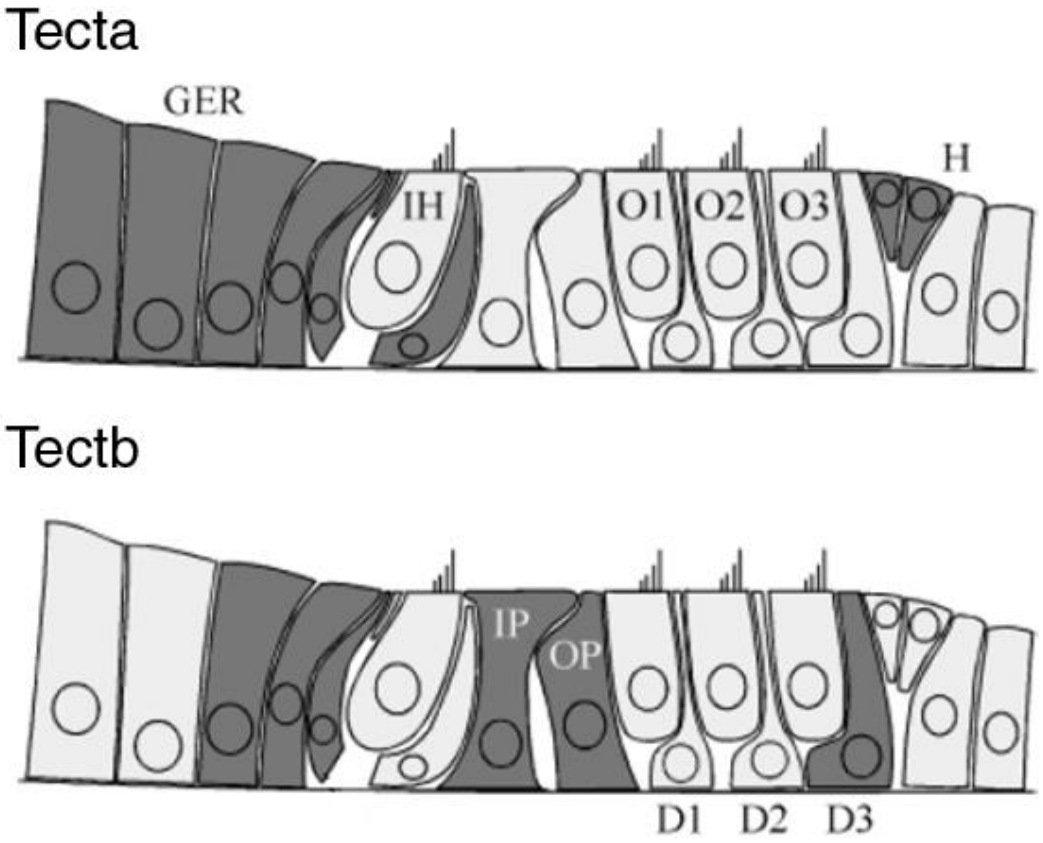

Figure 1.8. Tecta and Tectb protein expression patterns, for explanations refer to the text. GER – greater epithelial ridge, IH – inner hair cell, O1, O2, and O3 – three rows of outer hair cells, IP – inner pillar cell, OP – outer pillar cell, D1, D2 and D3 – three rows of Deiter's cells. Cells expressing tectorin mRNAs are shaded dark grey. Modified from Rau et al., 1999.

1.5.1.3. Deafness-causing mutations in Tecta

The *Tecta* gene, which encodes Tecta protein, contains 23 exons (Sagong et al., 2010). It was mapped to mouse chromosome 9 (Hughes et al., 1998) and to human chromosome 11q22 - q24 (Hughes et al., 1998; Verhoeven et al., 1997; Verhoeven et al., 1998). Mutations in *Tecta* gene have been shown to be responsible for sensorineural nonsyndromic hearing loss. They can be inherited either in an autosomal dominant

fashion causing ADNSHL or in an autosomal recessive manner resulting in ARNSHL (Alasti et al., 2008; Meyer et al., 2007). Missense mutations in Tecta produce ADNSHL with a variety of phenotypes (Moreno-Pelayo et al., 2001; Sagong et al., 2010; Verhoeven et al., 1998). ARNSHL, in contrast, is caused by truncating mutations (nonsense, frameshift, splice site) and are characterised by a common phenotype - moderate to profound prelingual deafness with mid-frequencies most affected (Meyer et al., 2007; Naz et al., 2003). However, a spontaneous missense mutation in the mouse *Tecta* gene which is recessive has also been described (Moreno-Pelayo et al., 2008).

As mentioned above, dominant missense mutations in Tecta result in different phenotypes depending on the domain and residue affected (Alloisio et al., 1999; Iwasaki et al., 2002; Meyer et al., 2007; Moreno-Pelayo et al., 2001; Plantinga et al., 2006; Sagong et al., 2010; Verhoeven et al., 1998) enabling potential genotype-phenotype correlations to be studied (Hildebrand et al., 2011). Some of these mutations are represented on Fig.1.9 along with the domain structure of Tecta.

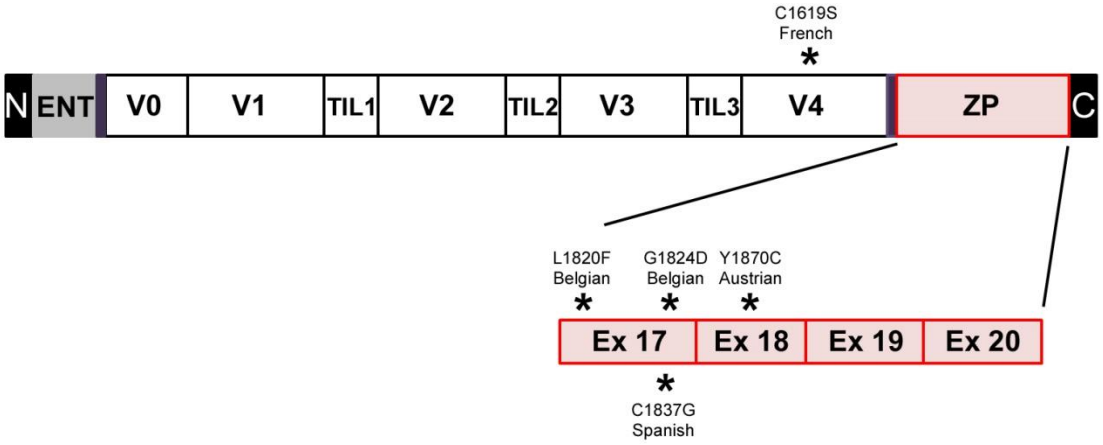

Figure 1.9. Tecta domains and the location of different deafness-causing missense mutations indicated by asterisks. V0-V4 – vWFC and vWFD repeats; TIL1, 2 and 3 - trypsin inhibitor like cysteine rich domains 1, 2 and 3; Ex 17-Ex 20 - exons encoding ZP domain. Modified from Moreno-Pelayo et al., 2001 and Hildebrand et al., 2011.

A dominant missense mutation found in a French family is located in the Tecta ZA domain (Fig.1.9) with a cysteine in the vWfD4 subdomain replaced by a serine (C1619S) (Alloisio et al., 1999). A cysteine to glycine substitution (C1837G) in the ZP domain of Tecta (Fig.1.9) results in ADNSHL in a Spanish family (Moreno-Pelayo et al., 2001). In a Belgian family the deafness phenotype is possibly caused by one of the two amino acid substitutions in the ZP domain (Fig.1.9) - leucine 1820 is replaced by phenylalanine (L1820F) and glycine 1824 is replaced by aspartic acid (G1824D) (Verhoeven et al., 1998). A mutation found in an Austrian family is another ZP domain mutation (Fig.1.9) with the substitution of a tyrosine for cysteine (Y1870C) (Verhoeven et al., 1998). The Belgian and the Spanish mutations are located in exon 17 of *Tecta*, the Austrian mutation maps to exon 18.

Four transgenic mice with dominant missense mutations in *Tecta* corresponding to the deafness-causing mutations in the French, Belgian, Spanish and Austrian families have been generated to understand how these mutations affect the assembly and function of the TM matrix (Coates, 2009; Legan et al., 2005).

The phenotypes described for mice heterozygous for the Spanish and Belgian mutations were comparable. In both mouse models, striated-sheet matrix was severely disrupted but only in the sulcal region, the marginal band was reduced and displaced medially and the covernet consisted of convoluted fibrils forming a mesh-like pattern that did not merge with the marginal band (Coates, 2009). In transgenic mice heterozygous for the Austrian mutation the limbal zone of the TM was reduced in thickness and the Kimura's membrane was detached from the main body of the TM. The marginal band and the Hensen's stripe were missing (Legan et al., 2005). The sulcal region of the TM lacked striated-sheet matrix and contained disorganised collagen fibrils (Legan et al., 2005). It

is likely that mutations in the ZP domain of Tecta disturb its interactions with other TM proteins and prevent tectorin assembly into striated-sheet matrix (Iwasaki et al., 2002). The phenotype of mice heterozygous for the French mutation provides a different model of protein-protein interactions within the TM with a much less disrupted striated-sheet matrix. The covernet is hardly distinguishable but still consists of the rod-like fibrils albeit of much finer diameter whilst the marginal band is fragmented (Coates, 2009). It is possible that a vicinal cysteine substitution by serine in the vWfD4 repeat changes Tecta assembly and cross-linking by affecting disulphide bond formation within the Tecta polypeptide (Iwasaki et al., 2002; Pfister et al., 2004).

Two missense mutations affecting the cysteine compliment within the Tecta ZP domain were chosen to study protein-protein interactions and filament assembly in this research: the Spanish mutation where a cysteine is replaced and the Austrian mutation where a new cysteine is introduced.

1.5.2. Ceacam16

1.5.2.1. General information about Ceacam16 protein

The carcinoembrionic antigen-related cell adhesion molecule (Ceacam) gene family (Kuespert et al., 2006) which includes the *Ceacam16* gene belongs to the immunoglobulin superfamily of cell adhesion molecules (IgCAM) (Hammarstrom, 1999; Kuespert et al., 2006). Ceacam proteins, which have so far only been discovered in mammals (Beauchemin et al., 1999), are characterised by the presence of at least one immunoglobulin (Ig)-like domain, and their genes are clustered on human chromosome 19 (Hammarstrom, 1999; Kuespert et al., 2006). The Ig-like domain consists of 85-110 amino acids (Kuespert et al., 2006) and has a characteristic structure which is referred to as an Ig fold (Barclay, 1999) or a “Greek key” (Vaughn and Bjorkman, 1996). The Ig

fold is made of seven to nine antiparallel β-strands arranged in two sheets (Barclay, 1999; Brooks, 2009; Halaby et al., 1999). On the basis of structural and sequence variations, the Ig fold domains have been subdivided into three groups: Ig variable (IgV) domain, Ig constant (IgC) type 1 domain and IgC type 2 domain (Kuespert et al., 2006; Vaughn and Bjorkman, 1996). IgV-like domain contains nine β-strands which are more variable in sequence (Brooks, 2009). The smaller IgC-like domain consists of seven β-strands, and the two sheets they form are connected via highly conservative disulfide bonds. There is some minor variation in β-strand organisation between IgC1 and IgC2-like domains (Vaughn and Bjorkman, 1996). The functions of Ceacam proteins include cell-cell interactions, tissue homeostasis, angiogenesis and tumorigenesis and, in addition, they can act as pathogen receptors (Benchimol et al., 1989; Hammarstrom, 1999; Hauck et al., 2006; Horst et al., 2006; Kuespert et al., 2006).

Ceacam16 is a secreted glycoprotein with a signal peptide at its NH_2-terminus and a proteolytic cleavage site between the 23^{rd} and 24^{th} amino acids. There are no predicted transmembrane domains or a GPI-anchor (Zheng et al., 2011). It consists of two IgV-like, or N, domains flanking two IgC2-like domains in the middle (Fig.1.10) (Zebhauser et al., 2005; Zheng et al., 2011). Ceacam16 protein has 7 cysteines, 7 potential N-glycosylation sites (Fig.1.10) and there is only one known splice variant (Zheng et al., 2011). Transient transfection of HEK293 cells with a construct encoding Ceacam16 and a subsequent western blotting analysis suggests that Ceacam16 is secreted in the form of disulfide cross-linked dimers and tetramers (Zheng et al., 2011).

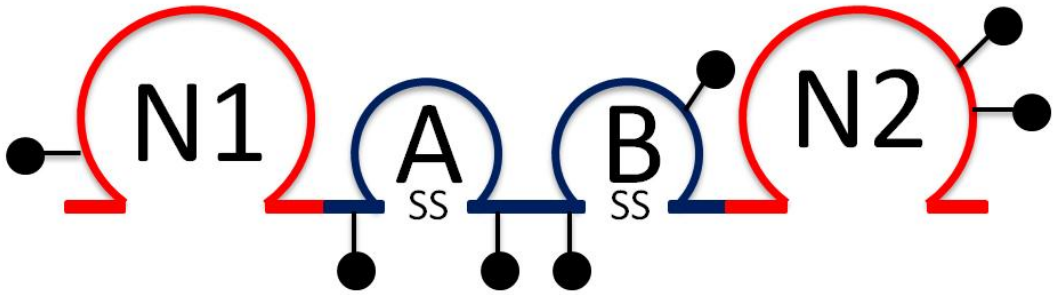

Figure 1.10. Schematic representation of the domain structure of Ceacam16 protein. N1 is an NH_2-terminal IgV-like domain, N2 is an COOH-terminal IgV-like domain. A and B are IgC2-like domains of subtype A and B. SS depicts highly conservative disulfide bridges in the IgC2-like domains. Pins represent potential N-glycosylation sites. Adapted from Zebhauser et al., 2005.

1.5.2.2. Ceacam16 in the inner ear

In the mouse cochlea, expression of *Ceacam16* mRNA is detected from E17 and lasts at least until P42 (Zheng et al., 2011). *In situ* hybridisation experiments suggested that Ceacam16 is expressed in OHCs, but not in IHCs or supporting cells (Zheng et al., 2011). Confocal microscopy suggested that the Ceacam16 protein expression located to the tips of OHC stereocilia. In addition, a strong anti-Ceacam16 labelling was detected in the main body of the TM, indicating that Ceacam16 is a component of this region (Zheng et al., 2011).

Finally, co-immunoprecipitation studies suggested that Ceacam16 protein might bind to Tecta in the TM and it was proposed that it would act as a component of attachment crowns linking the tips of OHC stereocilia to the TM (Zheng et al., 2011).

1.5.2.3. *Ceacam16* gene and human deafness DFNA4

The *Ceacam16* gene is highly conserved among mice, rats and humans (Zebhauser et al., 2005). In humans, it locates to chromosome 19q13.31 (Zheng et al., 2011). DFNA4 hearing loss detected in an American family maps to the same locus (Chen et al., 1995)

suggesting *Ceacam16* as a candidate gene for this type of deafness. Individuals affected by DFNA4 develop a severe-to-profound hearing loss across all frequencies with an onset in early adolescence and a deficit of up to 50 dB in adulthood (Chen et al., 1995). More recent studies have shown that DFNA4 hearing impairment is caused by a T140P (threonine to proline replacement) mutation in the *Ceacam16* gene which disrupts a highly conserved N-glycosylation site (Zheng et al., 2011). This might alter protein folding and, therefore, cause its degradation or instability (Zheng et al., 2011).

1.6. Aims of the thesis

Little is known about how the striated-sheet matrix develops. It is unclear how Tecta and Tectb proteins are secreted, processed and assembled and how deafness-causing mutations in Tecta could interrupt these processes. The recently described Ceacam16 protein might also be involved in the striated-sheet matrix assembly and could maintain its stability over the life time (Zheng et al., 2011). These problems set the aims of this thesis which can be formulated as follows:

1. The first aim is to create an *in vitro* model for studying the assembly of the TM matrix with an ultimate purpose to investigate how it is disrupted by the known Tecta deafness mutations.

2. The second aim of this study is to elucidate the role of Ceacam16 protein in normal hearing by creating a *Ceacam16* functional null mouse model and describing its phenotype.

CHAPTER 2

Materials and Methods

2.1. Gene cloning techniques

The process of gene cloning is used to create recombinant DNA molecules containing genes of interest and to achieve their replication within the host.

2.1.1. Polymerase chain reaction

Polymerase chain reaction (PCR) is used to amplify the DNA sequence of interest.

2.1.1.1. Amplification of PCR products for cloning

Pfu turbo DNA polymerase (Stratagene), an enzyme with a "proof reading" activity, was used to amplify inserts for ligation into plasmid constructs. A typical PCR reaction mixture was set up in a volume of 25 µl, its content is presented in a Table 2.1 (Insert amplification column). A standard PCR program used a heated lid and included following steps:

1. initial denaturation at 94^{o}C for 2 min
2. denaturation at 94^{o}C for 15 sec
3. annealing at 55^{o}C for 15 sec
4. extension at 72^{o}C, 1 min per 1 kb
5. final extension at 72^{o}C for 5 min

Steps 2 to 4 were usually repeated for 25 times. However, the annealing temperature and the number of cycles were varied to increase the yield of the product.

Amplified inserts were then gel purified to remove template and unincorporated dNTPs and primers (2.1.5).

To join two PCR products, A and B, in one PCR reaction, both were PCR amplified and gel purified (2.1.5). Both PCR products (100 ng each) were added to a Pfu reaction mix and amplified with a forward primer for A and a reverse primer for B as described above. Joined product was gel purified (2.1.5).

2.1.1.2. Mutagenic PCR

Stratagene QuickChange site-directed mutagenesis method was used to introduce point mutations into vectors. The technique utilises PCR with the Pfu turbo DNA polymerase (Agilent) and requires a special primer design. Forward and reverse mutagenic primers were made as complementary to each other oligonucleotides with the desired mutation flanked by 10-15 bases of correct sequence on each side. A PCR mixture set up in a volume of 50 µl included components as in the Table 2.1 (Mutagenic PCR column):

1. initial denaturation at 94^{o}C for 2 min
2. denaturation at 94^{o}C for 15 sec
3. annealing at 50^{o}C for 15 sec
4. extension at 68^{o}C, 1 kb in one min
5. final extension at 68^{o}C for 5 min

Steps 2 to 4 were repeated for 12 times. Although the annealing temperature could be varied, the number of cycles was kept quite low to minimise the chance of DNA polymerase errors.

To digest the parental DNA template a DpnI restriction enzyme that only cleaves at methylated sites was used. 2 µl of DpnI were added to the PCR reaction. It was

incubated at 37^{o}C for 2 hours and the desired product was gel purified (2.1.5) and transformed into XL1 Blue competent cells (Stratagene) (2.1.8).

Reagents	Insert amplification	Mutagenic PCR
10x cloned Pfu reaction buffer (Stratagene)	2.5 µl	5 µl
10 mM deoxynucleotide triphosphates (dNTPs) (Promega)	0.5 µl	1 µl
25 pmol/µl forward primer	0.5 µl	1 µl
25 pmol/µl reverse primer	0.5 µl	1 µl
Template	100 ng	50 ng
Pfu turbo DNA polymerase (Agilent)	1.25 units	2.5 units
Sterile H_2O	To 25 µl	To 50 µl

Table 2.1. PCR mixture content for insert amplification and mutagenic PCR.

2.1.1.3. AccuPrime PCR

AccuPrime Taq DNA polymerase High Fidelity (Invitrogen) was used to amplify large DNA fragments used to create targeting vectors and in case when Pfu polymerase failed to produce a satisfactory product. The following components were used in an AccuPrime reaction mixture:

Reagents	Amount used
10x AccuPrime PCR buffer I (Invitrogen)	5 µl
25 pmol/µl forward primer	1 µl

25 pmol/µl reverse primer	1 µl
Template	10 ng
AccuPrime Taq High Fidelity	0.2 µl
Sterile H_2O	To 50 µl

Table 2.2. PCR mixture content for AccuPrime PCR.

The PCR program used was similar to the mutagenic PCR program. The number of cycles used was varied between 25 and 35. The amplification product was analysed by TBE agarose gel electrophoresis (1.4) or gel purified if used for cloning (1.5).

2.1.1.4. PCR for In-Fusion cloning

DNA fragments for In-Fusion cloning (Clontech) were amplified with either Pfu turbo DNA polymerase (Stratagene) or AccuPrime Taq DNA polymerase High Fidelity (Invitrogen) as described in sections 2.1.1.1 and 2.1.1.3. The In-Fusion cloning technique allows joining of DNA fragments which have a 15-base overlap (Fig.2.1). This overlap is introduced by PCR with appropriately designed primers. A typical primer for in-fusion cloning has a 15-base overlap at its 5' end with the end of the DNA fragment it was meant to be joined. The 3' end is gene-specific to the target fragment sequence.

The PCR products were digested with DpnI and separated on a Tris-borate EDTA (TBE) agarose gel. The DNA was gel purified (2.1.5) and used in In-fusion cloning reactions (2.1.7).

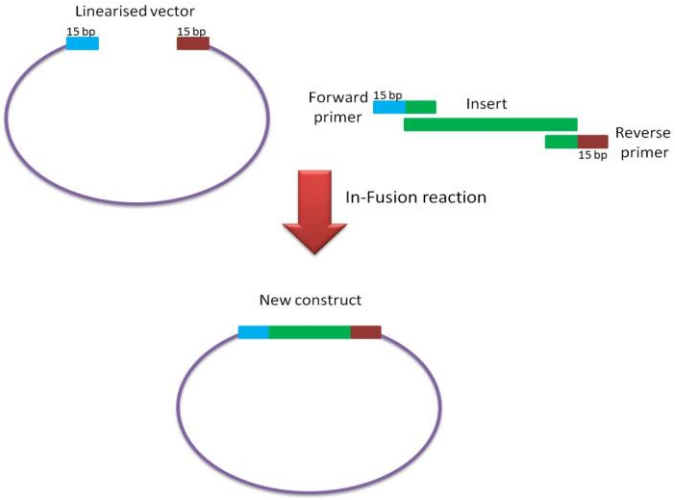

Figure 2.1. Directional cloning of a DNA fragment into a linearised vector. DNA fragment of interest was amplified with specially designed primers which contain 15 bp overlaps with the ends of the linearised vector.

2.1.1.5. PCR screening of bacterial colonies

PCR screening was used to determine the presence of the desired insert in transformed bacterial colonies. Single colonies were picked with autoclaved toothpicks, transferred to an LB agar master plate containing the appropriate antibiotic, and then dipped into a well of the PCR plate (BIOplastics) containing 25 µl of the PCR reaction mix. PCR mixture for one well included 2.5 µl of 10x NH4 reaction buffer (Bioline), 0.75 µl of 50 mM $MgCl_2$ (Bioline), 0.5 µl of 10 mM dNTPs (Promega), 0.5 µl of forward and the same amount of reverse primers (both primers at working concentration 25 pmol/µl), 20.15 µl of sterile H_2O and 0.1 µl of BIOTAQ DNA polymerase (Bioline). 2 drops of mineral oil were added to each well of the plate to prevent evaporation of the mixture during cycling. A plate was then placed in the thermocycler. A typical PCR program has an initial denaturation at 94^{o}C for 2 min followed by 25 cycles of denaturation at 94^{o}C 15 sec, annealing at 52^{o}C for 15 sec and extension at 72^{o}C 1 min for 1 kb. The annealing temperature and number of cycles, however, could be changed in some cases depending on primer sequences and yield of a product. A final extension at 72^{o}C lasted

for 5 min. Heated lid was used during cycling. Samples were then cooled down to 4^{o}C, separated on 0.7 % TBE agarose gels, stained with ethidium bromide and photographed under UV light (2.1.4).

The master plate was incubated on 37^{o}C overnight. Colonies positive by PCR were inoculated into 5 ml of LB medium with the appropriate antibiotic to obtain an overnight culture for plasmid minipreparation.

2.1.1.6. PCR clean-up

The NucleoSpin Extract II (Marchery-Nagel) was used to remove traces of primers, salts, enzymes and nucleotides from a PCR product. One volume of sample was mixed with two volumes of binding buffer (buffer NT). If the sample was less than 100 µl it was first made to 100 µl with buffer NT.

The mixture was loaded onto a NucleoSpin Extract II column, placed into a collection tube and centrifuged for one minute at 13,000 rpm. The flow-through was discarded and the column was washed with 700 µl of buffer NT3 by centrifugation for 1 min at 13,000 rpm. The flow-through was discarded and the column was centrifuged for 2 min at 13,000 rpm to remove the residual buffer NT3. DNA was eluted in 20-50 µl of elution buffer (buffer NE). To collect the eluate the column was incubated at room temperature for 1 min and then centrifuged for 1 min at 13,000 rpm.

2.1.2. DNA digestion with restriction enzymes

All digestion reactions were performed with NEB restriction endonucleases (New England BioLabs Inc.) in 50 µl of reaction mixture for PCR products and in 20 µl for vectors. DNA digests with two enzymes (double digests) were performed simultaneously, in one reaction tube, with a NEBuffer (New England BioLabs Inc.) in which both enzymes had the most activity. Ten units of an appropriate restriction

endonuclease were used per 1 µg of DNA. The typical digestion reaction mixture contained following components:

Reagents	20 µl reaction volume	50 µl reaction volume
Appropriate 10x NEBuffer (supplied by NEB with enzymes)	2 µl	5 µl
10x bovine serum albumin (BSA) if required (NEB)	2 µl	5 µl
Restriction enzyme (NEB)	0.5 µl – 1 µl	0.5 µl – 1 µl
DNA	0.5 µg – 1 µg	0.5 µg – 1 µg
Sterile H_2O	to 20 µl	to 50 µl

Table 2.3. Restriction endonuclease digestion reaction mixtures.

Digestion reactions were set up in microcentrifuge tubes, briefly centrifuged at 13,000 rpm and incubated on 37^{o}C for 1 hour.

2.1.3. Dephosphorylation

Vector re-circularisation during ligation reactions (2.1.6) was prevented by dephosphorylation of vector DNA with alkaline phosphatase to remove 5' phosphates from both ends of the linearised vector DNA.

One tenth of a volume of 10x Antarctic phosphatase reaction buffer (NEB) and 1 µl (5 units) of Antarctic phosphatase were added to the tube with cut DNA after the restriction endonuclease reaction was finished. The tube was then incubated at 37^{o}C for 15 min. Afterwards another 5 units of enzyme were added to the mixture and it was

incubated at 37^{o}C for additional 15 min. The phosphatase was heat inactivated at 65^{o}C for 5 min. Dephosphorylated vector DNA was then gel purified (2.1.5).

2.1.4. DNA gel electrophoresis

DNA was separated on horizontal slab 0.7 % agarose, 1x TBE gel. 1x TBE, used as electrophoresis buffer, contained 89 mM Tris base, 88 mM orthoboric acid and 2 mM EDTA. Agarose (BioGene Ltd) was dissolved in 1x TBE buffer and melted in a microwave oven. DNA samples were mixed with 0.1 vols of 10x loading dye (50 % glycerol, 1 mM Tris-HCl, pH 8.0, 0.25 % w/v bromophenol blue and 1 mM EDTA). One or two lanes of either 100 bp or 1 kb (depending on DNA fragment analysed) DNA size marker were run adjacent to sample lanes. Electrophoresis was performed in 1x TBE buffer. DNA on small gels was separated at constant voltage 100 V for 30 min, on big gels - at 220 V for 30 min.

Gels were then incubated in 0.5 µg/ml ethidium bromide in H_2O for 30 min. Preparative gels were incubated for 40 min. DNA bands were visualised on a UV (ultraviolet) transilluminator. Analytical gels were photographed with a CCD camera coupled to a thermal printer. Preparative gels were visualised on a long wavelength UV transilluminator and DNA bands of interest were excised for purification.

2.1.5. DNA purification from TBE agarose gels

The NucleoSpin Extract II kit (Macherey-Nagel) was used to extract DNA separated on 1x TBE agarose gels as described in 2.1.4. The DNA fragment of interest was excised from the agarose gel with a clean scalpel. The gel slice was weighted and mixed with 2 volumes of binding buffer (buffer NT). The mixture was incubated at 50^{o}C for 10-15 min with intermittent vortexing until the agarose slice was fully dissolved. A NucleoSpin Extract II column was placed into 2 ml collection tube. The sample was

loaded on the column and centrifuged for 1 min at 13,000 rpm. The flow-through was discarded. The column was then washed with 700 µl of wash buffer (buffer NT3) with added ethanol. The sample was then centrifuged 1 min at 13,000 rpm and the flow-through was discarded. The column was centrifuged for 2 min at 13,000 rpm to remove the residual buffer NT3. The column was then placed into a clean microcentrifuge tube. Elution buffer (buffer NE) was added to the column, 20 µl for vectors and 50 µl for inserts. The column was incubated for 1 min at room temperature to increase the yield of DNA and then centrifuged for 1 min at 13,000 rpm to collect the eluate. Eluate (2 µl) was loaded onto an analytical 1x TBE agarose gel to confirm recovery of the desired band.

2.1.6. Ligation

Vector and insert digested with the one restriction enzyme on the 5' end and a different enzyme on the 3' end to generate compatible overhangs and gel purified were joined together in a ligation reaction. Vector and insert DNA were used in 1:3 molar ratio. In addition, a tube with a double concentration of insert was set up. Ligation was carried out in four reactions referred as no ligase (-L), with ligase (+L), insert and ligase (+I+L) and double amount of insert with the same amount of enzyme ($+I_1+L$). –L and +L reactions contained only vector without insert and were used as a control. A typical ligation mixture included:

Components	-L	+L	+I+L	($+I_1+L$
10x ligase buffer (NEB)	1 µl	1 µl	1 µl	1 µl
Sterile H_2O	8 µl	8 µl	4 µl	-
Linearised vector	1 µl	1 µl	1 µl	1 µl

Insert	-	-	4 µl	8 µl
T4 DNA ligase (NEB)	-	0.5 µl	0.5 µl	0.5 µl

Table 2.4. The composition of ligation reactions.

The reactions were incubated at 14^{o}C in a cold water bath overnight. Next day all four reactions were transformed into competent E. coli cells.

2.1.7. In-fusion cloning

The In-Fusion HD cloning kit (Clontech) was used for fast precise cloning of PCR products without using restriction enzymes and DNA ligase. PCR reactions for In-Fusion cloning were set up as described in 2.1.1.4. PCR products were digested with DpnI and gel purified to use in the In-Fusion cloning reaction. A typical In-Fusion cloning reaction was set up in a 10 µl volume and contained 50 ng of vector, an equimolar amount of insert and 2 µl of 5x In-Fusion HD enzyme premix (Clontech). Negative control mixtures were carried out without In-fusion HD enzyme premix and without insert. Both reactions were incubated at 50^{o}C for 15 minutes, placed on ice and transformed into competent bacterial cells (2.1.8).

2.1.8. Bacterial transformation

2.1.8.1. Bacterial culture medium

Lysogeny broth, or LB medium, created by Bertrani, is a nutrient-rich medium used for growing bacterial cultures. It was prepared by adding 10 g of tryptone (Oxoid), 5 g of yeast extract (Oxoid) and 10 g of NaCl (Fisher chemical) to 950 ml of water. The pH was adjusted to 7.0 with 1 N NaOH and the volume was then made to 1 L. LB was autoclaved in Boxer 200/25LE benchtop autoclave at 121^{o}C. The whole cycle including warming up and cooling down takes about two hours.

To make LB agar plates containing selective antibiotics, 15 g of bacto agar (BD) was added to 1 L of LB and the mixture was autoclaved as described above. Afterwards the bottle was cooled down to 47^{o}C in a water bath and the appropriate selective antibiotic was added (Table 2.5). The bottle was swirled to mix in the antibiotic and the agar was poured into 90 mm petri dishes.

Selective antibiotic	Concentration
Ampicillin	50 µg/ml
Kanamycin	25 µg/ml

Table 2.5. Selective antibiotics and their concentration.

Super-optimal broth with catabolite repression (SOC medium) is a modification of LB for increased plasmid transformation efficiency. To prepare SOC medium 20 g of tryptone, 5 g of yeast extract, 0.58 g of NaCl, 0.186g of KCl (Fisons) and 0.952 g of $MgCl_2$ (Fisher Scientific) were added to 800 ml of water. The solution was mixed and made up to 980 ml with water once all the components were dissolved. SOC medium was autoclaved as described above. Once it was cooled down, 20 ml of filter-sterilized 1 M glucose was added. SOC medium was then aliquoted into 15 ml tubes (Cellstar) and stored at room temperature.

2.1.8.2. Bacterial transformation

DNA (ligation reactions, in-fusion cloning, mutagenic PCR products and plasmid minipreps) was transformed into chemically competent XL1 Blue cells (Stratagene) following the manufacturer instructions.

One vial (250 µl) of XL1 Blue competent cells from -80^{o}C was thawed on ice. For the transformation of ligation reactions two vials of XL1 Blue competent cells were used.

When thawed, cells were gently mixed and 100 µl were aliquoted in pre-chilled falcon tubes. 1.7 µl of β-mercaptoethanol were added to each aliquot and the mixture was swirled. Cells were incubated on ice for 10 min and swirled every 2 min. Afterwards 2 µl of the DNA containing mixture were added to the cells. The tubes were swirled and left on ice for 30 min. Meanwhile, the water bath and SOC medium were preheated to 42^{o}C. The cells were then heat-pulsed in the 42^{o}C water bath for 45 sec and incubated on ice for 2 min. 900 µl of SOC medium were added to each falcon tube and they were incubated at 37^{o}C shaking at 250 rpm for one hour. Afterwards each transformation reaction was plated on a labelled LB agar plate with an appropriate antibiotic in aliquots of 200 µl, 100 µl and 50 µl. Plates were incubated at 37^{o}C overnight. On the next day colonies were screened by PCR or set up as overnight cultures in LB with an appropriate antibiotic (Table 2.5) for the plasmid minipreparation.

2.1.9. DNA preparation

2.1.9.1. Plasmid minipreparation

Overnight cultures were prepared by introducing single bacterial colonies into 50 ml tubes (Cellstar) containing 5 ml of sterile LB supplemented with the appropriate antibiotic (Table 2.5). Cultures were grown at 37^{o}C shaking at 250 rpm overnight. Plasmid DNA was prepared using NucleoSpin plasmid DNA purification kit (Macherey-Nagel). Bacterial cells were pelleted from 3 ml of cell suspension in a benchtop centrifuge (accuSpin Micro, Fisher Scientific) by sequential 1 min spins at 13,000 rpm in microcentrifuge tubes. The remaining culture (2 ml) was used for preparing glycerol stocks (2.1.9.4) and inoculating a culture for plasmid maxipreparation. The supernatant was discarded and cell pellets were re-suspended in 250 µl of resuspension buffer (buffer A1) by pipetting up and down. 250 µl of lysis buffer (buffer A2) were added to each tube. Tubes were gently inverted 6-8 times to mix

the contents and then incubated for 5 min at room temperature. 300 µl of neutralisation buffer (buffer A3) was added to each tube, the contents were mixed by inverting the tubes 6-8 times and clarified by the centrifugation for 5 min in a benchtop centrifuge at 13,000 rpm. The clear supernatant was then transferred to a NucleoSpin Plasmid column placed in the collection tube and centrifuged for 1 min at 13,000 rpm. The flow-through was discarded, and 600 µl of wash buffer (buffer A4) containing ethanol were added to the column. The spin column was then centrifuged for 1 min at 13,000 rpm and the flow-through was discarded. The spin column was centrifuged again for 2 min at 13,000 rpm to remove traces of the wash buffer. The NucleoSpin Plasmid column was then placed into a clean microcentrifuge tube and 50 µl of elution buffer (buffer AE) were added. The columns were incubated at room temperature for 5 min and the eluate was collected by centrifugation for 1 min at 13,000 rpm. Concentrations of the eluted plasmids were measured (2.1.9.3).

2.1.9.2. Plasmid maxipreparation

Plasmid maxipreparation was performed using NucleoBond Xtra Maxi kit (Macherey-Nagel). 250 ml of LB with the appropriate antibiotic (Table 2.5) were inoculated with 2-5 ml of a starter bacterial culture and grown overnight (12-16 hours) at 37^{o}C with shaking at 250 rpm. The cells were pelleted by centrifugation for 10 min at 4^{o}C using a Sorvall GSA rotor (Dupont) at 5000 rpm. The supernatant was discarded and the cell pellet was resuspended in 12 ml of resuspension buffer (buffer RES) plus RNase A in a concentration of 60 µg/ml by pipetting up and down. When no clumps were detected in the suspension, 12 ml of lysis buffer (buffer LYS) were added. The tube was gently inverted 5 times and incubated at room temperature for 5 min. Meanwhile, a NucleoBond Xtra column was equilibrated by applying 25 ml of buffer EQU to the rim of the column filter so that the filter was thoroughly wetted. The bacterial lysate was

neutralised with 12 ml of neutralisation buffer (buffer NEU), mixed by gently inverting the tube 10-15 times and the lysate was loaded onto the column. The column filter was then washed with 15 ml of buffer EQU applied to the rim of the filter to wash out the remaining lysate. The column filter was then discarded and the column was washed with 25 ml of wash buffer (buffer WASH). The DNA was eluted with 15 ml of elution buffer (buffer ELU) and collected in an Oakridge tube. To precipitate the eluate, 10.5 ml of room-temperature isopropanol were added to it. The tube was vortexed and then centrifuged at 15,000 g for 30 min at 4^{o}C using a Sorvall SS-34 rotor (Dupont). The supernatant was discarded, the pellet was washed with 5 ml of 70 % ethanol and centrifuged at 15,000 g for 5 min at room temperature. Supernatant was then carefully discarded and the pellet was dried at room temperature for 15 min. The dry pellet was dissolved in 500 µl of buffer TE (10 mM Tris-HCl, 1 mM EDTA, pH 8.0). DNA concentration was measured with a Picodrop spectrophotometer (2.1.9.3).

2.1.9.3. DNA concentration measurement

DNA concentration was measured using a Picodrop spectrophotometer. The amount of DNA in a solution was quantified at 260 nm using the fact that the concentration of double stranded DNA in a 10 mm pathlength cell with OD_{260} of 1.0 equals 50 µg/ml.

The purity of the DNA sample was assessed by the ratio of absorbance at 260 nm to 280 nm. Pure DNA preparations had a value of 1.8.

2.1.9.4. Glycerol stocks

Clones of the constructs made were maintained as glycerol stocks at -80^{o}C. Bacterial cells were harvested from 5 ml overnight cultures. 800 µl of cell suspension were mixed with 200µl of sterile 80 % glycerol in an microcentrifuge tube and then frozen at -80^{o}C.

2.1.10. Cloning procedures

Vector DNA was obtained by plasmid minipreparation (2.1.9.1). DNA prepared by plasmid maxipreparation (2.1.9.2) was used as well after being diluted to a concentration of 10 – 50 ng/µl. The insert DNA was either cut out of a plasmid by restriction enzyme digest (2.1.2) or amplified by one of the PCR techniques mentioned above (2.1.1). The vector and the insert were then digested with the same restriction enzymes (2.1.2) and the vector DNA was dephosphorylated (2.1.3). Both DNAs were separated on a preparative 0.7 % TBE agarose gel (2.1.4), purified as described in 2.1.5 and ligated 2.1.6.

Basic steps for In-fusion cloning are described in 2.1.7.

Ligation and In-Fusion reactions were transformed into chemically competent *E. coli* XL1 Blue cells (2.1.8). The transformed colonies were screened either by colony PCR (2.1.1.5) or by sequencing. Clones containing the desired construct were used to make 5 ml overnight cultures. These cultures were used for DNA minipreparation. Extracted plasmid DNAs were either screened by sequencing or, in the case of PCR screening, digested with appropriate restriction endonucleases to confirm the size of the insert. Plasmid DNA from at least one positive clone was fully sequenced to confirm the orientation of the insert and to check that no unwanted mutations were introduced. Positive clones were stored as glycerol stocks at -80^{o}C (2.1.9.4). Plasmid maxipreparations were used to obtain a large amount of mammalian expression vector DNA. DNA was stored at -20^{o}C.

2.2. Cell culture techniques

2.2.1. Basic cell culture procedures

Cell culture procedures were performed in a laminar flow hood under sterile conditions. Madin-Darby canine kidney cells (MDCK) and human embryonic kidney 293 cells (HEK 293) were cultured in a Dulbecco's Modified Eagle's Medium (DMEM) (Sigma) supplemented with 10 % of fetal bovine serum (FBS) "Gold" (PAA), 20 mM L-glutamine (GibCo) and 20 mM penicillin/streptomycin (GibCo). Human colonic adenocarcinoma cells (CaCo2) were grown in DMEM supplemented with 20 % of FBS, 20 mM L-glutamine and 20 mM penicillin/streptomycin. To recover either of these three cell lines from liquid N_2 stocks, a cryovial, containing frozen cells, was quickly removed from liquid nitrogen and immediately placed into 37^{o}C water bath. Once thawed, cells were transferred to a 15 ml centrifuge tube containing 10 ml of a pre-warmed growth medium. The tube was gently inverted to re-suspend the cells and centrifuged for 5 min on 300 g in the accuSpin 400 centrifuge (Fischer Scientific). Supernatant was aspirated and the cell pellet was re-suspended in 5 ml of pre-warmed culture medium and transferred to a 75 cm^2 flask (Nunc) with 20 ml of culture medium in it. Cells were incubated in a humidified 5 % CO_2 incubator at 37^{o}C and their viability was assessed next day under the inverted microscope (diavert Leitz Wetzlar).

To prevent the exhaustion of nutrients in the medium, cells were passaged when they were about 70 % confluent, usually every five days. Cells were washed twice with sterile PBS (1x PBS contains 150 mM NaCl and 10 mM sodium phosphate, pH 7.4) to remove serum and 2 ml of trypsin/EDTA (Sigma) were added to the flask. The flask was gently shaken to distribute trypsin/EDTA over the cell monolayer and returned to the 37^{o}C incubator. MDCK and CaCo2 cells were incubated for 10 min and HEK 293

cells for 5 min only. To ensure that cells were completely detached from each other and from the culture surface, they were examined using the inverted microscope. Cells were then re-suspended in 8 ml of appropriate medium to inactivate trypsin. If cell number was required, a 20 µl of cell sample was applied to a counting slide (Fast Read 102 ISL) and cells were counted. The required amount of cell suspension was then transferred to a new cell culture flask containing growth medium. The remainder of the cell suspension was centrifuged for 5 min at 300 g in the accuSpin 400 centrifuge (Fischer Scientific), the supernatant was aspirated and the cell pellet was stored at – 20^{o}C and used for antibody preabsorption when needed.

Cells from early passages were frozen down and kept as a seed stock in liquid nitrogen. Cells were washed in PBS, trypsinised and re-suspended in growth medium as described above. They were then centrifuged for 5 min at 300 g. The supernatant was discarded and the cell pellet was re-suspended in pre-chilled growth medium containing 10 % dimethyl sulfoxide (DMSO) (Sigma). The cell suspension was then split into cryovials (Greiner Bio-One), 1 ml into each. Cryovials were placed in a penoplast box and transferred to -20^{o}C for 2 hours, then to -80^{o}C overnight and, finally, into liquid nitrogen tanks.

2.2.2. Cell transfection

The day before a transfection, cells were plated into 35 mm polystyrene petri dishes (Corning) either on sterile glass coverslips (if used for immunofluorescence) or directly into the dish (if used for western blot or stable cell line generation). On the day of transfection cells were 70-80 % confluent. In the morning, cells were fed with a medium without penicillin/streptomycin. Lipofectamine 2000 (Invitrogen) was used as the transfection reagent. The mass/volume ratio of DNA and lipofectamine 2000 was kept

at 1:5, using 4 µg plasmid DNA and 20 µl lipofectamine 2000 per dish. In the case of co-transfection with two different DNAs, 2 µg of each plasmid were used. To make the transfection mix, 20 µl of lipofectamine 2000 were added to 230 µl of OptiMEM. The plasmid DNA (4 µg) was diluted to 250 µl with Opti-MEM (GibCo). Both mixtures were incubated at room temperature for 5 min and then mixed together by pipetting. The mixture was incubated at room temperature for 20 min to form DNA-lipofectamine 2000 complexes and then added to 2.5 ml of growth medium without penicillin/streptomycin. The medium in transfection dishes was replaced with medium, containing DNA-lipofectamine complexes and cells were incubated in the humidified 5 % CO_2 incubator at 37^{o}C for 1 or 2 days.

2.3. Protein analysis

2.3.1. Sample preparation

Transiently or stably transfected cells expressing the protein of interest were plated in 35 mm polysterene petri dishes (Corning) and incubated at 37^{o}C until 70-80 % confluency was reached (usually 24 hours). Afterwards the medium was aspirated, cells were washed 3 times with PBS and incubated in 1 ml serum-free medium for two days. The medium was then harvested into clean microcentrifuge tubes and cell monolayers were washed 3 times with PBS. Cells were scraped off the dishes with a sterile tip, washed off with 1 ml of PBS and transferred into clean microcentrifuge tubes. Both medium and cell samples were centrifuged at 14,500 rpm for 5 min at 4^{o}C using a miniSpin^{plus} centrifuge (Eppendorf).

900 µl of the supernatant from the media samples were collected in fresh microcentrifuge tubes and trichloracetic acid (TCA) precipitated. One volume of 100 % TCA (Fluka) was added to nine volumes of supernatant. Samples were then incubated

on ice for 30 min and centrifuged at 4^{o}C on 14,500 rpm for 3 min in the miniSpin^{plus} centrifuge (Eppendorf). The supernatant was then discarded, and pellets were washed twice with IMS (Industrial methylated spirit), dried at room temperature and mixed with 30 µl of 1x non-reducing sample buffer (125 mM Tris, pH 6.8, 2 % SDS, 10 % glycerol (Sigma), 0.1 % bromophenol blue and sterile H_2O to 1 ml). To make a 1x reducing sample buffer 5 % of β-mercaptoethanol and 0.1 M DTT (dithiothreitol) were added to the mixture.

Supernatant from cell samples was discarded and cell pellets were mixed with 50 µl of 1x reducing or non-reducing sample buffer.

All samples were heated at 104^{o}C for 4 min, mixed by pipetting and centrifuged for 1 min at 13,000 rpm to get rid of air bubbles.

2.3.2. Sodium dodecyl sulphate polyacrylamide gel electrophoresis (SDS-PAGE)

Vertical SDS-PAGE gels were prepared using the BioRad mini-format gel system. The two gel plates were washed with 70 % ethanol and dried before use, clamped together and then placed in the gel pouring stand. A 5 cm-high resolving gel (Table 2.6) was poured by pipetting the mix between the plates and covered with a layer of water-saturated n-butanol to stop O_2 mediated inhibition of polymerisation. Once the resolving gel was polymerised, the n-butanol was discarded and any remaining drops removed using Whatman 3 MM paper. A stacking gel mixture (Table 2.7) was then poured on top of the resolving gel. A plastic comb was inserted between the plates to form wells in the stacking gel. Stacking gel was allowed to polymerise.

Components	7.5 % resolving gel	10 % resolving gel
Acrylamide	1 ml	1.33 ml
4x separation buffer (1.5 M Tris-HCl pH 8.8, 0.4 % SDS)	1 ml	1 ml
Ammonium persulphate (APS) 5 mg/ml	0.4 ml	0.4 ml
Sterile H_2O	1.6 ml	1.27 ml
Tetramethylethylenediamine (TEMED)	5 µl	5 µl

Table 2.6. Composition of 7.5 % and 10 % resolving gel solutions.

Components	Stacking gel
Sterile H_2O	1.1 ml
Acrylamide	0.2 ml
APS 5 mg/ml	0.2 ml
4x stacking buffer (0.5 M Tris-HCl pH 6.8, 0.4 % SDS)	0.5 ml
TEMED	5 µl

Table 2.7. Composition of stacking gel solution.

The gel plates were then clamped into the electrode assembly and placed in the electrophoresis tank. Two gel cassettes were usually mounted on the electrode assembly

to create the running buffer chamber. When only one gel cassette was used, a thick plastic blanking plate was mounted instead of the second gel plate.

1x SDS-PAGE running buffer (25 mM Tris, 192 mM glycine and 0.1% SDS) was poured between the gel plates to cover the sample wells and into the electrophoresis tank to one fourth of its level. The comb was carefully removed and samples were loaded into the wells. 5 µl of protein molecular weight marker Precision Plus Protein Standards Dual Color (BioRad) were loaded in at least one well on each gel. Electrophoresis was carried out at 20 mA (constant current) for one gel and 40 mA for two gels for about 1 hour.

2.3.3. Semi-dry western blotting and protein detection

Proteins separated on SDS-PAGE gels were transferred onto Hybond-P PVDF membrane (Amersham) by semi-dry blotting. For each gel, ten pieces of Whatman 3 MM paper 10 cm x 8 cm were prepared. While the gel was running, three sheets of paper were soaked in anode buffer I (300 mM Tris base, 20 % methanol, pH 10.4), two sheets - in anode buffer II (25 mM Tris base, 20 % methanol, pH 10.4) and five sheets - in cathode buffer (25 mM Tris base, 40 mM 6-amino-n-hexanoic acid, 20 % methanol, pH 9.4). 10 x 8 cm PVDF membrane was wetted in methanol and then soaked in anode buffer II.

Once the loading buffer ran off the bottom of the gel, the transfer was set up: the three sheets of Whatman 3MM, soaked in anode buffer I, were placed on the anodal plate of the blotter and a 10 ml glass pipette was rolled on top of the wetted paper stack to remove trapped bubbles. Two sheets from anode buffer II were then placed on top of the stack and the procedure with the glass pipette was repeated. After excessive buffer was drained off, the PVDF membrane was layered on top of the 3 MM paper stack and the

resolving gel was carefully aligned on its surface. The gel was covered with five cathode buffer-soaked Whatman sheets, ensuring no bubbles were trapped between them, and the cathode plate of the blotter was placed on top without disturbing the stack. The transfer was set up at 40 mA (constant current) for one gel and 80 mA for two gels for 1 hour.

After 1 hour the blotting apparatus was disassembled and the PVDF membrane was incubated in blocking solution for 1 hour on a shaker at room temperature. Blocking solution contains 3 % of skimmed milk powder in TBS-t (150 mM NaCl, 10 mM Tris-HCl, pH 7.4, 0.2 % Tween-20). After 1 hour the blocking solution was replaced with a primary antibody against the protein of interest diluted in blocking solution and the membrane was probed overnight on a shaker at 4^{o}C.

Sometimes to eliminate non-specific binding activity of a primary antibody, it was preabsorped on a frozen cell pellet (2.2.1) before use. Cell pellet was thawed at room temperature and washed three times in PBS. During each washing it was rotated for 5 min at room temperature and then centrifuged for 5 min on 300 g in the accuSpin 400 centrifuge (Fischer Scientific). The primary antibody was diluted to the desired concentration in 1-4 ml of PBS, added to the washed cell pellet, mixed by vortexing and rotated for 2 hours at room temperature. The preabsorbed antibody preparation was then centrifuged for 5 min at 300 g to pellet the cell debris and used for probing the PVDF membrane at 4^{o}C on a shaker overnight.

Next day the membrane was washed three times in TBS-t, each wash lasted for 10 min. The washes were followed by staining with an alkaline phosphatase-conjugated secondary antibody (DAKO), raised against the IgG of species which produced the primary antibody. The secondary antibody was used at a concentration of 1 vol in 1000

vols of blocking solution and the incubation was performed for 2 hours on a shaker at room temperature. Afterwards, the membrane was given three 10-minute washes in TBS-t and two 10-minute washes in TBS. During the last wash an alkaline phosphatase buffer (AP buffer) was prepared (Table 2.8). BCIP, which produces an insoluble purple-blue product in the presence of alkaline phosphatase, and NBT, which intensifies the colour and increases the sensitivity, were added to the AP buffer immediately before use. The blot was incubated in AP buffer for approximately 10 min, until the colour had developed sufficiently. The membrane was when washed several times in deionised water and dried on paper towels.

Component	Amount needed to prepare 10 ml of AP buffer
1 M $MgCl_2$	0.5 ml
1 M Tris-HCl pH 9.5	1 ml
4 M NaCl	0.25 ml
Sterile H_2O	8.25 ml
5-bromo-4-chloro-3-indolyl phosphate (BCIP)	10 µl
Nitro-blue tetrazolium chloride (NBT)	10 µl

Table 2.8. Composition of AP buffer.

2.4. Immunofluorescence

2.4.1. Paraformaldehyde fixation

Specimens (coverslips with cells, murine cochleae and cochlear cultures) were washed three times with PBS and fixed with 3.7 % formaldehyde in 0.1 M sodium phosphate

buffer, pH 7.4, for 1 hour at room temperature. Afterwards, fixed specimens were washed three times in PBS to remove the excess paraformaldehyde.

2.4.2. Cryosectioning

For fine microscopic analysis of complex tissues and anatomical structures, frozen sections were obtained from the fixed specimens. Bony structures, i.e. cochleae, required an additional step of decalcification in 0.5 M EDTA, pH 8.0, for 2-4 days, depending on the age of the animal. Older cochleae required prolonged incubation in EDTA. For any age the EDTA solution was always changed on the second day. The day before cryosectioning the specimens were placed in 30% sucrose (Fisher Scientific) in PBS and stored on 4^{o}C overnight. Next morning the specimens were embedded in cryoagar (1 % type 7 low geling temperature agar (Sigma-Aldrich) added to 18 % sucrose in PBS) poured into a 35 mm polystyrene petri dish, using a dissection microscope (Zeiss Stemi 2000) to visualise the tissue pieces. The cryoagar was allowed to set at room temperature for about 10 min and then placed at 4^{o}C for half an hour. The block with the specimens was cut out when the cryoagar became solid, instantly frozen with cryospray 134 (TAAB) and mounted on a metal base with optimal cutting temperature (OCT) compound (Tissue-Tek). Sections (15-20 µm thick) were taken using a Cryocut 1800 microtome (Reichert-Jung) at -30^{o}C. Sections were collected on glass slides (Thermo-Scientific) coated with 0.5 % gelatin (BDH Chemicals Ltd), dried in a 37^{o}C incubator overnight and then placed at -20^{o}C for storage.

2.4.3. Immunostaining

Prepared frozen sections (cell coverslips or cochlear cultures) were incubated in blocking solution (10 % Horse Serum in PBS) for 1 hour at room temperature. When detecting intracellular proteins in cells and cochlear cultures, they were permeabilised

by adding 0.1 % of Triton X-100 to the blocking solution. The blocking solution was then aspirated. A slide with sections was then rinsed with PBS (coverslips with cells and cochlear cultures were washed in a petri dish). Primary antibodies were diluted as required in 10 % Horse Serum in PBS and were added to the sections. Sections were then incubated overnight in a humid chamber at room temperature (coverslips with cells and cochlear cultures were incubated overnight on a rocker at 4^{o}C). On the next day the slides were washed three times in PBS. The secondary antibodies against the IgG of species that were the source of the primary antibody were diluted in 10 % Horse Serum in PBS and centrifuged for 5 min at 13,000 rpm at room temperature. The supernatant was carefully collected to avoid pellets and added to the specimens. Sometimes Texas Red®-X conjugated phalloidin at the dilution of 1:500 (Molecular Probes, Invitrogen) or fluorescein phalloidin in the dilution of 1:500 (Molecular Probes, Invitrogen) were used as a counter-stain by adding to the secondary antibody solution. The slides were incubated for 2 hours at room temperature either on a rocker (cell coverslips and cochlear cultures) or in a humid chamber (sections). They were then washed three times in PBS and mounted using Vectashield (Vector Laboratories) mounting medium. The specimens were examined by wide-field fluorescence microscopy (Zeiss Axioplan 2) and/or by confocal microscopy (Zeiss LSM S10).

2.5. Transmission and scanning electron microscopy techniques

Specimens were fixed, washed and incubated with a primary antibody as described in 2.4.1 and 2.4.3. The specimens were then washed five times with 1 % Horse Serum in PBS, 5 min each wash. Gold-conjugated secondary antibodies, specific for the IgG of the species which produced the primary antibody, were used to identify surface antigens by transmission electron microscopy (TEM) and scanning electron microscopy (SEM). To distinguish two secondary antibodies in the case of double-labelling with two

different primary antibodies, each secondary antibody was conjugated to a different size of a gold particle. Gold-conjugated secondary antibodies were purchased from Abcam® and were used at a dilution of 1:10 in 10 % Horse Serum, 1 mM EDTA, pH 8.0, 0.05 % Tween-20 and 0.1 mM in PBS. The specimens were incubated with the gold-conjugated secondary antibodies for 48 hours on a rocker at 4^{o}C and then given three 5-minute washes with 0.05 % Tween® 20 in PBS and two 5-minute washed in PBS only.

The specimens were then fixed in glutaraldehyde fixative (2.5 % glutaraldehyde, 0.1 M sodium cacodylate in sterile H_2O) for 2 hours. If the specimens were prepared for TEM, 1 % tannic acid (Sigma-Aldrich) was added to the fixative to enhance the electron density of protein filaments. After fixation, specimens were given three 5-minute washes in 0.1 M sodium cacodylate.

Specimens were then re-fixed with 1 % osmium tetroxide in 0.1 M sodium cacodylate for 1 hour. They were then washed three times with 0.1 M sodium cacodylate, rinsed with sterile water and dehydrated by using a graded series of ethanol. The specimens were first treated with 50 % ethanol, then sequentially transferred into 70 %, 80 % and 90 % ethanol. Each step lasted not more than 5 min to prevent the shrinkage of the tissue. Finally, the specimens were transferred to absolute ethanol for 10 min. This step was repeated two more times.

The samples for SEM were then placed into labeled porous plastic pots in 100 % ethanol and critical point dried to dry the tissue with preserving it 3D structure in a special apparatus. They were then mounted on aluminum stubs with silver paint. Carbon coating was performed with a Balzers BAF 400D freeze-fracture device. Carbon was evaporated from an electron beam gun at 90^{o} with sample rotation for 10-15 sec. Samples were then examined with a Jeol 6400 cold field emission scanning electron

microscope. Acceleration voltage was set up at 5 kV, an emission current at 10 mA and a probe current at 10 pA. Images were captured with different detection modes. The secondary electron image (SEI) mode was used for high-resolution pictures of a sample surface. The backscatter detector (BSD) was utilized for images of the gold labeling. Images were also captured in the Add-mode, which combines the SEI and the BSD.

The specimens for TEM were infiltrated in epoxy resin (Epon) (TAAB) with 100% ethanol mixed in a ratio of 1:1 for 1 hour at room temperature. They were then incubated in 3:1 Epon with 100% ethanol for 3 hours at room temperature. Finally, the specimens were transferred into pure Epon and incubated overnight at room temperature. On the next day the samples were moved into embedding molds containing pure Epon and incubated at 70^{o}C for 48 hours. Special polyethylene capsules, containing a piece of paper with a label, were filled with Epon and placed into 70^{o}C oven as well. Once the Epon was solid, the block with embedded specimen was extracted from the mold and glued onto the Epon-filled capsule that further served as a holder. The block was then filed and trimmed to make it easier to section. 1 µm sections were taken using an Ultracut E microtome (Reichert-Jung). They were stained with toluidine blue and examined on a Zeiss Axioplan 2 microscope. If the region of interest was present on 1 µm sections, sections of 90-100 nm thickness were taken using the same microtome and the diamond knife (TAAB). The sections were mounted on copper grids and stained with uranyl acetate for 30 min. They were then washed three times in sterile water and stained with lead citrate for 8 min. Afterwards the sections were given four washes with sterile water and dried. A Hitachi 7100 transmission electron microscope was used for examining sections. Images were captured with a Gatan Ultrascan 1000 CCD camera.

2.6. X-gal staining of mouse cochleae

Animals were killed by cervical dislocation. Cochleae were extracted and placed in PBS for dissection. The oval and round windows were removed and a small hole was made in the bony capsule and stria vascularis at the apex of each cochlea.

Cochleae were transferred to cold X-gal fixative (1 % formaldehyde, 0.25 % glutaraldehyde, 2 mM $MgCl_2$, 5 mM EGTA, 0.02 % NP-40 in 1x PBS) and fixed for 2 hours on ice. To prepare X-gal fixative 270 µl of 37 % formaldehyde (Sigma-Aldrich), 100 µl of 25 % glutaraldehyde (TAAB), 20 µl of 1 M $MgCl_2$, 250 µl of 200 mM EGTA, 20 µl of 10 % NP-40, 1000 µl of 10x PBS were diluted with sterile water to 10 ml. After fixation, cochleae were washed three times in room-temperature PBS. They were then transferred into 35 mm petri dishes each containing 3 ml of X-gal solution. X-gal solution was prepared according to the Table 2.9.

Reagent	Amount
Potassium ferricyanide	82.25 mg
Potassium ferrocyanide	105.5 mg
10 % sodium deoxycholate	50 µl
10 % NP-40	100 µl
1 M $MgCl_2$	100 µl
50 mg/ml X-gal (Melford Laboratories ltd) in dimethylformamide (Sigma)	1 ml
10x PBS	5 ml
Sterile H_2O	To 50 ml

Table 2.9. Composition of XGal solution.

Dishes with cochleae were stored in the dark at 4^{o}C for 5 days. On day 3 the X-gal solution was replaced with fresh solution. On the fifth day cochleae were washed three times in 0.02 % NP-40 in PBS, re-fixed in cold X-gal fixative for 2 hours on ice and washed three times with 0.02 % NP-40 in PBS again. Cochleae were then decalcified and cryosectioned as described in 4.2.

2.7. Materials and methods used for creating an *in vitro* model of the tectorial membrane

2.7.1. Vector design

2.7.1.1. pBK-Tecta-IRES-TurboFP635 construct

The internal ribosome entry site (IRES) was amplified using Pfu polymerase enzyme (Stratagene) (2.1.1.1) from pIRES2-EGFP bicistronic vector (Clontech) (Fig.2.2). The polymerase chain reaction (PCR) reaction was set-up with following primers (Table 2.10): TectaIRES-F1 was designed to join the 3' end of the Tecta open reading frame (ORF) with the 5' end of the IRES via a XhoI restriction site, and IRESturboFP635-R1 was made to join the 3' end of the IRES and the 5' end of the TurboFP635-N vector (Evrogen, Moscow, Russian Federation). Vector TurboFP635-N encodes far-red fluorescent protein TurboFP635 (Fig.2.3). The TurboFP635 ORF was amplified with Pfu polymerase and following primers (Table 2.10): IRESturboFP635-F1 which joins the 3' end of IRES ORF with the 5' end of TurboFP635 and TurboFP635-R1 designed to fuse the 3' end of TurboFP635, via an XhoI restriction site, with the SV40 polyadenylation signal of a plasmid pBK-Tecta-FL7 containing a full length Tecta ORF (pBK stands for plasmid backbone).

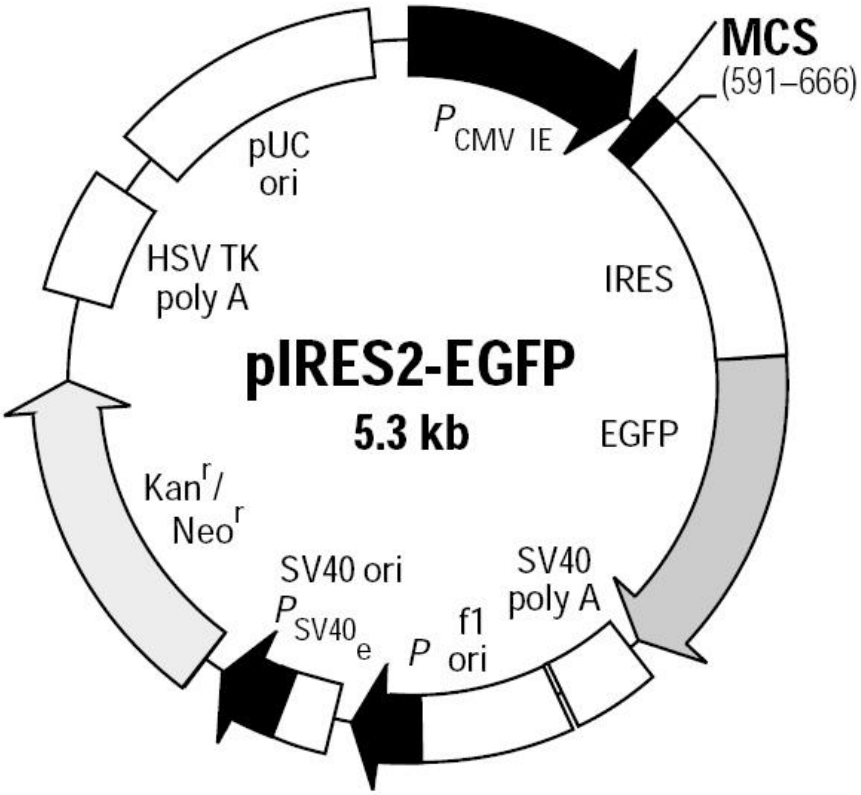

Figure 2.2. pIRES2-EGFP vector map (Clontech). The IRES sequence (584 bp) is located between the multiple cloning site (MCS) and the enchanced green fluorescent protein (EGFP) coding region. P CMV IE is the human cytomegalovirus immediate early promoter. SV40 poly A - the SV40 early mRNA polyadenylation signal is followed by the f1 single-strand DNA origin (f1 ori). The next is a bacterial promoter for expression of Kan^r gene. SV40 ori is the SV40 origin of replication, P SV40 e - SV40 early promoter/enhancer. Kan^r/Neo^r stands for the kanamycin/neomycin resistance gene. HSV TK poly A is herpes simplex virus thymidine kinase polyadenylation signal. pUC ori - pUC plasmid replication origin (from BD Biosciences Clontech information sheet).

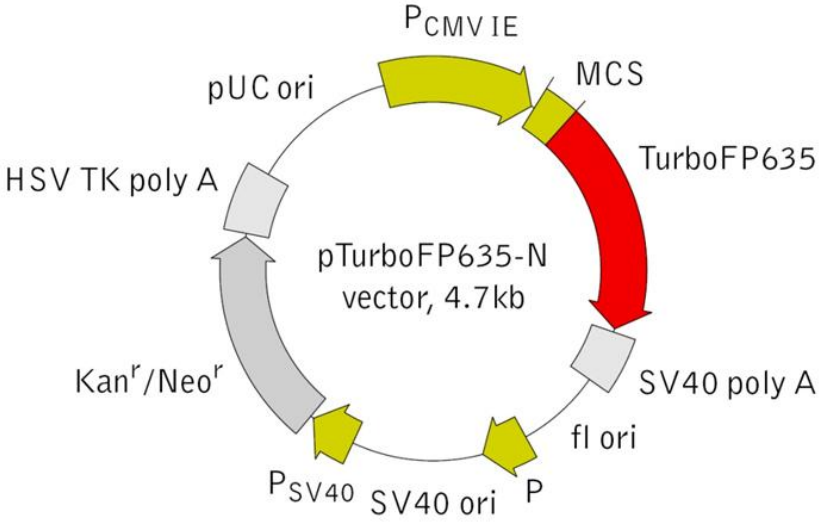

Figure 2.3. pTurboFP635-N vector map (Evrogen). The structure of the vector is similar to that of pIRES2-EGFP from Clontech. TurboFP635 ORF is located between MCS and SV40 early mRNA polyadenylation signal (from Evrogen data sheet).

The IRES and the TurboFP635 were amplified, mixed together and joined by PCR as described in 2.1.1.1 using Pfu polymerase and primers TectaIRES-F1 and TurboFP635-R1 (Table 2.10). The joined product was then digested with XhoI enzyme (2.1.2) and ligated (2.1.6) into the Tecta expression vector, pBK-Tecta-FL7 (Fig.2.4), which was also digested with XhoI and dephosphorylated (2.1.3). The ligation reaction was transformed into XL1 Blue competent cells and plated on LB plates containing kanamycin (2.1.8). Clones were screened using PCR (2.1.1.5) and the orientation of the insert was confirmed by restriction digestion of DNA mini preparations (2.1.9.1). One of the clones, pBK_Tecta_IRES_TurboFP635_23, was confirmed to be correct by DNA sequencing. Maxi-prepped plasmid (2.1.9.2) was used for mammalian cell transfection experiments. Fig.2.5, a, gives the schematic representation of the Tecta_IRES_TurboFP635 insert.

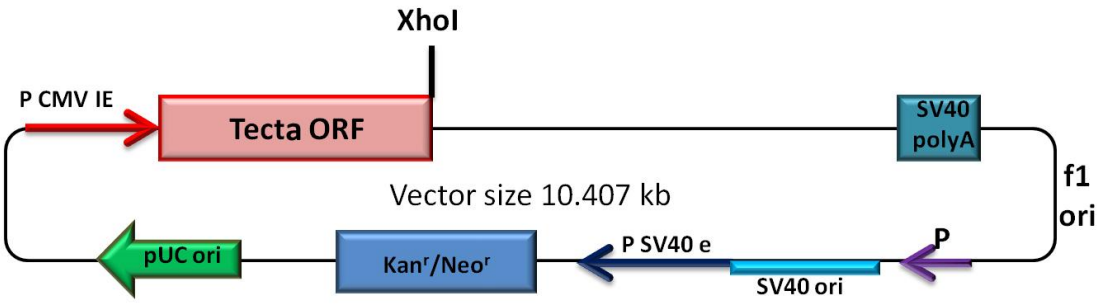

Figure 2.4. pBK-TectaFL7 vector, schematic representation. The full length Tecta ORF is located at the position 612 - 7065, between the MCS and the SV40 early mRNA polyadenylation signal. The abbreviations are as used above (Fig.2.1 and Fig.2.2).

2.7.1.2. pBK-mCherry-Tecta construct

Vector pBK-mCherry-Tecta encodes Tecta protein which is tagged with the mCherry fluorophore at its N-terminus (Fig.2.5, b). mCherry protein was selected due to its photostability and bright colour that makes it easy to trace during live imaging experiments. The Tecta signal peptide sequence was amplified from pBK-TectaFL7 construct (Fig.2.4) by PCR with Pfu enzyme and the following primers (Table 2.10): pBKTecta-F1 which joins the 5' end of the Tecta signal sequence to the plasmid backbone downstream from the CMV immediate early promoter and pBKChryTecta-R1 which joins the 3' end of the Tecta signal sequence and the 5' end of the mCherry ORF.

mCherry was amplified from the construct pBK-Tecta-mCherry which is similar to pBK-Tecta-IRES-TurboFP635 (Fig.2.5, a) with an IRES driving mCherry transcription. The PCR was set up with Pfu Taq and the primers (Table 2.10) pBKChryTecta-F1 and pBKChryTecta-R2. The first primer joins the 5' end of mCherry to 3' end of a Tecta signal peptide sequence, the latter fuses the 3' end of mCherry to the 5' end of Tecta ORF. The first 264 bp of Tecta ORF were amplified with Pfu polymerase and the primer pair: pBKChryTecta-F2 and pBKTecta-R3 (Table 2.10).

The three PCR products were then mixed and joined by PCR with Pfu polymerase and primers pBKTecta-F1 and pBKTecta-R3. The joined product was then digested with NheI and EcoRI and ligated into pBK-TectaFL7 backbone that had been cut with NheI and EcoRI and dephosphorylated.

2.7.1.3. Introducing deletions into the pBK-mCherry-Tecta construct

2.7.1.3.1. pBK-mCherry-MMMTecta construct

A construct containing mCherry fused in frame with MMM Tecta (Fig.1.7 for MMM Tecta, which is a part of the fourth vWFD repeat along with the ZP domain) was generated using the In-fusion cloning technique (2.1.7). First, a PCR reaction to amplify a required fragment from pBK-mCherry-Tecta was set up using Pfu Taq polymerase and primers ChTectaMMM-F that primes to the 5' end of the MMMTecta sequence and ChTectaMMM-R2 that anneals to mCherry ORF 3' end (Table 2.10). These primers amplify the plasmid backbone containing only mCherry and MMM Tecta thus introducing a deletion of LMM and HMM Tecta. 100 ng of the product were then used in the In-fusion cloning reaction.

2.7.1.3.2. pBK-mCherry-ZPTecta construct

pBK-mCherry-Tecta construct was modified so that C-terminus of mCherry became fused directly to the Tecta ZP domain (Fig.1.6). Entactin and ZA domains were both completely deleted. The deletion was introduced using In-fusion cloning approach. The plasmid backbone containing mCherry and ZP domain of Tecta was amplified with primers ChTectaDD-F that anneals to the 5' end of Tecta ZP domain and ChTectaDD-R2 that primes with the 3' end of mCherry ORF (Table 2.10). These primers amplify the plasmid backbone containing only mCherry and Tecta ZP domain. 100 ng of PCR product was added to an In-fusion cloning reaction.

2.7.1.4. pBK-EGFP-Tecta construct

pBK-EGFP-Tecta construct contains EGFP N-terminally fused to the Tecta ORF downstream from the Tecta signal peptide sequence (Fig.2.5, c).

EGFP was amplified from pBK-EGFP-Tectb construct described below using primers Tecta-EGFP and EGFP-Tecta (Table 2.10). Plasmid backbone was amplified from pBK-mCherry-Tecta construct (Fig.2.5, b) so that the mCherry coding sequence was excluded with primers TectamCherryt2EGFP-F and TectamCherry2EGFP-R (Table 2.10). 50 ng of each PCR product were used in the In-Fusion reaction.

2.7.1.5. pBK-EGFP-Tectb construct

pBK-EGFP-Tectb vector (Fig.2.5, d), encoding N-terminally EGFP-tagged Tectb protein, was designed to assess Tectb expression levels and localisation using live fluorescence imaging. The EGFP gene is located downstream of the Tectb signal sequence, and the 3' end of the EGFP ORF is fused in frame to 5' end of the Tectb ORF via the multiple cloning site (MCS). The expression of EGFP-Tectb fusion protein is driven by CMV immediate early promoter.

2.7.1.6. Introducing missense mutations for Tecta into Tectb

Mutations in ZP domain of Tecta protein, causing deafness in humans, were introduced into ZP domain of the Tectb protein. Tectb protein residues synonymous to those substituted in mutant forms of Tecta were identified by protein sequence alignment. The ZP modules of human Tecta and mouse Tectb proteins were aligned with other members of ZP protein family from a range of animal species using the ClustalV algorithm in DNASTAR MegAlign software (Lasergene).

2.7.1.6.1. C1837G (Spanish) mutation

The synonymous cysteine was replaced by glycine in mouse Tectb and transiently expressed in mammalian cells *in vitro*. The missense mutation that results in amino acid substitution was introduced in pBK-EGFP-Tectb construct by PCR site directed mutagenesis (2.1.1.2) using turbo Pfu polymerase. Mutagenic primers were designed to replace the first thymine in TGT codon by guanine which results in cysteine substitution with glycine (Table 2.10): TectbC59G-F1 and TectbC59G-R1.

2.7.1.6.2. Y1870C (Austrian) mutation

The conserved tyrosine residue in the ZP domain of mouse Tectb synonymous to human Tecta tyrosine 1870 was replaced by cysteine. An appropriate missense mutation changing A in TAC codon by G was introduced in pBK-EGFP-Tectb by PCR site directed mutagenesis with primers TectbC61T-F1 and TectbC61T-R1 (Table 2.10).

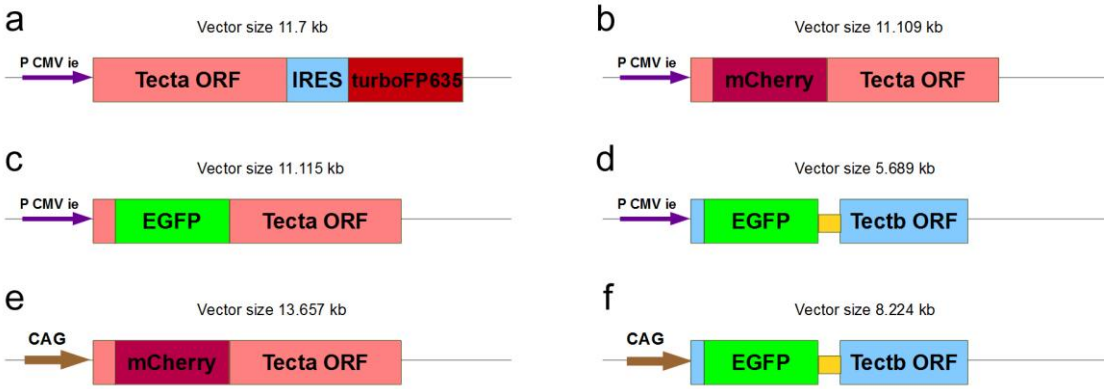

Figure 2.5. Inserts of the constructs generated in this work. A - pBK-Tecta-IRES-turboFP635, b - pBK-mCherry-Tecta, c - pBK-EGFP-Tecta, d - pBK-EGFP-Tectb, e - pCAG-mCherry-Tecta, f - pCAG-EGFP-Tectb. P CMV ie - CMV immediate early promoter, CAG - CAG promoter. Pink box between the promoter and the fluorescent protein in b, c and e stands for a Tecta signal peptide sequence. Blue bar downstream the promoter and upstream the EGFP sequence on d and f is a Tectb signal peptide sequence. Yellow box between the EGFP and the Tectb ORF stands for polylinker.

2.7.1.7. pCAG constructs

2.7.1.7.1. pCAG-mCherry-Tecta construct

Vector pCAG-EGFP (Fig.2.6) was a kind gift from Dr. Marcelo Rivolta, University of Sheffield, UK. pCAG-EGFP is a bicistronic construct with a CAG promoter driving EGFP and an IRES to express the puromycin resistance gene. CAG is a strong promoter obtained by connecting the CMV-IE enhancer sequence with AG , chicken βactin/rabbit β-globin hybrid promoter (Miyazaki et al., 1989; Niwa et al., 1991)

The vector was digested with XhoI and NotI restriction enzymes to remove EGFP ORF from the construct and dephosphorylated. A polylinker (Fig.2.7) was inserted into the digested plasmid backbone to introduce several new restriction sites. The polylinker was made from primers described in Table 2.10. pCAGlinker-F fuses with 3' sticky end of pCAG-EGFP which results from XhoI digest. Once ligated in the construct the primer destroys XhoI restriction site. pCAGlinker-R fuses to 5' end of NotI digested pCAG-EGFP and destroys the NotI restriction site.

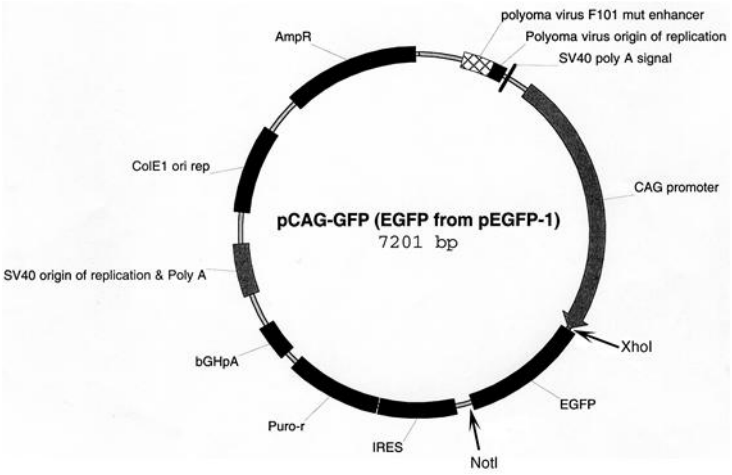

Figure 2.6. pCAG-EGFP vector map. Puro-r is puromycin resistance gene. bGHpa stands for the bovine growth hormone polyadenylation signal. ColE1 ori rep is E. coli ColE1 origin of replication site. AmpR is gene encoding bacterial ampicillin resistance (the map was kindly provided by Dr. Rivolta, University of Sheffield).

Figure 2.7. A polylinker which replaced EGFP in pCAG-EGFP construct.

Both primers were synthesized with 5' phosphate to enable ligation in the construct and annealed leaving protruding ends at both 5' and 3' sides. The annealing reaction used 1 µg of each primer, 5 µl of 10x ligation buffer (New England BioSciences) and sterile H_2O to 50 µl of volume. The mixture was incubated at 85^oC for 10 min and allowed to cool down to room temperature. The annealed oligonucleotides were then ligated into digested and dephosphorylated plasmid backbone.

pCAG plasmid backbone containing polylinker was digested with NheI and XhoI restriction enzymes and dephosphorylated. The mCherry-Tecta fusion was cut out from pBK-mCherry-Tecta construct with NheI and XhoI and ligated in pCAG backbone. The clones were screened by PCR and then by digestion of miniprepped DNA. Positive clone pCAG-mCherry-Tecta23 was re-confirmed by sequencing and a maxipreparation of the DNA was made. For schematic representation of mCherry-Tecta insert downstream the CAG promoter see Fig.2.5, e.

2.7.1.7.2. pCAG-EGFP-Tectb construct

The EGFP-Tectb fusion was amplified from the pBK-EGFP-Tectb construct using AccuPrime Taq DNA polymerase (2.1.1.3) and the following primers: PBK-F1 which anneals to the CMV immediate early promoter and the NheI restriction site between CMV immediate early and EGFP sequence, and mmTectbSal which introduces a SalI restriction site and a MluI restriction site at the 3' end of the EGFP-Tectb fragment (Table 2.10). SalI enzyme produces a sticky end which is compatible with XhoI cut

DNA. As ligation of SalI end and XhoI end eliminates both restriction sites, the primer introduces a MluI restriction site in case further cloning manipulations are required.

The PCR product EGFP-Tectb-SalI-MluI was digested with NheI and SalI restriction enzymes and the vector pCAG-polylinker was cut with NheI and XhoI and then dephosphorylated. The resultant DNA fragments were then ligated. Figure 2.5, f schematically represents the EGFP_Tectb insert in pCAG backbone.

Primer name	Primer sequence from the 5' end to the 3' end	Construct they were used to make	Positions and special features
TectaIRES-F1	CCTCATAACTCGAGATCCGC	pBK-Tecta-IRES-turboFP635	1-8 - complementary to the Tecta ORF 15-20 - to the IRES ORF XhoI restriction site is underlined
IRESturboFP635-R1	ACGCTATCCTCACCCACCATGGTTGTGGCCATATTATC	pBK-Tecta-IRES-turboFP635	1-23 - complementary to TurboFP635 ORF 24-38 - to IRES ORF
IRESturboFP635-F1	GATAATATGGCCACAACCATGGTGGGTGAGGATAGCGT	pBK-Tecta-IRES-turboFP635	Reverse complement to IRESturboFP635-R1

TurboFP635-R1	TGAGCTCGAG TCAGTTATTCA GCTGTGCCCCA GTTTGC	pBK-Tecta-IRES-turboFP635	1-14 - SV40 polyadenylation signal 15-24 - TurboFP635 ORF XhoI site is underlined
pBKTecta-F1	GCTAGCCACC ATGAATTATTC ATCATTACTTA G	pBK-mCherry-Tecta	1-10 - CMV immediate early promoter 11-33 - complement to the Tecta signal peptide sequence
pBKChryTecta-R1	CAAGCTCAGC CCAGGGAGCT CATGGTGAGC AAGGGCGAGG AG	pBK-mCherry-Tecta	1-21 - complementary to mCherry ORF 22-42 - Tecta signal peptide sequence
pBKChryTecta-F1	CAAGCTCAGC CCAGGGAGCT CATGGTGAGC AAGGGCGAGG AG	pBK-mCherry-Tecta	Reverse complement to the pBKmChryTecta-R1
pBKChryTecta-R2	GTCATTCTGCC AAAATGGATA CATCTTGTACA GCTCGTCCATG C	pBK-mCherry-Tecta	1-24 - Tecta ORF 25-44 - mCherry ORF
	GCATGGACGA	pBK-mCherry-	Reverse complement sequence

pBKChryTecta-F2	GCTGTACAAGATGTATCCATTTTGGCAGAATGAC	Tecta	to pBKChryTecta-R2
pBKTecta-R3	TTCTCTGTAATAGATCTCAC	pBK-mCherry-Tecta	Complementary to Tecta ORF sequence in the middle of exon 3
ChTectaMMM-F	AGCTGCAACGAGCTACAGTT	pBK-mCherry-MMMTecta	Complementary to the 5’ end of MMMTecta coding sequence
ChTectaMMM-R2	TAGCTCGTTGCAGCTCTTGTACAGCTCGTCCATG	pBK-mCherry-MMMTecta	1-18 - the 3’ end of mCherry ORF 19-34 - complementary to ChTectaMMM-F
ChTectaDD-F	ACCTGCAAGGCAGCCCAGATG	pBK-mCherry-ZPTecta	Complementary to the 5’ end of Tecta ZP domain
ChTectaDD-R2	GGCTGCCTTGCAGGTCTTGTACAGCTCGTCCATG	pBK-mCherry-ZPTecta	1-15 - overlap with ChTectaDD-F primer 16-34 - complementary to the 3’ end of mCherry ORF
Tecta-EGFP	CAGCCCAGGGAGCTCGTGAGCAAGGGCGAGGA	pBK-EGFP-Tecta	1-15 - complementary to the 5’ end of the Tecta signal peptide sequence 16-32 - to the 3’ end of the EGFP coding sequence

EGFP-Tecta	TCTTGTACAGCTCGTCCATGCCGAGAGTGAT	pBK-EGFP-Tecta	1 is the 3’ end of the Tecta ORF 2-31 - the 5’ end of the EGFP coding sequence
TectamCherryt2EGFP-F	ACGAGCTGTACAAGATGTATCCATTTTGGCAGAA	pBK-EGFP-Tecta	1-14 - complementary to the 5’ end of the EGFP coding sequence 15-34 - to the 3’ end of the Tecta ORF
TectamCherry2EGFP-R	GAGCTCCCTGGGCTGAGCTTGGTGCCGAA	pBK-EGFP-Tecta	Complementary to the 5’ end of the Tecta signal peptide sequence
TectbC59G-F1	CTGGCACTCGGGGGGCTGgGTTACAACGGGGTCCATGAAG	pBK-EGFP-Tectb C1837G	Mutagenic primer, mutated nucleotide is specified by lower case
TectbC59G-R1	CTTCATGGACCCCGTTGTAACcCAGCCCCCCGAGTGCCAG	pBK-EGFP-Tectb C1837G	Mutagenic primer, mutated nucleotide is specified by lower case
TectbC61T-F1	GTACAAGCCCCCCATCTgCCACTTCTACAGCCAC	pBK-EGFP-Tectb Y1870C	Mutagenic primer, mutated nucleotide is specified by lower case
TectbC61T-R1	GTGGCTGTAGAAGTGGcAGAT	pBK-EGFP-Tectb Y1870C	Mutagenic primer, mutated nucleotide is specified by lower

	GGGGGGCTTGTAC		case
pCAGlinker-F	TCGATGCGGCCGCTAGCGAATTCCCACCATGGCTCGAGGATCC	pCAG-mCherry-Tecta	Polylinker sequence
pCAGlinker-R	GGCCGGATCCTCGAGCCATGGTGGGAATTCGCTAGCGGCCGCA	pCAG-mCherry-Tecta	Polylinker sequence
PBK-F1	GAACCGTCAGATCCGCTAGC	pCAG-EGFP-Tectb	Complementary to CMV immediate early promoter Contains NheI restriction site (underlined)
mmTectbSalI	GGATCGTCGACacgcgtCTACAACACAGCCCAGGTCC	pCAG-EGFP-Tectb	Complementary to Tectb C-terminal sequence Introduces SalI restriction site (underlined) and MluI restriction site (in lower case)

Table 2.10. Primers used for making constructs described above.

2.7.2. Cell culture procedures

Cell culture procedures for the cell lines utilised in this study (MDCK and CaCo2) are described in section 2.2.1. Section 2.2.2. describes the lipofectamine 2000 transfection

method used in this chapter. The EGFP-Espin construct in which EGFP-Espin fusion is driven by CMV promoter was a kind gift from Prof. James R. Bartles (Northwestern University Feinberg School of Medicine, Chicago, USA) and was used to promote the formation of elongated microvilli on the apical surface of the cells transiently transfected with Tecta encoding constructs.

2.7.2.1. Generating stable cell lines

Two methods of generating stable cell lines were used in this research: cloning disks and the limiting dilution cloning technique.

MDCK cell line stably expressing the pBK-Tecta-IRES-TurboFP635 construct was generated using cloning disks. MDCK cells were first transfected with 4 µg of pBK-Tecta-IRES-TurboFP635 plasmid. After 48 hours the transfected cells were washed twice with phosphate buffered saline (PBS), trypsinised and resuspended in the MDCK media. Serial ten-fold dilutions of the cell suspension were then prepared and plated into 100 mm diameter culture dishes (Corning). G418, the antibiotic selective for the neomycin resistance gene, was added to the cell medium at a concentration of 0.5 mg/ml. Cells were selected for 7 days until distinct isolated colonies were formed. Plates were then screened for fluorescent colonies using a Zeiss IM35 inverted microscope equipped with a rhodamine filter set and a 50 W mercury lamp. Selected colonies were marked with a black pen on the underside of the plate. The plates were then washed twice with PBS, and 3 mm diameter cloning disks (Sigma-Aldrich) soaked in trypsin/ethylenediaminetetraacetic acid (EDTA) were placed on top of the selected colonies. Cells were incubated with trypsin/EDTA for 10 min at 37^{o}C. Each disk was then gently rubbed against the colony to pick up as many cells as possible and transferred into a 35 mm diameter polystyrene petri dish (Corning) containing growth

medium supplemented with geneticin (G418) at concentration 0.5 µg/ml. A duplicate dish for fixation and subsequent antibody staining was set up. When the culture reached 70-80 % confluency, ten-fold serial dilutions were set up again. The cloning procedure was repeated at least four times to ensure that the final line originated from a single transfected cell.

MDCK-based cell lines stably expressing either pCAG-mCherry-Tecta or pCAG-EGFP-Tectb were generated using cloning by limiting dilution. MDCK cells were transfected with 4 µg of the appropriate vector. Following 48-hour incubation, the cells were washed twice with sterile PBS and treated with trypsin/EDTA. Cells were then triturated 10 times with a sterile glass Pasteur pipette, re-suspended in medium and counted. Cell density was adjusted to 10^5 cells per ml with selection medium containing 5 µg/ml of puromycin (Sigma-Aldrich). Cell dilutions containing 100 and 10 cells per 1 ml of selection medium were prepared. Aliquots (100 µl) of high concentration cell suspension (100 cells per ml) were dispensed into 48 wells of a 96-well plate (Nunc). Aliquots (100 µl) of the 10 cell/ml cell suspension were dispensed into the remaining 48 wells. The plates were incubated for 14 days, changing the selection medium after the first seven days. They were then checked for the presence of isolated colonies on a Zeiss Cell Observer Axiovert 200M. mCherry and EGFP fluorescence were detected on the same microscope using rhodamine and fluorescein isothiocyanate (FITC) filters respectively. Clones that appeared to be derived from a single cell and expressing the appropriate fluorescent protein were selected. Cells were washed, trypsinised and transferred to 35 mm diameter petri dishes with selection medium. Cloning was repeated three more times.

2.7.2.2. Mitomycin C treatment of MDCK stable cell lines

MDCK cells stably transfected with pBK-Tecta-IRES-turboFP635 construct were dispensed in two 35 mm diameter petri dishes containing sterile glass coverslips and medium. G418 was not added to the medium to enhance the protein expression. The medium of one dish was supplemented with 10 µg/ml of mitomycin C (Sigma). Both dishes were incubated at 37^{o}C for 2 hours. The medium from both dishes was then aspirated and they were washed 3 times with PBS. Cells were then fed with a standard culture medium and incubated for 8 days at 37^{o}C. The coverslips with cells were then washed three times in PBS and fixed (2.4.1). They were then pre-blocked with Triton X-100 and stained with antibodies (Table 2.11) (2.4.3). Cells were then examined by wide-field fluorescence microscopy (Zeiss Axioplan 2).

2.7.2.3. Cell cultivation on different substrates

MDCK cells stably transfected with pBK-Tecta-IRES-turboFP635 were grown on sterile glass coverslips covered with special substrates which allow cell adhesion and spreading: BD Matrigel^{TM} (BD Biosciences), laminin (Sigma-Aldrich), poly-D-lysine (PDL) (Sigma-Aldrich) and ammonium polymerised collagen.

Glass coverslips were placed into 35 mm diameter petri dishes using sterile forceps and coated with individual substrates.

BD Matrigel^{TM} was thawed overnight at 4^{o}C and mixed with a pre-chilled pipette to ensure homogeneity. It was then diluted with cold culture medium without FBS to a concentration of 3 mg/ml. The diluted BD Matrigel^{TM} was added to glass coverslips so that it covered the entire cell growth surface. Dishes were incubated at room temperature for 1 hour while the BD Matrigel^{TM} polymerised onto the coverslip.

Afterwards, the medium was removed by aspiration, the dishes were rinsed with sterile PBS and used for culturing cells.

Laminin was diluted with HBSS (GibCo) to a concentration of 5 µg/ml and added onto the coverslips to cover the cell growth area. The dishes were incubated for 2 hours at 37^{o}C. The coating solution was then removed by aspiration and dishes were carefully washed with PBS.

Poly-D-lysine (PDL) working solution had a concentration 20 µg/ml and was prepared with sterile H_2O. Before culturing cells, dishes were incubated with PDL solution at room temperature overnight and rinsed with PBS.

Collagen substrate was prepared by spreading a drop of rat tail collagen (BD Biosciences) onto a glass coverslip with the back of the hook of a bent sterile glass Pasteur pipette in order to cover the entire surface of the coverslip with a thin layer of collagen. In a fume hood, 2 ml of 25 % ammonia solution (Fisher Chemical) was mixed with 1 ml of sterile H_2O and soaked into a piece of filter paper. It was then placed in a 140 mm petri dish (Sterilin) together with the petri dishes containing coverslips. The lids of the 35 mm diameter petri dishes were shifted to expose the coverslips. The ammonium polymerisation lasted for 25 min. Afterwards the petri dishes with the coverslips were covered with the lids again, transferred to the cell culture hood and left there for additional 15 min. The coverslips were then washed twice with sterile H_2O and used for culturing cells.

After a week of growing on coated coverslips and on one uncoated control coverslip, cells were fixed, preblocked with 0.1 % of Triton X-100 to permeabilise cell membranes and stained with antibodies (Table 2.11). The cells were then examined by wide-field immunofluorescence and confocal microscopy.

2.7.2.4. Generating cell spheres

To prepare the collagen - BD Matrigel™ master mix (CMM) the following compounds were mixed on ice in the order given: 700 µl acid-soluble rat tail collagen (BD Biosciences), 1700 µl sterile H_2O, 400 µl 10x minimum essential medium (MEM) (Sigma-Aldrich), 80 µl 1M hydroxyethyl-piperazine ethanesulafonic acid (HEPES) (Sigma), 36 µl 3 M NaOH, 360 µl fetal bovine serum (FBS) "Gold" (PAA), 40 µl 200 mM L-glutamine, 120 µl of a 11% $NaHCO_3$ solution and 640 µl BD Matrigel™ (BD Biosciences) (Sourisseau et al., 2006). 200 µl of CMM were placed on sterile glass coverslips in 35 mm petri dishes and allowed to set for 1 hour at 37°C. MDCK cells stably transfected with pCAG-mCherry-Tecta plasmid were washed twice with sterile PBS, treated with trypsin/EDTA, re-suspended in standard culture medium and counted. Cell concentration was adjusted with culture medium and the suspension was dispensed into 15 ml tubes, 10^5 cells per tube. The tubes were then centrifuged at 300g for 5 min (accuSpin™ 400 centrifuge, Fisher Scientific). The supernatant was aspirated, 200 µl of CMM was added to each tube and mixed with the cell pellet. The mixture was added on the top of the CMM layer on the coverslip, using the contents of one tube for each coverslip. Coverslips were incubated for 1 hour at 37° C and then 3 ml of MDCK medium was carefully added to each dish. The cells were grown for 1 week and 2 weeks at 37°C, they were then fixed, cryosectioned (2.4) and stained.

2.7.4. Gene-gun transfection of cochlear cultures

2.7.4.1. Mouse cochlear culture preparation

Mouse cochlear cultures were prepared by using a technique previously described (Russell and Richardson, 1987). P2 CD1 and *Tecta*$^{\Delta ENT/\Delta ENT}$/*Tectb* null mouse pups were killed by cervical dislocation. After the cartilaginous capsule was removed, cochleae were dissected in HEPES buffered (10 mM, pH 7.2) Hank's balanced salt solution

(HBSS). The stria vascularis and the modiolar tissue were removed and the cochlear coils were divided into apical and basal parts. The apical and basal coils were then explanted onto a rat tail collagen coated glass coverslip and fed with a drop of medium containing 93 % Dulbecco's modified Eagle's medium (DMEM) F-12 Ham nutrient mixture (Sigma) and 7 % FBS "Gold" (GE Healthcare, PAA) with 10 µg/ml ampicillin. Explanted cultures were sealed into Maximow slide assemblies with a mixture of wax and vaseline and grown for 24 hours at 37^{o}C.

2.7.4.2. Gene-gun gold bullets preparation

25 mg of 1 µm gold particles (Bio-Rad) were used to prepare each set of bullets. 10 mg of polyvinylpyrrolidone (PVP) (Bio-Rad) were diluted in 500 µl of fresh dry 100 % ethanol. 35 µl of this solution were added to 7 ml of fresh 100 % ethanol (Fisher Scientific) to obtain a PVP solution of final concentration 0.02 mg/ml. A stock solution of 0.5 M spermidine trihydrochloride was prepared as follows: 31.75 mg of spermidine trihydrochloride (Sigma) were added to 250 µl of sterile H_2O. The stock solution was then diluted ten-fold to prepare a 0.05 M working solution.

Spermidine trihydrochloride (50 µl of the 0.05 M working solution) was added to 25 mg of gold particles. The resulting gold suspension was vortexed (Spinmix) for 10 sec, sonicated for 10 sec in a Decon sonic bath (Ultrasonics Ltd.), then vortexed for 10 sec again and sonicated again for 10 sec. Plasmid DNA (50 µg) was added, and the mixture was vortexed for 5 sec. An equal volume of 1 M $CaCl_2$ was added to the mixture drop by drop, vortexing for 5 sec after the addition of each drop. The suspension was allowed to stand for 10 min at room temperature and then centrifuged for 15 sec in a bench centrifuge (accuSpin Micro, Fisher Scientific). The supernatant was discarded and the pellet was washed 3 times with 100% ethanol. The pellet was then re-suspended in 200

µl of 0.02 mg/ml PVP in ethanol, carefully mixed by pipetting up and down, and transferred to a microcentrifuge tube with the remaining 6.8 ml of 0.02 mg/ml PVP. The suspension was gently shaken for about 10 min to prevent gold particles from clumping. Bullets were made using Tefzel tubing with an external diameter of 3.175 mm and internal diameter of 2.36 mm (Bio-Rad). The tubing was pulled through the tubing holder of the Tubing Prep Station and dried with nitrogen for 10 min. Afterwards the gold-DNA suspension was loaded into the tubing with a syringe and allowed to settle for 5 min. The PVP solution was then slowly aspirated by the syringe. The tubing holder was first rotated through 180^{o}, allowed to stand for 4 sec to spread the gold and then rotated continuously for 30 sec to allow the gold to spread evenly on the inside surface of the tube. Nitrogen gas was flushed through the rotating tubing for 5 min at 0.35 l/min to dry the gold particles attached to the wall. After the coated tubing was removed from the holder the sparsely and unevenly coated ends were trimmed with a razor blade. The remaining part of the tube was cut on a Tubing Cutter (Bio-Rad) into individual cartridges of 1.27 cm length. Cartridges were stored at 4^{o}C in labelled 15 ml tubes with a bed of silica gel particles (BDH) isolated with foil.

2.7.4.3. Gene gun transfection

Cochlear cultures were transfected with the required plasmid DNA using a Helios^{TM} gene gun. The gene gun was connected to a helium gas tank and the pressure was set at 110 psi. An empty cartridge holder was inserted into the gun, and the gun was discharged 3 times to pressurise the system. Bullets were then loaded into the cartridge, and the cartridge was placed back in the gun. Cochlear cultures were taken out from the Maximow slide assembly, excess culture medium was aspirated with a piece of sterile filter paper. The coverslip with the culture attached was placed at the centre of the pedestal, covered with a fresh 3 µm cell culture insert (Becton Dickinson Labware) and

positioned directly under the gene gun. The gene gun was discharged once with a single bullet. The coverslip was immediately placed into the 35 mm petri dish and examined under the dissection microscope (Zeiss Stemi 2000). The "shot" was repeated if no gold was detected on the explants. 2 ml of Rat Cochlear culture Medium (RCM) (93 % of DMEM F-12, 7 % of FBS, 0.1 % of 10 µg/ml ampicillin) were added to the dish and the culture was incubated at 37^{o}C in a CO_2 incubator for 24 or 48 hours to allow gene expression.

2.7.5. Correlative light-electron microscopy

Wild type mouse cochlear cultures at P2+1 days *in vitro* (DIV) were gene gun transfected with pBK-EGFP-Tectb DNA, incubated for 24 hours at 37^{o}C, fixed and stained with goat anti-GFP (FITC) antibody (Abcam) at a dilution of 1:2000. Stained cultures were placed in a chamber with PBS and photographed using a SPOT camera mounted on a Zeiss Axioplan 2 microscope. Using wide-field fluorescence images, a montage was created in Adobe Photoshop 7.0 where cells of interest were marked. Cultures were then incubated with R7 primary antibody to Tectb and double-labelled with 10 nm gold-conjugated donkey anti-rabbit antibody (BBInternational) as described in section 5 of Appendix. They were then processed for either scanning electron microscopy (SEM) or transmission electron microscopy (TEM) (2.5). Montage maps obtained with light microscopy were used to identify and image cells of interest in the electron microscopy.

2.7.6. Western blotting

Cell and medium samples were collected as described in section 2.3.1 of. SDS-PAGE gel and blotting procedures were carried out as previously described (2.3.2 and 2.3.3).

For samples expressing Tecta a 7.5 % resolving gel was used; a 10 % resolving gel was prepared for samples expressing Tectb (2.3.2).

To detect Tecta protein in a medium or cell lysates R9 rabbit antiserum to chick α1-tectorin subunit (Knipper et al., 2001) was used at a dilution of 1:1000. mCherry protein was detected with a rat monoclonal antibody to monomeric red fluorescent proteins (ChromoTek) at a dilution of 1:1000. R7, rabbit antiserum to chick Tectb (Knipper et al., 2001) at a dilution of 1:1000 was used for Tectb protein detection. For EGFP protein anti-GFP rabbit serum (Invitrogen, Molecular probes), 1:1000, was used. Anti-rat alkaline phosphatase (AP)-conjugated IgG, generated in goat (DAKO), 1:1000, was utilised to detect anti red primary antibody. For other primaries, goat anti-rabbit AP-conjugated IgG (DAKO) was used at a dilution of 1:1000.

2.7.7. Immunolabelling and microscopy

The detailed procedures of sample preparation for immunofluorescence microscopy and TEM/SEM are described in sections 2.4 and 2.5. The list of antibodies used for immunofluorescence microscopy is shown in Table 2.11, for SEM/TEM - in Table 2.12. When phalloidin staining was used, the cells and cochlear cultures were first permeabilised with Triton X-100 (2.4.3).

Protein	Primary antibody	Primary antibody dilution	Secondary antibody (Molecular Probes, Invitrogen)	Secondary antibody dilution
Tecta	Anti-Tecta (R9)	1:1000	Alexa Fluor 488 goat anti-rabbit or 555 donkey anti-rabbit	1:500
Tectb	Anti-Tectb (R7)	1:1000	Alexa Fluor 488 goat	1:500

			anti-rabbit or 555 donkey anti-rabbit	
EGFP	Goat anti-GFP (FITC) (Abcam)	1:2000	Alexa Fluor 488 donkey anti-goat IgG	1:500
Stereocilin	Rabbit anti-stereocilin antibody	1:1000	Alexa Fluor 488 goat anti-rabbit	1:500

Table 2.11. Primary and secondary antibodies used for immunofluorescence microscopy

Protein	Primary antibody	Primary antibody dilution	Gold-conjugates	Gold-conjugate dilution
Tecta	Anti-Tecta (R9)	1:1000	10 nm gold-conjugated donkey anti-rabbit (BBInternational) Or 25 nm gold-conjugated donkey anti-rabbit IgG (Abcam)	1:10
Tectb	Anti-Tectb (R7)	1:1000	10 nm gold-conjugated donkey anti-rabbit (BBInternational)	1:10

Table 2.12. Primary antibodies and gold-conjugates used for TEM/SEM.

2.8. Materials and methods used for generating and studying Ceacam16 null mutant mouse

2.8.1. Making the Ceacam16 null mutant mouse

JM8A1.N3 embryonic stem (ES) cells (C57BL/6N background) with confirmed targeting of the *Ceacam16* gene were obtained from the Knockout Mouse Consortium (IKMC Project ID: 69148; UC Davis, California, USA), indirectly through the Wellcome Trust Sanger Institute (Cambridge, UK). The vector used for targeting *Ceacam16* in ES cells is shown in Fig.2.8.

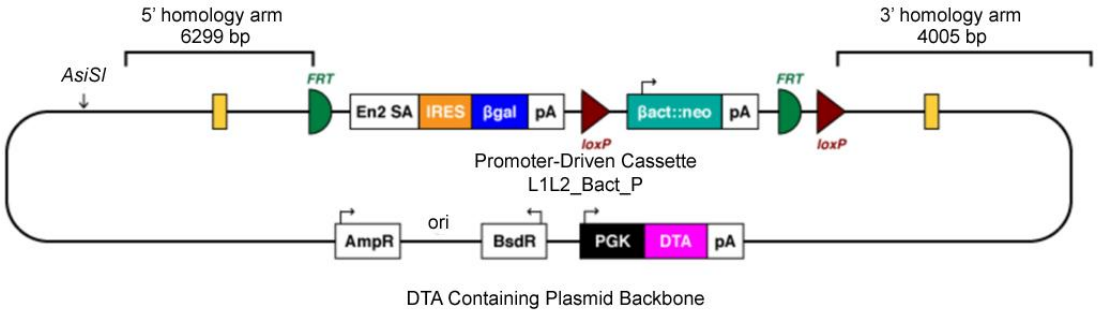

Figure 2.8. Construct used for ES cell targeting. Homology arms of 6299 bp (5') and 4005 bp (3') flank an L1L2 targeting cassette. Yellow rectangles in the 5' and 3' homology arms represent exons 1 and 6 respectively of *Ceacam16*. En2SA stands for En2 splice acceptor, IRES - internal ribosome entry site, βgal - β-galactosidase gene, pA - SV40 polyadenylation site. The neomycin resistance gene (neo) is driven by a human β-actin promoter. LoxP - lox P sites for cutting by Cre-recombinase, FRT-sites - flippase recognition target sites for interaction with the flippase recombination enzyme. The targeting cassette is inserted into R3R4_pBR_DTA+_Bsd_amp plasmid backbone which includes: a DTA (diptheria toxin A) negative selection cassette, a phosphoglycerate kinase 1 promoter (PGK), a blasticidin resistance sequence (BsdR), an ampicillin resistance sequence (AmpR) and a site for AsiSI restriction enzyme. Ori is an origin of replication site. The picture was obtained from the Wellcome Trust Sanger Institute webpage.

The *Ceacam16* gene in the ES cell line contains a targeted replacement of exons 2 to 5 with a bacterial lacZ ORF. The LacZ reporter encodes β-galactosidase that can catalyse the hydrolysis of X-Gal, producing a blue stain in cells in which *Ceacam16* is expressed. Therefore, in the cochlea of the *Ceacam16* null mutant mouse model a blue staining will appear in the cells that would normally express the *Ceacam16* gene.

I microinjected targeted ES cells into the blastocysts from the albino C57BL/6J-*Tyr*$^{c\text{-}2J}$ mice (Charles Rivers, UK). Microinjected blastocysts were surgically transferred into F1 pseudopregnant females. If the coat of a mouse pup obtained from the injections consisted of black and white patches, I identified the animal as chimeric (Fig.2.9). Non-chimeric newborns were albino. Chimeric male mice were then mated to C57BL/6J-*Tyr*$^{c\text{-}2J}$ animals of albino background. Patched offspring confirmed germ line transmission.

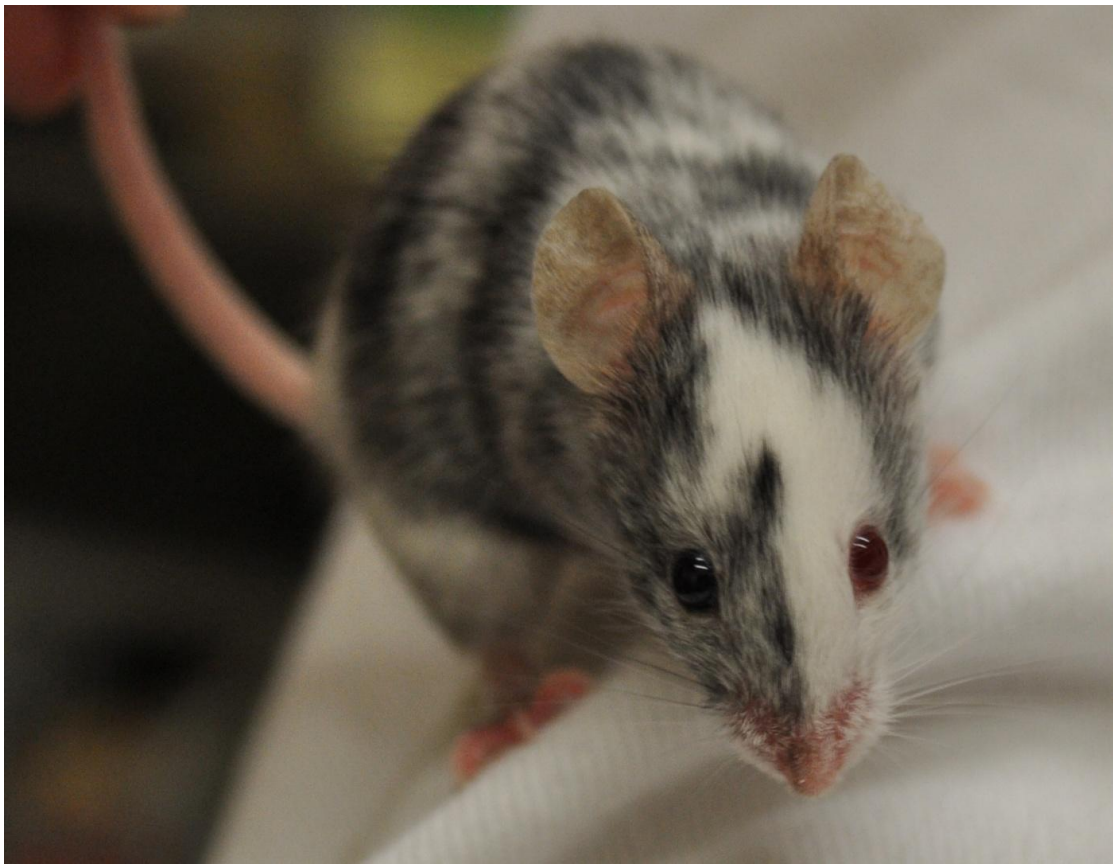

Figure 2.9. A chimeric mouse pup is identified by a coat which is a mix of black and white patches. Note the left eye is black and therefore of C57B1/6N origin and the right eye is red and of C57BL/6J-*Tyr*$^{c\text{-}2J}$ albino origin.

2.8.2. Genotyping mice

For genotyping *Ceacam16* targeted mice, genomic DNA was isolated from tail snips (Legan et al., 2000). To minimise the number of steps in the genotyping protocol, DNA was not purified and its concentration was not measured. The PCR reaction mixture was set up as follows:

Reagents	Amount used
10x PCR reaction buffer with 20 mM $MgCl_2$	2.5 µl

10 mM dNTPs	0.5 µl
25 pmol forward primer	0.5 µl
25 pmol reverse primer	0.5 µl
Uracil-DNA Glycosylase (Roche)	0.4 units
Extracted DNA	2 µl
FastStart Taq DNA polymerase (Roche)	0.5 units
Sterile H_2O	18.65 µl

Table 2.13. Genotyping PCR mixture.

The following primers were used:

Primer	Sequence	Location
CeagenF1	5'GGGGCATACCTAGCAAGAGTAAGG3'	located at the 3' end of exon5
Lar3.1	5'GTGTTGCCCAAGAAGACAATCAGG3'	anneals to the 5' end of the en2-intron
CeagenF2	5'CAAGGACCTGCTAGTCTATGCCTG3'	complementary to the middle of exon5
CeagenR2	5'AGGGTAGGGTGTGACGAGTGAGTG3'	located at the 5' end of intron 5

Table 2.14. Primers used for genotyping PCR.

Reactions were cycled as listed:

6. initial denaturation at 94^{o}C for 2 min
7. denaturation at 94^{o}C for 15 sec
8. annealing at 60^{o}C for 20 sec

9. extension at 72^{o}C for 30 sec
10. final extension at 72^{o}C for 5 min

Steps 2 to 4 were repeated 40 times. PCR products were analysed by gel electrophoresis (Appendix 1.4). For wild type mice a product of 265 bp was amplified with CeagenF2 and CeagenR2 primers. Primers CeagenF1 and Lar3.1 amplified a 308 bp fragment in mutant mice. Both products were detected in heterozygous animals.

2.8.3. Transient expression of Ceacam16 and Tectb in HEK 293 cells

HEK 293 cells were cultured as described in 2.2.1, and transiently transfected with plasmid constructs according to 2.2.2. Two plasmids were used, pcDNA6-Ceacam16-V5His (a kind gift from Dr. Jing Zheng, Northwestern University, Chicago, USA) expressing Ceacam16 C-terminally tagged with V5 and 6His tags (Fig.2.10) and pBK-EGFP-Tectb, expressing N-terminally EGFP tagged Tectb (Fig.2.5, b).

HEK 293 cells were transfected with individual plasmids and also co-transfected with both plasmids. Sham transfected controls were used. All transfections were performed in duplicate. 24 hours after transfection cells were fed with a serum-free medium. 48 hours later the medium was collected and used for western blotting.

2.8.4. Co-immunoprecipitation of Tetctb and Ceacam16 proteins from culture medium and western blotting

Serum free cell culture medium was collected as described in Appendix 3.1 and then centrifuged at 50,000 rpm for 15 min at 4^{o}C using a Beckman TL-100 Ultracentrifuge to pellet cell debris. One set of culture media from Sham, Tectb, Ceacam16 and Tecb+Ceacam16 transfections was incubated with 0.6 mg/ml rabbit anti-Tectb IgG pooled serum. The antibody was prepared by Dr. Kevin Legan to the amino acid sequence HPSFPPKKKLPSFWKR from the ZP domain of Tectb.

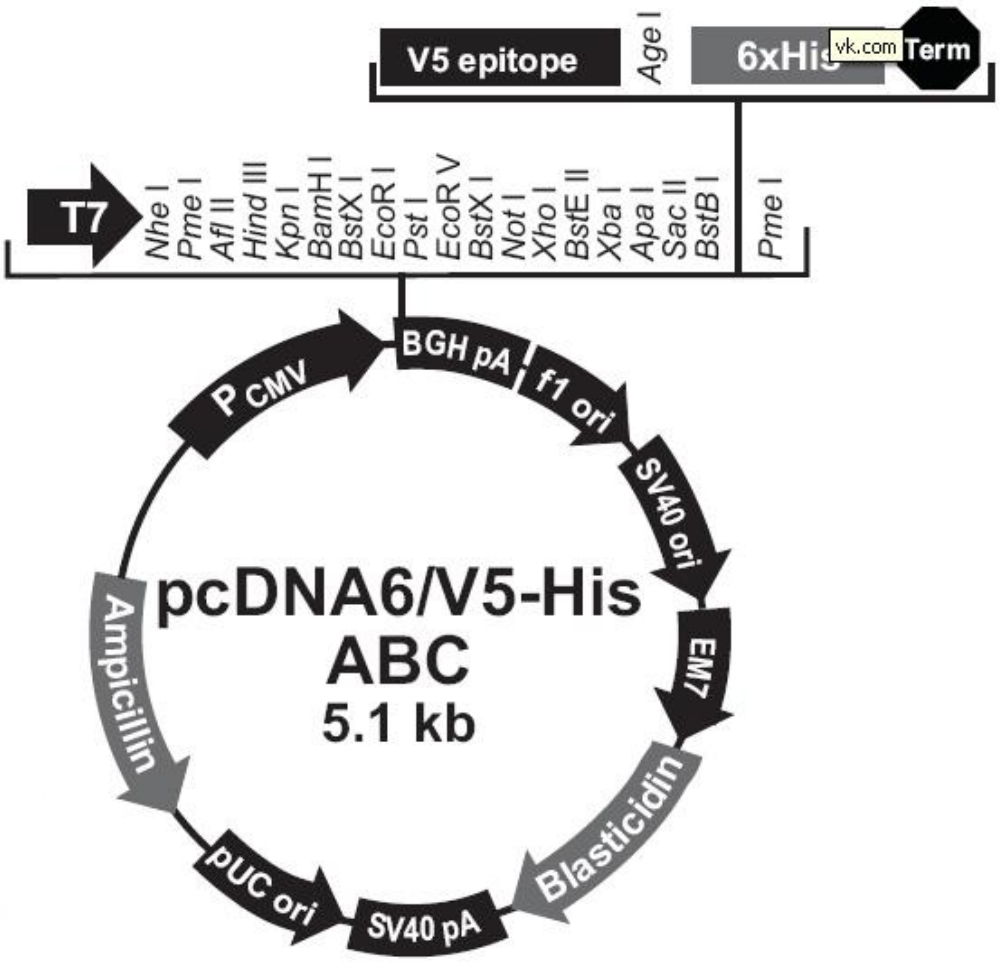

Figure 2.10. Schematic representation of pcDNA6/V5HisB plasmid. pCMV - human cytomegalovirus immediate early promoter, BGH pA - bovine growth hormone polyadenylation sequence, f1 ori - origin of replication site, SV40 ori - SV40 promoter and origin, EM7 - bacterial EM7 promoter, Blasticidin - blasticidin resistance gene ORF, SV40 pA - SV40 polyadenylation sequence, pUC ori - pUC origin of replication, Ampicillin - ampicillin resistance gene ORF. T7 promoter sequence is followed by a polylinker, which contains V5 epitope connected to 6xHis tag through an AgeI restriction site. Term stands for a termination codon sequence (map is modified from an Invitrogen data sheet).

Culture media from the second set of Sham, Tectb, Ceacam16 and Tecb+Ceacam16 transfectants was incubated with rabbit polyclonal anti-V5 antiserum (Sigma, V8137) at a dilution of 1:2000. This process of pulling protein complexes from the culture medium is further referred as a pull down.

Tubes were incubated at 4^{o}C for 24 hours on the rotator. Meanwhile, 25 mg of protein A-Agarose (Sigma-Aldrich) were re-suspended in 1 ml of PBS. The mixture was centrifuged at 13,000 rpm for 1 min at room temperature using a benchtop centrifuge (accuSpin Micro, Fisher Scientific). The supernatant was discarded and the pellet of a swollen protein A-agarose was washed twice more with PBS. Afterwards, 40 µl of the 1:1 protein A-agarose suspension in PBS were added into each immunoprecipitation mixture. Tubes were then rotated for an additional 2 hours at 4^{o}C. The protein A-agarose was then pelleted by brief centrifugation at 13,000 rpm at room temperature and then washed three times with PBS. The pellets were mixed with 30 µl of 1x RSB, boiled at 104^{o}C for 4 min, mixed by pipetting, centrifuged for 1 min at 13,000 rpm and then electrophoresed through a 10 % SDS-PAGE gel (2.3.2). Western blotting and protein visualization were performed as in 2.3.3. Duplicate western blots were set up for each immunoprecipitation reaction. Antibodies used for probing the polyvinylidene difluoride (PVDF) membrane are summarised in Table 2.15. All primary and secondary antibodies were used at a dilution of 1:1000.

Antibodies used for pulling down proteins from the culture medium	Antibodies used for probing PVDF membrane	
	Primary antibody	Secondary antibody
Rabbit anti-Tectb IgG pooled serum	Rabbit anti-Tectb IgG pooled serum	Goat anti-rabbit AP-conjugated IgG (DAKO)
	Monoclonal anti-V5 antibody (Invitrogen)	Goat anti-mouse AP-conjugated IgG (DAKO)

Rabbit polyclonal anti-V5 antiserum	Rabbit anti-Tectb IgG pooled serum	Goat anti-rabbit AP-conjugated IgG (DAKO)
	Monoclonal anti-V5 antibody (Invitrogen)	Goat anti-mouse AP-conjugated IgG (DAKO)

Table 2.15. Antibodies used for protein immunoprecipitation and for western blotting.

2.8.5. Western blotting of tectorial membranes lysates

The TMs were dissected from cochleae into HEPES-buffered (10 mM, pH 7.2) HBSS. The TM lysates were prepared according to the procedure described in Legan et al., 2000. A modified step-gradient gel was used to perform SDS-PAGE electrophoresis. 4 µl of each sample (approximately two tectorial membranes) were loaded onto the 4 % stacking gel and resolved on a complex resolving gel consisting of the 8.25 % resolving gel on top and the 12 % resolving gel underneath. Proteins were transferred onto Hybond-P membrane using a wet transfer protocol. For the wet transfer, gel pad, membrane, filter papers and transfer foams were equilibrated with transfer buffer (25 mM Tris, 192 mM glycine, 10 % methanol). The transfer sandwich was assembled as follows: negative electrode, the transfer foam, three sheets of Whatman 3 MM paper, the gel, the PVDF membrane, three pieces of Whatman 3 MM paper, the transfer foam and the positive electrode. The sandwich was clamped vertically and placed in the tank with a transfer buffer. The transfer was performed overnight at 30 V (constant voltage) keeping the buffer temperature at 4^{o}C. The membranes were probed with rabbit purified IgG to the CGRLEIHRNKNSTTVESK amino acid sequence of Tecta at a dilution of 1:1000, rabbit purified IgG to the CYNKNPLDDFLRPDGR amino acid sequence of Tectb at a dilution of 1:1400 (both antibodies generated by Dr. Kevin Legan) and rabbit

anti collagen type IX antibody at a dilution of 1:1500. Anti-Ceacam16 staining was performed with anti Ceacam16 antibody (kindly provided by Dr. Jing Zheng, Northwestern University, Chicago, USA) which was generated to SLLVQKLNLTDAGRYTLKTVT amino acid sequence of IgV-like N2 domain of Ceacam16 (Fig.2.11) and used at a dilution of 1:20000. The secondary antibody used for all four primary antibodies was horseradish peroxidase (HRP)-linked anti-rabbit IgG (True-blot, eBioscience) at a dilution of 1:1000. The band densitometry analysis was performed using Image J software. The amount of Tecta and Tectb in the TMs of *Ceacam16*$^{\beta gal/\beta gal}$ mice was expressed as a percentage of that seen for Tecta and Tectb in *Ceacam16*$^{+/\beta gal}$ mice. Collagen type IX was used to normalise the amount of protein present when quantifying the density of the Tecta and the Tectb bands.

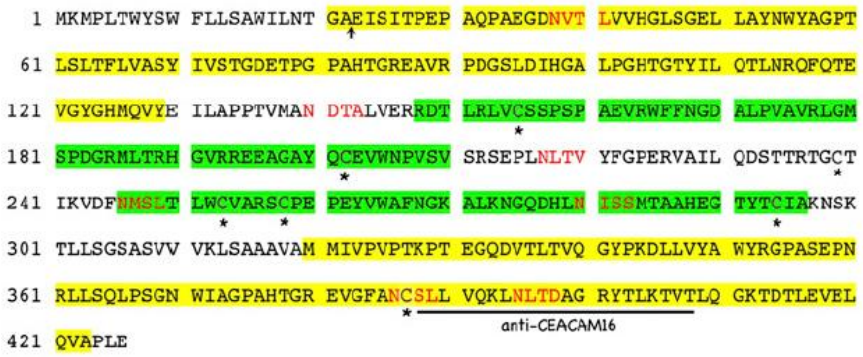

Figure 2.11. Amino acid sequence of Ceacam16. Yellow colour marks IgV-like domains, green indicates IgC-like domains. Seven predicted N-glycosylation sites are shown in red. The arrow marks the proteolytic cleavage site downstream from the signal peptide, a characteristic of secreted or transmembrane proteins, asterisks indicate cysteine residues. The peptide sequence used to generate the anti-Ceacam16 antibody is underlined. From Zheng et al., 2011.

2.8.6. Light and transmission electron microscopy

Animals were killed by cervical dislocation. Cochleae were rapidly removed and placed in PBS for dissection, the oval and round windows were opened, and the apex of each cochlea was punctured. For TEM about 50 µl of fixative (2.5) was perfused through the

openings, and the cochleae were fixed in the same fixative for additional 2 hours. After the fixation, cochleae from animals older than 3 weeks were decalcified with 0.5 M EDTA (pH 8.2) for 7 days at 4^{o}C. Cochleae were then postfixed in 1 % OsO_4 (detailed description in 2.5). The cochleae were then dehydrated, equilibrated with propylene oxide and imbedded in Epon as described in section 2.5. For light microscopy, 1 µm sections were stained with toluidine blue and then photographed with a SPOT camera mounted on a Zeiss Axioplan 2 microscope. Ultrathin sections for TEM were prepared according to section 2.5.

2.8.7. Immunofluorescence microscopy and X-Gal staining detection

Cochleae were dissected as in 2.8.6 and used either for staining with X-Gal (2.6) or cryosectioned (2.4.2) for immunostaining (2.4.3). Whole mounts of cochleae stained with X-Gal were photographed under a Leica MZ10F microscope using a ProgRes C3 camera and then re-fixed, cryosectioned and imaged using Zeiss Axioplan 2 microscope. Cryosections of the cochleae for immunostaining were preblocked with 10 % HS in PBS and then stained with primary antibodies (Table 2.16) overnight in a humid chamber. Afterwards, the slides were washed 3 times in PBS, stained with a secondary antibody, washed again and mounted as described in 2.4.3. Sections were analysed using a fluorescence Zeiss Axioplan 2 microscope.

Protein	Primary antibody	Primary antibody dilution	Secondary antibody	Secondary antibody dilution
β-galactosidase	anti-β-galactosidase (anti-βgal)	1:200	Alexa Fluor 488 goat anti-rabbit	1:500

	(Promega)			
Ceacam16	anti-Ceacam16 (CC16)	1:1000	Alexa Fluor 488 goat anti-rabbit	1:500
Otoancorin	anti-otoancorin (OA)	1:1000	Alexa Fluor 488 goat anti-rabbit	1:500
Tecta	anti-Tecta (R9)	1:1000	Alexa Fluor 488 goat anti-rabbit	1:500
Tectb	anti-Tectb (R7)	1:1000	Alexa Fluor 488 goat anti-rabbit	1:500
Collagen IX	anti-collagen IX (M2)	1:1000	Alexa Fluor 488 goat anti-rabbit	1:500
Otogelin	anti-otogelin (OG)	1:1000	Alexa Fluor 488 goat anti-rabbit	1:500

Table 2.16. Antibodies against proteins expressed in the organ of Corti of *Ceacam16* null mutant mice and the dilutions at which they were used.

For lectin staining sections were preblocked with 3 % bovine serum albumin (BSA) (Sigma-Aldrich) in PBS for an hour and then stained with FITC-conjugated soybean agglutinin (SBA) (Vector labs) at a dilution of 1:1000. Staining was performed overnight in a humid chamber.

Texas Red phalloidin or fluorescein phalloidin were used as counter-stains at a dilution of 1:500.

2.8.8. Cochlear microdissection

When sectioning fixed cochleae for immunofluorescence/toluidine blue staining, the blade goes through the organ of Corti as shown in Fig.2.12. Therefore four turns of the organ of Corti named apical 1, apical 2, basal 1 and basal 2 are observed in the cross-section through the cochlea (refer to Fig.2.12).Unless stated otherwise, apical 2 and basal 2 turns are described in the results section.

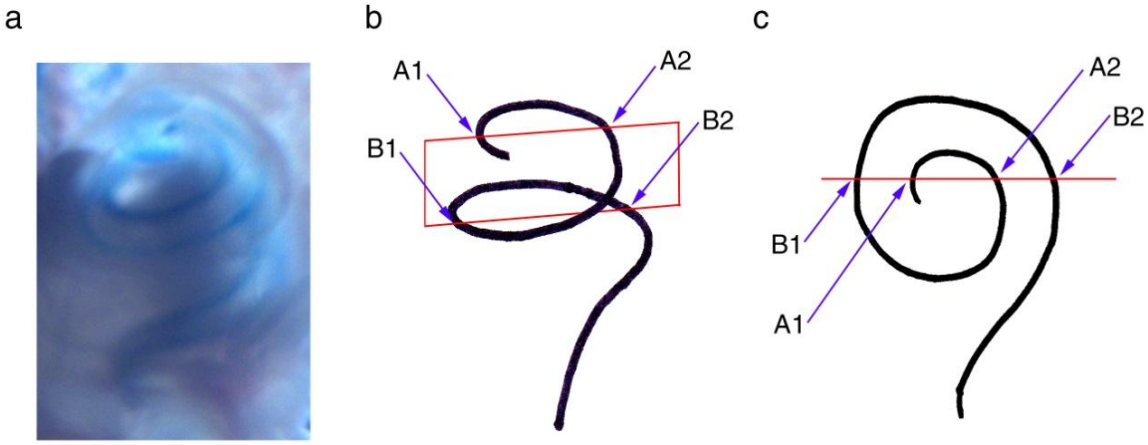

Figure 2.12. Sectioning of the mouse cochlea. Panel a - fixed cochlea whole mount from a *Ceacam16* null mutant mouse showing the spiral of the organ of Corti stained with X-Gal. B and c are schematic representations of the organ of Corti in back/front (b) and up/down (c) views. The red rectangle in b and red line in c represent the sectioning blade. As a result, four cochlear turns are observed in the cross-section: apical 1 (A1), apical 2 (A2), basal 1 (B1) and basal 2 (B2).

CHAPTER 3

Development of an *in vitro* model system for studying the processing, secretion and assembly of tectorial membrane proteins

3.1. Introduction

Alpha-tectorin (Tecta) and beta-tectorin (Tectb) are glycoproteins that are found exclusively in the inner ear. Through interaction with each other and with other proteins they form the secreted matrix of the otoconial and tectorial membranes. In the tectorial membrane (TM), Tecta and Tectb form the striated-sheet matrix which surrounds the radially orientated collagen fibrils (Hasko and Richardson, 1988). The structure of both tectorins suggests that they can form hetero- or homopolymers. It is, however, unclear how these proteins are secreted, processed and assembled into the matrices observed, and how deafness-causing mutations in Tecta influence these processes.

As the epithelial cells of the inner ear that produce the tectorins *in vivo* are extremely difficult to access and isolate, the aim of this project was to create an *in vitro* cell transfection model which could help to examine some of these processes (Zheng at al, 2010). Unpublished observations from the host laboratory indicated that non-polarised cell lines, such as human embryonic kidney 293 cells (HEK293), failed to secrete tectorins on their surfaces. Thus I transiently transfected polarised Madin-Darby canine kidney (MDCK) and colorectal adenocarcinoma 2 (CaCo2) cell lines of epithelial origin with fluorescently-tagged tectorin constructs to determine whether these proteins can be

expressed *in vitro*. Microvilli which are similar in structure to hair cell stereocilia were elongated by transient over-expression of fluorescently-tagged espin (Zheng et al., 2010). MDCK derived cell lines stably expressing tectorin constructs were utilised to study processing and secretion of the tectorins. Stable cells grown in a mixture of collagen and Matrigel^{TM} formed polarised epithelial spheres expressing tectorin filaments in the lumen (Witteveen, 2008). To circumvent some disadvantages of cell monolayer and sphere models, I used gene gun transfection to transfect the recombinant tectorin constructs into various cell types in neonatal mouse cochlear cultures. Mutations in the ZP domain of Tecta that are known to cause human hereditary hearing loss I introduced by site directed mutagenesis into the ZP domain of Tectb encoding plasmid, and studied their effect on matrix formation.

3.2. Results

3.2.1. The MDCK cell monolayer system as an *in vitro* model for studying tectorin secretion and assembly

3.2.1.1. Choosing an appropriate cell line

As hair and supporting cells of the organ of Corti are epithelial cells, it is possible that certain characteristics of epithelial cells, e.g. apical-basal polarity, specialised cell to cell contacts and free apical surface, might be essential for expressing tectorial membrane proteins. Thus, the choice fell on established fast-growing epithelial cell culture models, MDCK and CaCo2 cells. Both cell types were transiently transfected with pBK-Tecta-IRES-turboFP635 plasmid to induce Tecta expression. The transfection experiment was repeated at least three times to ensure that the obtained results are reliable. Due to the presence of the IRES, turboFP635 was expressed as a separate protein. Cells were co-transfected with Espin-EGFP encoding construct to elongate the

apical microvilli which are related to hair cell stereocilia. Both transfected cell lines expressed Tecta protein (Fig.3.1, a, a') and displayed enhanced microvilli growth (Fig.3.1, b, b'). Confocal microscopy indicated that MDCK cells secreted Tecta on their apical surface where it aggregated among the microvilli (Fig.3.2, a, c). CaCo2 cells, in contrast, did not show any signs of extracellular Tecta expression and accumulated the protein in the cytoplasm (Fig.3.2, d, f). Based on these observations, MDCK cells were selected for further *in vitro* work.

3.2.1.2. pBK-Tecta-IRES-turboFP635 stably transfected cells

To study how tectorins form extracellular matrix and how deafness causing mutations in Tecta can disrupt this process, high levels of protein expression are required. Having a cell monolayer where every cell expresses tectorins on its apical surface would greatly facilitate TEM and SEM investigations. To achieve a long-term high-rate of expression of tectorins by MDCK cells, a stable transfection protocol was utilised. G418 positive selection of MDCK cells stably transfected with the pBK-Tecta-IRES-turboFP635 construct revealed that the red fluorescence of turboFP635 protein, with an excitation wavelength of 588 nm (similar to that of Texas Red phalloidin), was not detected with the rhodamine filter during the live fluorescence microscopy screening. Thus, the screening was performed on fixed duplicate dishes stained with anti-Tecta antibody.

After the cloning was repeated twice (the procedure is detailly explained in 2.7.2.1), two cell lines expressing Tecta were selected from derived neomycin-resistant colonies of a number greater than 15: line 7 (Fig.3.3, a - c) and line 11 (Fig.3.3, a' - c'). The majority of cells in both cell lines seemed not to express Tecta on their apical surface, although a few of the line 7 cells might have secreted Tecta extracellularly (Fig.3.3, a and c).

Confocal microscopy of cell line 7 indicated that Tecta-positive cells secrete amorphous Tecta aggregates on their cell apical surface (Fig.3.4, a' and c'). Tecta expression in line 11 cells was seen throughout the cytoplasm in a non-polarised manner with no signs of secretion on the cell surface (Fig.3.5, a' and c'). Based on the presence of extracellular Tecta expression, line 7 was chosen for further work.

3.2.1.3. Mitomycin C treatment of Tecta expressing cells

It is possible that to effectively secrete Tecta on the apical surface, MDCK cells first need to accumulate enough protein inside. The process of protein accumulation would be disrupted by mitosis. Mitomycin C was used to prevent cell division in the pBK-Tecta-IRES-turboFP635 stable cell line. Wide-field fluorescence microscopy showed that Tecta expression in both control and Mitomycin C treated cells was intracellular and no bright surface-associated aggregates were observed (Fig.3.6, c and c'). Intracellular Tecta expression in non-Mitomycin C treated cells (Fig.3.6, a and c) was even brighter than in Mitomycin C treated ones (Fig.3.6, a' and c'). Although Mitomycin C treatment did not increase Tecta expression, it increased the size of the cells (Fig.3.6, b' and c').

3.2.1.4. Influence of different substrates on Tecta expression

As epithelial cells grow on a basement membrane *in vivo*, it is possible that cultivating stably transfected MDCK cells on various extracellular matrices would enhance cell polarisation and increase extracellular Tecta expression.

Line 7 cells cultured on laminin (LM), poly-D-lysine (PDL), Matrigel^{TM} (MG) as well as control cells grown directly on a glass coverslip did not show a significant increase in the levels of extracellular Tecta expression (Fig.3.7, a, b, c and e). Interestingly, cells grown on MG could be characterised as sphere-shaped (Fig.3.7, c'). The highest levels

of Tecta expression that might be extracellular were observed for cells grown on ammonia-polymerised collagen (CG) (Fig.3.7, d and d'). Confocal microscopy of the CG-grown cells confirmed the extracellular localisation of Tecta aggregates (Fig.3.8).

However, despite some success with enhancing extracellular expression of Tecta by culturing cells on an appropriate substrate, the small numbers of Tecta-positive cells still posed a problem in creating an effective model of Tecta expression.

3.2.1.5. Stable cell lines generated with CAG promoter constructs

New mammalian expression vectors utilising the CAG promoter composed of the cytomegalovirus immediate early enhancer (Foecking and Hofstetter, 1986) upstream of the chicken β-actin/rabbit β-globin (AG) promoter (Miyazaki et al., 1989; Niwa et al., 1991) were used for stable transfection of MDCK cells. To enable cell screening for Tecta-positive cells with live fluorescence microscopy, mCherry, a red fluorescent protein with improved brightness and photostability, was fused to the N-terminal end of the Tecta protein. Fusing the mCherry and Tecta coding sequences gives an advantage of determining Tecta expression and localisation by mCherry fluorescence signal.

Transient transfection of MDCK cells with pCAG-mCherry-Tecta along with EGFP-Espin showed that the mCherry fluorescence signal had an intensity high enough to be detected at both low (Fig.3.9, a) and high (Fig.3.9, a') magnifications. EGFP-Espin co-transfection caused the prolongation of microvilli on cell apical surfaces. A cell line expressing mCherry-Tecta without EGFP-Espin was generated, as this allowed immunolabelling of Tecta through the GFP channel.

After a final round of cloning, the cell monolayers of at least five selected clones observed using wide-field fluorescent microscopy appeared to be monoclonal in origin with each cell expressing mCherry (Fig.3.10, b). After seven days of culturing *in vitro*

the presence of several matrix aggregates on the cell apical surfaces was revealed by anti-Tecta staining (Fig.3.10, a and c). Confocal microscopy of the aggregates enclosed in the box on Fig.3.11 showed that mCherry-Tecta fusion protein formed amorphous aggregates on cell apical surface and green (Tecta) and red (mCherry) fluorescence signals co-localised as expected (Fig.3.11, c and c'). However, the co-localisation of Tecta and mCherry signals was not observed in all cells. Fig.3.12 shows an example of a cell found on the same glass coverslip as the cell in Fig.3.11. It displayed aggregates stained with anti-Tecta antibody as well as mCherry-only aggregates on the apical surface.

Western blots of cell lysates and culture medium probed with anti-Tecta (R9) antibody revealed a broad band of approximately 260 kDa (Fig.3.13, b, lanes 3 and 4) which possibly represented the mCherry-Tecta fusion and was more distinct in cell lysates. Anti-RFP antibody detected a similar band with more protein and of slightly heavier mass in cell lysates (Fig.3.13, c, lane 5). In culture medium it revealed a double band which might represent glycosylated (larger band) and unglycosylated (smaller band, also detected with R9) forms of mCherry-Tecta (Fig.3.13, c, lane 6). These data might suggest that R9 does not react with glycosylated form of Tecta. Anti-RFP reacted with two additional bands of 60 and 63 kDa in both cell lysates and culture medium. As these bands were not detected by R9 antibody they possibly represent mCherry protein fused with a fragment of N-terminal Tecta. The western blotting experiments were repeated at least three times with consistent results.

SEM of stable mCherry-Tecta cells detected mCherry-Tecta protein on the cell's apical surface (Fig.3.14, a). However, Tecta failed to form filaments similar to those observed *in vivo*, and gold particles appeared to be tightly associated with microvilli and

protrusions (Fig.3.14, a). Since *in vivo* the TM matrix is normally formed by both Tecta and Tectb proteins, it was reasoned that co-expression with Tectb might enhance matrix formation. Confocal microscopy of the stable mCherry-Tecta cells co-transfected with the pBK-EGFP-Tectb construct showed that both Tecta and Tectb were secreted as small aggregates on cell apical surfaces. The expression patterns of the two proteins, however, hardly overlapped (Fig.3.15). No enhancement of tectorin aggregates was observed in response to co-expression.

Hence, although using the pCAG-mCherry-Tecta vector enabled live selection by red fluorescence, the model still displayed some issues:

1. mCherry-Tecta expressed on the apical cell surface could diffuse or be shed into the culture medium.

2. Time course experiment repeated minimum three times showed that at least 7 days of incubation were required for cells to accumulate sufficient extracellular mCherry-Tecta for detection by fluorescence microscopy (Fig.3.16).

Consistent with the data for stable mCherry-Tecta cells, only a few extracellular EGFP-Tectb punctae were observed in a minimum five examined clones of MDCK cells stably transfected with the pCAG-EGFP-Tectb construct after seven days of incubation (Fig.3.17). EGFP and anti-Tectb signals did not necessarily co-localise (Fig.3.17, c). Confocal microscopy provides an example of EGFP-Tectb fusion protein aggregates (Fig.3.18).

Western blotting of cell lysates and culture medium with both anti-Tectb (Fig.3.19, b) and anti-GFP (Fig.3.19, d) antibodies repeated at least three times revealed a broad band at around 65 kDa corresponding to the mass expected for an EGFP-Tectb fusion protein.

In addition, the anti-Tectb antibody detected a broad band of approximately 43 kDa in both the cell lysates and the culture medium (Fig.3.19, b, lanes 3 and 4) which would correspond to Tectb protein lacking the EGFP fusion. EGFP protein was observed as multiple bands of around 25 kDa in the culture medium lane only (Fig.3.19, d, lane 8). The EGFP-Tectb and the Tectb proteins secreted into the culture medium were of a slightly higher mass than the proteins detected in cells.

Thus, the Tectb stable cell line model encountered the same problems as the Tecta line: it took several days to produce matrix and much of the exported protein was secreted into the culture medium.

3.2.2. Epithelial cell spheres as a model of Tecta expression

Because one of the main disadvantages of a monolayer model was the loss of tectorins into the culture medium, the ability of MDCK cells to form hollow cysts in collagen-Matrigel^{TM} mix (Sourisseau et al., 2006) was exploited to create a cellular "trap" for secreted proteins. The apical surfaces of the cells in such structures are directed inwards. Confocal microscopy of spheres formed from stably transfected mCherry-Tecta cells grown in collagen-Matrigel^{TM} mix for two weeks showed that mCherry-Tecta fusion protein accumulated within the lumen (Fig.3.20, a and b). mCherry signal was also detected within the cells (Fig.3.20, b and c).

TEM analysis revealed that the sphere lumen was packed with matrix-like material (Fig.3.21). It consisted of fine branched interconnecting filaments with a diameter of 6-9 nm which were attached to the microvilli.

Thus polarised epithelial spheres were able to accumulate Tecta and produce a filamentous matrix in the lumen. However, the spheres took up to two weeks to produce high amounts of matrix which is consistent with previous studies (Witteveen, 2008).

Over this time cellular debris could accumulate inside the spheres too, making interpretation difficult.

3.2.3. Matrix production in mouse cochlear cultures transiently transfected with recombinant tectorin constructs

It is possible that problems observed in the epithelial cell monolayer and 3D culture models might be solved by using cultures of inner ear sensory epithelium, a system which normally builds the TM *in vivo* and might, therefore, meet all the requirements for effective tectorin secretion and matrix assembly. EGFP-Tectb and mCherry-Tecta encoding plasmids were delivered into wild type and *Tecta*$^{\Delta ENT/\Delta ENT}$/*Tectb* null (Legan et al., 2000; Russell et al., 2007) mice cochlear explants by biolistic transfection with a helium gene gun.

3.2.3.1. EGFP-Tectb expression

Live fluorescence microscopy of wild type mouse inner ear explants revealed that gene gun transfection with pBK-EGFP-Tectb DNA triggered a robust production of matrix-like material by different cell populations just 24 hours after transfection (Fig.3.22). Outgrowth zone cells produced a significant amount of EGFP-positive matrix forming either vermiculate structures (Fig.3.22, a and c) or amorphous masses (Fig.3.22, b) which appeared to be situated on the apical surfaces of the cells. In outer and inner hair cells, EGFP-signal appeared to associate with the hair bundle (Fig.3.22, d, e and f). Supporting cells of the GER that are characterised by a long narrow body and a small apical surface area expressed Tectb within the cytoplasm and produced a single patch of matrix on their apex (Fig.3.22, g, h and i). The same rapid EGFP-Tectb matrix production was observed in gene gun transfected cochlear cultures prepared from *Tecta*$^{\Delta ENT/\Delta ENT}$/*Tectb* null mutant mice (Fig.3.23).

Confocal microscopy confirmed the extracellular nature of the EGFP-positive matrix aggregates generated by outgrowth zone cells (Fig.3.24). These aggregates ranged in shape and size from small grain-shaped matrix particles (Fig.3.24, a) to bigger amorphous aggregates (Fig.3.24, b and c) and thick strips of EGFP-positive material (Fig.3.24, d) that stayed in close contact with the plasma membrane (Fig.3.24, a', b', c' and d'). GER cells expressed a fluffy-looking EGFP-positive material which was secreted onto the apical surface of the cell and appeared to be attached to the microvilli (Fig.3.25). In Deiter's cells, amorphous matrix material covered the entire cell apical surface (Fig.3.26, a, b and c) and stayed in a close contact with cell microvilli as well (Fig.3.26, panels a', b' and c'). Fig.3.27 gives another example of Deiter's and GER cells secreting extracellular matrix. In transfected outer and inner hair cells, EGFP-positive matrix was detected at the distal area of the hair bundle where it formed a matrix cap around the tip of each stereocilium (Fig.3.28). Some EGFP-positive material was also present around the edge if the cell and had an extracellular nature (Fig.3.29). However, due to the damage caused by gene gun only five EGFP-Tectb transfected hair cells were examined in this thesis: three cells by confocal microscopy and two cells by TEM.

Thus using gene gun transfection of mouse cochlear cultures as a model for studying Tectb expression provided the following advantages:

1. Rapid matrix production was observed within 24 hours of transfection.

2. Matrix production could be studied in different cell types.

3.2.3.2. Correlative light-electron microscopy of mouse cochlear cultures transiently expressing EGFP-Tectb

Fig.3.30 shows a photomontage created from immunofluorescence images of a mouse cochlear culture that were transiently transfected with the construct encoding EGFP-Tectb and stained with goat anti-GFP antibody after fixation. An outgrowth zone cell expressing high levels of EGFP-positive matrix on its apical surface organised in a few discrete bean-shaped aggregates (Fig.3.30, a and b) was chosen and subsequently identified using SEM. Prior to SEM imaging, the culture was re-stained with anti-Tectb antibody and labelled with gold-conjugated anti-rabbit antibody. Fig.3.31 illustrates the correlation between the light microscopy image of one of the matrix aggregates (Fig.3.31, a) on the apical surface of the outgrowth zone cell described above and the same structure imaged using SEM (Fig.3.31, b). SEM revealed that the bean-shaped aggregate on the surface of the outgrowth zone cell was an amorphous 3D structure which was attached to the cell by microvilli protruding from its edges (Fig.3.31, c). The aggregate was labelled with gold particles and therefore contains Tectb protein (Fig.3.31, d).

Toluidine blue staining of a cross-section through an outgrowth zone cell that was first located by immunofluorescence labelling (Fig.3.32, a) and had EGFP-positive aggregates on its apical surface showed that these aggregates consist of amorphous extracellular material (Fig.3.32, b). TEM immunogold labelling confirmed the presence of Tectb (Fig.3.32, c) and showed that it consisted of amorphously organised material. No signs of filaments were detected (Fig.3.32, d).

In an EGFP-positive hair cell detected in the second row of OHCs in a P2+1 wild type mouse cochlear culture (Fig.3.33, a) the signal localised to the hair bundle (Fig.3.33, b).

The correlative TEM of this OHC is shown on Fig.3.33, c. Gold labelling was detected at the distal tips of stereocilia which is consistent with the confocal microscopy results (Fig.3.28). Further investigation revealed that the EGFP-Tectb matrix expressed on the top of the hair bundle of OHCs and IHCs was of amorphous nature similar to that of the outgrowth zone cells (Fig.3.33, Fig.3.34).

Thus mouse cochlear cultures were easier to map than cell monolayers, and transfected cells detected at light microscopy level could be found and then analysed by electron microscopy.

3.2.3.3. mCherry-Tecta expression

Despite the high levels of extracellular EGFP-Tectb expression observed in biolistically transfected outgrowth zone cells from neonatal mouse cochlear cultures, a similar effect was not detected using mCherry-Tecta encoding plasmids.

Confocal microscopy investigation revealed that although pBK-mCherry-Tecta transfected outgrowth zone cells formed grain-shaped matrix punctae, these punctae were retained in the cell cytoplasm (Fig.3.35). In outgrowth zone cells transfected with the pCAG-mCherry-Tecta plasmid, mCherry-Tecta also formed discrete particles distributed intracellularly (Fig.3.36).

To investigate whether the large size of the mCherry-Tecta protein can prevent outgrowth zone cells from secreting it as matrix, two constructs encoding shorter modifications of Tecta protein, pBK-mCherry-MMMTecta and pBK-mCherry-ZPTecta, were used for gene gun transfection. As shown by confocal microscopy, outgrowth zone cells transfected with these constructs had a large amount of protein aggregates distributed throughout the cell cytoplasm (Fig.3.37, a and b). These aggregates were, however, not secreted or deposited on the cell surface (Fig.3.37, a’ and b’).

Although transfected outgrowth zone cells failed to form extracellular matrix, mCherry-Tecta secretion was sometimes detected on other cell types of mouse cochlear cultures. Fig.3.38 shows a confocal image of a Hensen's cell transfected with the pBK-mCherry-Tecta construct with an outburst of extracellular mCherry expression. Grain-shaped protein aggregates were present within the cell cytoplasm and were also found on its apical surface (Fig.3.38, a' and c').

Confocal microscopy of a transfected OHC revealed that mCherry localised to the distal tips of the hair bundle (Fig.3.39). In contrast to EGFP-Tectb which formed a solid cap around the tips of stereocilia (Fig.3.28), mCherry-Tecta appeared like small spherical aggregates attached to the hair bundle (Fig.3.39, b). However, only two transfected OHCs were detected, and this observation needs to be supported by increasing the number of performed hair cell transfections.

In contrast to mCherry-Tecta transfected cells, a pBK-EGFP-Tecta construct promoted a robust extracellular expression of EGFP-positive aggregates in outgrowth zone cells (Fig.3.40) which resembled that in outgrowth zone cells transfected with the EGFP-Tectb encoding construct. However, EGFP-Tecta transfected cells also retained the protein inside the cell bodies (Fig.3.40). Deiter's cells also expressed protein inside and secreted it on their apical surface (Fig.3.41). GER cells displayed a high level of protein expression and produced a thick layer of extracellular matrix on their apical surfaces (Fig.3.42).

3.2.3.4. Introduction of deafness-causing ZP domain mutations into Tectb

Alignment of ZP domains from various proteins (chick Tectb, mouse Tecta, ZP3 proteins from pig, mouse, human and hamster, mouse ZP2 protein, rat and human uromodulins, dog and rat GP2 proteins) identified cysteine and tyrosine amino acids in

mouse Tectb protein that are synonymous to those in human Tecta and are affected in human Spanish (C1837G) and Austrian (Y1870C) families with hereditary hearing loss (Fig.3.43).

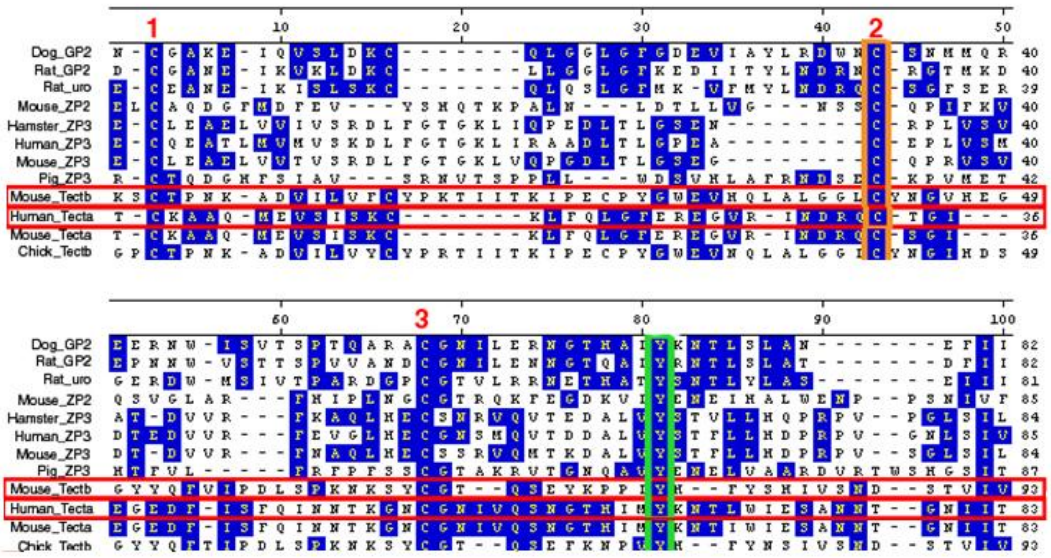

Figure 3.43. Fragments of ZP domains of various ZP proteins. Red horizontal boxes show mouse Tectb and human Tecta amino acid sequences. Red numbers mark the conserved cysteines, three of eight are shown. Orange box identifies the conserved cysteine replaced with glycine in the Spanish family. Green box shows the conserved tyrosine replaced with a cysteine in the Austrian family.

Wide-field live fluorescence imaging showed that outgrowth zone cells transfected with the wild type Tectb-encoding construct formed bright matrix aggregates which localise extracellularly (Fig.3.44, a). However, cells transfected with the C1837G and Y1870C Tectb constructs lacked any matrix structures (Fig.3.44, b and c), and the even distribution of EGFP fluorescence signal throughout the cell body indicated the proteins derived from the mutated constructs were not secreted.

Confocal microscopy results are consistent with live fluorescence imaging (Fig.3.45). Thus mutations in the ZP domain disrupt the process of matrix secretion.

3.3. Discussion

The transient transfection experiment with the Tecta-IRES-turboFP635 construct showed that CaCo2 cells selected as a cell culture model for epithelia were unable to apically target recombinant Tecta. One of the possible explanations is that CaCo2 cells misinterpret the Tecta targeting signal. However, Tecta belongs to a group of GPI-anchored proteins (Witteveen, 2008) which were shown to be secreted exclusively to the apical surface in epithelial cells with a very few exceptions (Brown and Breton, 2000). Thus it is more likely that CaCo2 cells either fail to process and/or fold the protein correctly, which might result in the GPI signal being obscured. MDCK cells, in contrast, expressed a significant amount of Tecta aggregates among the apical microvilli. This result was supported by previous studies in which an MDCK cell line was successfully used as a model for apical expression of GPI-anchor proteins (Lisanti et al, 1988).

Following the results of the transient transfection, an MDCK cell line was utilised as a model system for investigating the secretion and assembly of tectorin matrix. While transient transfection is suitable for studying short-term protein production, stable extracellular expression of both tectorins is desirable for investigating the ultrastructure of secreted matrix by electron microscopy. A cell monolayer spread on a coverslip contains a large number of cells all of which have a similar form and it is hard to relocate transfected cells expressing fluorescent proteins in the electron microscope. Thus having a model in which every cell produces an extracellular matrix would significantly facilitate analysis by SEM and/or TEM. To determine how matrix assembly might be disrupted by deafness causing mutations in Tecta, a considerable surface expression of tectorins is required. Thus, MDCK-based cell lines stably

expressing Tecta and Tectb were generated by carefully selecting cells showing an extracellular tectorin expression.

The first problem revealed while selecting cells stably transfected with the pBK-Tecta-IRES-turboFP635 construct was an absence of fluorescence signal from the far-red turboFP635 protein during live imaging. As previous studies reported an excellent performance of turboFP635 in various *in vivo* applications, including cell selection, (Kelmanson, 2009), it was suggested that the construct used contained a mutation either in the coding sequence of turboFP635 thus affecting its fluorescent properties or in the IRES, disrupting the translation of the fluorescent protein. Sequencing of the construct revealed a point mutation in the IRES which might explain why it was not possible to do live imaging. It is not known, however, whether this mutation affects IRES function.
Other difficulties experienced while generating a Tecta-IRES-turboFP635 stable cell line were the low number of immunoreactive with anti-Tecta antibody, yet G418 resistant, cells and even lower number of cells expressing Tecta on their apical surfaces. The Tecta encoding sequence was driven from the human CMV immediate early promoter. The efficiency of the CMV promoter is known to vary between different cell lines, being strong in some cell types and much weaker in others (Qin et al., 2010). In addition, silencing of this promoter was reported to be a problem while generating stable cell lines (Brooks et al., 2004; Löser et al., 1998). Silencing might occur due to the methylation of promoter sequences or histone deacetylation (Brooks et al., 2004; Grassi et al., 2003) and can explain the low number of cells in which Tecta expression could be detected.

It was assumed that the appearance of Tecta on the cell's apical surface might be a time-dependent process and protein would have to accumulate to a certain level before it

could be detected. In any cell line that is actively dividing, the accumulation process might be disrupted by mitosis. This hypothesis was not confirmed as Mitomycin C-induced block of cell division did not enhance the extracellular Tecta expression.

It was further assumed that a suitable substrate imitating a basement membrane to which epithelial cells are attached *in vivo* might promote cell spreading, proliferation and the secretion and accumulation of matrix (Themistocleous et al., 2004). Cells were therefore grown on a collagen matrix composed of reconstituted collagen fibres that might simulate the cell- extracellular matrix (EMC) interactions that occur *in vivo* within epithelium systems. As predicted, it slightly promoted apical targeting of Tecta.
As was mentioned above, the downregulation of the human CMV promoter while selecting for stably transfected cells prevented the accumulation of Tecta protein matrix. The composite CAG promoter (Niwa et al., 1991) was previously reported to be an invaluable tool for driving high-level and long-term gene expression from mammalian expression vectors (Alexopoulou et al., 2008; Chen et al., 2011; Nishijima et al., 2009). Fluorescent proteins are known to fold and function correctly when joined to other proteins (Snapp, 2010), so it should be possible to use the fluorescently tagged tectorins to directly study tectorin expression and distribution in live cells. This would also facilitate cell screening. Hence, a new set of Tecta and Tectb encoding constructs utilising the CAG promoter placed upstream of the fluorescent fusion protein coding sequence was designed.

Although the CAG-based mammalian expression vectors allowed the generation of cell lines stably expressing Tecta and Tectb, the levels of extracellular matrix production remained quite low and it took about a week of culturing to obtain a detectable amount of surface-associated tectorin aggregates. In addition, both mCherry-Tecta and EGFP-

Tectb were subjected to proteolysis and cleaved into mCherry and mCherry fused to LMM Tecta (Legan et al., 1997) and EGFP and Tectb, respectively. Interestingly, EGFP was only found in the medium and not in the cells. The abundant extracellular secretion of GFP protein was previously reported for different cell lines, however, only the improperly folded and thus non-fluorescent forms of protein were excreted (Tanudji, 2002). The appearance of EGFP in culture medium and its absence in cell lysates probably reflects proteolysis of the secreted protein, possibly in the linker region between the two protein sequences. A slightly larger mass of the EGFP-Tectb and Tectb proteins detected in the medium might be explained by some posttranslational modification occurring before secretion, probably glycosylation.

To circumvent the loss of protein into the culture medium, polarised epithelial cell spheres which "trap" secreted proteins in their lumen were generated from a mCherry-Tecta stable cell line. With TEM, material could be detected inside the spheres that had assembled into fine interconnecting filaments with a diameter of 6-9 nm. Similar irregular branched filaments were detected in the TM of *Tectb*$^{-/-}$ mutant mouse with completely disrupted striated-sheet matrix (Fig.3.46) (Russell et al., 2007). These filaments are thought to be made from Tecta and can be localised between the collagen fibrils (Fig.3.46, b). These data suggest that the fibrils detected in the sphere lumen might be formed of Tecta protein as well.

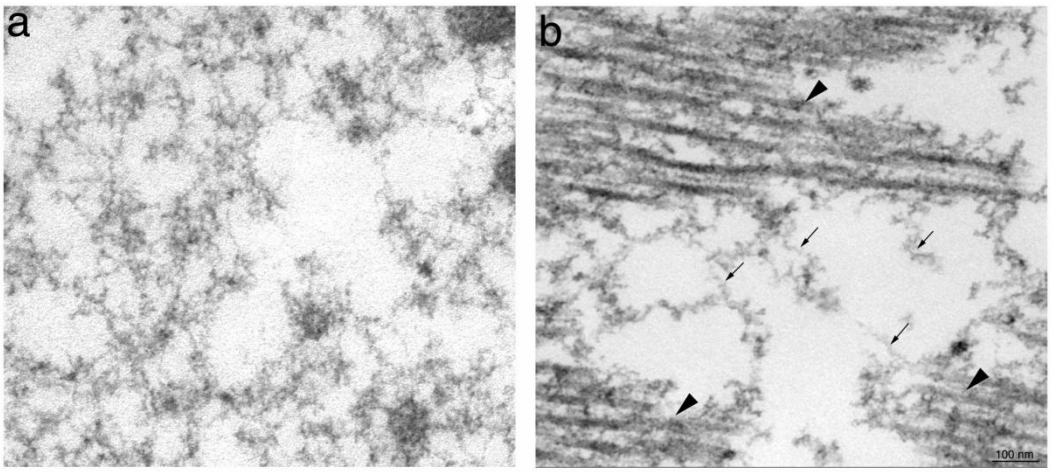

Figure 3.46. TEM images of the fibrils from the lumen of a sphere formed of cells stably transfected with mCherry-Tecta (a) and similar fibrils that are observed in the TM matrix of *Tectb*$^{-/-}$ mouse (b). Fluffy branched filaments depicted in panel a are about 6-9 nm diameter and are similar to the 8 nm diameter filaments that are formed by Tecta (arrows) in the TM of the *Tectb* null mouse. Collagen fibrils are marked by arrowheads. Scale bar is 100 nm

For *in vitro* matrix production, the best results were achieved using neonatal mouse cochlear cultures that had been transiently transfected with EGFP-Tectb encoding constructs using a gene gun. In addition to the cell types normally expressing Tectb protein *in vivo*, e.g. GER and Deiter's cells, apical tectorin targeting was observed in transfected hair cells and outgrowth zone cells.

An outgrowth zone emerges from the edge of the cochlear culture and has both epithelial and mesenchymal origins (He, 1997). It consists of mesenchymal cells and giant flat epithelial cells spread over the culture substrate. Transfected outgrowth zone cells secreted significant amounts of extracellular Tectb matrix to their apical surfaces just 24 hours after transfection. However, they failed to secrete mCherry-Tecta and its shortened versions which instead accumulated in the cytoplasm, indicating that the

failure of Tecta apical expression is not dependent on protein size. Interestingly, cells transfected with the EGFP-Tecta construct cause a robust extracellular matrix production in various cell-types. It is therefore possible that the mCherry fluorescent tag interferes with apical targeting of Tecta protein.

The observed distribution of ectopically expressed tectorins in hair cells suggests the presence of a special receptor for Tecta and Tectb at the tip of a hair bundle. It is possible that the tectorins that are located to the distal end of stereocilia in transfected OHCs are becoming associated with the attachment crowns and interact with stereocilin. However, anti-stereocilin staining of the neonatal cochlear cultures showed that at the age of P2+1 stereocilin is expressed only in a kinocilium (Fig.3.47). Alternatively Tecta and Tectb may simply accumulate at the tips of stereocilia as a similar distribution is observed in IHCs, the mature bundles of which do not interact with the TM.

TEM analysis revealed that outgrowth zone cells and hair cells express an amorphous Tectb matrix in which filaments cannot be resolved. It is possible that Tectb protein is unable to form a filament-based matrix without Tecta as was suggested to be the case in $Tecta^{\Delta ENT/\ \Delta ENT}$ mice (Legan et al., 2000). However, it also might be the case that the initial fixation was not good enough to preserve filaments.

The final goal of this research was to study how deafness-causing mutations influence matrix assembly. The *Tecta* C1837G and *Tecta* Y1870C mutations were introduced into orthologous residues in the mouse Tectb ZP domain, and the mutated constructs were transfected into cochlear cultures. Outgrowth zone cells transfected with the mutated Tectb constructs failed to apically target the mutated polypeptides which accumulated instead in the cell cytoplasm. This result is consistent with the study of the $Tecta^{C1837G/+}$ mouse (Coates, 2009) and the $Tecta^{Y1870C/+}$ (Legan et al., 2005) mouse in which the

striated-sheet matrix is disrupted. Previous studies have showed that mutation synonymous to Y1870C in ZP2 protein essentially decreases its ability to incorporate in the zona pellucida and abolishes its extracellular expression in transfected CHO cells (Jovine et al., 2002). Both mutations affect the cysteine composition of ZP domain and hence might disrupt intrachain disulphide bond formation (Iwasaki et al., 2002). As a result, the incorrectly folded polypeptide will not be able to be exported to the cell's apical membrane.

Finally, the inability of Tecta and Tectb to form organised matrix might also be due to the absence of some other component of the TM which could be essential for proper protein assembly. This unknown component could be Ceacam16, a molecule recently described as a component of TM matrix that interacts with Tecta (Zheng et al., 2011).

3.4. Conclusions

The major findings of this study can be summarised as follows:

1. MDCK cell lines stably expressing mCherry-Tecta and EGFP-Tectb produce limited amounts of "matrix" after prolonged periods *in vitro*.

2. mCherry-Tecta forms filament-based matrix within the lumen of epithelial cell spheres.

3. Transiently transfected epithelial cells in neonatal mouse cochlear cultures rapidly produce Tectb extracellular matrix.

4. Deafness-causing ZP domain mutations prevent matrix formation *in vitro*.

3.5. Future perspectives

The ultimate aim of this project was to study how deafness-causing mutations in *Tecta* affect TM matrix assembly. Thus the future work should aim to generate deafness-causing mutations in the pBK-EGFP-Tecta construct using site directed mutagenesis and transfect the mutated vectors into the *in vitro* model system based on the neonatal mouse cochlear cultures. A higher transfection level might be possibly achieved by using electroporation as a transfection technique instead of the gene gun. Finally, the model developed might be useful for investigating the role of the recently described TM protein Ceacam16 in the maintenance of the striated-sheet matrix (Zheng et al., 2011).

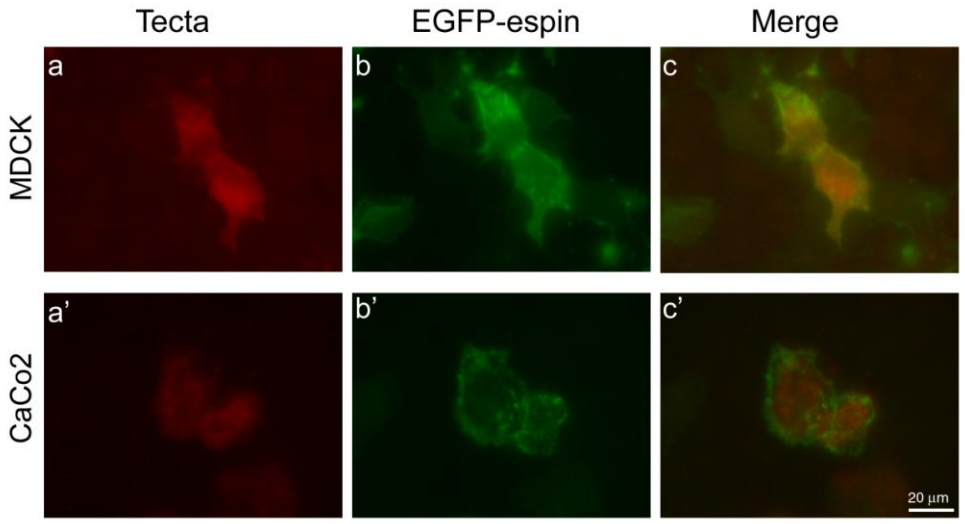

Figure 3.1. MDCK and CaCo2 cells transiently transfected with the pBK-Tecta-IRES-turboFP635 and EGFP-Espin plasmids. Cells were treated with Triton X-100 and stained with anti-Tecta antibody (red) and anti-GFP antibody (green). Anti-Tecta staining reveals Tecta expression in both MDCK and CaCo2 (a, a'). Tecta expressing cells form elongated EGFP-positive microvilli on their surface. Scale bar 20 μm.

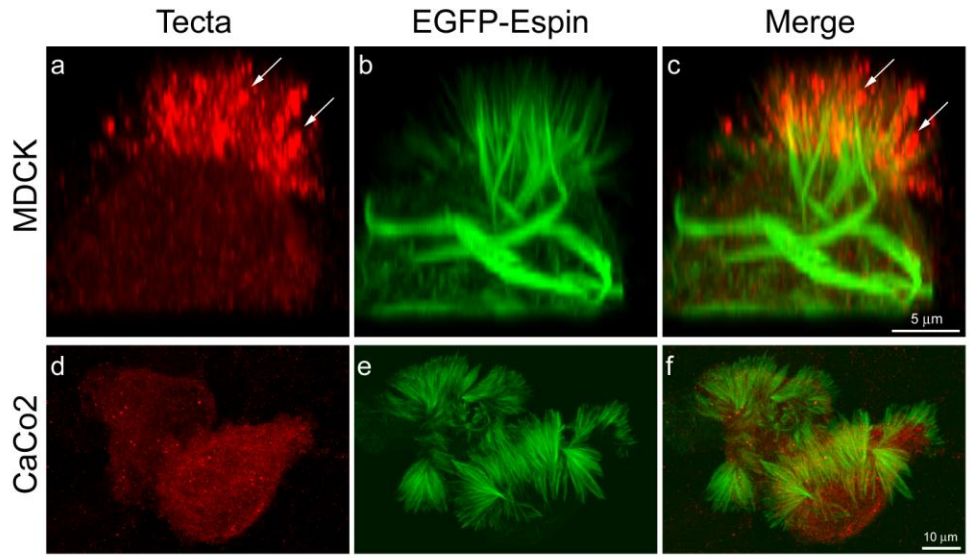

Figure 3.2. Confocal microscopy of MDCK (a, b and c) and CaCo2 (d, e and f) cells transiently transfected with the Tecta and EGFP-Espin encoding constructs and stained with anti-Tecta (red) and anti-GFP (green) antibodies after Triton X-100 treatment. Tecta protein in MDCK cells is expressed on the apical surface and associates with elongated microvilli (a, c, arrows). In CaCo2 cells, however, Tecta is retained in the cytoplasm. Scale bar for panels a, b and c is 5 μm, for panels d, e and f - 10 μm.

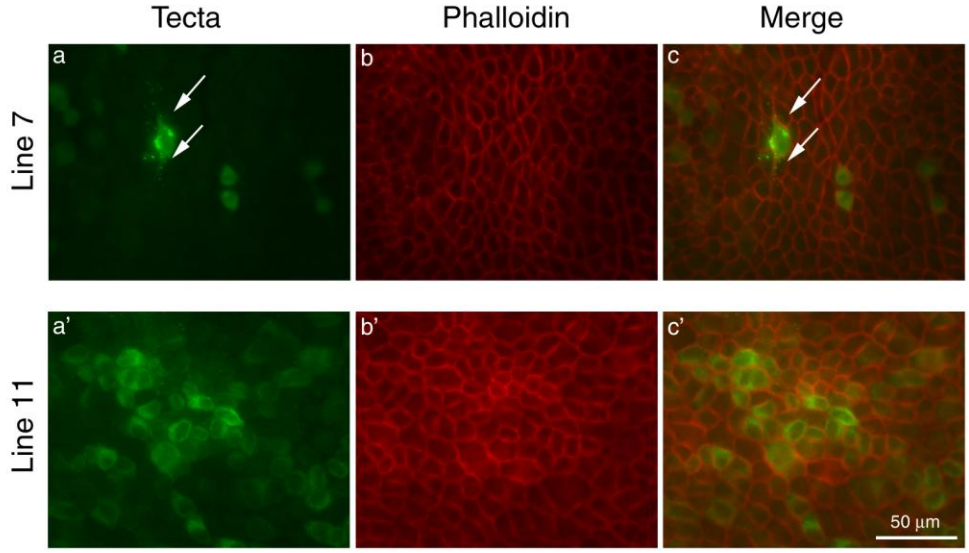

Figure 3.3. Wide-field fluorescent microscopy of MDCK-based cell lines 7 (a, b and c) and 11 (a', b', c') permeabilised with Triton X-100 and stained with anti-Tecta antibody (green) and Texas Red phalloidin (red). Only a few line 7 cells from imaged region are stained with anti-Tecta antibody (a), just one of the cells has green particles which are likely to be on its apical surface (a and c, arrows). Line 11 contains a larger number of Tecta-positive cells (a'), none of them, however, display any signs of extracellular Tecta expression. Scale bar 50 µm.

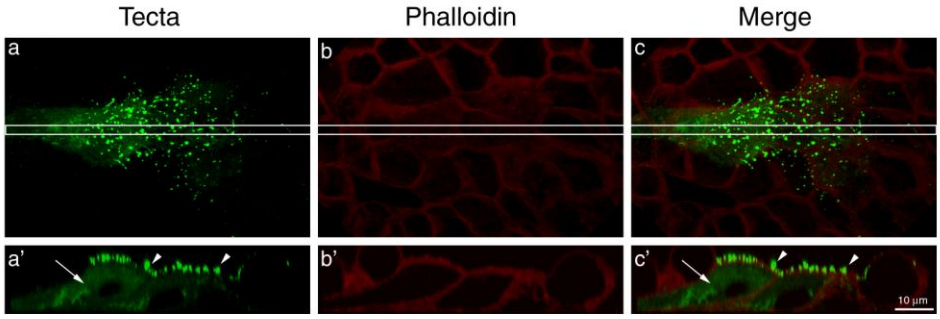

Figure 3.4. Confocal microscopy of line 7 cells (a, b and c) and a compressed Z-stack projection of the region outlined by the white lines (a', b' and c'). Cells were permeabilised with Triton X-100 and stained with anti-Tecta antibody (green) and Texas Red phalloidin (red). Along with the moderate intacellular Tecta expression (a and c, arrows), the cells also produce extracellular Tecta particles on their apical surface (a and c, arrowheads). Scale bar 10 μm.

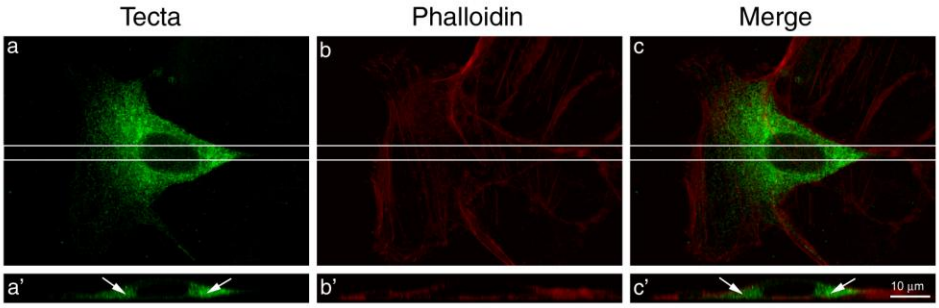

Figure 3.5. Confocal microscopy of line 11 cells permeabilised with Triton X-100 and stained with anti-Tecta antibody (green) and Texas Red phalloidin (red). The region outlined by the white lines was projected around the Z-axis (a', b' and c'). Tecta protein retains inside the cell (a' and c', arrows). Scale bar 10μm.

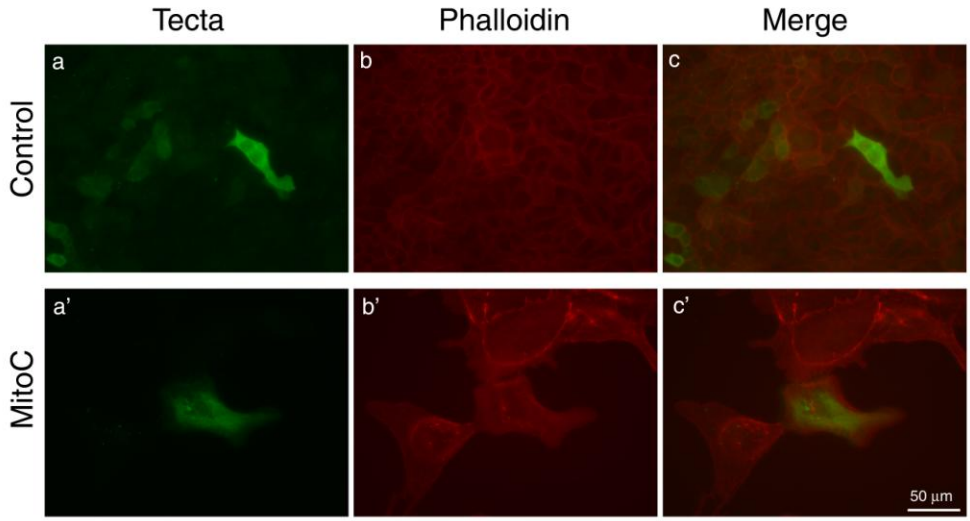

Figure 3.6. Stable Tecta-IRES-turboFP635 cells cultured without (a, b and c) and with (a', b' and c') Mitomycin C. Cells were permeabilised with Triton X-100 and stained with anti-Tecta antibody (green) and Texas Red phalloidin (red). In both control (c) and Mitomycin C-treated (c') cells, Tecta protein is retained in the cytoplasm. Although not promoting Tecta extracellular expression, Mitomycin C increases the cell size (b' and c'). Scale bar 50 µm.

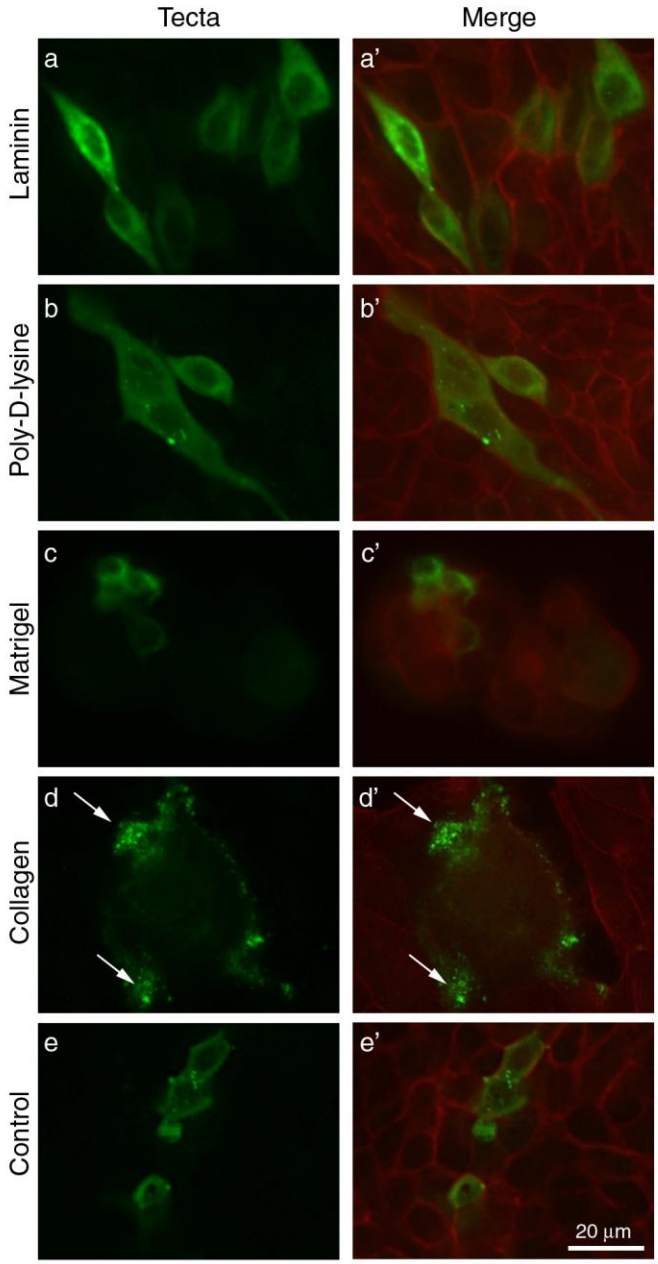

Figure 3.7. Line 7 cells cultivated on laminin (LM) (a, a'), poly-D-lysine (PDL) (b, b'), Matrigel (MG) (c, c'), ammonia-polymerised collagen (CG) (d, d') and control cells grown on an uncoated glass coverslip (e, e'). Cells were permeabilised with Triton X-100 and stained with anti-Tecta antibody (green) and Texas Red phalloidin (red). The levels of extracellular Tecta expression in cells grown on LM, PDL and MG are comparable to those in the control cells. MG-cultured cells form round colonies (c'). Cells cultured on CG produce Tecta aggregates (d and d', arrows) which are possibly localised on the cell apical surfaces. Scale bar 20 µm.

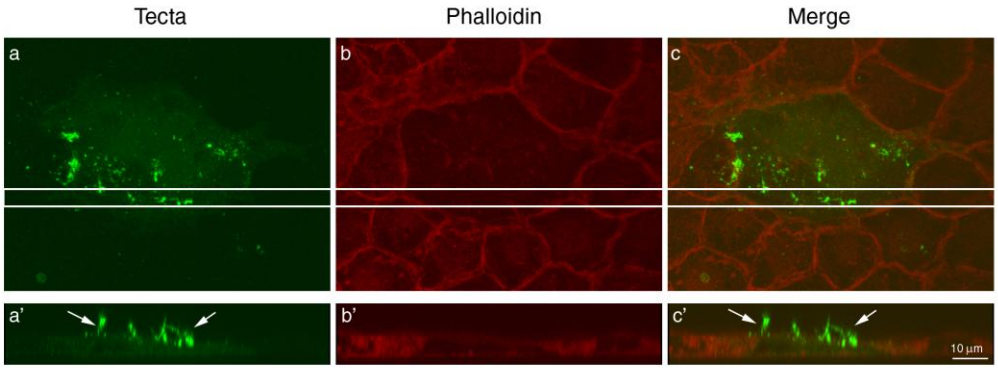

Figure 3.8. Confocal microscopy (a, b and c) and a Z-axis projection of the region outlined by the white lines (a', b' and c') of line 7 cells cultured on ammonia-polymerised collagen. Cells were preblocked with Triton X-100 and stained with anti-Tecta (green) and Texas Red phalloidin (red) antibodies. Tecta protein is present within the cell cytoplasm, however, it also forms bright aggregates associated with cell microvilli (a' and c', arrows). Scale bar 10 µm.

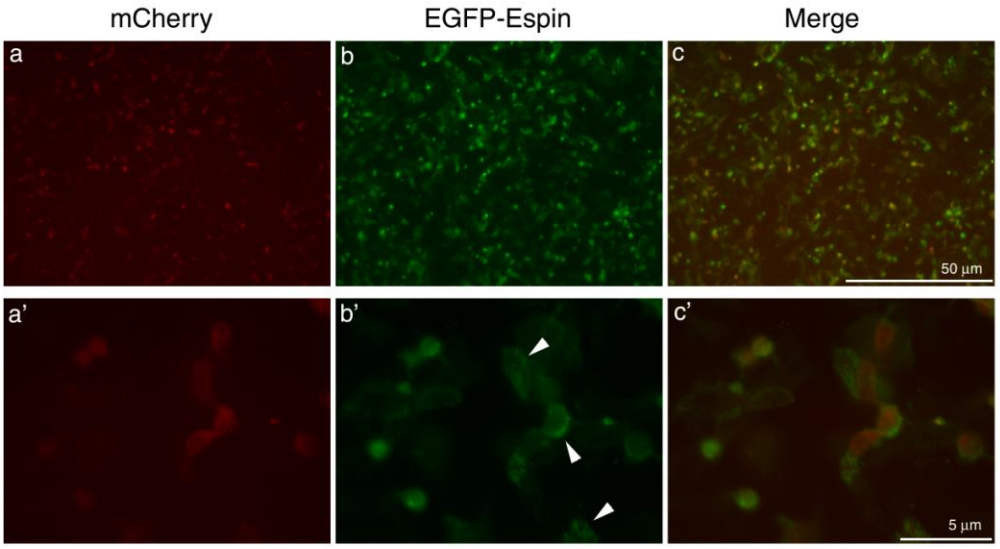

Figure 3.9. MDCK cells transiently co-transfected with the pCAG-mCherry-Tecta and EGFP-Espin plasmids and live-imaged with x10 (a, b and c) and x63 (a', b' and c') lenses. mCherry signal (red) is easily detected in both low- (a) and high-magnification (a') images. EGFP-Espin (green) generates prolonged microvilli on cell surfaces (b', arrowheads). Scale bar for panels a, b and c 50 μm. Scale bar for panels a', b' and c' is 5 μm.

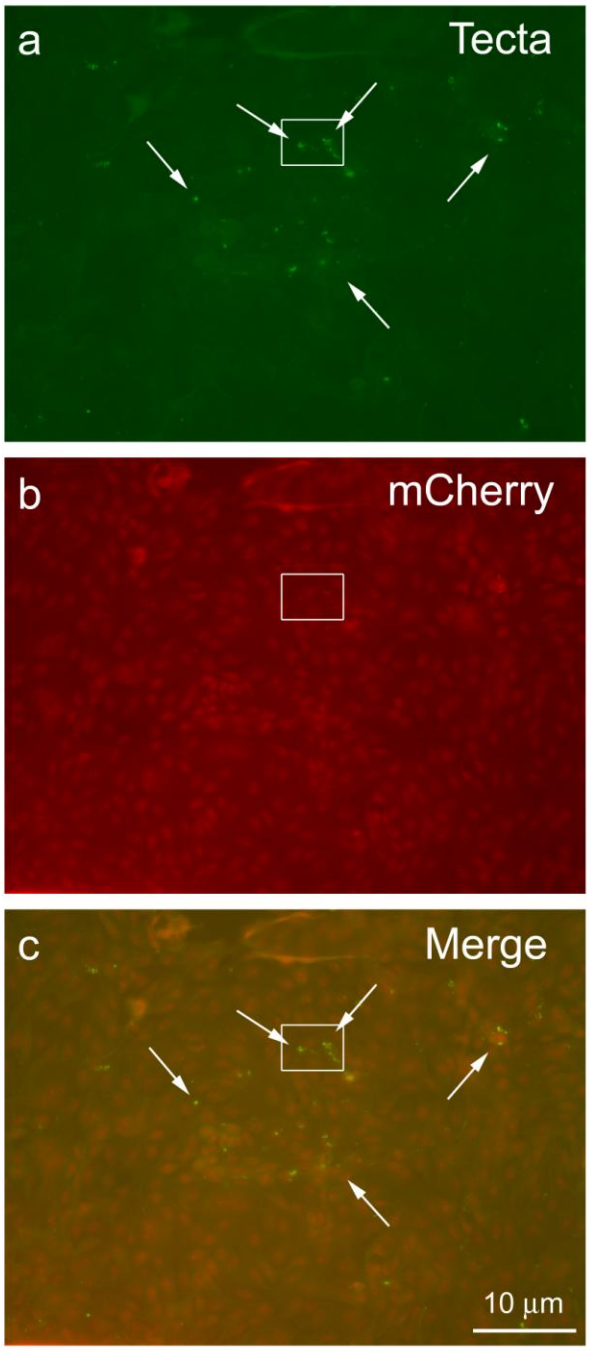

Figure 3.10. MDCK cells stably transfected with the pCAG-mCherry-Tecta construct after seven days *in vitro*. In order to reveal extracellular Tecta expression no Triton X-100 was used. Cells were stained with anti-Tecta (green) antibody. Every cell imaged seems to express mCherry protein. However, only a few extracellular aggregates immunoreactive with anti-Tecta antibody are observed on the monolayer surface (some examples are indicated by arrows). The boxed region was used for confocal microscopy (next figure). Scale bar 10 μm.

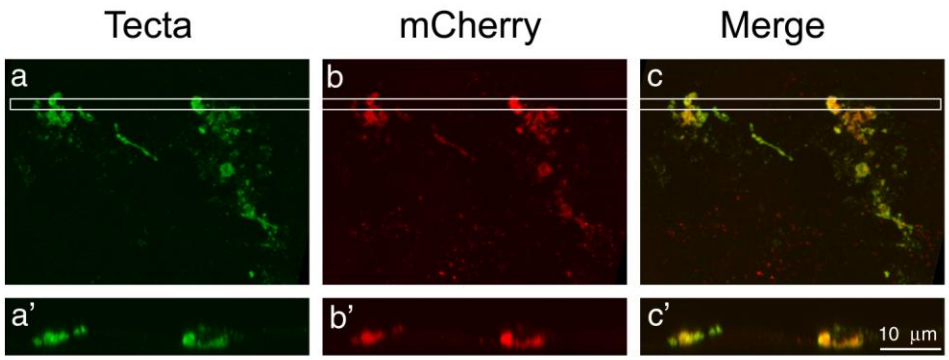

Figure 3.11. Confocal microscope image (a, b and c) and a Z-stack projection of the region outlined by the white lines (a', b' and c') of aggregates produced by stable mCherry-Tecta cells after seven days of incubation. Anti-Tecta staining (green) which co-localises with mCherry signal present (red) confirms that the aggregates produced are formed of mCherry-Tecta fusion protein and secreted on cell apical surfaces (c'). Scale bar 10 μm.

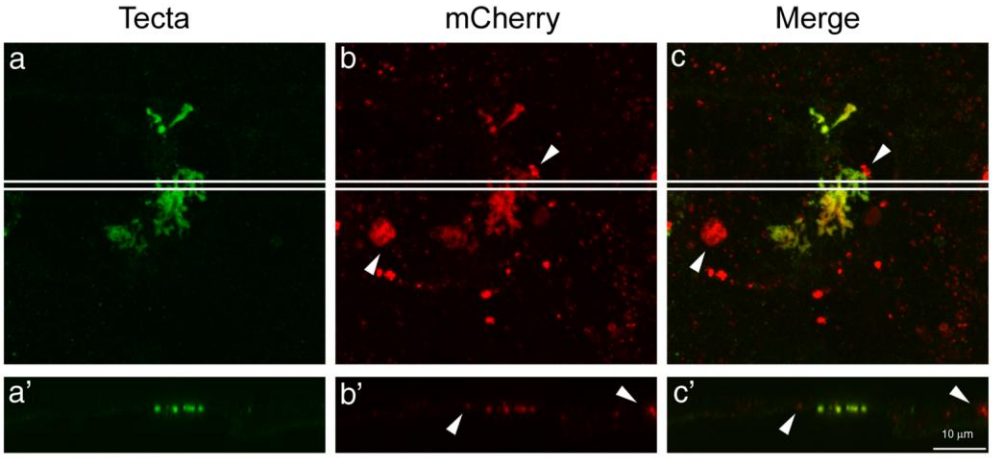

Figure 3.12. Confocal microscope image (a, b and c) and a Z-stack projection of the area outlined by the white lines (a', b' and c') of a stable mCherry-Tecta cell stained with anti-Tecta antibody (green). mCherry-Tecta fusion protein forms a matrix-like aggregate on the cell's apical surface. However, mCherry-only aggregates are also secreted (b and b', c and c', arrowheads). Scale bar 10 μm.

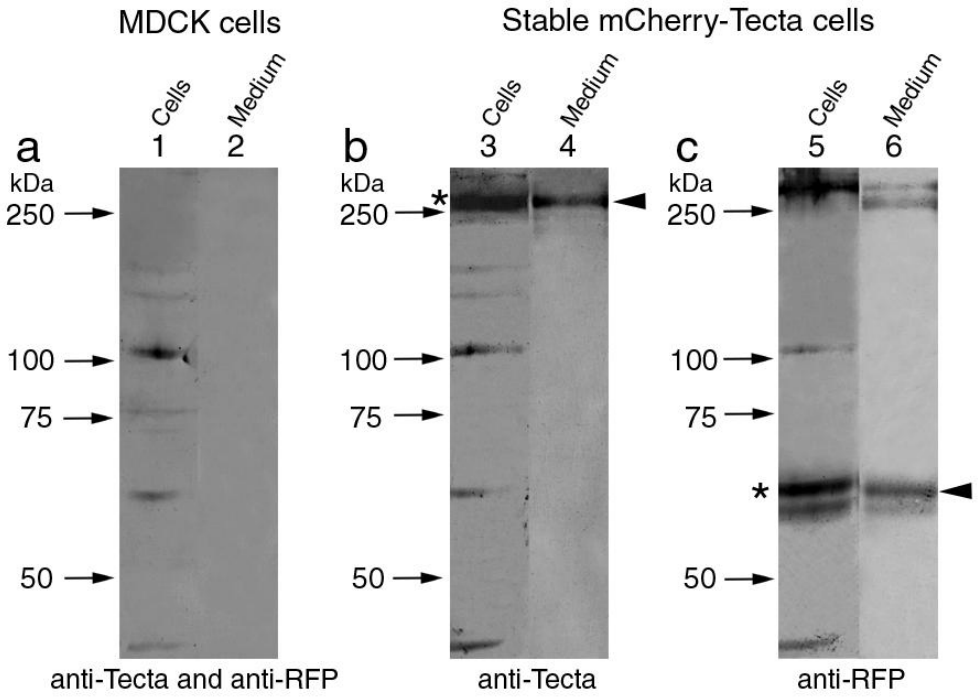

Figure 3.13. Western blot of cell lysates and culture medium from nontransfected MDCK and stable mCherry-Tecta MDCK-derived cells probed with anti-Tecta (R9) and anti-RFP antibodies. Anti-Tecta antibody detects a band of about 260 kDa in both cell lysates (b, lane 3, asterisk) and culture medium (b, lane 4, arrowhead), possibly mCherry-Tecta fusion protein. The same band is revealed with anti-RFP antibody in cell lysates (c, lane 5) and is represented by two bands in culture medium (c, lane 6). Anti-RFP also reacts with smaller bands of 60 and 63 kDa (asterisk in lane 5 and arrowhead in lane 6). Other bands i cell lysates are nonspecific and are also detected in the negative control (a, lane 1). Negative control for culture medium appears to be clear (a, lane 2).

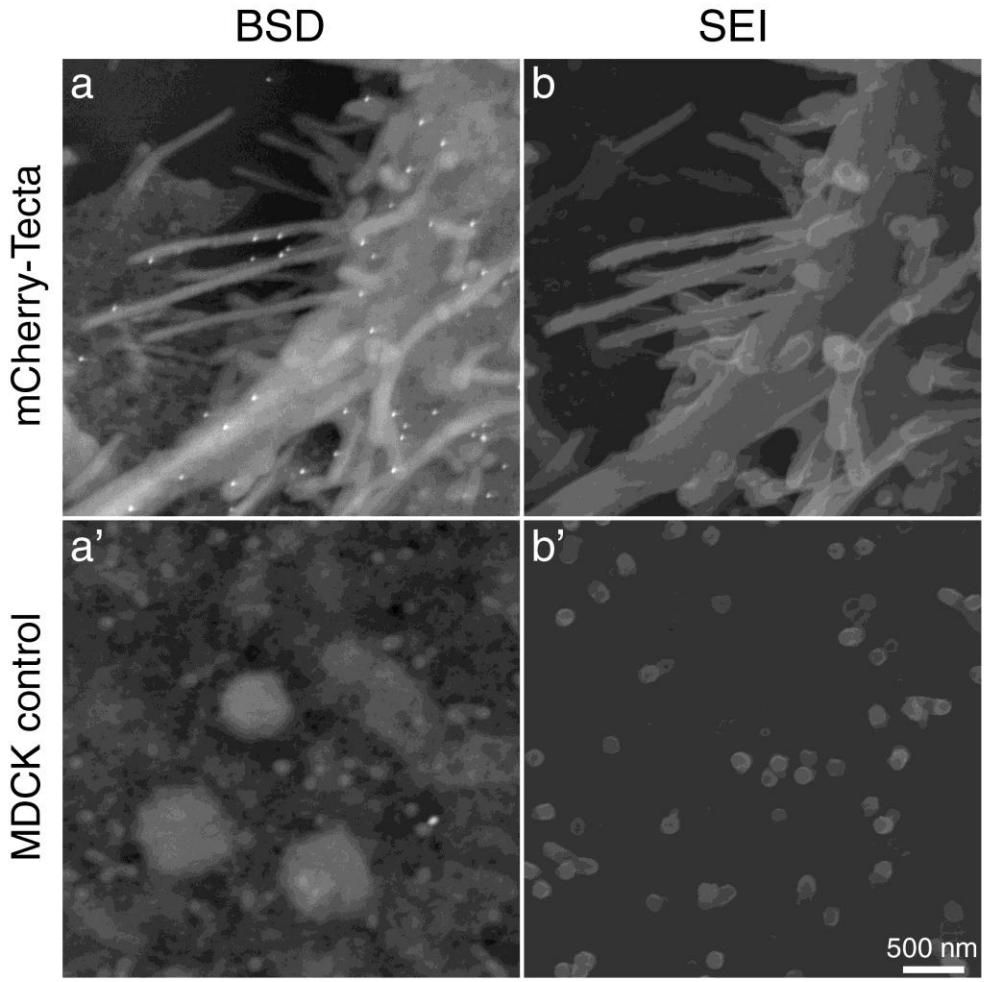

Figure 3.14. Backscatter detector (BSD) images (a, a') and secondary electron images (SEI) (b, b') of stable mCherry-Tecta and control MDCK cells stained with anti-Tecta antibody and labeled with 25 nm gold-conjugated anti-rabbit antibody. Gold labelling is associated with cell microvilli and protrusions. No filamentous structures are observed. Scale bar 500 nm.

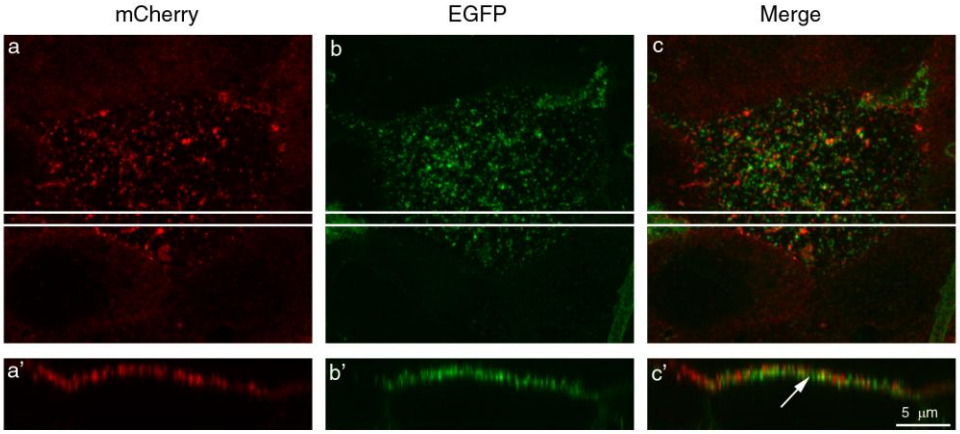

Figure 3.15. Confocal microscope images (a, b and c) and a Z-stack projection of the region outlined by the white lines (a', b' and c') of a stable mCherry-Tecta cell transiently co-transfected with the EGFP-Tectb encoding construct. No Triton X-100 was applied, cells were stained with anti-Tecta (red) and anti-GFP (green) antibodies. Both mCherry-Tecta and EGFP-Tectb form aggregates associated with apical microvilli, however, only a small area of overlap between red and green signals is seen (c', arrow). No enhancement in Tecta matrix formation is detected. Scale bar 5 µm.

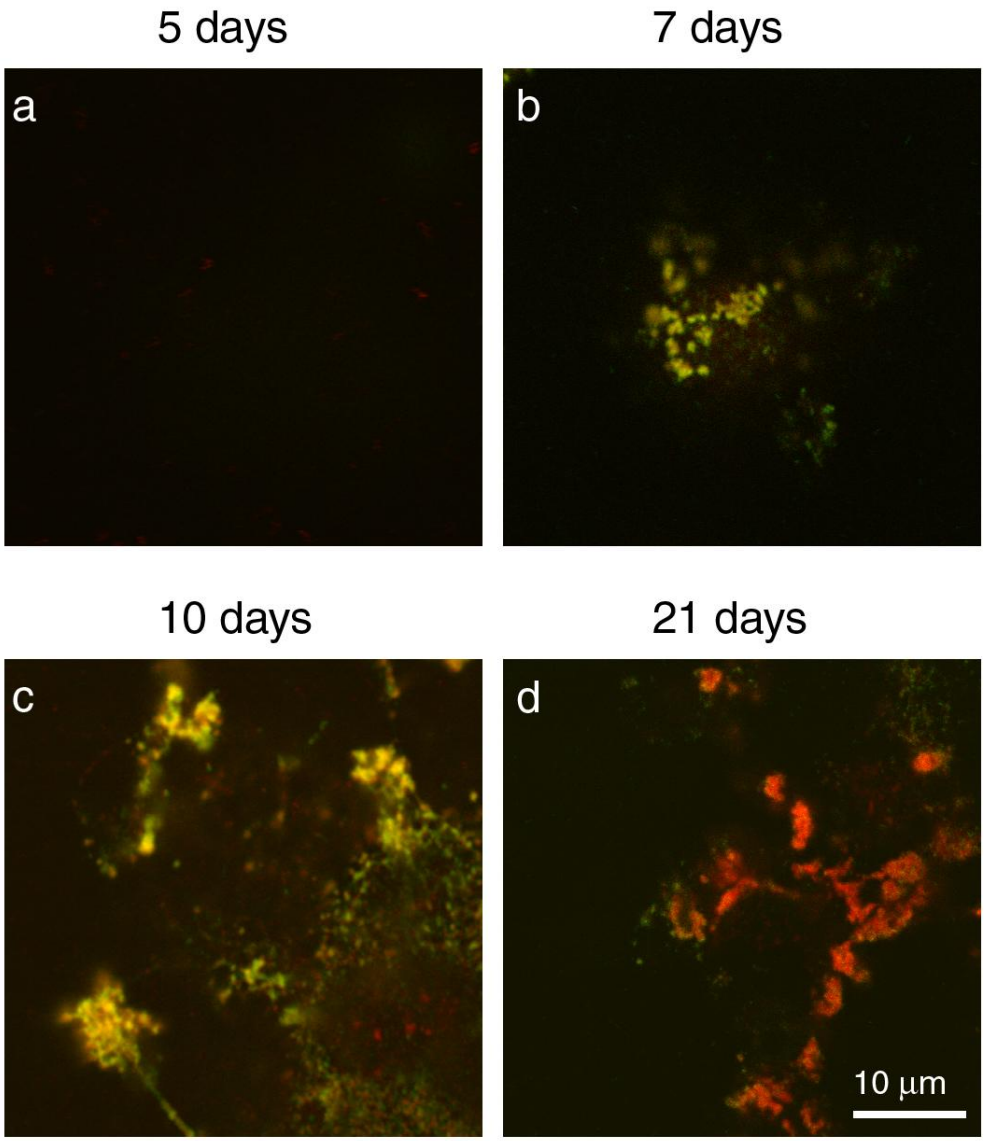

Figure 3.16. Confocal microscope images of stable mCherry-Tecta cells incubated for 5, 7, 10 and 21 days. No Triton X-100 was applied. Cells were stained with anti-Tecta antibody (green signal), and the mCherry signal (red) was not amplified. From four time points examined, extracellular matrix is first detected at day seven. No significant difference is detected between day 10 and day 21. Scale bar 10 μm.

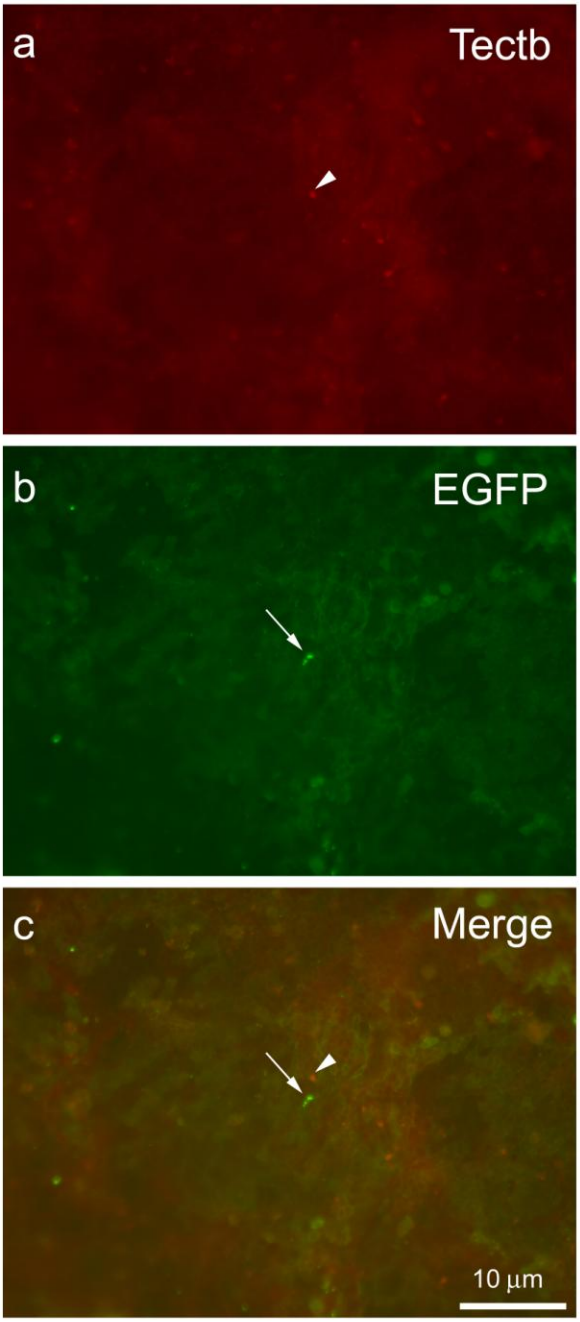

Figure 3.17. MDCK cells stably transfected with the pBK-EGFP-Tectb construct and cultured for seven days. No Triton X-100 was applied. Cells were stained with anti-Tectb (red) and anti-GFP (green) antibodies. Only a few extracellular punctae are observed over the cell's apical surfaces. Arrowhead points to Tectb-only aggregate, arrow indicates EGFP-only aggregate. Scale bar 10 μm.

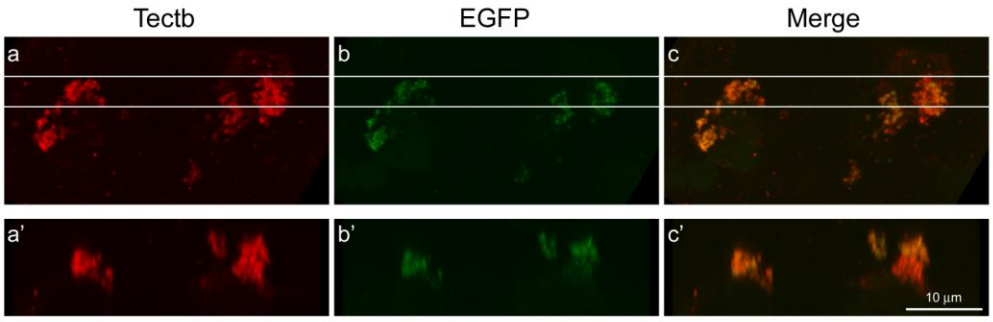

Figure 3.18. Confocal microscope image (a, b and c) and a Z-stack projection of the region outlined by the white lines (a', b' and c') of stable EGFP-Tectb cells after seven days of incubation. No Triton X-100 was used. Cells were stained with anti-Tectb (red) and anti-GFP (green) antibodies. Extracellular matrix detected shows a significant co-localisation of red and green fluorescence signals (c, c'). Scale bar 10 µm.

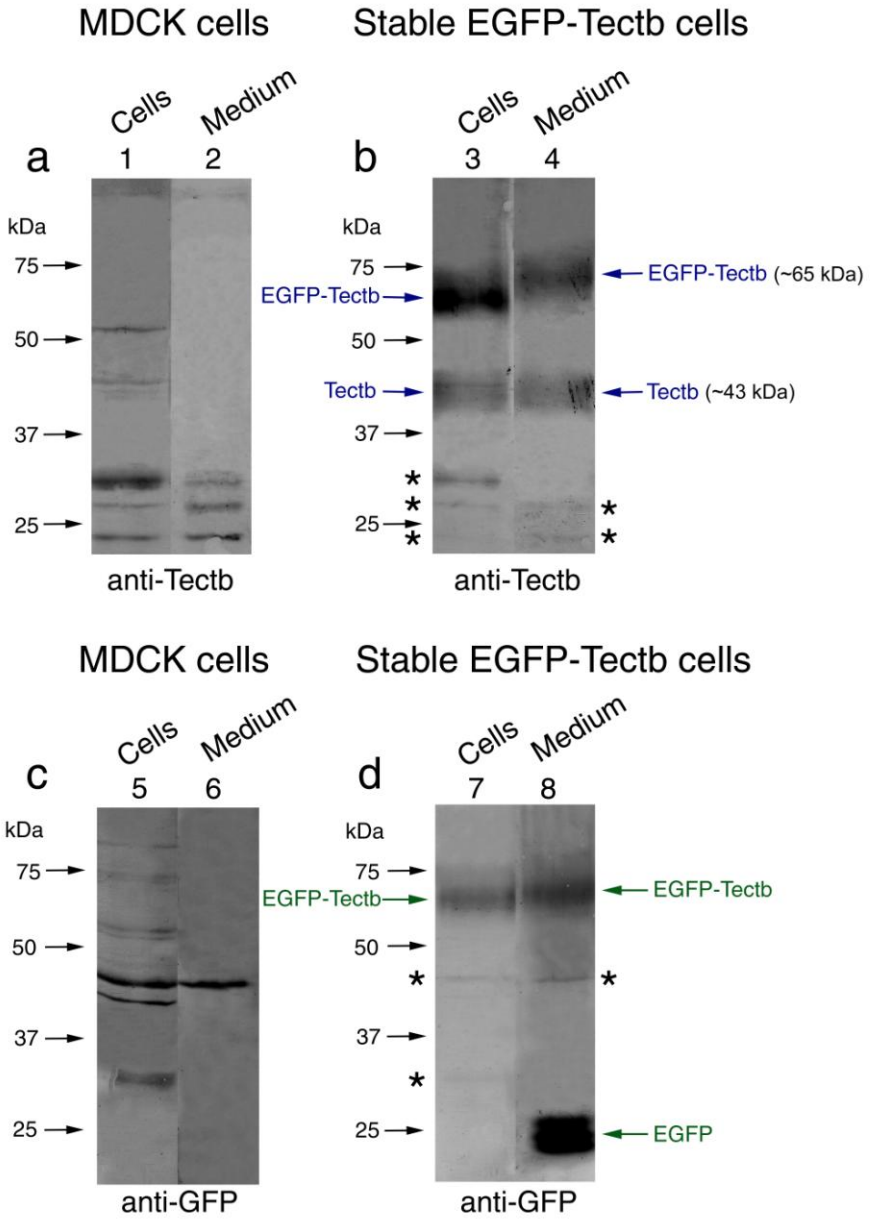

Figure 3.19. Western blotting of stable EGFP-Tectb cell lysates and culture media labelled with anti-Tectb (b) and anti-GFP antibodies (d). Panels a and c are western blotting of nontransfected MDCK cells and their culture medium used as a control. Both anti-Tectb and anti-GFP antibodies detect an EGFP-Tectb band of around 65 kDa in cell lysates and culture medium (b and d). Anti-Tectb antibody reveals Tectb only band of about 43 kDa in cell lysates and culture medium (b). The bands found in culture medium lanes are of slightly higher mass. EGFP protein forms multiple bands in culture medium only (d, lane 8). Non-specific bands in b and d are marked with asterisks and are revealed on negative controls (a and c).

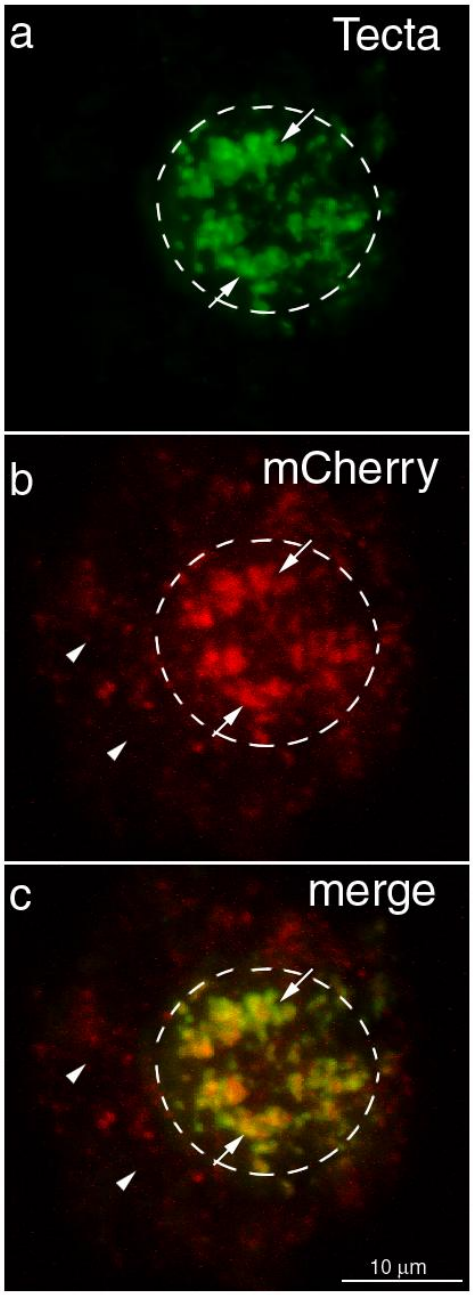

Figure 3.20. Confocal microscopy of a polarised epithelial sphere formed by stably transfected mCherry-Tecta cells after two weeks of growth in collagen-Matrigel™. Spheres were stained with anti-Tecta antibody. Both Tecta (green) and mCherry (red) signals are detected within the cell lumen with a high degree of co-localisation (arrows). mCherry fluorescence signal is also detected within cells (arrowheads). Dashed line indicates the shere's cavity. Scale bar 10 μm.

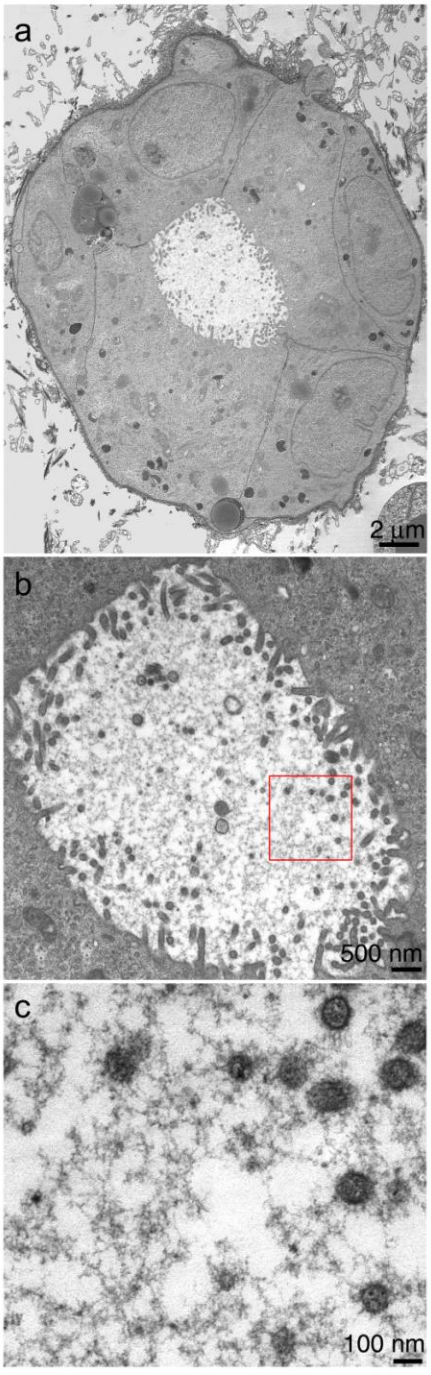

Figure 3.21. TEM images of a 2-week sphere expressing mCherry-Tecta. Panel a shows a low magnification overview of the polarised epithelial cells of the sphere with their apical surfaces directed inwards and forming a central cavity. Panel b presents a higher magnification image of the cavity filled with a secreted material. Panel c is an enlargement of the red-boxed region in panel b. It shows that the extracellular material is formed of fine interconnecting filaments, some of which are attached to the microvilli. Scale bar for a is 2 µm, for b - 500 nm, for c - 100 nm.

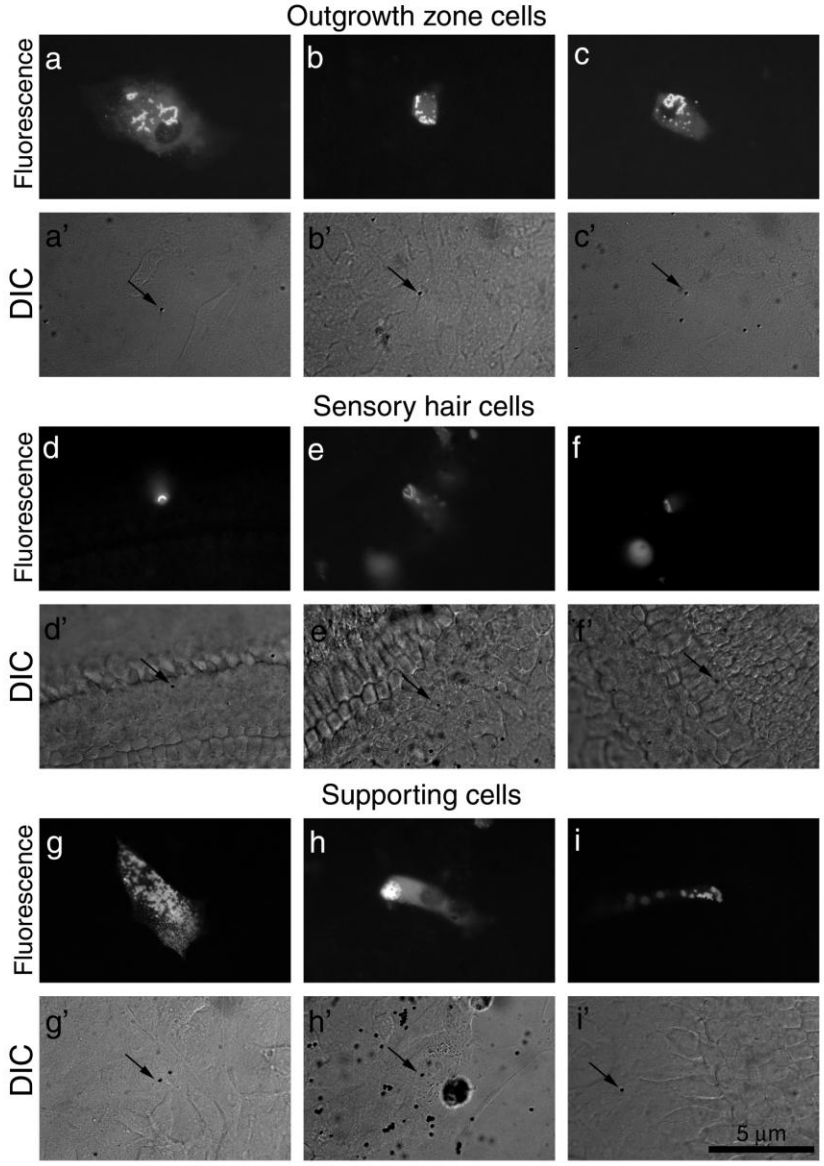

Figure 3.22. Outgrowth zone cells, hair cells and supporting cells live imaged after biolistic transfection with the pBK-EGFP-Tectb construct. Panels a, b, c, d, e, f, g, h and i are wide-field fluorescence images of transfected cells. Panels a', b', c', d', e', f', g', h' and i' are DIC images of the same cells, arrows indicate positions of a gold microcarrier in cell nuclei. Alongside the observed intracellular Tectb expression, cells express matrix-like aggregates on their apical surface. Outgrowth zone cells demonstrate especially high levels of extracellular expression. In hair cells matrix seems to be associated with microvilli. Tectb extracellular expression in supporting cells is limited by their small apical surface. Scale bar 5 μm.

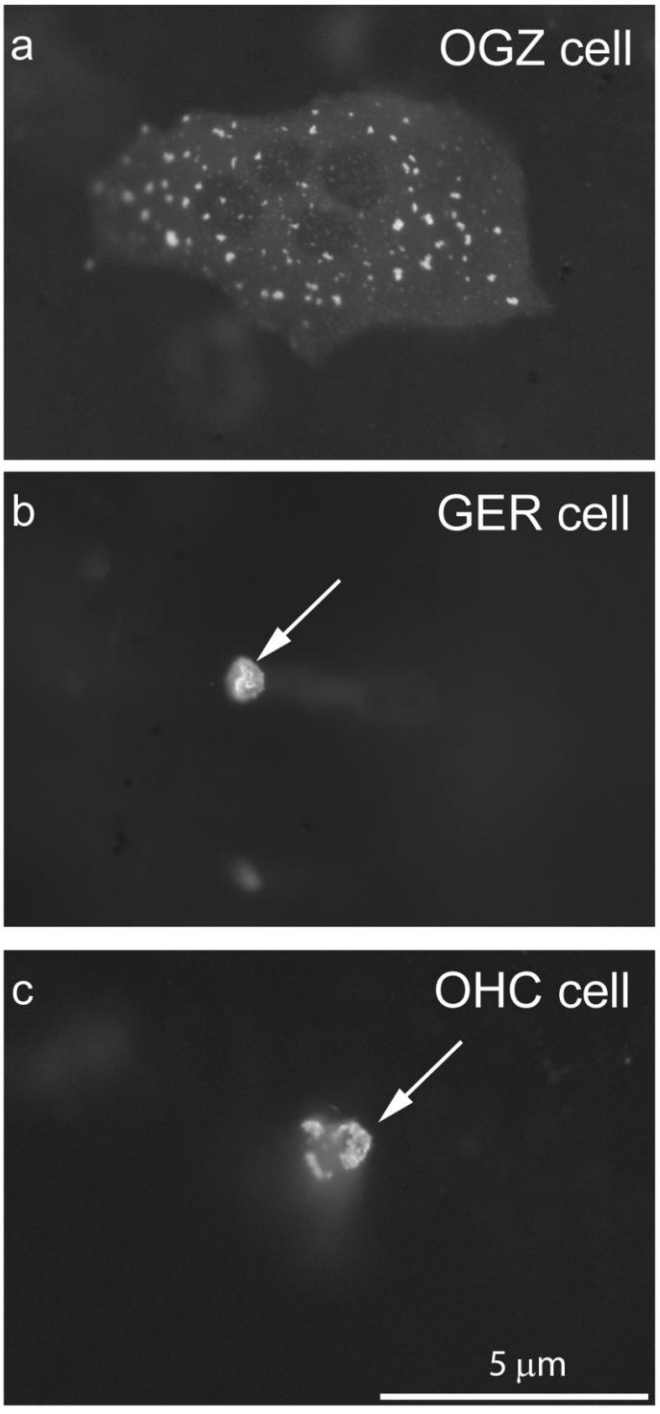

Figure 3.23. Live imaging of cells from the *Tecta*$^{\Delta ENT/\Delta ENT}$/*Tectb* null mouse cochlear culture biolostically transfected with the construct encoding EGFP-Tectb. Panel a displays outgrowth zone (OGZ) cells producing grain-shaped EGFP-positive aggregates. A GER cell generates a vermiculate-shaped lump of matrix at its apex (b, arrow). An OHC without a hair bundle (probably damaged by an accelerated gold microcarrier) has an amorphous matrix at its apical surface (c, arrow). Scale bar 5 μm.

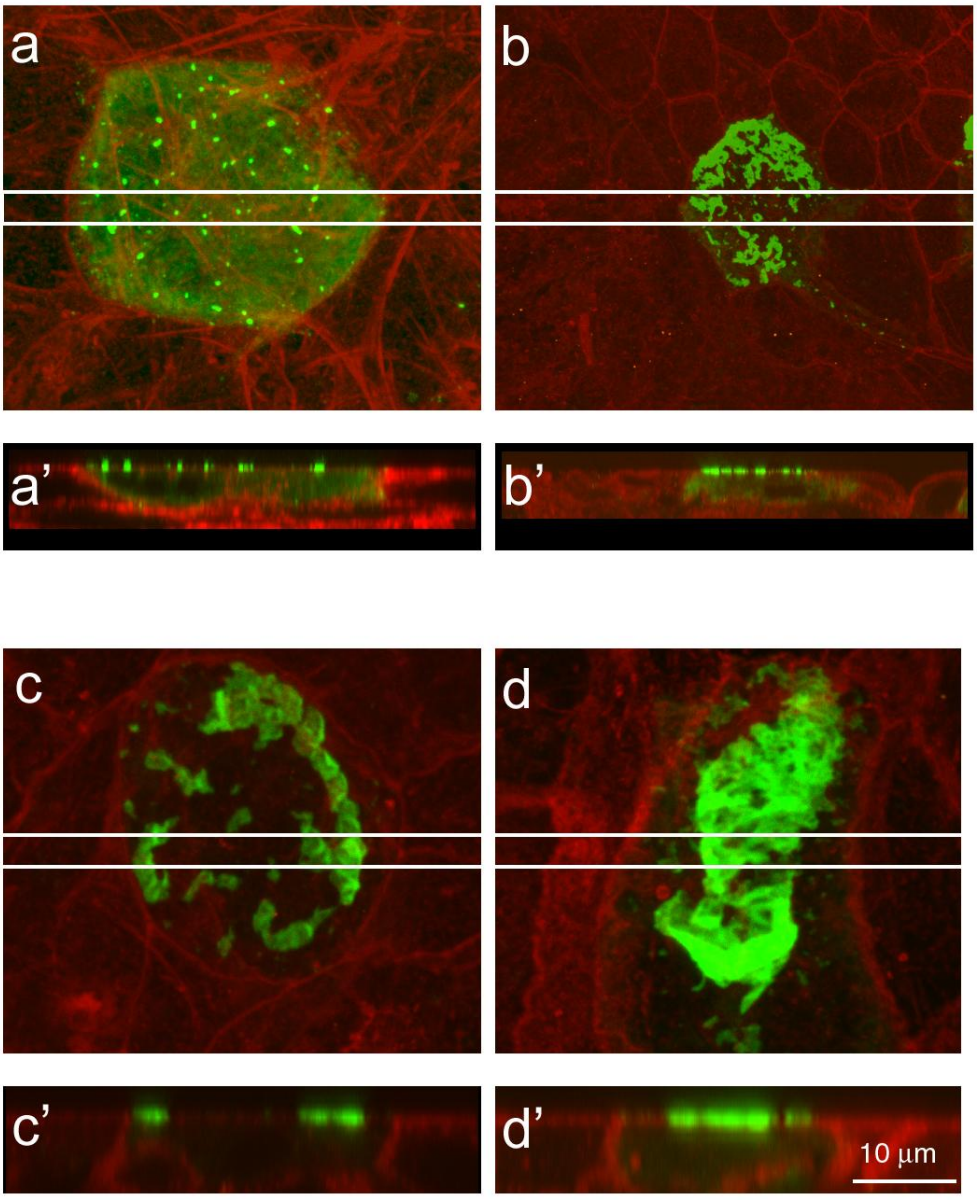

Figure 3.24. Confocal microscope images (a, b, c and d) and Z-stack projections of the region outlined by the white lines (a', b', c' and d') of the outgrowth zone cells from *Tecta*$^{\Delta ENT/\Delta ENT}$/*Tectb* null mouse cochlear cultures transfected with the EGFP-Tectb encoding construct and stained with anti-GFP antibody and Texas Red phalloidin. After 24 hours of incubation outgrowth zone cells produce EGFP-Tectb aggregates of various shape and size which locate extracellularly and remain attached to the apical cell surface. EGFP signal is also detected inside the cell where it is evenly distributed at low levels throughout the cytoplasm. Scale bar 10 µm.

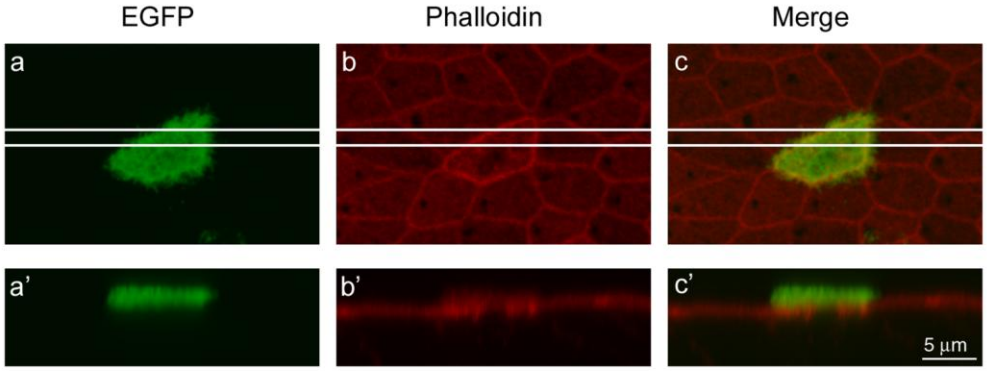

Figure 3.25. Confocal microscope image (a, b and c) and a Z-stack projection of the region outlined by the white lines (a', b' and c') of a GER cell from wild type mouse cochlear culture transfected with the pBK-EGFP-Tectb construct and stained with anti-GFP antibody and Texas Red phalloidin. After 24-hour incubation GER cell generates EGFP-positive matrix material which is secreted on the cell's apical surface and seems to be associated with cell microvilli. Scale bar 5 μm.

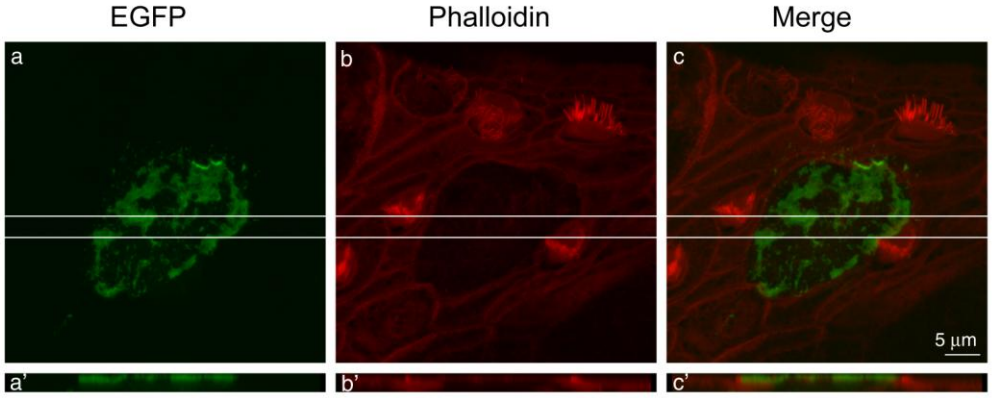

Figure 3.26. Confocal microscope image (a, b and c) and a Z-stack projection of the region outlined by the white lines (a', b' and c') of a Deiter's cell from a wild type mouse cochlear culture transfected with the pBK-EGFP-Tectb construct and stained with anti-GFP and Texas Red phalloidin. Deiter's cells produce an amorphous EGFP-positive matrix that is secreted extracellularly and is closely associated with cell apical surface. Scale bar 5 μm.

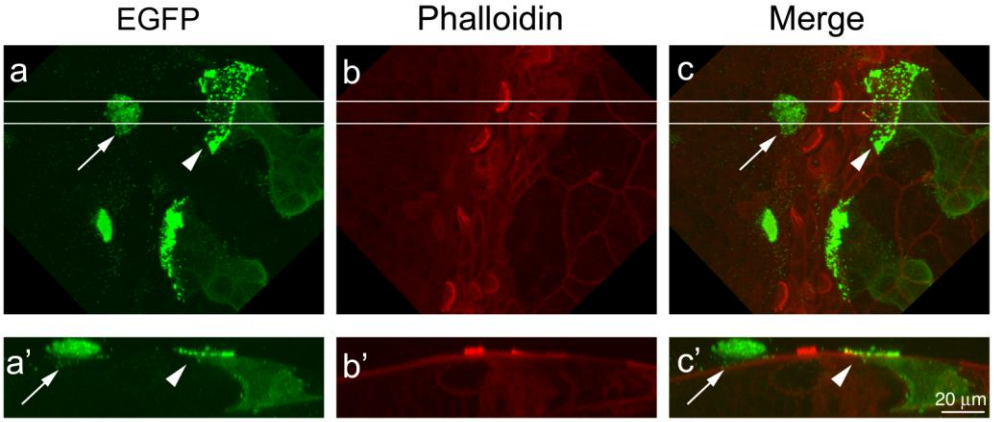

Figure 3.27. Confocal image (a, b and c) and a Z-stack projection (a', b' and c') of the region outlined by the white lines of GER (arrow) and Deiter's (arrowhead) cells from wild type mouse cochlear cultures transfected with the construct encoding EGFP-Tectb and stained with anti-GFP antibody and Texas Red phalloidin. In the Deiter's cell EGFP-positive material is detected within the cell cytoplasm, bright aggregates are secreted extracellularly and stay attached to cell microvilli (a' and c', arrowheads). GER cell forms a thicker layer of matrix which is loosely attached to the cell apical surface (a' and c', arrowheads). Scale bar 20 µm.

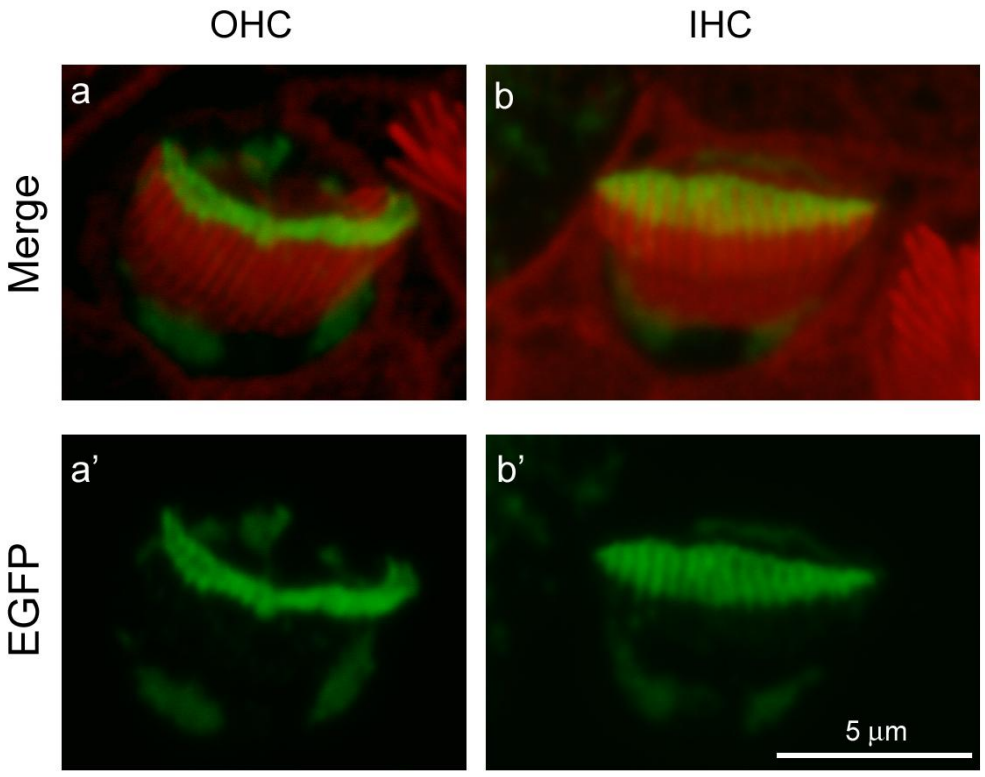

Figure 3.28. Compressed Z-stack confocal projections of an OHC (a and a') and an IHC (b and b') from a wild type mouse cochlear culture transfected with the pBK-EGFP-Tectb plasmid and stained with anti-GFP antibody and Texas Red phalloidin. In both cells Tectb locates to the distal tip of the hair bundle. Scale bar 5 μm.

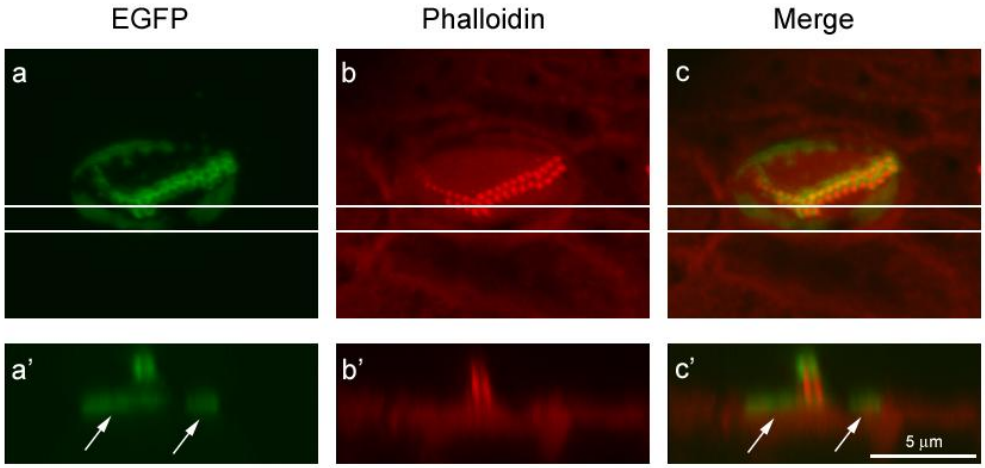

Figure 3.29. OHC from a wild type mouse cochlear culture transfected with the pBK-EGFP-Tectb construct and stained with anti-GFP antibody and Texas Red phalloidin. Confocal microscopy indicates EGFP-Tectb caps at the tips of the stereocilia and an amorphous matrix surrounding the base of the hair bundle (panels a, b and c). The region outlined with the white lines projected around Z-axis (panels a', b' and c') reveals that the matrix-like structure at the base of a hair bundle is located extracellularly (arrows). Scale bar 5 μm.

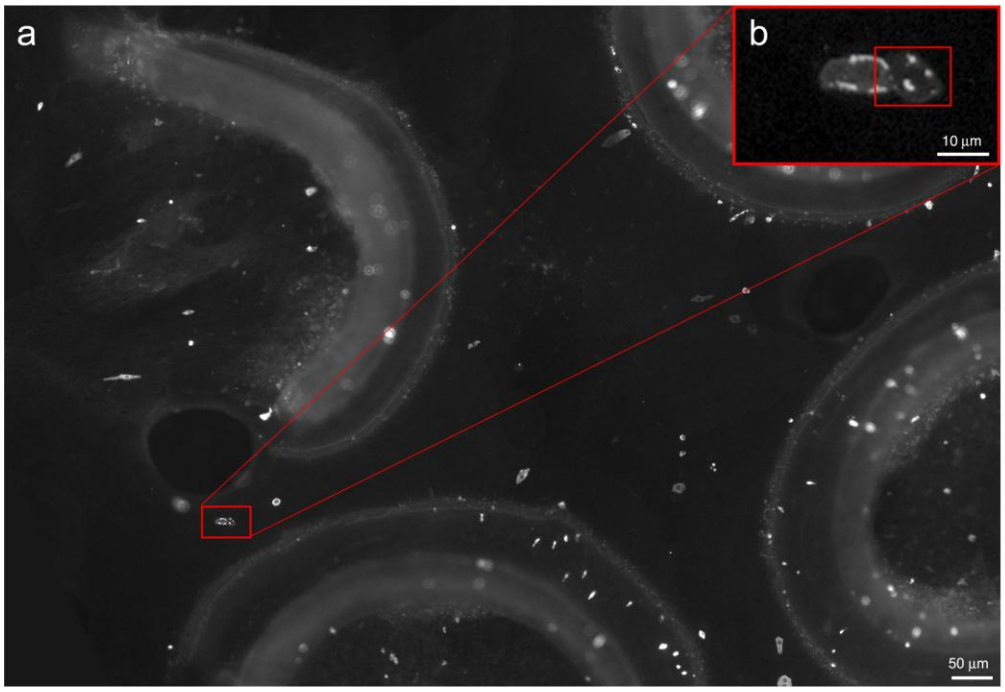

Figure 3.30. Wide-field fluorescence photomontage of a wild type mouse cochlear culture transiently transfected with the pBK-EGFP-Tectb construct using gene gun and stained with anti-GFP antibody to amplify EGFP signal. A small proportion of the cells is transfected, including some cells of the outgrowth zone (a). One example of an outgrowth zone cell transfected with EGFP-Tectb is highlighted (red box) and shown in a bigger magnfication (b). Scale bar for a is 50 µm, scale bar for b is10 µm.

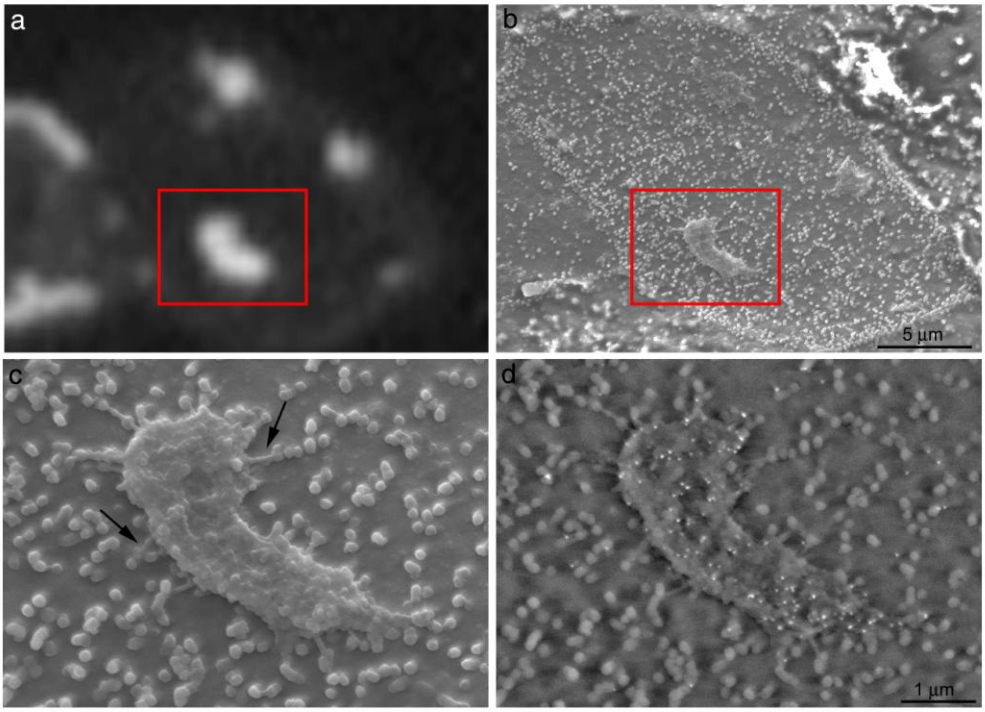

Figure 3.31. A bean-shaped EGFP-positive aggregate is on the surface of the outgrowth zone cell from a wild type neonatal mouse cochlear culture biolistically transfected with pBK-EGFP-Tectb and stained with anti-GFP antibody (a, red box). After cultures were labelled with anti-Tectb antibody and double-labelled with 10 nm anti-rabbit gold-conjugated IgG, the same cell was found under SEM (b), the corresponding matrix lump is enclosed in a red box. Panel c shows a SEI scan of the cell surface with a matrix aggregate attached to cell microvilli with thin filamentous structures (arrows). BSD image (d) reveals the gold labelling on the surface of the aggregate. Scale bar for panels a and b 5 µm, for panels c and d 1 µm.

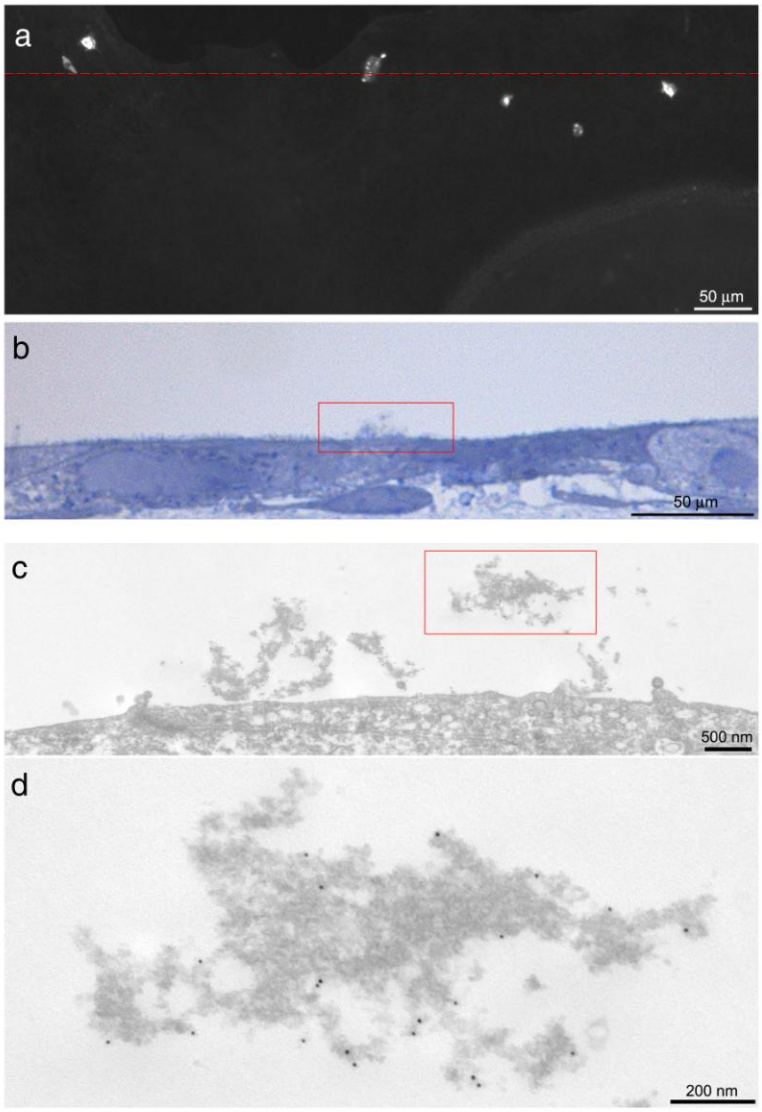

Figure 3.32. Correlative light-transmission electron microscopy of an outgrowth zone cell from a wild type neonatal mouse cochlear culture transfected with the pBK-EGFP-Tectb plasmid using the gene gun. Panel a represents a photomontage of the culture fragment containing an outgrowth zone cell with EGFP-positive aggregates on its surface. Red line indicates a place where the sections were taken after the culture was processed for TEM. Panel b shows a light microscope image of a 1 µm thick cross-section through the outgrowth zone cell stained with toluidine blue. Surface matrix material is enclosed in a red box. A 100 nm section analysed with TEM is shown in panel c. A fragment of matrix included in the red box is shown at higher magnification in panel d. The matrix is labelled with gold particles bound to anti-Tectb antibody and has an amorphous structure. Scale bars: panel a is 100 µm, panel b is 50 µm, panel c is 500 nm and panel d is 200 nm.

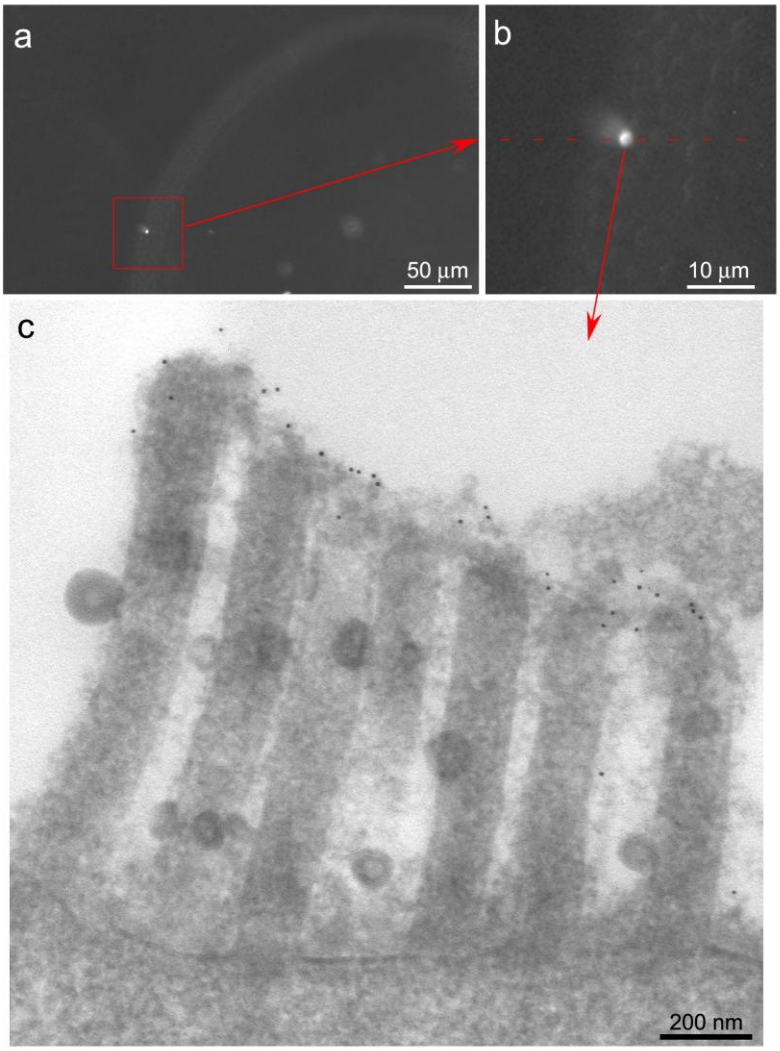

Figure 3.33. Correlative light-transmission electron microscopy of an EGFP-expressing OHC in a neonatal wild type mouse cochlear culture biolistically transfected with the pBK-EGFP-Tectb construct. Panel a is a wide-field fluorescence image of four hair cell rows. Bright fluorescence signal (EGFP amplified with anti-GFP) detected in one of the second row OHCs is enclosed in a red box and shown in a higher magnification in panel b. TEM indicates that gold labelling associated with anti-Tectb staining is observed on the surface of the distal tips of stereocilia. Scale bars: panel a is 50 µm, panel b is 10 µm, panel c is 200 nm.

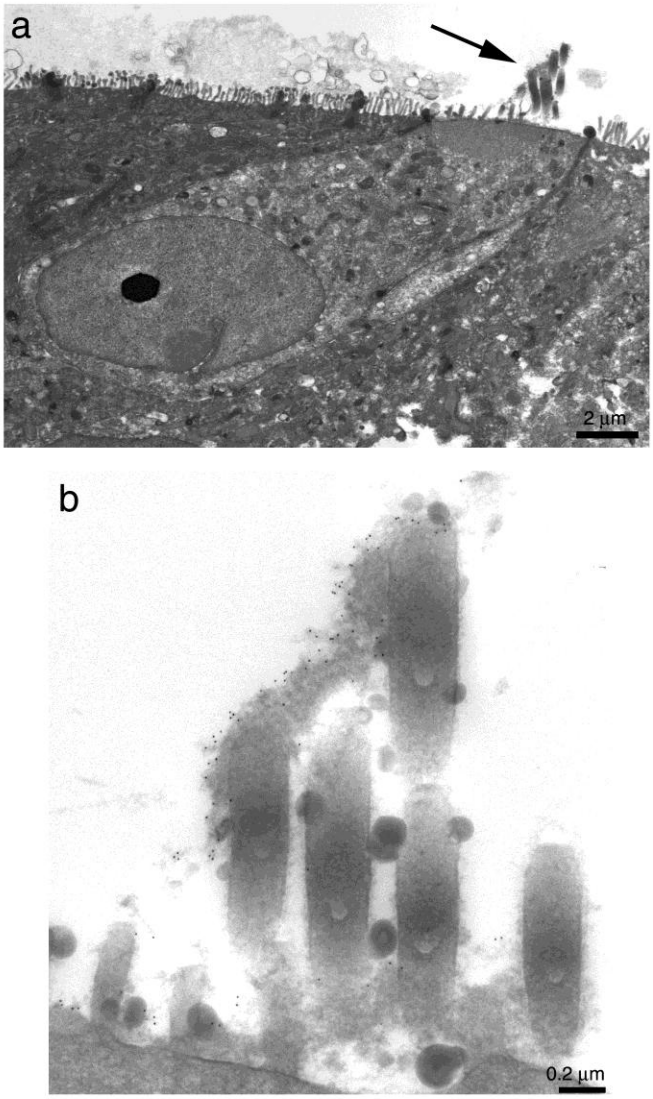

Figure 3.34. TEM images of an IHC from a neonatal wild type mouse cochlear culture transfected with the pBK-EGFP-Tectb construct, stained with anti-Tectb antibody and double-labelled with an anti-rabbit gold-conjugated antibody. Panel a shows a low magnification image of a transfected IHC with a gold microcarrier in its nucleus. Hair bundle is indicated by an arrow. Panel b is a high magnification image of the hair bundle. As shown on panel b, gold labelling localises to the amorphous matrix coating at the tips of stereocilia. Scale bar for panel a is 2 µm, for panel b is 0.2 µm.

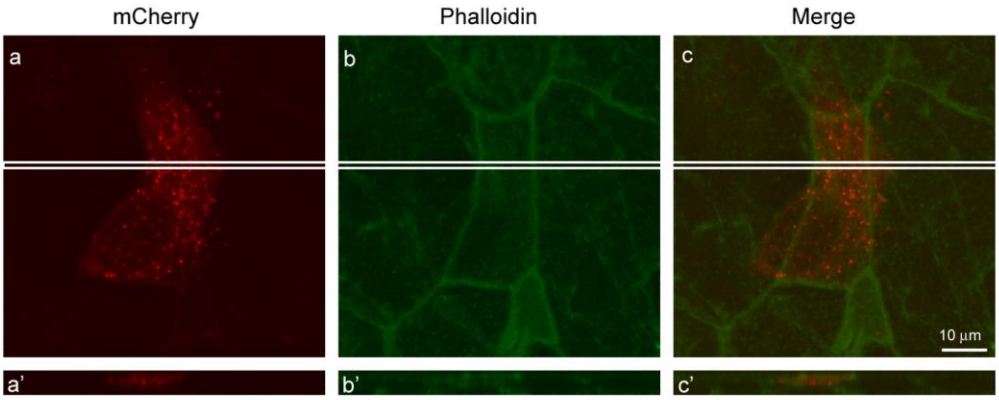

Figure 3.35. Confocal microscope image (a, b and c) and a compressed Z-stack projection of the region outlined by the white lines (a', b' and c') of an outgrowth zone cell from a neonatal wild type mouse cochlear culture transfected with the pBK-mCherry-Tecta construct and stained with fluorescein phalloidin. Although mCherry-Tecta forms punctae, they are localised intracellularly. Scale bar 10 µm.

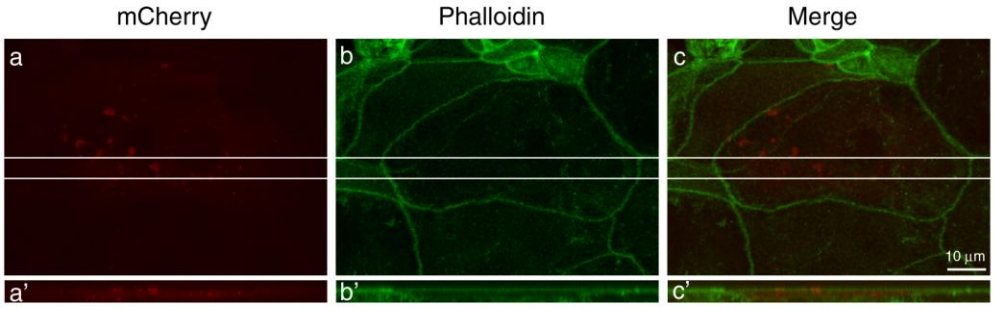

Figure 3.36. Confocal microscope image (a, b and c) and a compressed Z-stack projection (a', b' and c') of the region outlined by the white lines of an outgrowth zone cell from a neonatal wild type mouse cochlear culture transfected with the pCAG-mCherry-Tecta plasmid and stained with fluorescein phalloidin. mCherry-positive matrix forms discrete particles (a and c) most of which localise within the cell body. Scale bar 10 µm.

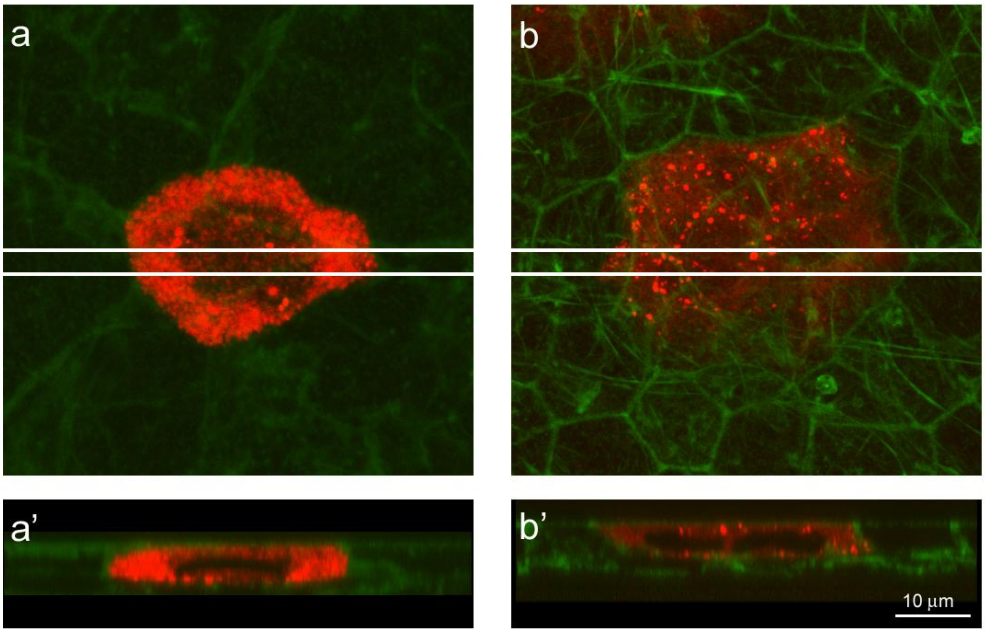

Figure 3.37. Confocal microscope images (a and b) and compressed Z-stack projections of the region outlined by the white lines (a' and b') of outgrowth zone cells from a neonatal mouse wild type cochlear culture transfected with the pBK-mCherry-MMMTecta and pBK-mCherry-ZPTecta constructs using the gene gun and stained with fluorescein phalloidin. Both cells show a significant level of mCherry expression. mCherry-MMMTecta and mCherry-ZPTecta form matrix aggregates which fill the cytoplasm. However, no signs of extracellular expression are observed. Scale bar 10 μm.

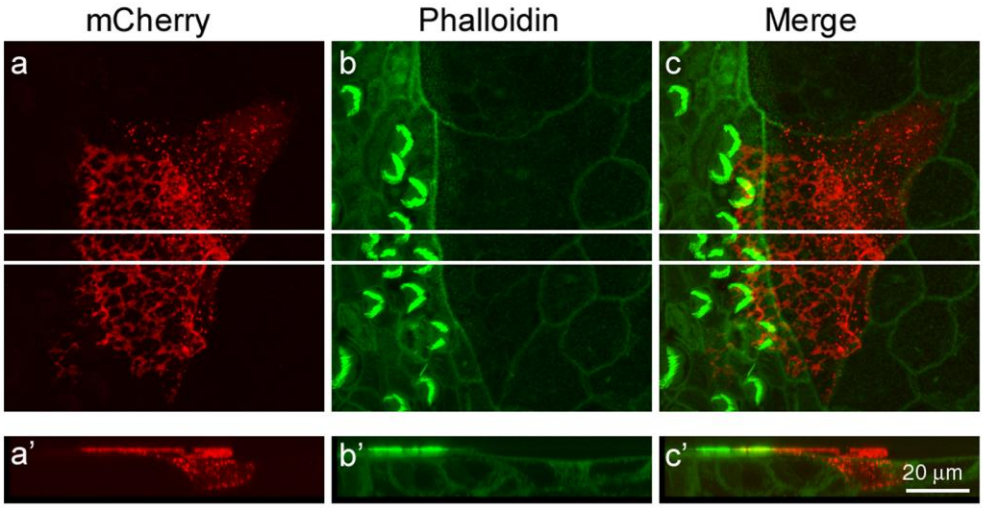

Figure 3.38. Confocal microscope image (a, b and c) and a compessed Z-stack projection of the region outlined by the white lines (a', b' and c') of a Hensen's cell in a neonatal wild type mouse cochlear culture transfected with the pBK-mCherry-Tecta construct using the gene gun and stained with fluorescein phalloidin. mCherry-positive aggregates are produced in the cell cytoplasm and secreted onto its apical surface where it forms a layer of meshwork-like matrix. Scale bar 20 µm.

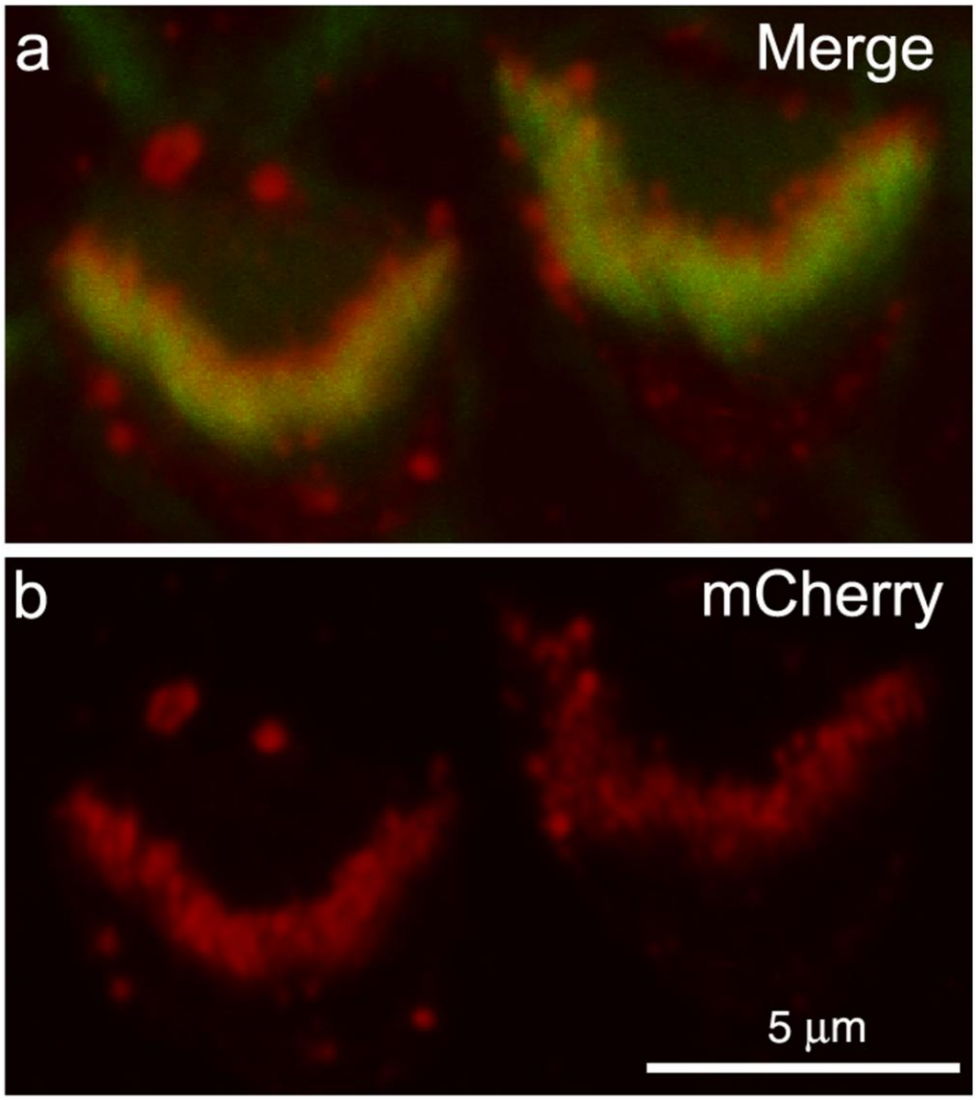

Figure 3.39. Confocal image of OHCs from a neonatal mouse cochlear explant transfected with the pCAG-mCherry-Tecta construct and stained with fluorescein phalloidin. As well as EGFP-Tectb agregates, mCherry-positive aggregates are secreted at the distal end of the hair bundle where they stay attached to the tips of stereocilia. However, mCherry-Tecta looks different than EGFP-Tectb (see Fig.3.28). Scale bar 5 μm.

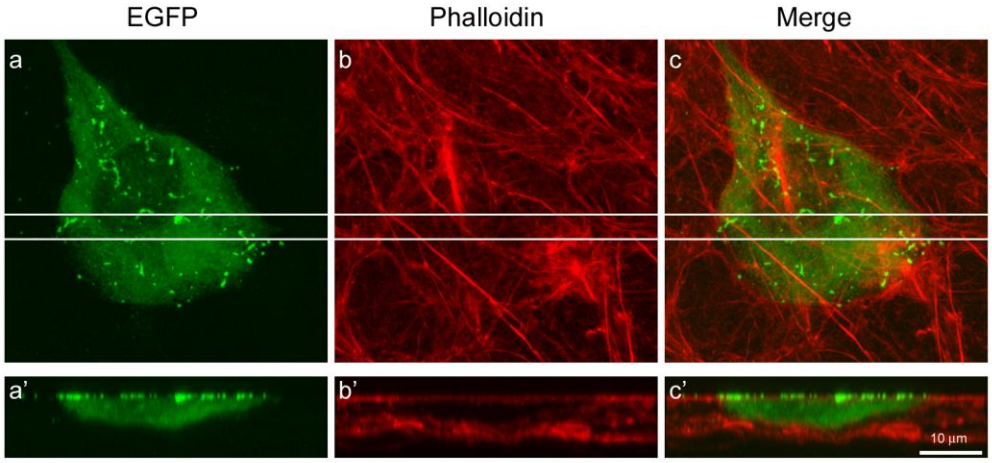

Figure 3.40. Confocal microscope image (a, b and c) and a compressed Z-stack projection of the region outlined by the white lines (a', b' and c') of an outgrowth zone cell from a neonatal mouse cochlear culture transfected with the pBK-EGFP-Tecta construct and stained with anti-GFP antibody and Texas Red phalloidin. Anti-GFP antibody reacts with the content of the outgrowth zone cell indicating intracellular EGFP-Tecta expression. The cell also secretes EGFP-positive aggregates on its apical surface. Scale bar 10 µm.

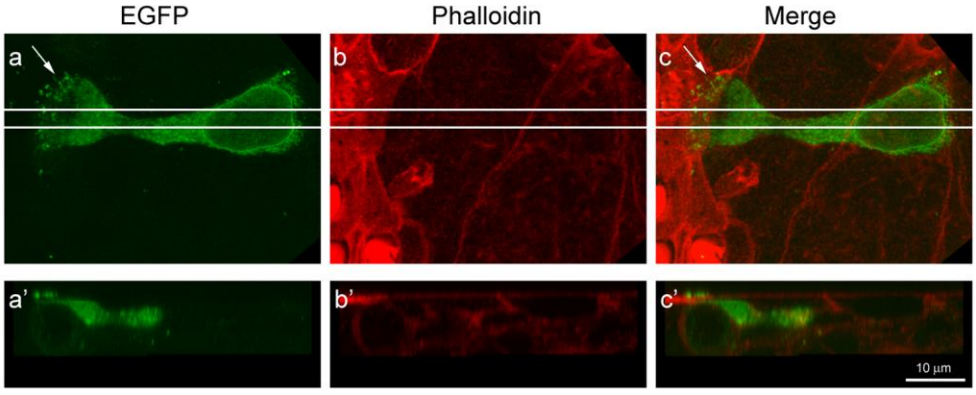

Figure 3.41. Confocal microscope image (a, b and c) and a compressed Z-stack projection of the area outlined by the white lines (a', b' and c') of a Deiter's cell from a neonatal mouse cochlear culture transfected with the pBK-EGFP-Tecta construct and stained with anti-GFP antibody and Texas Red phalloidin. Deiter's cells reveal an intracellular EGFP-Tecta expression and also produce matrix aggregates on their apical surface (arrows). Scale bar 10 µm.

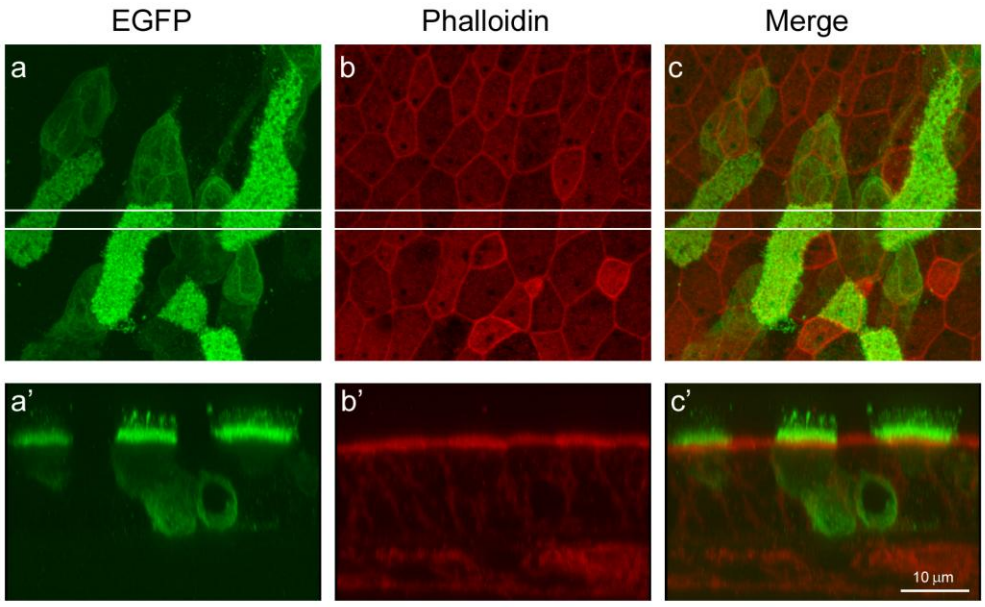

Figure 3.42. Confocal microscope image (a, b and c) and a compressed Z-stack projection of the region outlined by the white lines (a', b' and c') of GER cells from a neonatal mouse cochlear culture transfected with the pBK-EGFP-Tecta construct and stained with anti-GFP antibody and Texas Red phalloidin. Each GER cell secretes a thick EGFP-positive matrix layer on its apical surface. Scale bar 10 μm.

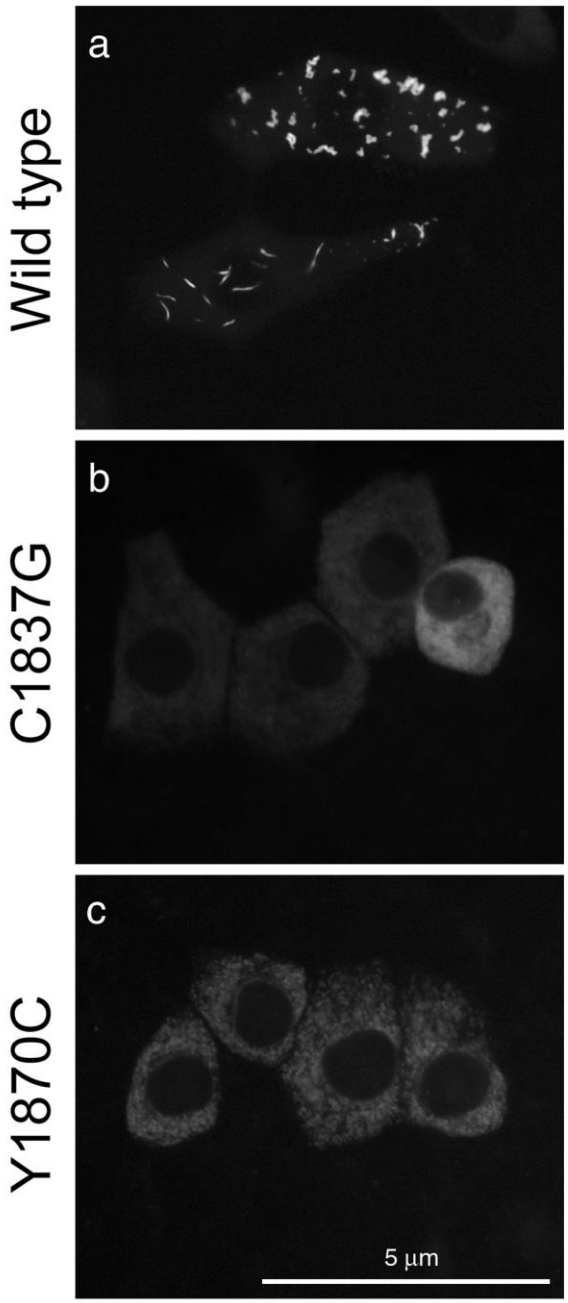

Figure 3.44. Live immunofluorescence images of outgrowth zone cells from neonatal mouse cochlear cultures transfected with the wild type and mutated Tectb constructs using gene gun. Images were obtained 24 hours post transfection. While outgrowth zone cells transfected with wild type Tectb produce EGFP-positive aggregates (a), EGFP signal in outgrowth zone cells with a mutant Tectb DNA is evenly distributed in the cytoplasm and matrix aggregates are not detected (b and c). Scale bar 5 µm.

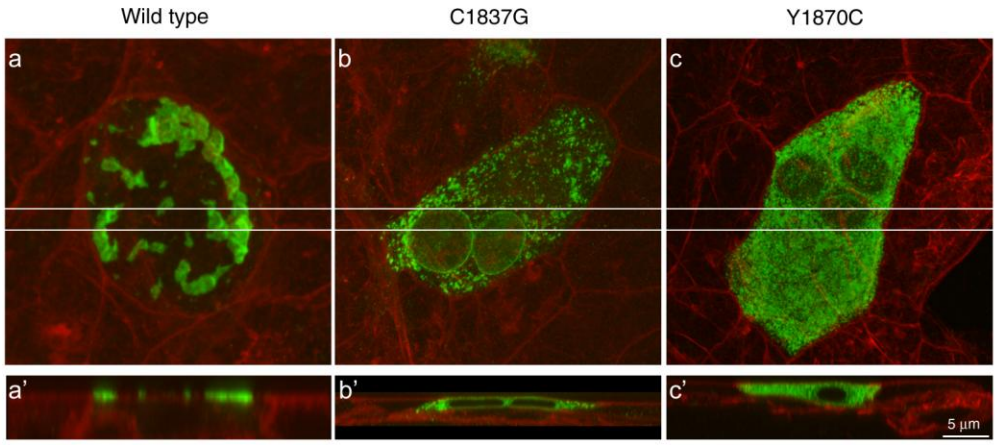

Figure 3.45. Confocal microscope images (a, b and c) and compressed Z-stack projections of the area outlined by the white lines (a', b' and c') of outgrowth zone cells from neonatal wild type mouse cochlear cultures transfected with the wild type and mutant Tectb constructs using gene gun and stained with anti-GFP antibody and Texas Red phalloidin. Outgrowth zone cell transfected with the wild type Tectb construct secretes amorphous matrix on its surface (a and a'). In contrast, outgrowth zone cells transfected with the C1837G and Y1870C Tectb constructs are characterised only by intracellular EGFP-Tectb expression. Scale bar 5 µm.

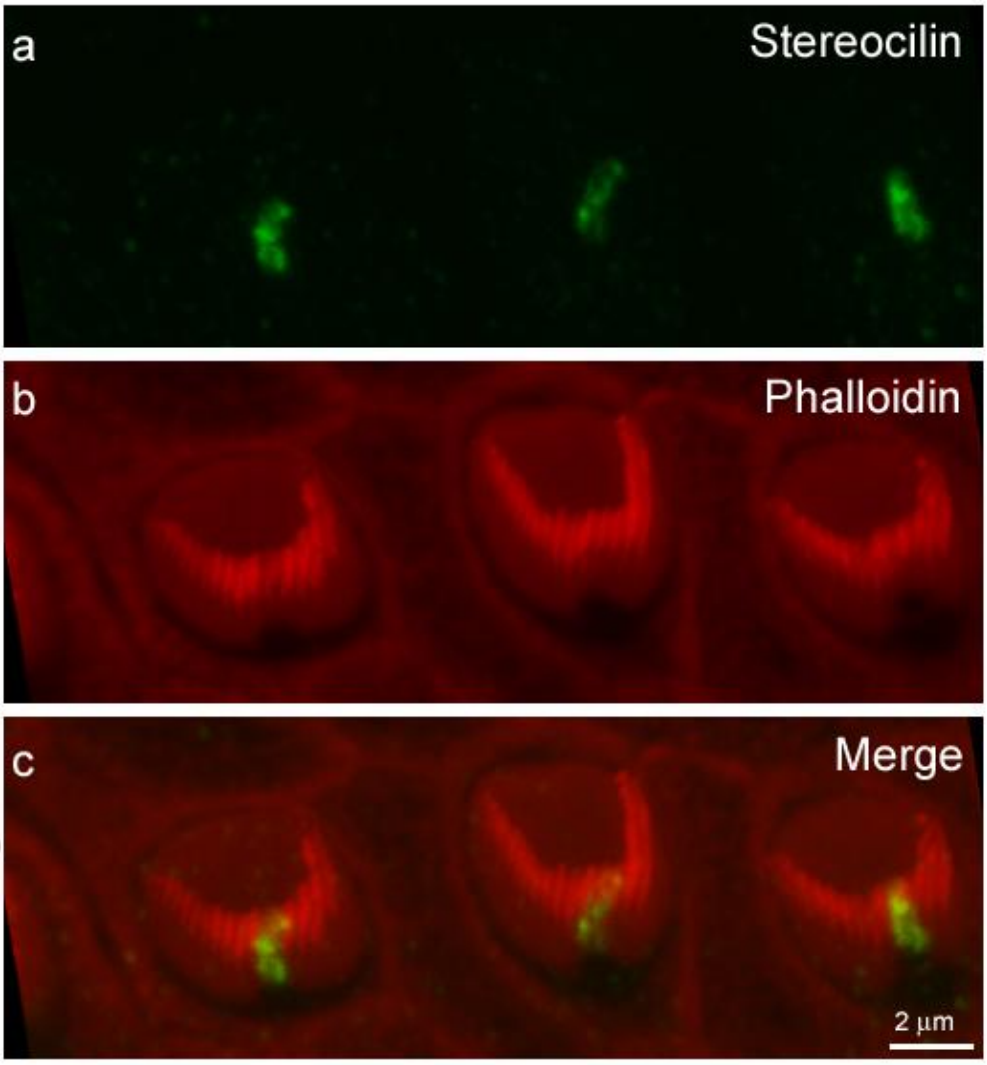

Figure 3.47. Confocal microscope image of outer hair cells from a neonatal mouse cochlear culture stained with anti-stereocilin antibody (green) and Texas Red phalloidin (red). Anti-stereocilin antibody indicates that at the age examined (P2+1) stereocilin is only present on the kinocilia. Scale bar 2 μm.

CHAPTER 4

Phenotypic analysis of Ceacam16 null mutant mouse

4.1. Introduction

Ceacam16, a member of a large group of mammalian immunoglobulin-related glycoproteins , is a secreted protein specifically expressed in the inner ear . A mutation in the *Ceacam16* gene is thought to be the cause of human ADNSHL discovered in an American family . However, the role of Ceacam16 in normal hearing is unclear. To reveal its possible function a *Ceacam16* null mutant mouse model was generated.

To study the changes in the inner ear morphology caused by the absence of Ceacam16 and hence to understand its function in hearing and deafness, I analysed the phenotype of *Ceacam16* null mutant mouse model generated as a part of this thesis.

4.2. Results

4.2.1. Ceacam16 expression in a non-mutant mouse model

To study the time course of Ceacam16 expression and the localisation of secreted Ceacam16 protein in a non-mutant mouse model, a CD1 mouse strain was used. Cryosections of cochleae obtained from CD1 mice pups of different ages were stained with anti-Ceacam16 antibody and Texas Red phalloidin. Although Ceacam16 protein is absent in the basal turn of the cochlea at P3 (Fig.4.1, a and a'), it can be detected at P9 as a narrow region of immunoreactivity with the anti-Ceacam16 antibody on the surface

of a spiral limbus (Fig.4.1, b'), in the place of the TM attachment (Fig.4.1, b and b'). At P14 the staining spreads to the limbal and marginal zones of the TM and also appears around the edge of the TM main body (Fig.4.1, c and c'). However, Ceacam16 is not detected in the main body itself at this stage (Fig.4.1, c). Although all zones of the TM appear to be positive for Ceacam16 at P22, the staining is still brighter at the limbal and marginal zones (Fig.4.1, d and d').

In the apical turns of the cochlea of a non-mutant mouse, Ceacam16 staining is not detected at P3 and P9 (Fig.4.2, a and a', b and b'), but appears at P14 at the limbal and marginal zones of the TM (Fig.4.2, c and c'). As in the basal turns of the cochlea, the main body of the TM is not stained for Ceacam16 at P14 (Fig.4.2, c and c'). At P22 the entire TM body is immunoreactive with anti-Ceacam16 antibody. Like in the basal parts of the TM, the limbal and marginal zones are stained stronger (Fig.4.2, d and d').

Western blotting of the TMs from P10, P12, P14 and P16 CD1 mouse pups indicates that Ceacam16 appears in the TM at P12 and produces a ladder of oligomeric forms under reducing conditions (Fig.4.3). The amount of Ceacam16 protein in the TM increases between P12 and P16 (Fig.4.3). As a reference, immunoblotting was also performed with antibodies to other TM proteins: Tecta, Tectb and collagen type IX. These proteins are already present in the TM at P10 and the levels of Tectb and collagen type IX expression stay stable through all the stages examined (Fig.4.3). Tecta expression, however, continue to grow over the period from P10 to P16.

Noteworthy, the onset of Ceacam16 expression precedes the appearance of clearly defined striated sheet matrix which gains its mature appearance by P16 (Fig.4.4). This observation is consistent with the idea of Kammerer et al., 2012 that Ceacam16 protein is required for striated-sheet matrix formation.

4.2.2. Ceacam16 null mutant mouse model

4.2.2.1 βgal reporter expression

In the *Ceacam16* null mutant mouse, exons 2-5 of the *Ceacam16* gene are replaced with a β-galactosidase reporter and the cells in which *Ceacam16* gene is active can be readily visualised with X-Gal staining. Fig.4.5 shows X-Gal-stained cochleae from P82 (a, b and c) and 6 months old (a', b' and c') *Ceacam16*$^{+/+}$, *Ceacam16*$^{\beta gal/+}$ and *Ceacam16*$^{\beta gal/\beta gal}$ mice. X-Gal staining is not detected in wild type cochleae (Fig.4.5, a and a'). In heterozygous and homozygous mutant cochleae the staining appears along the spiralling organ of Corti with the strongest stain seen in the proximity to the helicotrema (Fig.4.5, b and b', c and c'). X-Gal staining observed in heterozygotes (Fig.4.5, b and b') is, as expected with only one copy of the *βgal* gene, weaker than that seen in homozygous mutants (Fig.4.5, c and c'). However, in both heterozygotes and mutants, X-Gal staining is stronger at 6 months than in the earlier stages, indicating that Ceacam16 expression lasts up to 6 months of age and may continue to increase (Fig.4.5, compare b and c with b' and c').

The detailed examination of cryosections of the organ of Corti from *Ceacam16*$^{\beta gal/\beta gal}$ animals reveals that the β-galactosidase reporter is expressed in the epithelial cells of the spiral limbus and inner sulcus (Fig.4.6). X-Gal staining is also observed in the Deiter's cells, pillar cells and border cells (Fig.4.6). Obvious staining is not seen in outer and inner hair cells (Fig.4.6). Interestingly, there is a gradient in β-galactosidase reporter expression through the length of the organ of Corti. As revealed by X-Gal staining, lacZ expression is weaker in the apical turns of the cochlea (Fig.4.7, a), but becomes more prominent towards the basal part (Fig.4.7, b). A comparative developmental cryosection series from the apical and basal turns of X-Gal-stained cochleae from mutant mice confirm the presence of this gradient from the early stages

of postnatal development (Fig.4.8). Expression of βgal starts from the basal turn of the cochlea at P8 (Fig.4.8, b'), where X-Gal staining is detected in the border cells (supporting cells lying medial to the IHCs), and reaches the apical end by P14 (Fig.4.8, e). However, in the sections examined, βgal expression in the border cells of the basal turn of the cochleae is downregulated at P10 and only the small patch of spiral limbus epithelial cells appears to react with X-Gal (Fig.4.8, c'). By P12, lacZ reporter expression spreads through the surface of the spiral limbus and inner sulcus and is also detected in the border cells and the third row of Deiter's cells (Fig.4.8, d'). X-Gal staining becomes brighter by P14 and also appears in the two other rows of Deiter's cell and in the pillar cells (Fig.4.8, e'). It is, however, more prominent in the outer pillar cell. βgal expression gets even stronger at P16 (Fig.4.8, f'). In the apical region of the organ of Corti X-Gal staining appears in the spiral limbus only by P14 (Fig.4.8, e). At P16, weak staining can be detected in the border and Deiter's cells (Fig.4.8, f). Fig.4.9 demonstrates that βgal expression is detected in the all cell types at stages of postnatal development later than P16. In mutant mice examined at P82, 6 months and 1 year, X-Gal staining is observed in the spiral limbus, border cells, pillar cells and Deiter's cells.

4.2.2.2. LacZ reporter is not expressed in OHCs

In situ hybridisation experiments suggested that Ceacam16 is expressed in OHCs, but is absent in the supporting cells. However, in the present study, X-Gal staining of cryosections from the cochleae of *Ceacam16* null mutant mice indicates that Ceacam16 protein is expressed in Deiter's cells, but not OHCs. To confirm this finding, cryosections were stained with anti-βgal antibody and analysed using confocal microscopy (Fig.4.10, a). Fluorescein phalloidin was used to define cell borders (Fig.4.10, b). Consistent with the results obtained with X-Gal, anti-βgal immunostaining

is detected in Deiter's cells (Fig.4.10, c), OHC bodies, however, do not react with the anti-βgal antibody (Fig.4.10, c).

4.2.2.3. Staining for Ceacam16 protein in the vestibular system of *Ceacam16* null mutant mouse

X-Gal staining is not detected in the vestibular system of *Ceacam16*$^{\beta gal/+}$ and *Ceacam16*$^{\beta gal/\beta gal}$ mice at the stages of postnatal development that were examined (P21, P82, 6 months and 1 year). As shown in Fig.4.11, the lateral crista, saccule and utricle from a P21 mutant animal do not have any signs of βgal reporter expression.

4.2.2.4. Protein composition of the TM in *Ceacam16* null mutant mouse

Cryosections of the cochleae from *Ceacam16*$^{+/+}$, *Ceacam16*$^{+/\beta gal}$ and *Ceacam16*$^{\beta gal/\beta gal}$ mice at P21 were stained with soybean agglutinin (SBA, or lectin) which binds to carbohydrate-containing structures to study the distribution of the glycoconjugates recognised by this lectin in the TM of mice with these three genotypes. Wide-field immunofluorescence microscopy indicates that the distribution appears to be similar in the wild type, heterozygous and homozygous mutant animals. Fig.4.12 demonstrates that SBA reacts with the marginal band, covernet and the limbal zone of the TM in all three genotypes.

To determine whether the lack of Ceacam16 protein can influence the expression of other inner ear components, cryosections from the cochleae of *Ceacam16*$^{+/+}$, *Ceacam16*$^{+/\beta gal}$ and *Ceacam16*$^{\beta gal/\beta gal}$ mice at P21 were stained with antibodies to the following proteins: Tecta, Tectb, collagen type IX, otogelin and the TM attachment protein otoancorin (Fig.4.13). Staining for Ceacam16 was also performed, and in accordance with expectations it is strong in the *Ceacam16*$^{+/+}$ mouse cochlea (Fig.4.13, a), weaker in the *Ceacam16*$^{+/\beta gal}$ (Fig.4.13, b) and is completely absent in the

Ceacam16$^{\beta gal/\beta gal}$ mouse (Fig.4.13, c). Ceacam16 staining in both wild type and heterozygous animals locates to the limbal and marginal zones of the TM (Fig.4.13, a, and b). No differences in the distribution or expression levels of the other proteins are observed.

It is possible that the protein composition and arrangement in the inner ear of a mutant mouse might change with time. Thus the staining with antibodies to inner ear proteins was repeated for *Ceacam16*$^{+/+}$, *Ceacam16*$^{+/\beta gal}$ and *Ceacam16*$^{\beta gal/\beta gal}$ mice at 6 months of age. As indicated in Fig.4.14, the results obtained are similar to P21 data: staining with anti-Ceacam16 antibody is present only in wild type and heterozygous animals (a and b), mainly in the marginal and limbal zones of the TM; no differences in the distribution of otoancorin, Tecta, otogelin and collagen type IX are detected. However, Tectb protein levels in the main body of the TM appear to be decreased in homozygous mutants (Fig.4.14, l) which might indicate a time dependent drop-off in Tectb levels in *Ceacam16*$^{\beta gal/\beta gal}$ mice. The Tectb staining in heterozygote and wild type TMs is comparable.

To verify whether the amount of tectorins in the TM of *Ceacam16*$^{\beta gal/\beta gal}$ mice decreases with time, quantification from western blots of TMs harvested from heterozygous and mutant animals at the age of 1 month and 6 months was carried out. No visible difference is detected for Tecta and Tectb bands between *Ceacam16*$^{+/\beta gal}$ and *Ceacam16*$^{\beta gal/\beta gal}$ animals at 1 month of age (Fig.4.15, a). Although the tectorin bands are weaker at 6 months of age for both heterozygotes and mutants, the Tectb protein band from *Ceacam16*$^{\beta gal/\beta gal}$ mice seems to be the most drastically affected (Fig.4.15, a). Quantification of the western blots confirms that Tecta levels do not differ significantly at 1 month and 6 months of age in the mutant mice (Fig.4.15, b). However, the amount

of Tectb in *Ceacam16*$^{\beta gal/\beta gal}$ mice at 6 months of age is considerably less than at one month of age (Fig.4.15, b).

To identify whether Tectb and Ceacam16 proteins interact once secreted, culture medium from HEK293 cells transiently transfected with constructs encoding Tectb and Ceacam16-V5 was analysed using co-immunoprecipitation (Co-IP) and immunoblotting. The antibodies used for pulling down proteins and western blotting, as well as the results expected for a Tectb/Ceacam16 interaction are presented in Table 4.1.

Antibody used for Co-IP	Antibody used for western blotting	Transient transfection used to obtain culture medium			
		Sham	Tectb	Ceacam16-V5	Tectb+Ceacam16-V5
Anti-Tectb	Anti-Tectb	-	+	-	+
	Monoclonal anti-V5	-	-	-	+
Polyclonal anti-V5	Anti-Tectb	-	-	-	+
	Monoclonal anti-V5	-	-	+	+

Table 4.1. The expected results of Co-IP assay and western blotting in case secreted Tectb and Ceacam16 are interacting partners. Sign "-" marks the combination of antibodies and culture medium where no bands are expected on PVDF membrane. Sign "+" identified the position where the bands are expected.

As shown in Fig.4.16, proteins pulled down with anti-Tectb and then blotted with anti-Tectb and anti-V5 antibodies reveals a similar pattern of background staining for both PVDF membranes with no secreted Tectb band detected (Fig.4.16, a). No proof of interaction between Ceacam16 and Tectb is detected (Fig.4.16, a and b). Anti-Tectb staining of samples pulled down by anti-V5 antibody as well uncovers only non-specific

bands (Fig.4.16, c). Anti-V5 staining of anti-V5 co-immunoprecipitates gives two specific bands in the Ceacam16 lane and one band in Ceacam16+Tectb lane (Fig.4.16, d). The high molecular weight material at 160 kDa forms a narrow band in the top of the Ceacam16 lane. The broad 65-75 kDa band is detected in the Ceacam16 lane, a lesser density band of 175 kDa is found in the Ceacam16+Tectb lane. These bands are likely to represent those Ceacam16 oligomers which are secreted in the culture medium.

4.2.2.5. No changes in Ceacam16 expression are detected in mouse models for Tecta deafness-causing mutations

As was suggested by studies of , Ceacam16 protein might directly interact with Tecta. However, no changes in Tecta content in the TM of *Ceacam16*$^{+/\beta gal}$ and *Ceacam16*$^{\beta gal/\beta gal}$ mice were observed using immunofluorescence microscopy and quantifying western blotting. It is possible, however, that deafness mutations in Tecta which cause alterations in the TM matrix, might have an effect on Ceacam16 protein expression. Hence, cryosections of cochleae from three transgenic mice generated as models for Tecta mutations found in Spanish (C1837G), French (C1619S) and Belgian (L1820F, G1824D) families with ADNSHL (1.5.1.3) were stained with anti-Ceacam16 antibody and examined using confocal microscopy. As shown in Fig.4.17, in the transgenic mice models for Tecta mutations examined, Ceacam16 protein is expressed in apical and basal turns of the cochleae throughout the entire body of the TM in all genotypes.

4.2.2.6. The TM matrix is less dense in the apical turn of the cochlea in *Ceacam16*$^{\beta gal/\beta gal}$ mice

Toluidine blue staining of 1 μm sections from the organ of Corti of *Ceacam16* null mutant mice indicates that the density of the TM in *Ceacam16*$^{\beta gal/\beta gal}$ animals is reduced (Fig.4.18). The lack of the matrix in the main body of the TM is especially prominent in

the apical turn of the cochlea (Fig.4.18, c). A less severe decrease in the TM density is observed in the 20 kHz (basal 1) region of the organ of Corti (Fig.4.18, f). Although the TM in the 40 kHz (basal 2) region has a normal density, it lacks Hensen's stripe (Fig.4.18, i) which is present in wild type and heterozygous animals (Fig.4.18, g and h). The organ of Corti of *Ceacam16*$^{+/\beta gal}$ mice appears to be similar to that of wild type animals, hence, no obvious phenotype is present in heterozygotes up to 6 months of age at the light microscopy level.

4.2.2.7. Ultrastuctural analysis of the TM in *Ceacam16*$^{+/\beta gal}$ and *Ceacam16*$^{\beta gal/\beta gal}$ mice

TEM analysis confirms the normal appearance of striated-sheet matrix in the apical and basal cochlear turns of *Ceacam16*$^{+/\beta gal}$ mice (Fig.4.19, a and a'). In the *Ceacam16*$^{\beta gal/\beta gal}$ mouse disrupted striated-sheet matrix can be seen at P30, the earliest stage examined (Fig.4.19, b and b'). The apical turn of the mutant cochlea is characterised by sparsely packed filaments located between collagen fibrils. The matrix of the mutant basal TM is densely packed but does not appear to be clearly structured (Fig.4.19, b'). The covernet has a normal organisation in the *Ceacam16*$^{+/\beta gal}$ and the *Ceacam16*$^{\beta gal/\beta gal}$ mice (Fig.4.20). TEM analysis also confirms the observation that the TM of mutant animals lacks Hensen's stripe in the basal turns of the cochlea (Fig.4.21).

4.3. Discussion

X-Gal staining reveals that the main sources of Ceacam16 expression in the adult mouse cochlea (P21) are interdental cells of the spiral limbus, epithelial cells of the inner sulcus epithelia, border cells, pillar cells and Deiter's cells. Expression in the Deiter's cells and its absence in OHCs, however, conflicts with the findings of Zheng et al., 2011, who located *Ceacam16* mRNA to OHCs and did not detect it in Deiter's cells of

P42 mice. This can possibly be explained by the optical overlap of the Deiter's cells protrusions with the bodies of OHCs causing Zheng et al. to misidentify the origin of the staining. It might be argued that the Deiter's cells protrusions are secreting Ceacam16 protein which diffuses to the main body of the TM .

Lectin staining demonstrated the presence of glycoconjugates in the limbal zone, covernet and marginal zone of the TM in the *Ceacam16* null mutant mouse. No abnormalities were described for the content and distribution of collagen IX, otogelin and otoancorin proteins in *Ceacam16*$^{+/\beta gal}$ and *Ceacam16*$^{\beta gal/\beta gal}$ mice at P21 and 6 months of age. Previous studies suggested that Ceacam16 and Tecta proteins might be interacting partners . However, no decrease in Tecta levels was detected in *Ceacam16* null mutant mice using immunofluorescence staining and quantitative western blotting. Ceacam16 protein was also detected in the TM of mouse models for Tecta missense mutations in the ZA (French mutation) and ZP (Belgium and Spanish mutations) domains which potentially can disrupt the ability of Tecta to interact with other proteins. However, a significant decrease in the levels of Tectb in the TM of the *Ceacam16*$^{\beta gal/\beta gal}$ mice was observed by the age of 6 months, suggesting that Tectb might interact with Ceacam16. Co-immunoprecipitation assays and western blotting detected high levels of Ceacam16 protein secreted in the cell culture medium but failed to detect extracellular Tectb secretion. One of the possible explanations might be that the anti-Tectb antibody was unable to pull down the proteins in a co-immunoprecipitation assay. However, a Ceacam16 band observed in the Ceacam16+Tectb co-transfection lane is much weaker than in the Ceacam16-only lane which might indicate that Tectb remains within the cytoplasm where it interacts with Ceacam16 protein and prevents its secretion.

The data obtained from the toluidine blue stained sections of the organ of Corti showed that the main body of the TM in the apical turns of the cochlea of *Ceacam16*$^{\beta gal/\beta gal}$ mice contains a reduced amount of matrix. The TEM data revealed a complete disruption of the striated-sheet matrix in the apical TM of mutant animals which may explain the low frequency hearing loss in DFNA4 patients. In the basal turns of the TM the phenotype is, however, less prominent and includes amorphous filaments densely packed between collagen fibrils and the absence of Hensen's stripe. Interestingly, X-Gal staining reveals transient βgal expression in the border cells, located underneath the developing Hensen's stripe, in the basal turn of the organ of Corti in a mutant mouse at P8. This observation indicates that Ceacam16 expression from border cells might be essential for the development of the Hensen's stripe.

In summary, the data indicate that Ceacam16 is involved in the formation of the striated-sheet matrix of the TM. A possible mechanism of interaction between Ceacam16, Tecta and Tectb proteins has been proposed by Kammerer et al., 2012 (Fig.4.22). Tecta and Tectb proteins were suggested to interact through their ZP domains thus producing dark fibrils of striated-sheet matrix. Ceacam16 proteins might form dimers through the disulfide bonds between their IgC2-like subtype B domains. They might then interact with each other through their IgV-like domains thus giving the light-stained fibrils. Dark and light-stained fibrils could be connected by the bridges formed by Tecta. This model, however, does not suggest the direct interaction between Tectb and Ceacam16.

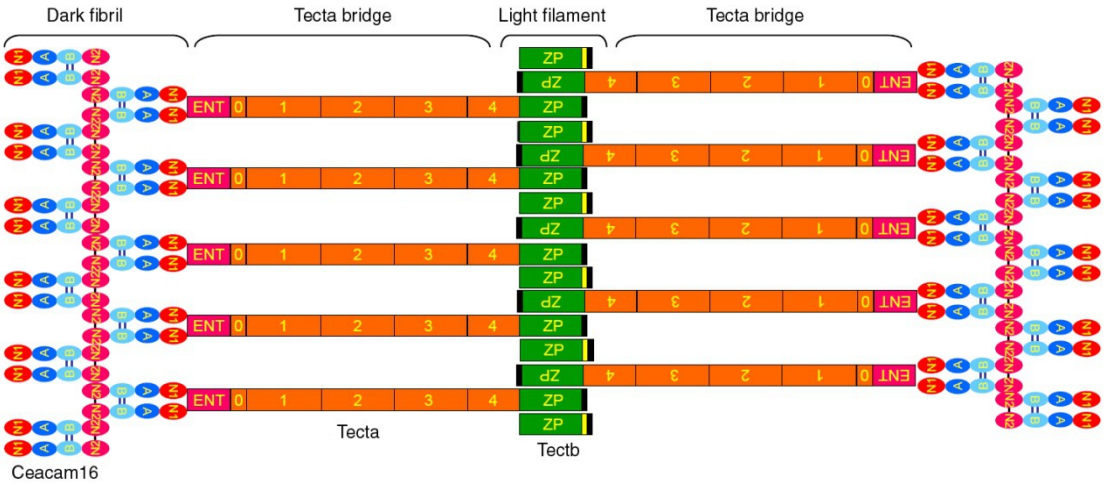

Figure 4.22. Possible organisation of Tecta, Tectb and Ceacam16 in striated-sheet matrix. Ceacam16 molecules interact through their IgC-like B domains forming two disulfide bonds and thus associating in dimers. IgV-like N2 domains of Ceacam16 molecules from different dimers form one disulfide bond connecting Ceacam16 dimers in a staggered structure that might form a dark filament. Light filaments are supposed to be formed by the ZP domain of Tecta and Tectb proteins. Dark fibrils are attached to the Ent domain of Tecta through IgV-like N1 domains. Hence, Tecta protein forms bridges between alternating dark and light fibrils. N1 - IgV-like N1 domain, A and B - IgC-like domains subtypes A and B. Ent - Tecta entactin domain, 0-4 - Tecta von Willebrand factor domains, ZP - Tecta zona pellucida domain. Yellow bar depicts a region of no significant homology with other proteins, black bar indicates for GPI-anchor. Modified from .

These studies also suggest that Ceacam16 might be involved in the long-term maintenance of the TM. In the cochleae of non-mutant mice, the onset of *Ceacam16* mRNA expression is detected at E17 and overlaps with the expression of tectorin mRNAs which starts from E12.5 but shuts down by P15 . While Ceacam16 expression lasts into adulthood, Tecta and Tectb are synthesised in a 3-week period and stay stable throughout the life time of the organism (Rau et al., 1999). This suggests that Ceacam16 might act as a matrix-stabiliser and is essential for preservation of TM composition . Although both tectorins are expressed in the vestibular system, X-Gal staining does not reveal Ceacam16 expressing cells in the vestibule of the *Ceacam16* null mutant mice.

These data are consistent with Ceacam16 role in formation of striated-sheet matrix and maintenance of its stability (Kammerer et al., 2012; Zheng et al., 2011). In a non-mutant mouse model, Ceacam16 protein is detected by P9 as a thin cover over the spiral limbus and by P12 appears in the TM as a ladder of oligomeric forms confirming the results obtained by Zheng et al. in 2011.

No physiological measurements for *Ceacam16* null mutant mice were performed in this research project. However, the 4 weeks old *Ceacam16* null mice with targeted deletion of exons 2-4 and a part of exon 5 generated by Kammerer et al. had hearing impairment which progressed with age. The mutant animals displayed an elevated hearing threshold for frequencies below 10 kHz and above 22 kHz and reduced cochlear amplification. However, the vulnerability of *Ceacam16* to noise exposure was comparable to that in wild type animals. In addition, age-related hearing in both mutant and wild type animals progressed in a similar way.

4.4. Conclusions

The major findings regarding the role of Ceacam16 protein in the TM are summarised below:

1. Ceacam16 expression in the TM precedes the striated-sheet matrix formation and the onset of hearing.

2. Ceacam16 protein is essential for striated-sheet matrix formation and may maintain stability of this matrix over time.

3. The amount of Tectb protein drastically decreases with time in the *Ceacam16*$^{\beta gal/\beta gal}$ mouse.

4. Loss of striated-sheet matrix from the apical end of the tectorial membrane may account for the low frequency hearing loss in DFNA4 patients.

5. No phenotype was discovered in *Ceacam16*$^{+/\beta gal}$ animals.

4.5. Future prospectives

Future studies of *Ceacam16* null mutant mouse model are needed to find out whether there is a special phenotype for *Ceacam16*$^{+/\beta gal}$ mice. Although no phenotype was discovered for heterozygotes up to 6 months, preliminary TEM data indicate that it might appear later. It is worth studying whether *Ceacam16* null mutant mice are more vulnerable to noise exposure or if they age differently to non-mutant animals. The central focus of research should, however, be on physiological assessment of the mutant mice hearing. To describe the heterozygous and mutant phenotypes fully it will be necessary to perform auditory brainstem response (ABR) and distortion product otoacoustic emissions (DPOAE) measurements, to define changes in TM stiffness and to measure compound action potential (CAP). An *in vitro* model of TM matrix assembly described in Chapter 2 might be helpful for finding out the potential interactions of Ceacam16 protein with other components of the TM.

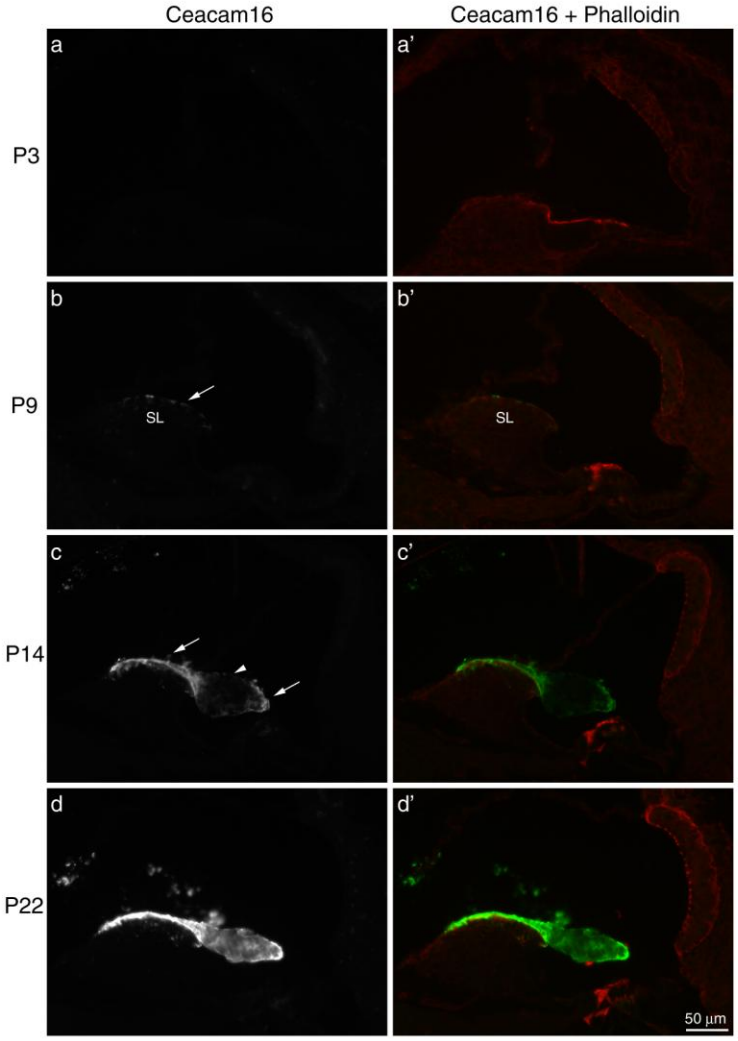

Figure 4.1. Staining for Ceacam16 in the basal turn of the cochlea of a non-mutant CD1 mouse during cochlear maturation. Cryosections, stained with anti-Ceacam16 antibody and Texas Red phalloidin, were obtained from P3, P9, P14 and P22 animals. Panels a, b, c and d are black and white images of anti-Ceacam16 staining, panels a', b', c' and d' are merged images of anti-Ceacam16 staining (green) and phalloidin staining (red). Ceacam16 expression is not detected at P3. At P9 Ceacam16 is expressed only in a narrow zone in the area of the attachment to the spiral limbus (SL, arrow on b). At P14 immunoreactivity with anti-Ceacam16 antibody is detected in the limbal and marginal zones of the TM (arrows on c). The staining is absent from the main body of the TM (arrowhead on c). At P22 all zones of the TM appear to be immunoreactive with anti-Ceacam16 antibody. Scale bar 50 μm.

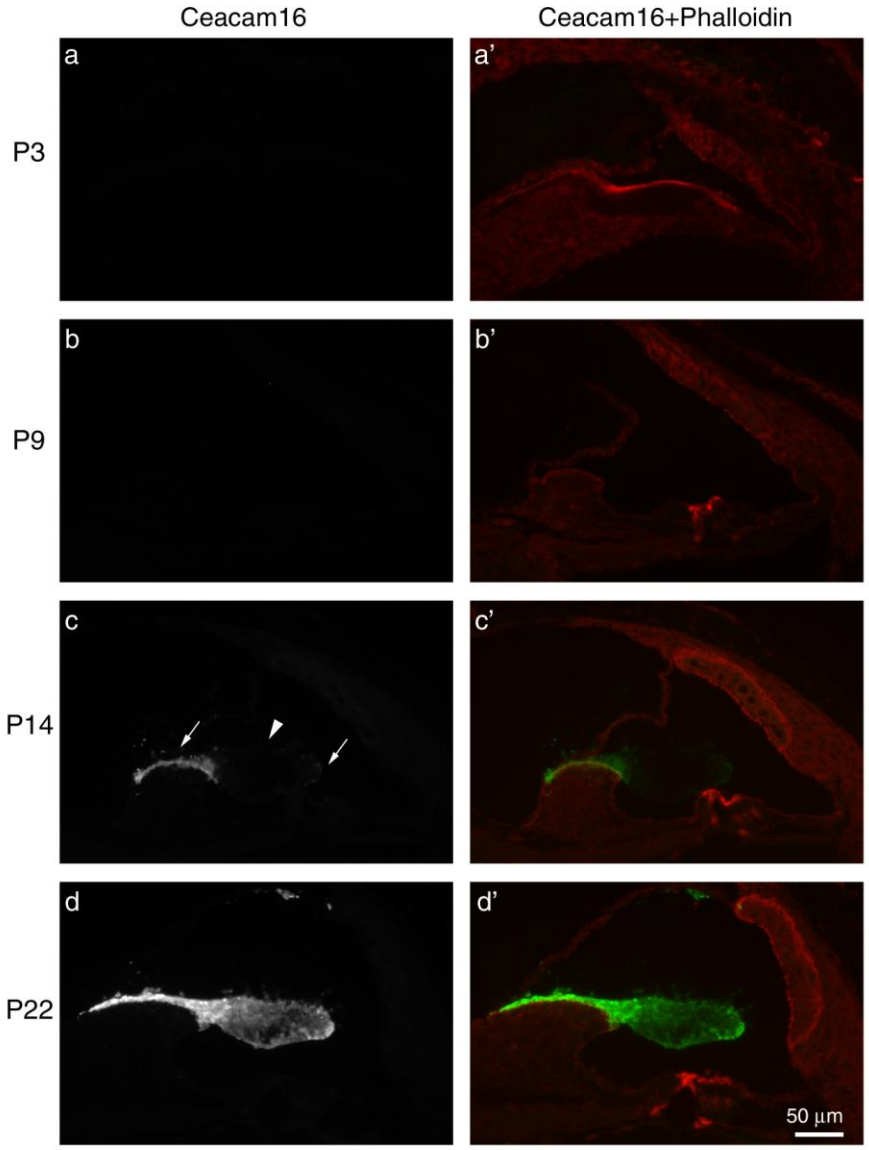

Figure 4.2. Cryosections from the apical turn of the cochleae of CD1 mice at the ages of P3, P9, P14 and P22, stained with anti-Ceacam16 antibody and Texas Red phalloidin. Panels a, b, c and d show the staining for Ceacam16 in black and white, merged images of anti-Ceacam16 (green) and phalloidin (red) staining are displayed on panels a', b', c' and d'. Immunoreactivity with anti-Ceacam16 antibody is not observed at P3 and P9. At P14 Ceacam16 staining appears in the limbal and in the marginal zones (c, arrows). The main body is, however, not immunofluorescent (c, arrowhead). At P22 the TM is fully immunoreactive with anti-Ceacam16 antibody. Scale bar 50 µm.

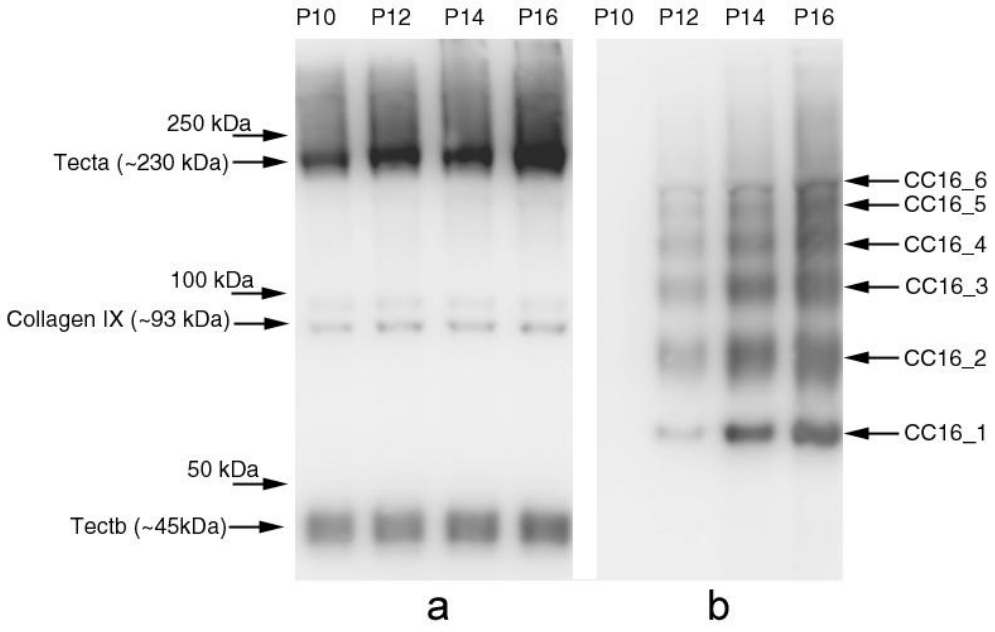

Figure 4.3. Western blot analysis of the tectorial membranes of non-mutant CD1 mice at P10, P12, P14 and P16. Panel a - membrane blotted with anti-Tecta, anti-collagen type IX and anti-Tectb antibodies, panel b - membrane blotted with anti-Ceacam16 antibody. Ceacam16 is first observed in the TM at P12. Expression gets stronger by P16. As indicated by previous studies of Zheng et al., 2011, Ceacam16 forms a ladder of oligomers. Reference staining for Tecta, Tectb and collagen type IX indicates that these proteins are present in the TM at all stages examined. The levels of Tectb and collagen type IX expression stay unchanged. Tecta increases between P10 and P16.

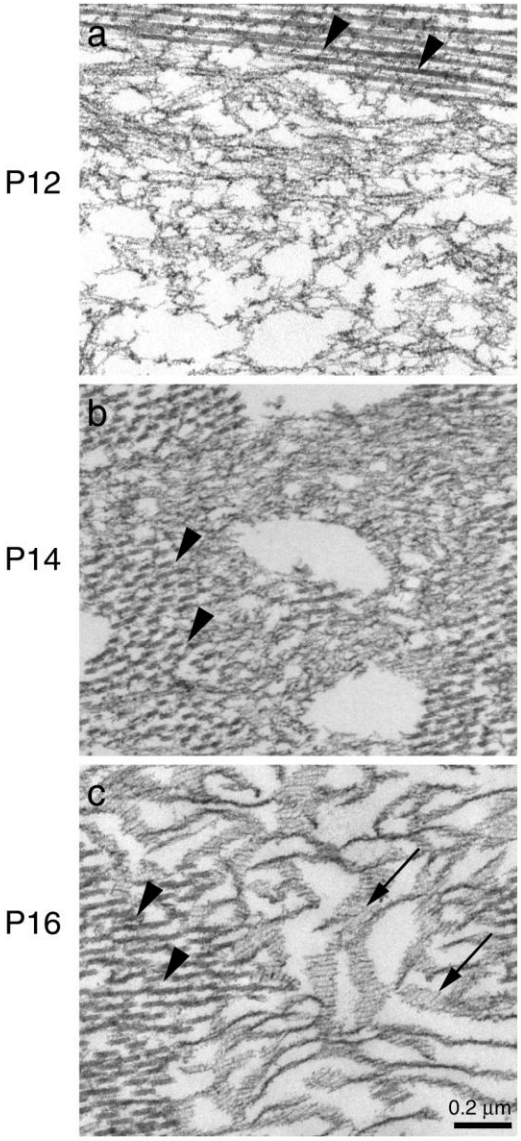

Figure 4.4. TEM of the main body of the TM from non-mutant CD1 mice at P12, P14 and P16. Collagen fibrils are marked by arrowheads. At P12 (a) the space between collagen bundles is filled with sparsely distributed filaments. They get denser by P14 (b) but only form a mature striated-sheet matrix by P16 (c, arrows). Scale bar 0.2 µm.

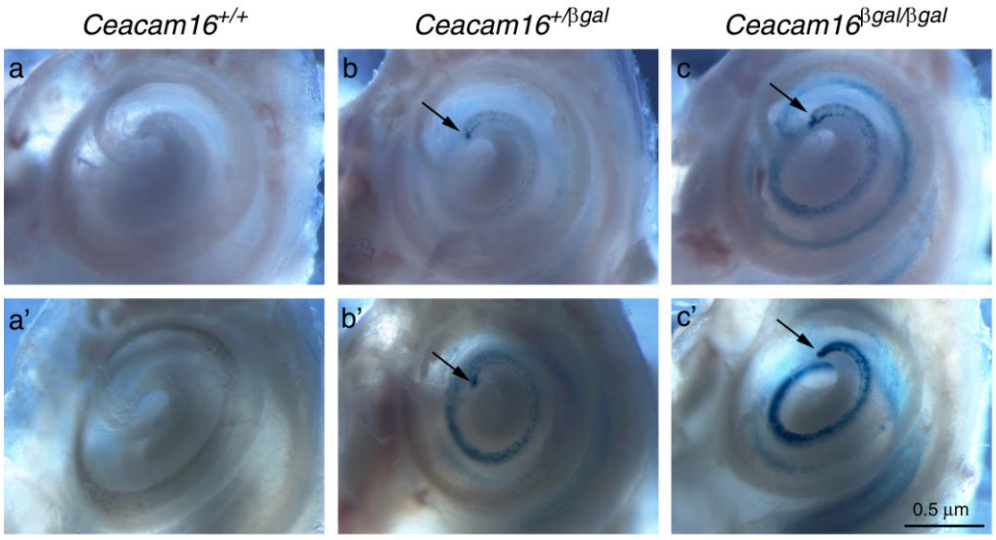

Figure 4.5. Wholemount images of X-Gal-stained cochleae from *Ceacam16*$^{+/+}$, *Ceacam16*$^{+/\beta gal}$ and *Ceacam16*$^{\beta gal/\beta gal}$ animals. Panels a, b and c are cochleae from P82 mice, panels a', b' and c' show cochleae obtained from 6 months mice. As expected, there is no X-Gal staining in wild type at both P82 (a) and 6 months (a'). X-Gal staining is detected in the organ of Corti of heterozygous and homozygous mutant animals (b and b', c and c'). However, it is weaker in heterozygotes as they contain only one copy of the lacZ reporter. Both heterozygous and homozygous mutant mice have a darker patch of X-Gal staining near the helicotrema (arrows). X-Gal staining is darker in 6 months mice. Scale bar 0.5 µm.

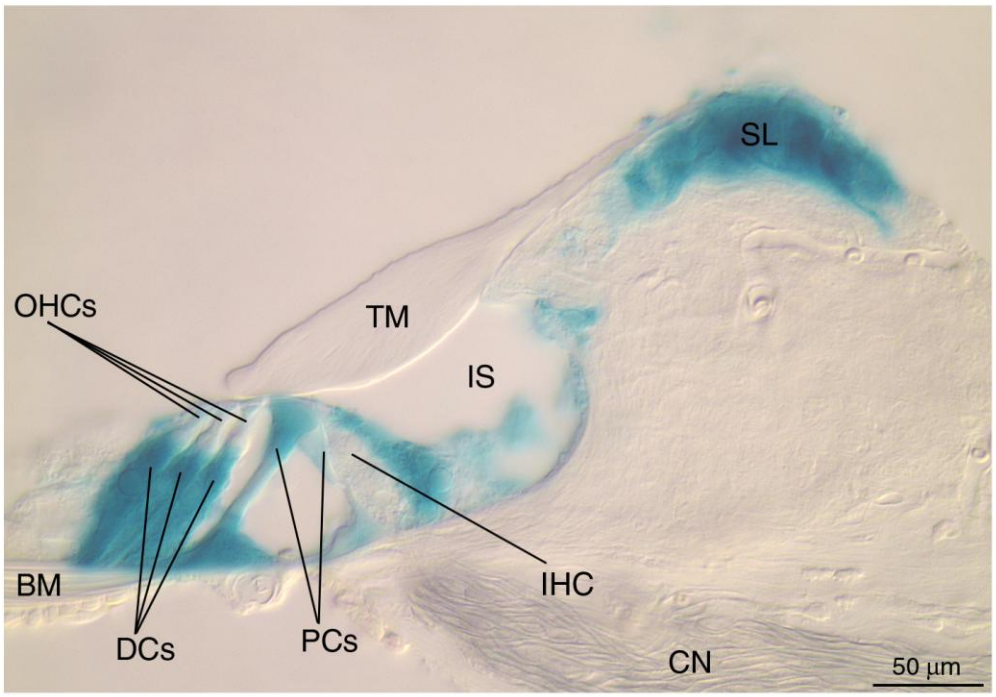

Figure 4.6. X-Gal staining for lacZ reporter expression in the basal turn of the cochlea of a *Ceacam16*$^{\beta gal/\beta gal}$ mouse at P21. SL - spiral limbus, IS - inner sulcus, CN - cochlear nerve, BM - basilar membrane, DCs - Deiter's cells, OHCs - outer hair cells, PCs - pillar cells, TM - tectorial membrane. X-Gal staining is detected in the epithelial cells of the spiral limbus and inner sulcus, in the pillar and Deiter's cells and in the border cells. Staining is not observed in the hair cells. Scale bar 50 μm.

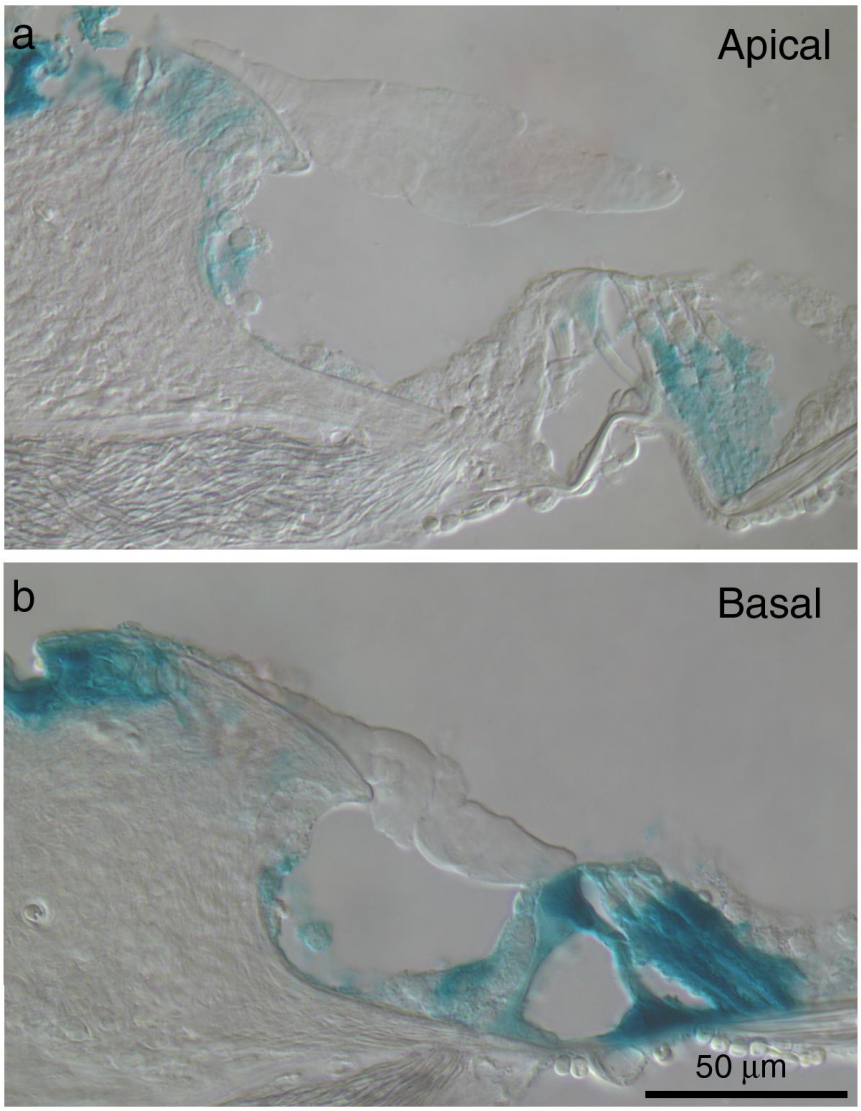

Figure 4.7. X-Gal staining in the apical (a) and basal (b) turns of the cochlea of a *Ceacam16*$^{\beta gal/\beta gal}$ mouse at P43. β-galactosidase expression in the apical part is visibly weaker than in the basal region. Scale bar 50 μm.

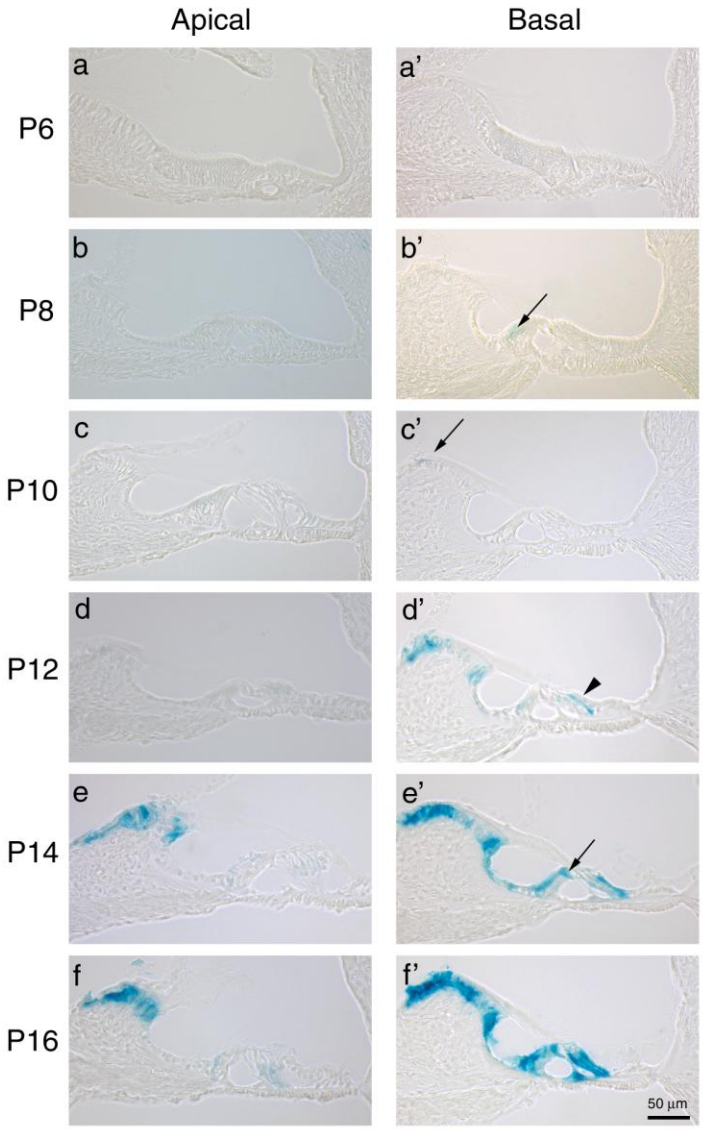

Figure 4.8. Cryosections from X-Gal stained cochleae of *Ceacam16*$^{\beta gal/\beta gal}$ mice obtained at different ages during postnatal development. In the apical turn of the cochlea (a, b, c, d, e and f), X-Gal staining is first observed at P14 in the spiral limbus (e). At P16 it is detected in Deiter's cells and border cells; staining, however, is much weaker than that seen in the spiral limbus (f). In the basal part of the organ of Corti, lacZ reporter expression is first detected at P8 as a patch of X-Gal staining in the border cells (b', arrow). This staining disappears by P10 and β-gal expression is seen in a small area of the spiral limbus epithelium instead (c', arrow). This staining spreads over the spiral limbus epithelium and appears in the 3rd row of Deiter's cells (arrowhead) at P12. It spreads further within the organ of Corti at P14 and P16 and becomes very prominent by P16 (f'). Staining in pillar cells is first detected at P14 (e', arrow). Scale bar 50 µm.

Figure 4.9. Cryosections of X-Gal stained organ of Corti from *Ceacam16*$^{\beta gal/\beta gal}$ mice examined at ages P82, 6 months and 1 year. In all three ages analysed, βgal expression is observed within the same cell types as detected at P16: spiral limbus, border cells, pillar cells and Deiter's cells. Scale bar 50 μm.

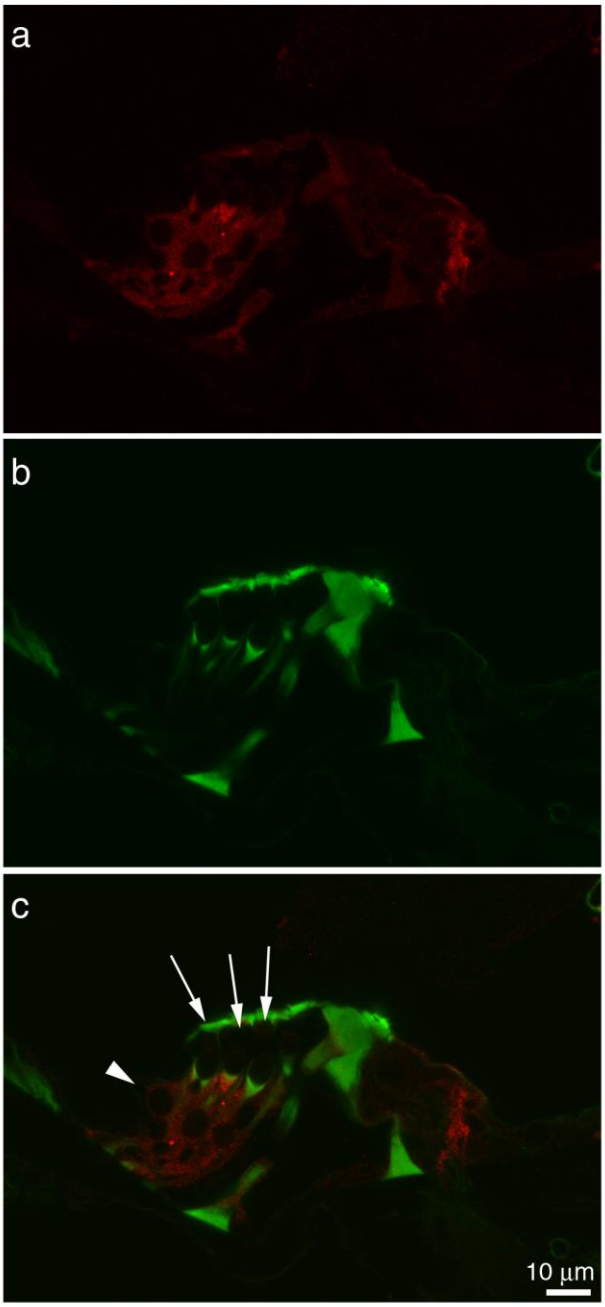

Figure 4.10. Single confocal slice of a cryosection from a *Ceacam16*$^{+/\beta gal}$ mouse cochlea expressing lacZ reporter at P21. The section was stained with anti-βgal antibody (red, a) and fluorescein phalloidin (green, b). Anti-βgal staining is detected in Deiter's cells (c, arrowhead). However, immunoreactivity with anti-βgal antibody is not observed in OHCs (c, arrows). Scale bar 10 μm.

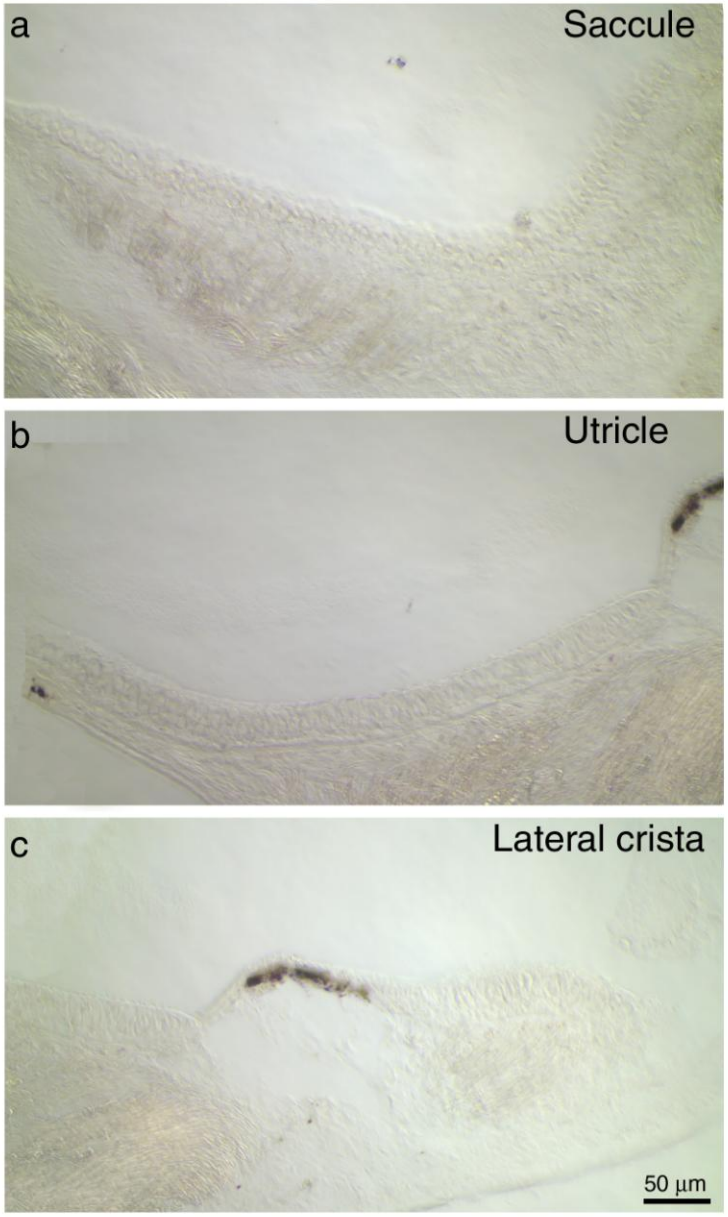

Figure. 4.11. Cryosections through the vestibular partition of the X-Gal-stained inner ear from a *Ceacam16*$^{\beta gal/\beta gal}$ mouse at P21. LacZ reporter expression is not observed in any vestibular structures. Scale bar 50 µm.

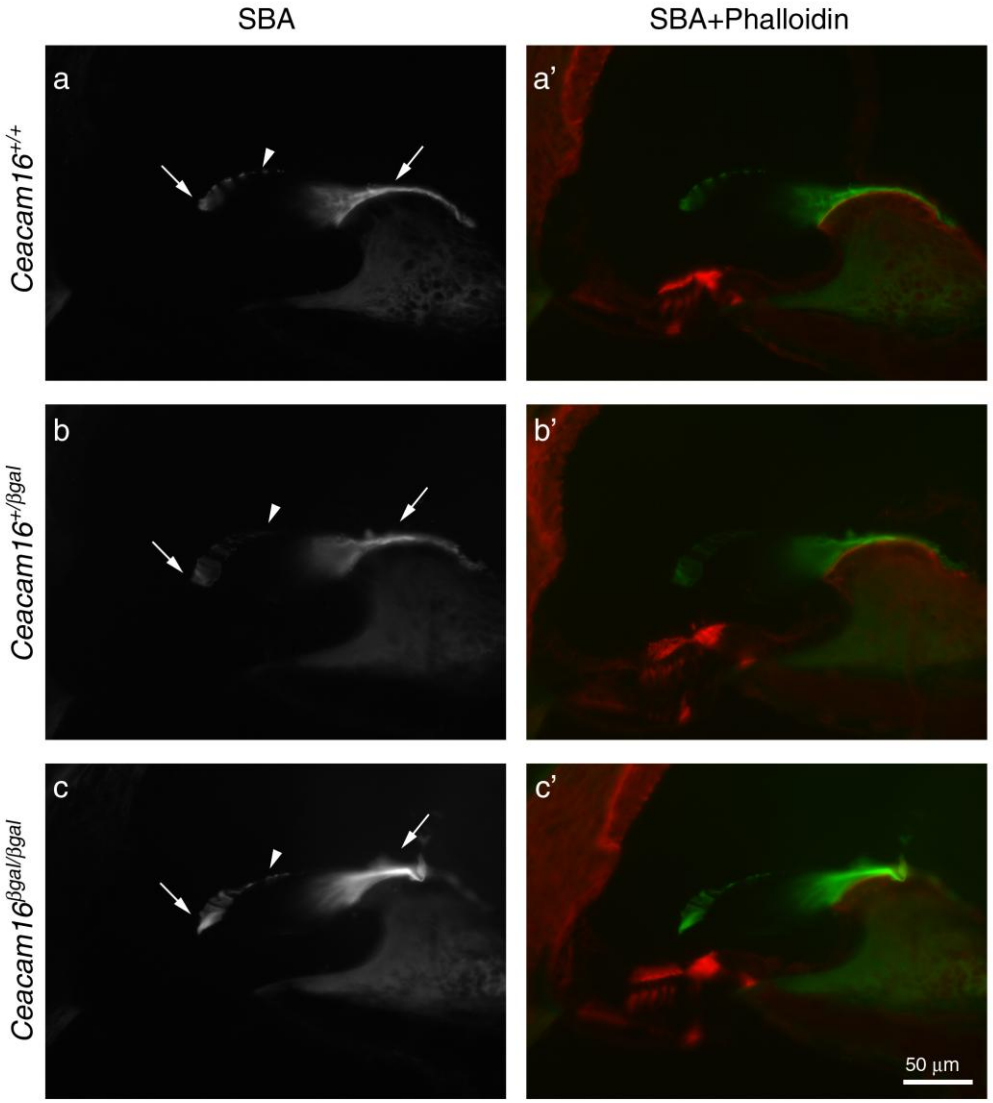

Figure 4.12. SBA-labelled cryosections from the organ of Corti of Ceacam16$^{+/+}$ (a and a'), Ceacam16$^{+/\beta gal}$ (b and b') and *Ceacam16*$^{\beta gal/\beta gal}$ (c and c') at P21 counter-stained with Texas Red phalloidin. Panels a, b and c are black and white images of SBA-staining, panels a', b' and c' are merged images of SBA (green) and phalloidin (red) staining. All three genotypes have a similar pattern of SBA staining in the TM which includes marginal and limbal zones (arrows) and the covernet (arrowheads). Scale bar 50 µm.

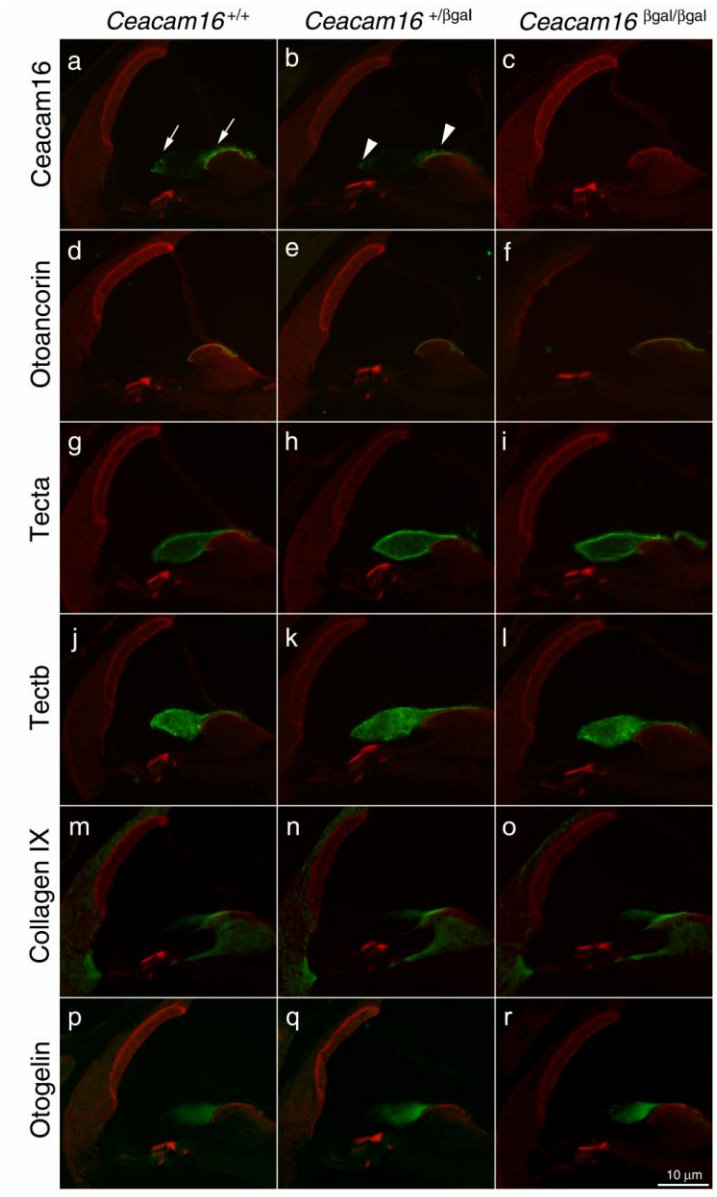

Figure 4.13. Immunofluorescence images of cryosections from *Ceacam16*$^{+/+}$, *Ceacam16*$^{+/βgal}$ and *Ceacam16*$^{βgal/βgal}$ cochleae at P21 stained with Texas Red phalloidin (red) and with antibodies for various TM proteins (green): anti-Ceacam16, anti-otoancorin, R9 for Tecta, R7 for Tectb, M2 for collagen type IX and anti-otogelin. As expected, staining for Ceacam16 is not detected in the *Ceacam16*$^{βgal/βgal}$ mouse cochlea. Immunoreactivity for Ceacam16 is detected in *Ceacam16*$^{+/+}$ mice (a, arrows) and in *Ceacam16*$^{+/βgal}$ mice but weaker (b, arrowheads). Variations in staining for the other TM proteins are not detected between the three genotypes. Scale bar 10 μm.

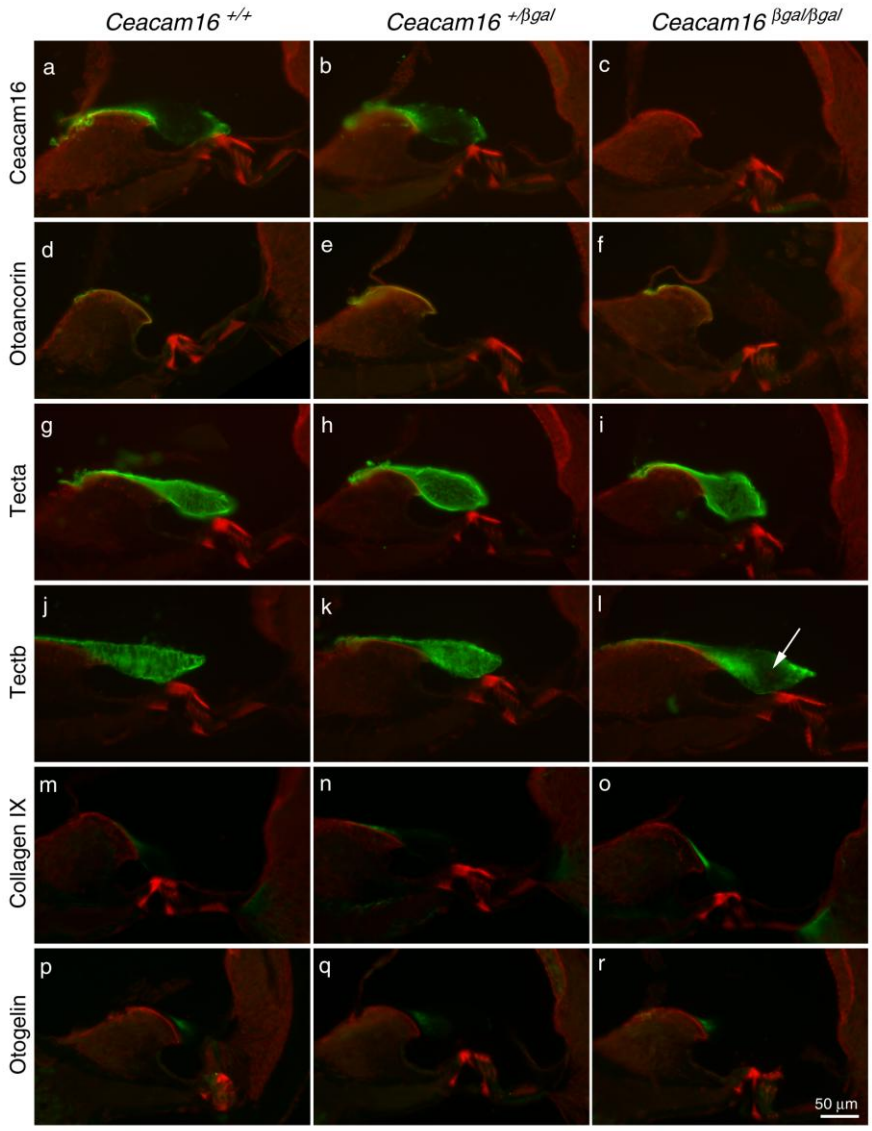

Figure 4.14. Cryosections from *Ceacam16*$^{+/+}$, *Ceacam16*$^{+/\beta gal}$ and *Ceacam16*$^{\beta gal/\beta gal}$ cochleae at 6 months of age stained with Texas Red phalloidin (red) and antibodies to different TM proteins (green): anti-Ceacam16, anti-otoancorin, R9 for Tecta, R7 for Tectb, M2 for collagen type IX and anti-otogelin. Staining for Ceacam16 is detected in wild type (a) and heterozygous (b) animals only. Anti-Tectb staining in the main body of the TM is weaker in *Ceacam16*$^{\beta gal/\beta gal}$ mice (l, arrow) than in *Ceacam16*$^{+/\beta gal}$ or *Ceacam16*$^{+/+}$ mice. Differences in immunoreactivity for other proteins are not observed. Scale bar 50 µm.

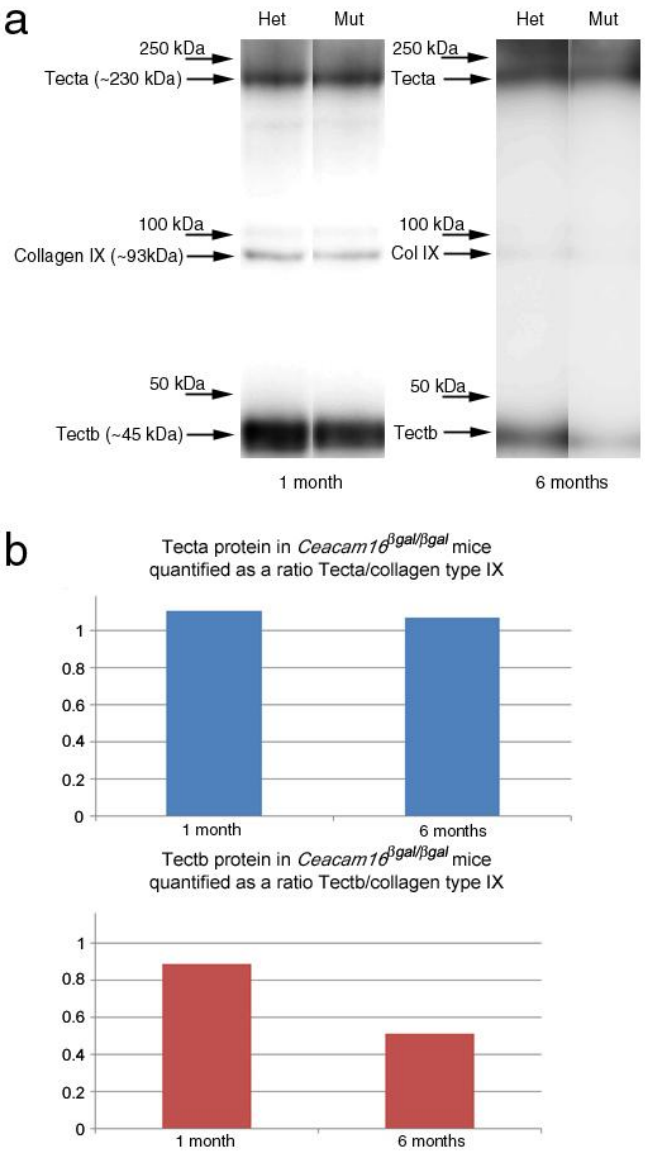

Figure 4.15. a. Western blot of TM proteins from *Ceacam16*$^{+/\beta gal}$ (Het) and *Ceacam16*$^{\beta gal/\beta gal}$ (Mut) mice at 1 month and 6 months of age labelled with anti-Tecta, anti-Tectb and anti-collagen type IX antibodies. The bands for the three proteins appear to be similar for heterozygous and homozygous mutants at 1 month of age. At 6 months, the levels of Tectb decrease in both *Ceacam16*$^{+/\beta gal}$ and *Ceacam16*$^{\beta gal/\beta gal}$ mice with a severe drop-off in Tectb levels in homozygous mutants. **b.** Quantification of the western blot bands. The protein content in the TMs of heterozygotes was considered to be 1. Tecta and Tectb levels were normalised to the levels of the collagen type IX. The Tecta levels do not show significant difference between 1 and 6 months of age. Tectb in homozygous mutants at 6 months of age drastically drops down in comparison to 1 month.

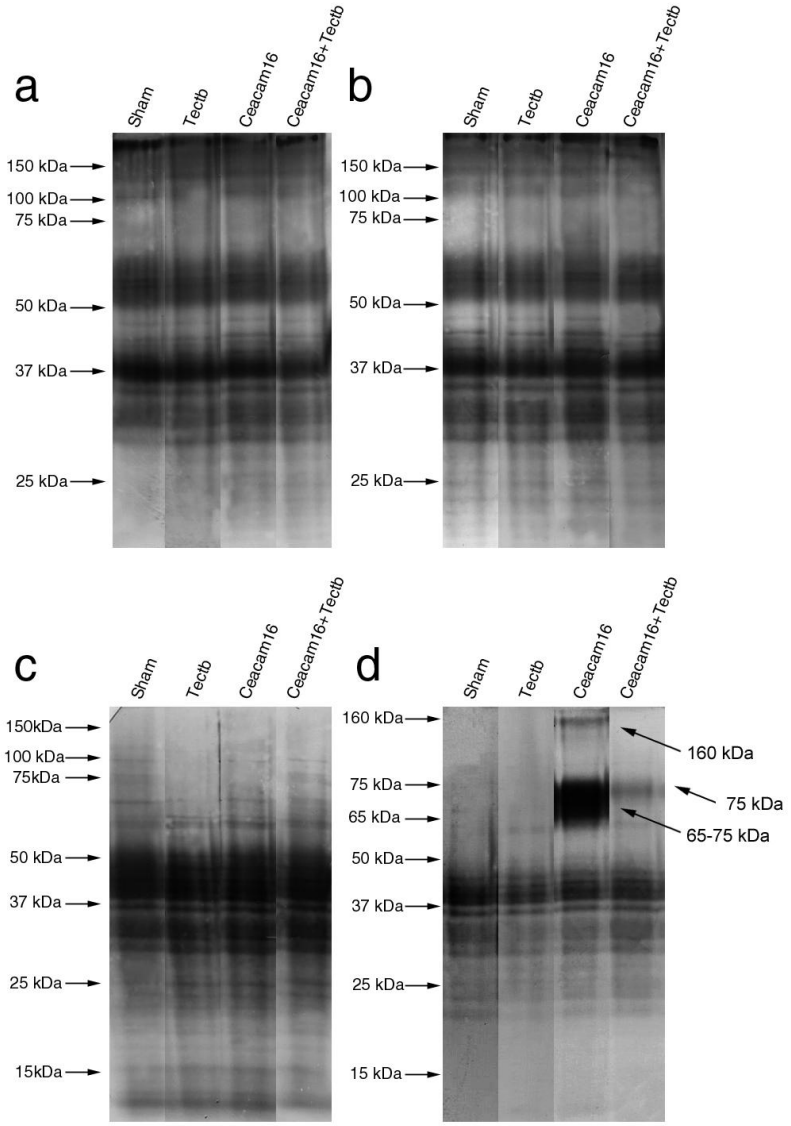

Figure 4.16. Western blotting of Tectb and Ceacam16 proteins co-immunoprecipitated with specific antibodies from the culture medium of transiently transfected HEK 293 cells. Panel a - proteins pulled down and blotted with anti-Tectb antibody, b - immunoprecipitation performed with anti-Tectb antibody, PVDF membrane was probed with monoclonal anti-V5 antibody, c - polyclonal anti-V5 antibody for immunoprecipitation and anti-Tectb antibody for western immunoblotting, d - proteins pulled down with polyclonal anti-V5 antibody and membrane probed with monoclonal anti-V5 antibody. No specific bands are detected on a, b and c. Two bands of ~ 160 kDa and ~ 65-75 kDa are detected in the Ceacam16 lane on d. In the Ceacam16+Tectb lane only one band of ~ 75 kDa is visible (d).

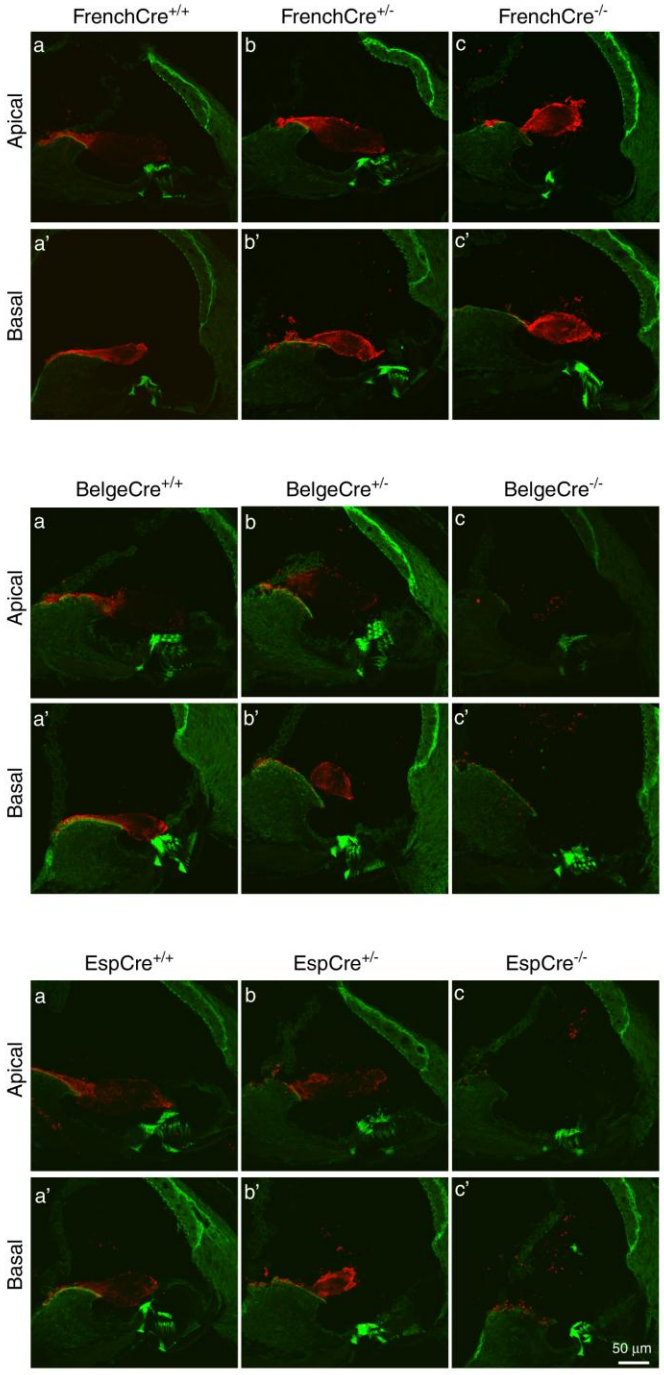

Figure 4.17. Cryosections of cochleae from transgenic mouse models of French, Belgium (Belge) and Spanish (Esp) Tecta mutations of +/+ (wild type), +/- (heterozygous) and -/- (mutant) genotypes stained with anti-Ceacam16 antibody and fluorescein phalloidin. Both apical and basal turns of the cochleae were examined. Ceacam16 is detected in the TMs of all three genotypes. In wild type and heterozygous mice Tecta is distributed throughout the TM body. It is also detected in the remnants of the TMs in mutant animals. Scale bar 50 µm.

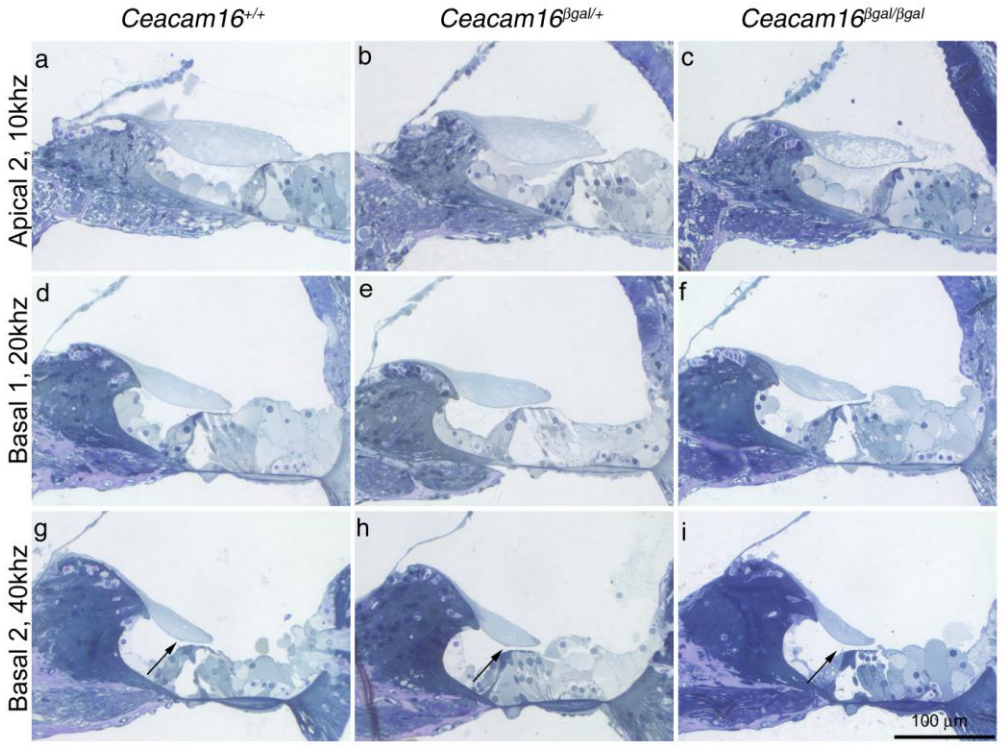

Figure 4.18. One micron thick, toluidine blue stained sections from the cochleae of *Ceacam16*$^{+/+}$, *Ceacam16*$^{+/\beta gal}$ and *Ceacam16*$^{\beta gal/\beta gal}$ mice at 6 months of age. The sections were taken from the 10 kHz (apical 2; a, b and c), 20 kHz (basal 1; d, e and f) and 40 kHz (basal 2; g, h and i) regions of the organ of Corti. Differences are not observed between wild type (a, d, g) and heterozygous (b, e, h) phenotypes. The TM in the 10 kHz turn of the organ of Corti in homozygous mutants (c) has a severe reduction in the density of its main body. Some decrease in the TM matrix content is also observed in the 20 kHz region of *Ceacam16*$^{\beta gal/\beta gal}$ animals (f). Although the matrix density of the 40 kHz TM region in the homozygous mutant is similar to that seen in the wild type and heterozygotes, it lacks Hensen's stripe (i, arrow), which is clearly defined in the other two genotypes (g and h, arrows). Scale bar 100 µm.

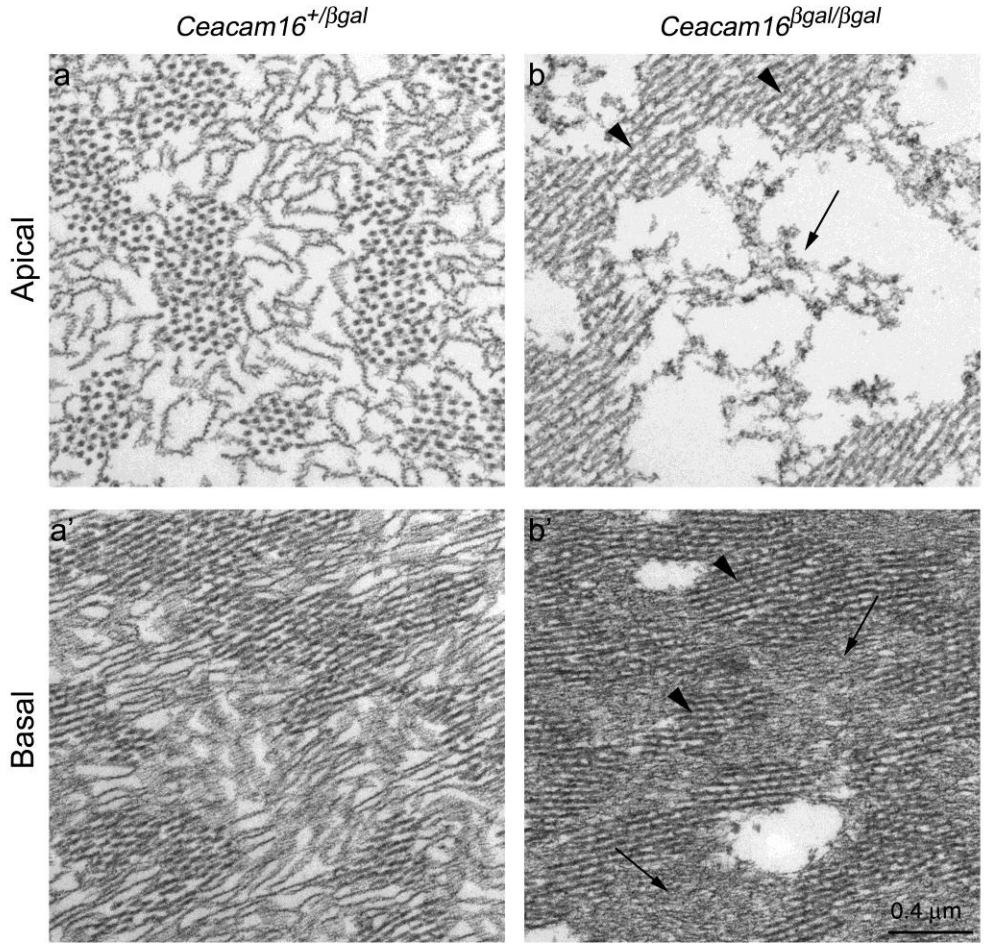

Figure 4.19. TEM of the TMs from the cochleae of Ceacam16$^{+/\beta gal}$ (a and a') and Ceacam16$^{\beta gal/\beta gal}$ (b and b') mice at P30. Clearly defined striated-sheet matrix is observed in both apical (a) and basal (a') turns of the organ of Corti in heterozygous mice. In homozygous mutants, however, striated-sheet matrix is not visible and consists of unstructured filaments (arrow in b) scattered among the collagen bundles (arrowheads in b). Panel a' shows normal looking striated-sheet matrix in the basal turns of the cochleae of Ceacam16$^{+/\beta gal}$ animals, panel b' displays disrupted matrix in homozygous mutants. Scale bar 0.4 µm.

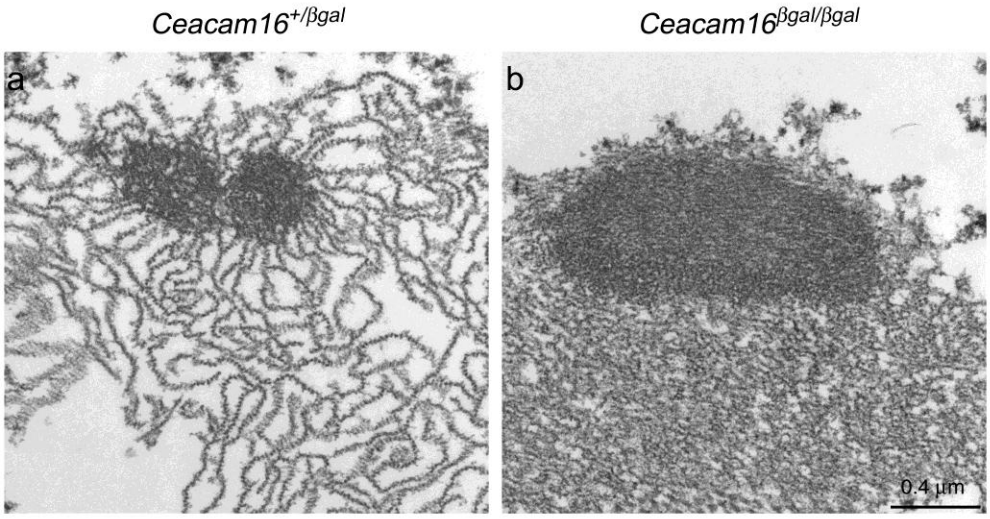

Figure 4.20. TEM images of the covernet in the apical TM from Ceacam16$^{+/\beta gal}$ (a) and Ceacam16$^{\beta gal/\beta gal}$ (b) mice at P30. Abnormalities in the covernet organisation are not detected in either heterozygous or homozygous mutant mice. The striated-sheet matrix has a normal appearance in Ceacam16$^{+/\beta gal}$ mice whereas its structure is completely disrupted in homozygous mutants. Scale bar 0.4 μm.

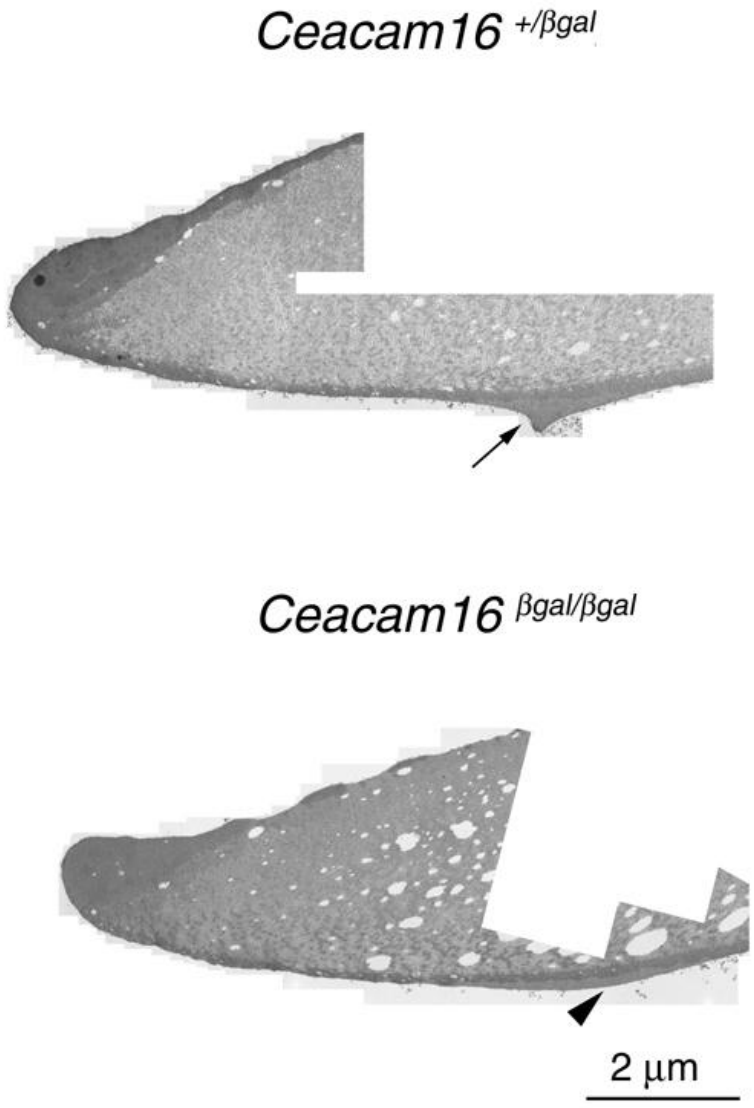

Figure 4.21. TEM images of the TMs from the basal turn of the organ of Corti from Ceacam16$^{+/\beta gal}$ and Ceacam16$^{\beta gal/\beta gal}$ mice at P30. \Whereas heterozygotes possess a clearly defined Hensen's stripe (arrow), homozygous mutants display only a thickening of Kimura's membrane (arrowhead). Scale bar 2 μm.

CONCLUSIONS

This work has been focused on the non-collagenous components of the tectorial membrane matrix which are involved in the striated-sheet matrix formation. It has provided an *in vitro* model for studying the processing, secretion and assembly of the tectorins and an *in vivo* model for revealing the function of newly described inner ear protein Ceacam16. The major conclusions of this thesis can be summarised as follows:

1. Epithelial cells in primary cultures of the early postnatal cochlea are the best suited for studying the production and assembly of extracellular tectorin-based matrix.

2. Outgrowth zone cells of the neonatal mouse cochlear cultures probably possess enzymes and chaperons necessary for extracellular tectorin secretion *in vitro*.

3. Ceacam16 protein is required for striated-matrix formation and/or for maintenance the TM stability over time.

REFERENCES

1.Abnet, C. and Freeman, D. (2000). Deformations of the isolated mouse tectorial membrane produced by oscillatory forces. *Hearing research*, 144 (1-2), 29-46.

2. Alasti, F. Sanati M.H., Behrouzifard, A.H., Sadeghi, A., de Brouwer, A.P.M., Kremer, H., Smith, R.J. and Van Camp, G. (2008). A novel TECTA mutation confirms the recognizable phenotype among autosomal recessive hearing impairment families. *International journal of pediatric otorhinolaryngology*, 72(2), 249–55.

3. Alexopoulou, A.N., Couchman, J.R. and Whiteford, J.R. (2008). The CMV early enhancer/chicken beta actin (CAG) promoter can be used to drive transgene expression during the differentiation of murine embryonic stem cells into vascular progenitors. *BMC cell biology*, 9, 2-13.

4. Alloisio, N., Morlé L., Bozon M., Godet J., Verhoeven K., Van Camp G., Plauchu H., Muller P., Collet L. and Lina-Granade G. (1999). Mutation in the zonadhesin-like domain of alpha-tectorin associated with autosomal dominant non-syndromic hearing loss. *European journal of human genetics*, 7(2), 255–8.

5. Barclay, A.N. (1999). Ig-like domains: evolution from simple interaction molecules to sophisticated antigen recognition. *Proceedings of the National Academy of Sciences of the United States of America*, 96(26), 14672–14674.

6. Beauchemin, N., Draber P., Dveksler G., Gold P., Gray-Owen S., Grunert F., Hammarström S., Holmes K.V., Karlsson A., Kuroki M., Lin S.H., Lucka L., Najjar S.M., Neumaier M., Obrink B., Shively J.E., Skubitz K.M., Stanners C.P., Thomas P., Thompson J.A., Virji M., von Kleist S., Wagener C., Watt S. and Zimmermann W. (1999). Redefined Nomenclature for Members of the Carcinoembryonic. *Experimental Cell Research*, 249, 243–249.

7. Bekesy Von, G. (1948). On the elasticity of the cochlear partition. *The Journal of the Acoustical Society of America*, 20(3), 227–241.

8. Bekesy Von, G. (1960). *Experiments in hearing*, New York: McGraw-Hill, 745 pp.

9. Benchimol, S., Fuks, A., Jothy, S., Beauchemin, N., Shirota, K. and Stanners, C.P. (1989). Carcinoembryonic antigen, a human tumor marker, functions as an intercellular adhesion molecule. *Cell*, 57(2), 327–34.

10. Bork, P. and Sander, C. (1992). A large domain common to sperm receptors (ZP2 and ZP3) and TGF-beta type III receptor. *FEBS letters*, 300(3), 237–40.

11. Bosher, S.K. and Warren, R.L. (1978). Very low calcium content of cochlear endolymph, an extracellular fluid. *Nature*, 273(5661), 377–378.

12. Brooks, A.R. Harkins, R.N., Wang, P., Qian, H.S., Liu, P. and Rubanyi, G.M. (2004). Transcriptional silencing is associated with extensive methylation of the CMV promoter following adenoviral gene delivery to muscle. *The journal of gene medicine*, 6(4), 395–404.

13. Brooks, M.J. (2009). *Characterization of CEACAM binding by Human Specific Pathogens*, Toronto: University of Toronto, 168 pp.

14. Brown, D. and Breton, S. (2000). Sorting proteins to their target membranes. *Kidney international*, 57(3),.816–24.

15. Brownell, W.E., Bader, C.R., Bertrand, D. and de Ribaupierre, Y. (1985). Evoked mechanical responses of isolated cochlear outer hair cells. *Science*, 227, 194-200.

16. Carugo, O., Cemazar, M., Zahariev, S., Hudáky, I., Gáspári, Z., Perczel, A. and Pongor, S. (2003). Vicinal disulfide turns. *Protein Engineering Design and Selection*, 16(9),.637–639.

17. Chen, A.H., Ni L., Fukushima K., Marietta J., O'Neill M., Coucke P., Willems P. and Smith R.J. (1995). Linkage of a gene for dominant non-syndromic deafness to chromosome 19. *Human molecular genetics*, 4(6), 1073–6.

18. Chen, C., Krohn, J., Bhattacharya, S.and Davies, B. (2011). A comparison of exogenous promoter activity at the ROSA26 locus using a PhiC31 integrase mediated cassette exchange approach in mouse ES cells. *PloS One*, 6(8), e23376.

19. Coates, B. (2009). *Three deaf mice, a study of tectorial membrane structure in mouse models of human hereditary deafness*, Brighton UK: University of Sussex, 60 pp.

20. Cohen-Salmon, M., El-Amraoui A., Leibovici M. and Petit C. (1997). Otogelin: a glycoprotein specific to the acellular membranes of the inner ear. *Proceedings of the National Academy of Sciences of the United States of America*, 94(26), 14450–14455.

21. Dallas, P. (1992). The active cochlea. *The journal of neuroscience*, 12 (12), 4575-4585.

22. Deans, M.R., Peterson, J.M. and Wong, G.W. (2010). Mammalian Otolin: a multimeric glycoprotein specific to the inner ear that interacts with otoconial matrix protein Otoconin-90 and Cerebellin-1. *PloS One*, 5(9), e12765.

23. Fettiplace, R. and Hackney, C.M. (2006). The sensory and motor roles of auditory hair cells. *Nature reviews. Neuroscience*, 7(1), 19–29.

24. Foecking, M.K. and Hofstetter, H. (1986). Powerful and versatile enchancer-promoter unit for mammalian expression vectors. *Gene*, 45, 101–105.

25. Freberg, L. (2009). *Discovering Biological Psychology*, Belmont C.A.: Cengage Learning, 608 pp.

26. Geisler, C.D. (1998). *From sound to synapse: physiology of the mammalian ear*, New York: Oxford University Press US, 381 pp.

27. Ghaffari, R., Aranyosi, A.J. and Freeman, D.M. (2007). Longitudinally propagating traveling waves of the mammalian tectorial membrane. *Proceedings of the National Academy of Sciences of the United States of America*, 104(42), 16510–16515.

28. Goodyear, R.J. and Richardson, G.P. (2002). Extracellular matrices associated with the apical surfaces of sensory epithelia in the inner ear: molecular and structural diversity. *Journal of neurobiology*, 53(2), 212–227.

29. Grassi, G., Maccaroni P., Meyer R., Kaiser H., D'Ambrosio E., Pascale E., Grassi M., Kuhn A., Di Nardo P., Kandolf R. and Küpper J.H. (2003). Inhibitors of DNA methylation and histone deacetylation activate cytomegalovirus promoter-controlled reporter gene expression in human glioblastoma cell line U87. *Carcinogenesis*, 24(10),1625–1635.

30. Halaby, D.M., Poupon, A. and Mornon, J. (1999). The immunoglobulin fold family: sequence analysis and 3D structure comparisons. *Protein engineering*, 12(7), 563–571.

31. Hammarstrom, S. (1999). The carcinoembryonic antigen (CEA) family: structures, suggested functions and expression in normal and malignant tissues. *Seminars in Cancer Biology*, 9(2), 67-81.

32. Hasko, J.A. and Richardson, G.P. (1988). The ultrastructural organization and properties of the mouse tectorial membrane matrix. *Hearing research*, 35(1), 21–38.

33. Hauck, C.R., Agerer, F., Muenzner, P., Schmitter, T. (2006). Cellular adhesion molecules as targets for bacterial infection. *European journal of cell biology*, 85(3-4), 235–242.

34. He, D.Z. (1997). Relationship between the development of outer hair cell electromotility and efferent innervation: a study in cultured organ of corti of neonatal gerbils. *The Journal of neuroscience : the official journal of the Society for Neuroscience*, 17(10), 3634–3643.

35. Hildebrand, M.S., Morín, M., Meyer, N.C., Mayo, F., Modamio-Hoybjor, S., Mencía, A., Olavarrieta, L., Morales-Angulo, C., Nishimura, C.J., Workman, H., DeLuca, A.P., del Castillo, I., Taylor, K.R., Tompkins, B., Goodman, C.W., Schrauwen, I., Wesemael, M.V., Lachlan, K., Shearer, A.E., Braun, T.A., Huygen, P.L., Kremer, H., Van Camp, G., Moreno, F., Casavant, T.L., Smith, R.J. and Moreno-Pelayo, M.A. (2011). DFNA8/12 Caused by TECTA Mutations is the Most Identified Subtype of Non-syndromic Autosomal Dominant Hearing Loss. *Human Mutation Variation, Informatics, and Disease*, 32(7), pp.825–834.

36. Horst, A.K., Ito, W.D., Dabelstein, J., Schumacher, U., Sander, H., Turbide, C., Brümmer, J., Meinertz, T., Beauchemin, N. and Wagener, C. (2006). Carcinoembryonic antigen – related cell adhesion molecule 1 modulates vascular remodeling *in vitro* and *in vivo*. *The journal of clinical investigation*, 116(6), 1596-1605.

37. Hughes, D.C., Legan, P.K., Steel, K.P. and Richardson, G.P. (1998). Mapping of the alpha-tectorin gene (TECTA) to mouse chromosome 9 and human chromosome 11: a candidate for human autosomal dominant nonsyndromic deafness. *Genomics*, 48(1), 46–51.

38. Iwasaki, S., Harada, D., Usami, S., Nagura, M., Takeshita, T., Hoshino, T. (2002). Association of Clinical Features With Mutation of Tecta in a Family With Autosomal Dominant Hearing Loss. *Archives of Otolaryngology - Head and Neck Surgery*, 128(8), 913–917.

39. Jovine, L., Qi, H., Williams, Z., Litscher, E. and Wassarman, P.M. (2002). The ZP domain is a conserved module for polymerization of extracellular proteins. *Nature cell biology*, 4(6), 457–61.

40. Jovine, L., Darie, C.C., Litscher, E.S. and Wassarman, P.M. (2005). Zona pellucida domain proteins. *Annual review of biochemistry*, 74, .83–114.

41. Kammerer, R., Rüttiger, L., Riesenberg, R., Schäuble, C., Krupar, R., Kamp, A., Sunami, K., Eisenried, A., Hennenberg, M., Grunert, F., Bress, A., Battaglia, S., Schrewe, H., Knipper, M., Schneider, M.R. and Zimmermann, W. (2012). Loss of mammal-specific tectorial membrane component carcinoembryonic antigen cell adhesion molecule 16 (CEACAM16) leads to hearing impairment at low and high frequencies. *The Journal of biological chemistry*, 287(26), 21584–21598.

42. Kelmanson, I. (2009). Enhanced red and far-red fluorescent proteins for *in vivo* imaging. *Nature Methods*, 6(5), 355-358.

43. Killick, R. and Richardson, G.P. (1997). Antibodies to the sulphated, high molecular mass mouse tectorin stain hair bundles and the olfactory mucus layer. *Hearing research*, 103, 131–141.

44. Kimura, R.S. (1966). Hairs of the cochlear sensory cells and their attachment to the tectorial membrane. *Acta otolaryngologica*, 61(1), 55–72.

45. Klinke, R. (1986). Neurotransmission in the inner ear. *Hearing Research*, 22(1-3), 235–243.

46. Knipper, M., Richardson, G., Mack, A., Müller, M., Goodyear, R., Limberger, A., Rohbock, K., Köpschall, I., Zenner, H.P. and Zimmermann, U. (2001). Thyroid hormone-deficient period prior to the onset of hearing is associated with reduced levels of beta-tectorin protein in the tectorial membrane: implication for hearing loss. *The Journal of biological chemistry*, 276(42), 39046–39052.

47. Kuespert, K., Pils, S. and Hauck, C.R. (2006). CEACAMs: their role in physiology and pathophysiology. *Current opinion in cell biology*, 18(5), 565–71.

48. Lagostena, L., Ashmore, J.F., Kachar, B. and Mammano, F. (2001). Purinergic control of intercellular communication between Hensen ' s cells of the guinea-pig cochlea. The *Journal of Physiology*, 531(Pt3), 693–706.

49. Lea, I.A., Sivashanmugam, P. and O'Rand, M.G. (2001). Zonadhesin: characterization, localization, and zona pellucida binding. *Biology of reproduction*, 65(6), 1691–1700.

50. Legan, P.K., Rau, A., Keen, J.N. and Richardson, G.P. (1997). The mouse tectorins. Modular matrix proteins of the inner ear homologous to components of the sperm-egg adhesion system. *The Journal of biological chemistry*, 272(13), 8791–8801.

51. Legan, P.K., Lukashkina, V.A., Goodyear, R.J., Kössi, M., Russell, I.J. and Richardson, G.P. (2000). A targeted deletion in alpha-tectorin reveals that the tectorial membrane is required for the gain and timing of cochlear feedback. *Neuron*, 28(1), 273–285.

52. Legan, P.K., Lukashkina, V.A., Goodyear, R.J., Lukashkin, A.N., Verhoeven, K., Van Camp, G., Russell, I.J. and Richardson, G.P. (2005). A deafness mutation isolates a second role for the tectorial membrane in hearing. *Nature Neuroscience* , 8(8), 1035–1042.

53. Lim, D.J. (1980). Cochlear anatomy related to cochlear micromechanics. A review. *The Journal of the Acoustical Society of America*, 67(5), 1686–95.

54. Lim, D.J. (1987). Development of the tectorial membrane. *Science*, 28, 9–21.

55. Lim, D.J. and Rueda, J. (1992). Structural development of the cochlea. In Romand, R. (Ed), *Development of auditory and vestibular systems 2*, Amsterdam: Elsevier Science Publ., 33–58.

56. Lisanti, M.P., Sargiacomo, M., Graeve ,L., Saltiel, A.R. and Rodriguez-Boulan, E. (1988). Polarized apical distribution of glycosyl-phosphatidylinositol-anchored proteins

in a renal epithelial cell line. *Proceedings of the National Academy of Sciences of the United States of America*, 85(24), 9557–9561.

57. Löser, P., Jennings, G.S., Strauss, M. and Sandig, V. (1998). Reactivation of the Previously Silenced Cytomegalovirus Major Immediate-Early Promoter in the Mouse Liver : Involvement of NF κ B. *Journal of Virology*, 72(1), 180-190.

58. McGuirt, W.T., Prasad, S.D., Griffith, A.J., Kunst, H.P., Green, G.E., Shpargel, .KB., Runge, C., Huybrechts, C., Mueller, R.F., Lynch, E., King, M.C., Brunner, H.G., Cremers, C.W., Takanosu, M., Li, S.W., Arita, M., Mayne, R., Prockop, D.J., Van Camp, G., Smith, R.J. (1999). Mutations in COL11A2 cause non-syndromic hearing loss (DFNA13). *Nature genetics*, 23(4), 413–419.

59. Meyer, N.C., Alasti, F., Nishimura, C.J., Imanirad, P., Kahrizi, K., Riazalhosseini, Y., Malekpour, M., Kochakian, N., Jamali, P., Van Camp, G., Smith, R.J. and Najmabadi, H. (2007). Identification of three novel TECTA mutations in Iranian families with autosomal recessive nonsyndromic hearing impairment at the DFNB21 locus. *American journal of medical genetics.* 143A(14), 1623–1629.

60. Miyazaki, J., Takaki, S., Araki, K., Tashiro, F., Tominaga, A., Takatsu, K. and Yamamura, K. (1989). Expression vector system based on the chicken beta-actin promoter directs efficient production of interleukin-5. *Gene*, 79, 269–277.

61. Moreno-Pelayo, M.A., del Castillo, I., Villamar, M., Romero, L., Hernández-Calvín, F.J., Herraiz, C., Barberá, R., Navas, C. and Moreno, F. (2001). A cysteine substitution in the zona pellucida domain of alpha-tectorin results in autosomal dominant, postlingual, progressive, mid frequency hearing loss in a Spanish family. *Journal of medical genetics*, 38(5), E13.

62. Moreno-Pelayo, M.A., Goodyear, R.J., Mencía, A., Modamio-Hoybjor, S., Legan, P.K., Olavarrieta, L., Moreno, F. and Richardson, G.P. (2008). Characterization of a spontaneous, recessive, missense mutation arising in the Tecta gene. *Journal of the Association for Research in Otolaryngology : JARO*, 9(2), 202–214.

63. Munnamalai, V., Hayashi, T. and Bermingham-McDonogh, O. (2012). Notch Prosensory Effects in the Mammalian Cochlea Are Partially Mediated by Fgf20. *The Journal of Neuroscience*, 32(37), 12876–12884.

64. Naz, S., Alasti, F., Mowjoodi, A., Riazuddin, S., Sanati, M.H., Friedman, T.B., Griffith, A.J., Wilcox, E.R. and Riazuddin, S. (2003). Distinctive audiometric profile associated with DFNB21 alleles of TECTA. *Journal of medical genetics*, 40(5), 360–363.

65. Nishijima, H., Yasunari, T., Nakayama, T., Adachi, N. and Shibahara, K. (2009). Improved applications of the tetracycline-regulated gene depletion system. *Bioscience Trends*, 3(5), 161–167.

66. Niwa, H., Yamamura, K. and Miyazaki, J., (1991). Efficient selection for high-expression transfectants with a novel eukaryotic vector. *Gene*, 108(2), 193–199.

67. Pfister, M., Thiele, H., Van Camp, G., Fransen, E., Apaydin, F., Aydin, O., Leistenschneider, P., Devoto, M., Zenner, H.P., Blin, N., Nürnberg, P., Ozkarakas, H. and Kupka, S. (2004). A Genotype-Phenotype Correlation with Gender- Effect for Hearing Impairment Caused by TECTA Mutations. *Cellular Physiology and Biochemistry*, 14(4-6),369–376.

68. Pickles, J.O. (1988). *An introduction to the physiology of hearing*, New York: Academic Press, 400 pp.

69. Plantinga, R.F., de Brouwer, A.P., Huygen, P.L., Kunst, H.P., Kremer, H. and Cremers, C.W. (2006). A novel TECTA mutation in a Dutch DFNA8/12 family confirms genotype-phenotype correlation. *Journal of the Association for Research in Otolaryngology : JARO*, 7(2), 173–181.

70. Qin, J.Y., Zhang, L., Clift, K.L., Hulur, I., Xiang, A.P., Ren, B.Z. and Lahn, B.T. (2010). Systematic comparison of constitutive promoters and the doxycycline-inducible promoter. *PloS One*, 5(5), e10611.

71. Raphael, Y. and Altschuler, R.A. (2003). Structure and innervation of the cochlea. *Brain Research Bulletin*, 60(5-6), 397–422.

72. Rau, A., Legan, P.K. and Richardson, G.P. (1999). Tectorin mRNA Expression Is Spatially and Temporally Restricted During Mouse Inner Ear Development. *Journal of Comparative Neurology*, 280(, 271–280.

73. Richardson, G.P., Russell, I.J., Duance, V.C., Bailey, A.J. (1987). Polypeptide composition of the mammalian tectorial membrane. *Hearing research*, 25(1), 45–60.

74. Robles, L. and Ruggero, M.A. (2001). Mechanics of the mammalian cochlea. *Physiological reviews*, 81(3), 1305–1352.

75. Rosowski, J. (1996). *Models of external and middle ear function.* In: Auditory computation. New York: Springer, 15-61.

76. Rueda, J., Cantos, R. and Lim, D.J. (1996). Tectorial membrane-organ of Corti relationship during cochlear development. *Anatomy and embryology*, 194(5), 501–514.

77. Russell, I.J. and Richardson, G.P. (1987). The morphology and physiology of hair cells in organotypic cultures of the mouse cochlea. *Hearing research*, 31(1), 9–24.

78. Russell, I.J., Legan, P.K., Lukashkina, V.A., Lukashkin, A.N., Goodyear, R.J. and Richardson, G.P. (2007). Sharpened cochlear tuning in a mouse with a genetically modified tectorial membrane. *Nature neuroscience*, 10(2), 215–223.

79. Sagong, B., Park, R., Kim, Y.H., Lee, K.Y., Baek, J.I., Cho, H.J., Cho, I.J., Kim, U.K., Lee, S.H. (2010). Two novel missense mutations in the TECTA gene in Korean families with autosomal dominant nonsyndromic hearing loss. *Annals of clinical and laboratory science*, 40(4), 380–385.

80. Schraders, M., Ruiz-Palmero, L., Kalay, E., Oostrik, J., del Castillo, F.J., Sezgin, O., Beynon, A.J., Strom, T.M., Pennings, R.J., Seco, C.Z., Oonk, A.M., Kunst, H.P., Domínguez-Ruiz, M., García-Arumi, A.M., del Campo, M., Villamar, M., Hoefsloot, L.H., Moreno, F., Admiraal, R.J., del Castillo, I. and Kremer, H. (2012). Mutations of the gene encoding otogelin are a cause of autosomal-recessive nonsyndromic moderate hearing impairment. *American journal of human genetics*, 91(5), 883–889.

81. Simmler, M.C., Cohen-Salmon, M., El-Amraoui, A., Guillaud, L., Benichou, J.C., Petit, C. and Panthier, J.J. (2000). Targeted disruption of OTOG results in deafness and severe imbalance. *Nature genetics*, 24(2), 139–143.

82. Snapp, E. (2005). Design and use of fluorescent fusion proteins in cell biology. *Current protocols in cell biology*, 21 (4).

83. Sourisseau, T., Georgiadis, A., Tsapara, A., Ali, R.R., Pestell, R., Matter, K., Balda, M.S. (2006). Regulation of PCNA and Cyclin D1 Expression and Epithelial Morphogenesis by the ZO-1-Regulated Transcription Factor ZONAB / DbpA. *Molecular and cell biology*, 26(6), 2387–2398.

84. Spoendlin, H. (1985). Anatomy of cochlear innervation. *American journal of otolaryngology*, 6(6), 453–67.

85. Sugasawa, M., Erostegui, C., Blanchet, C. and Dulon D. (2013). ATP activates a cation conductance and Ca^{2+} -dependent Cl^- conductance in Hensen cells of guinea pig cochlea. *American journal of physiology. Cell physiology*, 271 (6), 1817-1827.

86. Tanudji, M. (2002). Improperly folded green fluorescent protein is secreted via a non-classical pathway. *Journal of Cell Science*, 115(19), 3849–3857.

87. Themistocleous, G.S., Katopodis, H., Sourla, A., Lembessis, P., Doillon, C.J., Soucacos, P.N., Koutsilieris, M. (2004). Three-dimensional type I collagen cell culture systems for the study of bone pathophysiology. *In vivo*, 18(6), 687–696.

88. Tolomeo, J. and Holley, M. (1997). Mechanics of microtubule bundles in pillar cells from the inner ear. *Biophysical journal*, 73(4), 2241–2247.

89. Vaughn, D.E. and Bjorkman, P.J. (1996). The (Greek) key to structures of neural adhesion molecules. *Neuron*, 16(2), 261–273.

90. Verhoeven, K., Van Camp, G., Govaerts, P.J., Balemans, W., Schatteman, I., Verstreken, M., Van Laer, L., Smith, R.J., Brown, M.R., Van de Heyning, P.H., Somers, T., Offeciers, F.E., Willems, P.J. (1997). A gene for autosomal dominant nonsyndromic hearing loss (DFNA12) maps to chromosome 11q22-24. *American journal of human genetics*, 60(5), 1168–1173.

91. Verhoeven, K., Van Laer, L., Kirschhofer, K., Legan, P.K., Hughes, D.C., Schatteman, I., Verstreken, M., Van Hauwe, P., Coucke, P., Chen, A., Smith, R.J., Somers, T., Offeciers, F.E., Van de Heyning, P., Richardson, G.P., Wachtler, F., Kimberling, W.J., Willems, P.J., Govaerts, P.J. and Van Camp, G. (1998). Mutations in the human alpha-tectorin gene cause autosomal dominant non-syndromic hearing impairment. *Nature genetics*, 19(1), 60–62.

92. Witteveen, J. (2008). *Development of an in vitro model system for studying tectorin targeting and tectorial membrane assembly*. Brighton: University of Sussex, 51 pp.

93. Xia, A., Gao, S.S., Yuan, T., Osborn, A., Bress, A., Pfister, M., Maricich, S.M., Pereira, F.A. and Oghalai, J.S. (2010). Deficient forward transduction and enhanced reverse transduction in the alpha tectorin C1509G human hearing loss mutation. *Disease models & mechanisms*, 3(3-4), 209–223.

94. Yariz, K.O., Duman, D., Seco, C.Z., Dallman, J., Huang, M., Peters, T.A., Sirmaci, A., Lu, N., Schraders, M., Skromne, I., Oostrik, J., Diaz-Horta, O., Young, J.I., Tokgoz-Yilmaz, S., Konukseven, O., Shahin, H., Hetterschijt, L., Kanaan, M., Oonk, A.M., Edwards, Y.J., Li, H., Atalay, S., Blanton, S., Desmidt, A.A., Liu, X.Z., Pennings, R.J., Lu, Z., Chen, Z.Y., Kremer, H. and Tekin, M. (2012). Mutations in OTOGL, encoding the inner ear protein otogelin-like, cause moderate sensorineural hearing loss. *American journal of human genetics*, 91(5), 872–882.

95. Zebhauser, R., Kammerer, R., Eisenried, A., McLellan, A., Moore, T. and Zimmermann, W. (2005). Identification of a novel group of evolutionarily conserved members within the rapidly diverging murine Cea family. *Genomics*, 86(5), 566–580.

96. Zheng, J., Miller, K.K., Yang, T., Hildebrand, M.S., Shearer, A.E., DeLuca, A.P., Scheetz, T.E., Drummond, J., Scherer, S.E., Legan, P.K., Goodyear, R.J., Richardson, G.P., Cheatham, M.A., Smith, R.J. and Dallos, P. (2011). Carcinoembryonic antigen-related cell adhesion molecule 16 interacts with alpha-tectorin and is mutated in autosomal dominant hearing loss (DFNA4). *Proceedings of the National Academy of Sciences of the United States of America*, 108(10), 4218–4223.

97. Zheng, L., Zheng, J., Whitlon, D.S., García-Añoveros, J. and Bartles, J.R. (2010). Targeting of the hair cell proteins cadherin 23, harmonin, myosin XVa, espin, and prestin in an epithelial cell model. *The journal of neuroscience*, 30(21), 7187-7201.